8th Taiwan - Japan International Workshop on Hydrological and Geochemical Research for Earthquake Prediction

September 29,2009

National Cheng Kung University, Tainan, Taiwan

-PROCEEDINGS-

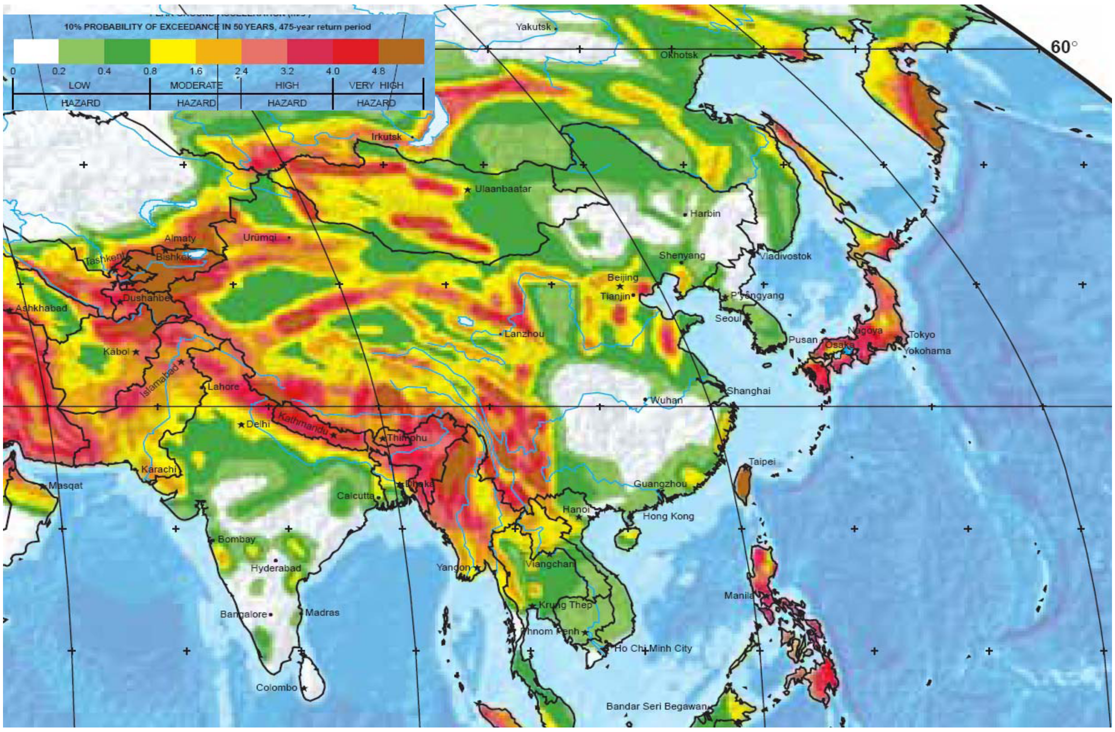

Edited by Chjeng-Lun Shieh, Naoji Koizumi and Norio Matsumoto

GSJ Open-File Report No.522

Disaster Prevention Research Center
National Cheng Kung University

No.1,Ta-Hsueh Rd. Tainan 701, Taiwan

GEOLOGICAL SURVEY OF JAPAN

NATIONAL INSTITUTE OF

ADVANCED INDUSTRIAL SCIENCE AND TECHNOLOGY (AIST)

1-1 Higashi 1-Chome, Tsukuba, Ibaraki, 305-8567 Japan

2010

8th Taiwan - Japan International Workshop on Hydrological and Geochemical Research for Earthquake Prediction

September 29,2009
National Cheng Kung University, Tainan, Taiwan

Sponsor：

Disaster Prevention Research Center, National Cheng Kung University

Taiwan Disaster Prevention Society

Co-Sponsor：

Earth Science Research Promotion Center, National Sciences Council

Geological Survey of Japan, National Institute of Advanced Industrial Science and Technology

Water Resource Agency, Ministry of Economic Affairs

Preface

Both of the NCKU-DPRC (the Disaster Prevention Research Center, National Cheng Kung University, Taiwan) and the IG-GSJ (Institute of Geoscience, Geological Survey of Japan, National Institute of Advanced Industrial Science and Technology) agreed to pursue scientific and technical cooperation about hydrological and geochemical research for earthquake prediction in Taiwan in February 2002. In 2005 NCKU-DPRC and GSJ agreed to continue the cooperation.

Based on the cooperation agreement, DPRC-NCKU and GSJ have been carrying out cooperative research activities on (1) Investigation of groundwater anomalies associated with the earthquake in Taiwan; (2) Analysis of the natural groundwater level changes in correlation to the geotectonic and meteorological activities; (3) Improving methodologies in monitoring and studying the groundwater anomalies with respect to geotectonic activities and/or other aspect as well; (4) Compiling the future periodically-monitored information of groundwater chemical and physical properties, and geotectonic anomalies; and(5) Analysis of the groundwater anomalies as earthquake precursors.

The 1st International Workshop on Hydrological and Geochemical Research for Earthquake prediction was held on Sep. 24, 2002 at GSJ, AIST, Tsukuba, Japan. The workshop was a good beginning to promote the research cooperation between Japan and Taiwan. The main purpose of the workshop this time is to proceed the collaboration and to provide an opportunity to share the precious experience with other researchers. In total, seventeen papers will be presented in this workshop.

Although the earthquake prediction is a hard scientific challenge in the century, keeping on study and making any kind of approach are the better way to contribute earthquake hazard mitigation. We hope that this workshop will offer the good ideas and experiences for related works. In view of this sincerecooperation, we absolutely believe this workshop will help us to preserve more safety for our life.

September 2009

Chjeng-Lun Shieh and Naoji Koizumi

8th Taiwan - Japan International Workshop on Hydrological and Geochemical Research for Earthquake Prediction, Workshop Program(September 29,2009)

【Sep.29 】Place: International Conference Room, National Cheng Kung University

Place	Time	Program		
Lobby	09:10~09:40	Registration		
Conference Hall	09:40~10:00	Opening Ceremony		
Place	**Time**	**Speaker**	**Title**	**Coordinator**
International Conference Room, National Cheng Kung University	10:00~10:20	Naoji Koizumi	Integrated groundwater observation for forecasting the Tonankai and Nankai earthquakes	Director Shieh
	10:20~10:40	Ruey-Juin Rau	Precursory swarms of moderate-sized earthquakes in eastern Taiwan	
	10:40~11:00	Yasuhiro Asai	Dynamic strain variations and co-seismic groundwater level changes associated with the August 2009 Suruga-bay earthquake (M6.5) observed at the Tono area, Central Japan.	
	11:00~11:15	Coffee Break		
	11:15~11:35	Masataka Ando	Geological, seismological, tsunami and folklore studies related to giant earthquakes along the Ryukyu trench	Dr. Koizumi
	11:35~11:55	Kuo-Fong Ma	Modeling and Scaling for Earthquakes in Taiwan Region	
	11:55~12:15	Mamoru Nakamura	Interplate coupling and slow slip events along the Ryukyu trench	
	12:15~13:30	Lunch Time		
	13:30~13:50	Nobuhisa Matsuta	Comparison of the deformation between geological term and geodetic term across the Yuli fault by precise leveling survey, Southeast Taiwan	Prof. Ando
	13:50~14:10	Masayuki Murase	Creeping distribution on the Longitudinal valley fault at Yuli area estimated by precise leveling survey, Southeast Taiwan	
	14:10~14:30	Chi-Ching Liu	Borehole Strain and GPS Strain in Eastern Taiwan	
	14:30~14:50	Kuniyo Kawabata	Structure of long-term sealing in the fault zone during aseismic period – examples from the Chelungpu fault in Taiwan	
	14:50~15:20	Coffee Break		

Place	Time	Speaker	Title	Coordinator
	15:20~15:40	Fumiaki Tsunomori	Semi-continuous groundwater gas monitoring at Kashima observatory	Deputy Director Lai
	15:40~16:00	M. C. Tom Kuo NCKU	Estimation of fracture porosity using radon as a tracer	
	16:00~16:20	Shigeki Tasaka	Underground water observations in hot spring, central part of Japan	
	16:20~16:40	Duo-Xing Yang	Responses of well water-level changes to the stress wave due to Wenchuan MS 8.0 strong earthquake	
	16:40~17:00	Kuo-Chin Hsu	Characterization of earthquake-induced water level fluctuation using data mining techniques	
	17:00~17:20	Wen-Chi Lai	Dynamic effects on coseismic groundwater level changes	

Content

Integrated groundwater observation for forecasting the Tonankai and Nankai earthquakes

N.Koizumi, Y.Kitagawa, S.Itaba, N.Matsumoto and R.Ohtani
Geological Survey of Japan, AIST

Abstract

Geological Survey of Japan (GSJ), AIST has been monitoring groundwater in the Tokai area for earthquake prediction since 1970's. Given the “pre-slip” model indicating that slow aseismic slip occurs at the tectonic plate boundary a few days before an earthquake, our network can detect the groundwater level changes that may precede the occurrence of the Tokai earthquake. However, the possibility of occurrence of the Tonankai and Nankai earthquakes has also been increasing. In addition recent studies have found that episodic slow slips with deep low frequency tremors occur near the source regions of the Tokai, Tonankai, and Nankai earthquakes. The slow slips resemble the pre-slip. Therefore we constructed 12 new integrated groundwater observatories in the Tonankai and Nankai regions by January 2009 (Fig.1). Each of these includes three wells that monitor groundwater levels and temperatures, crustal deformation, and seismic activity (Fig.2). Using the data from the new observatories, we already detected strain changes related to more than ten episodic slow slips with the tremors in the plate boundary near the Tonankai region for the recent two years (Fig.3).

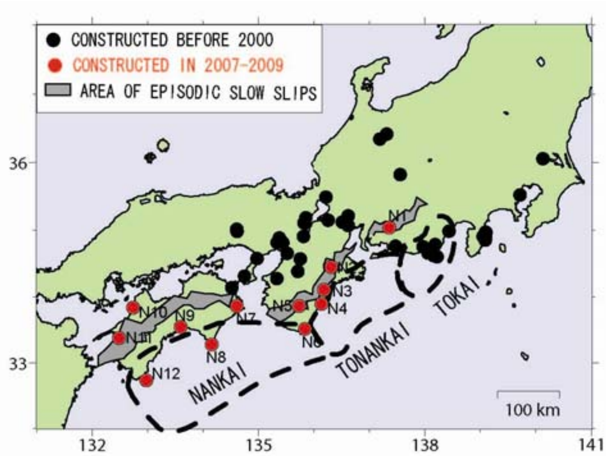

Fig.1 Integrated groundwater observatories of GSJ, AIST.

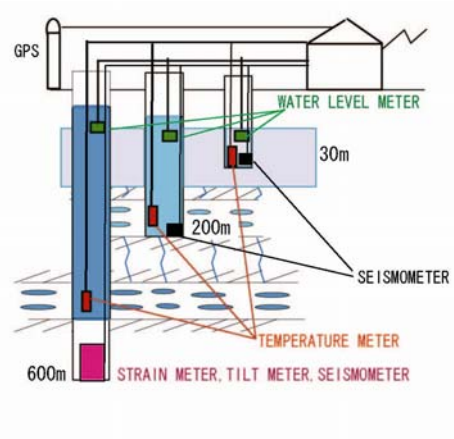

Fig.2 Schematic figure of the system of our new observatory (N1-N12) in Fig.1.

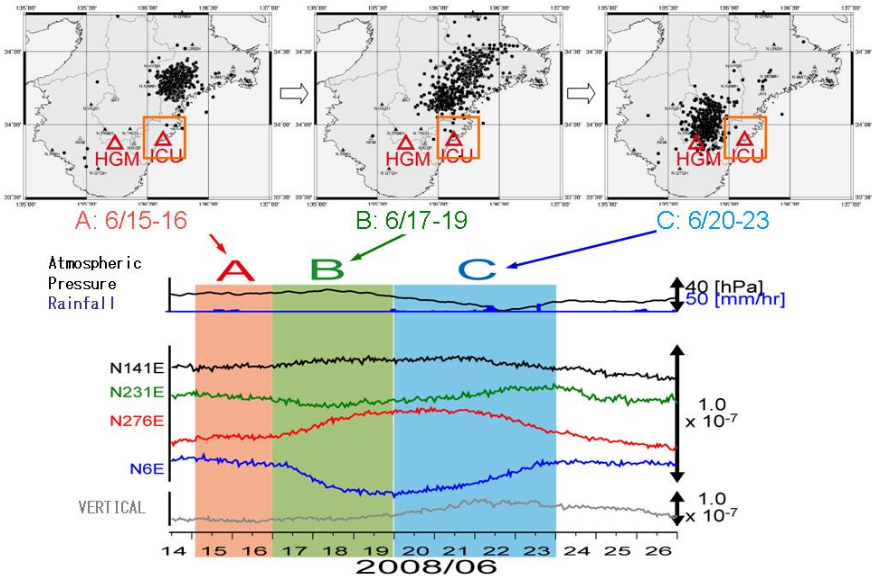

Fig.3 (Upper): Distribution of tremors (small balck circles) detected from June 15-23, 2008 by the Automatic Tremor Monitoring System (ATMOS) of Hiroshima University.

(Lower): Hourly strain changes at ICU accompanying the tremors.

Integrated groundwater observation for forecasting the Tonankai and Nankai earthquakes

*Naoji Koizumi, N.Matsumoto, R.Ohtani, Y.Kitagawa,S.Itaba and N.Takeda
(Geological Survey of Japan, AIST)

OUTLINE

1) Introduction of the Nankai and Tonankai Earthquakes and Groundwater Changes Related to the Past Nankai Earthquake

2) Recent Detection of Deep Low-Frequency Tremors and Episodic Slow Slips (SSE) on the Plate Boundary

3) System of our New Integrated Groundwater Observation

4) Preliminary Results

OUTLINE

1) Introduction of the Nankai and Tonankai Earthquakes and Groundwater Changes Related to the Past Nankai Earthquake

2) Recent Detection of Deep Low-Frequency Tremors and Episodic Slow Slips (SSE) on the Plate Boundary

3) System of our New Integrated Groundwater Observation

4) Preliminary Results

Earthquake-Related Groundwater Change ⟷ Crustal Deformation

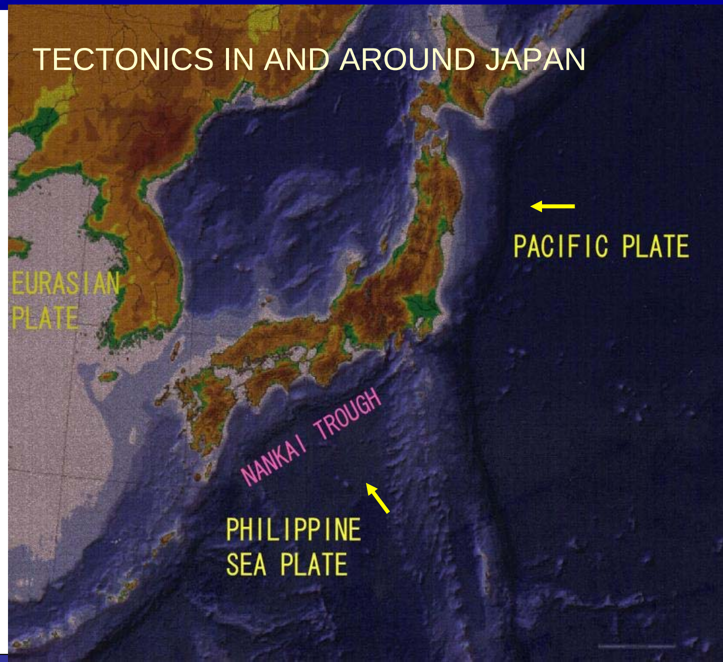

AIST

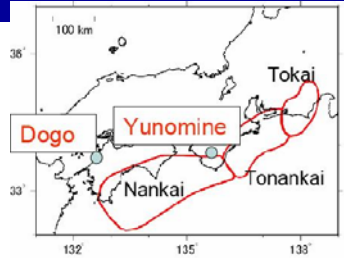

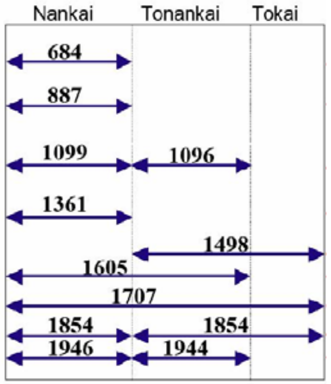

Sangawa (1992)

NANKAI, TONANKAI AND TOKAI EARTHQUAKES

HISTORY OF THE EARTHQUAKES
- 9 TIMES ←HISTORICAL DOCUMENTS

- M7.9 – M8.4
- INTERVAL: 100 - 200 years

AIST

Dogo hot spring: Groundwater level decreases after the 1946 Nankai earthquake

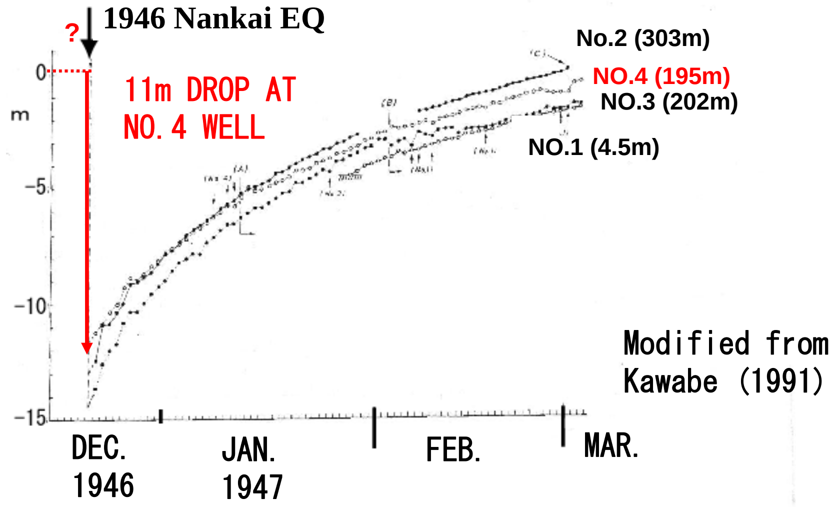

Modified from Kawabe (1991)

AIST

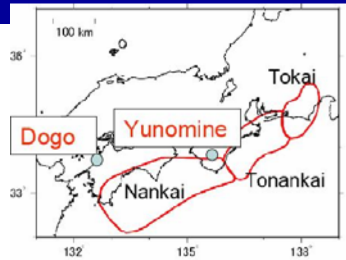

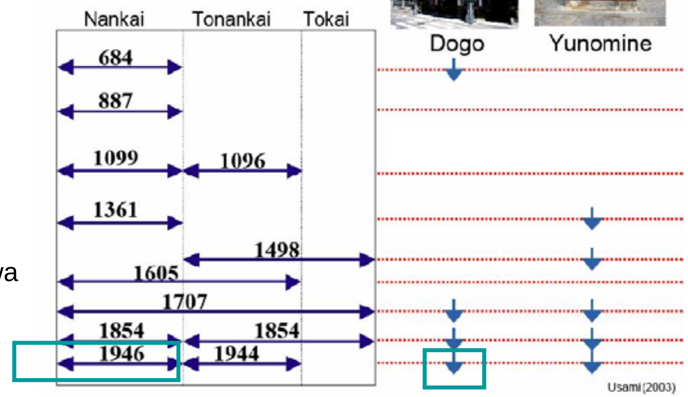

Sangawa (1992)

DECREASE IN GROUNDWATER DISCHARGE OR LEVEL AT HOT SPRINGS ASSOCATED WITH THE EARTHQUAKES

Dogo

Yunomine

AIST

Preseismic groundwater anomalies

1-10 days before the 1854 Nankai earthquake

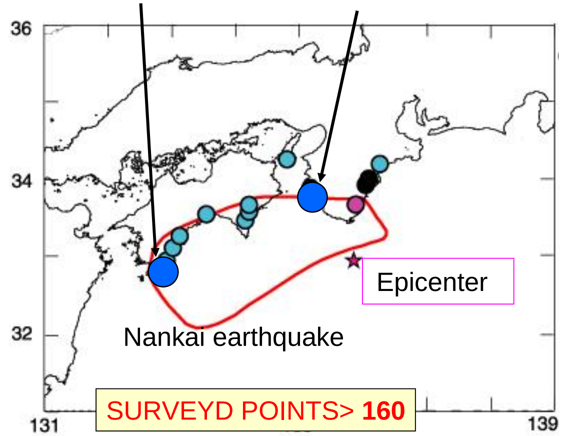

Shigetomi et al.(2005)

A Few Large Anomalies Occurred in a Wide Area

0.5-1m ?

- 11 DROPS in shallow unconfined groundwater level
- 1 Decrease in hot spring water discharge
- Getting turbid

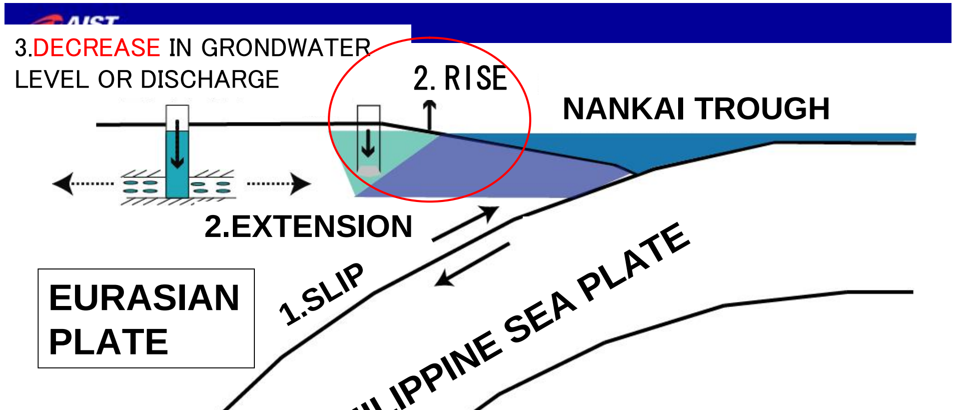

A Few Large Groundwater Anomalies Occurred in a **Wide Area**

Possible Mechanism

・Preseismic Small Crustal Deformation in the Wide Area by a Slow Slip and Lodcal Groundwater System Amplifying the small Crustal Deformation.

Deep Low-Frequency Tremors and Episodic Slow Slip Events (SSE)

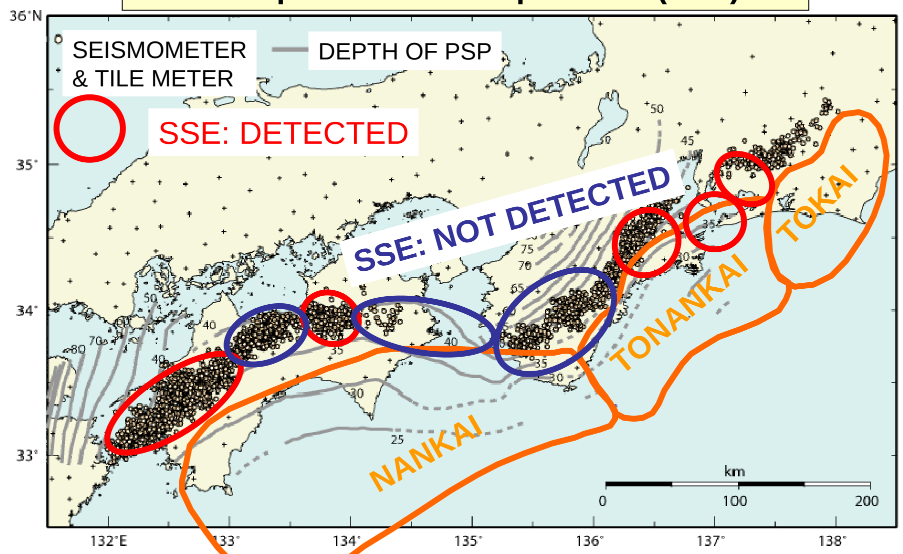

Modified From Obara,(2002) and Schwartz and Rokosky (2007)

OUTLINE

1) Introduction of the Nankai and Tonankai Earthquakes and Groundwater Changes Related to the Past Nankai Earthquake
2) **Recent Detection of Deep Low-Frequency Tremors and Episodic Slow Slips (SSE) on the Plate Boundary**

3) System of our New Integrated Groundwater Observation
4) Preliminary Results

OUTLINE

1) Introduction of the Nankai and Tonankai Earthquakes and Groundwater Changes Related to the Past Nankai Earthquake
2) Recent Detection of Deep Low-Frequency Tremors and Episodic Slow Slips (SSE) on the Plate Boundary
3) **System of our New Integrated Groundwater Observation**

4) Preliminary Results

Integrated Groundwater Observatory

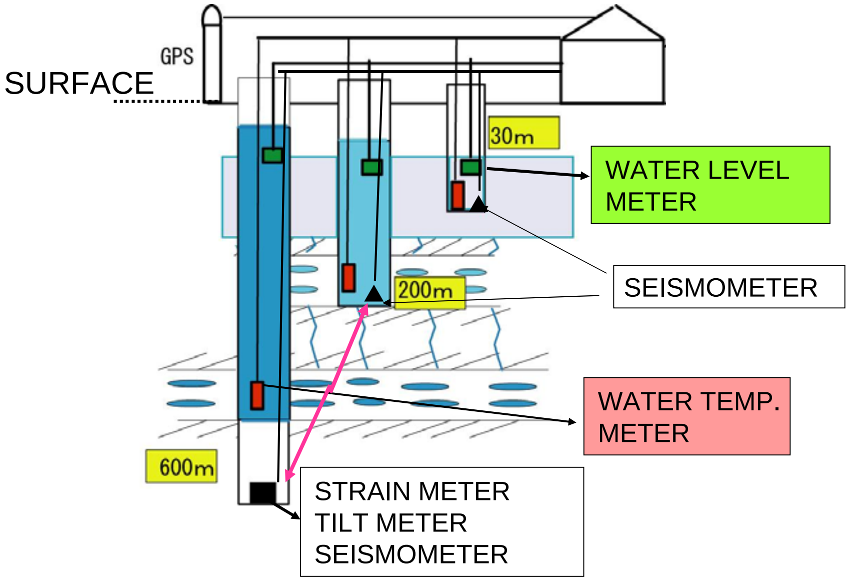

OUTLINE

1) Introduction of the Nankai and Tonankai Earthquakes and Groundwater Changes Related to the Past Nankai Earthquake

2) Recent Detection of Deep Low-Frequency Tremors and Episodic Slow Slips (SSE) on the Plate Boundary

3) System of our New Integrated Groundwater Observation

4) Preliminary Results

4-1) Detection of SSE in the Southern Part of the Kii Peninsula

4-2) Anomalous Changes in Strain and Groundwater Level Just After the Earthquake off Muroto on July 22,2009

Deep Low-Frequency Tremors and Episodic Slow Slip Events (SSE)

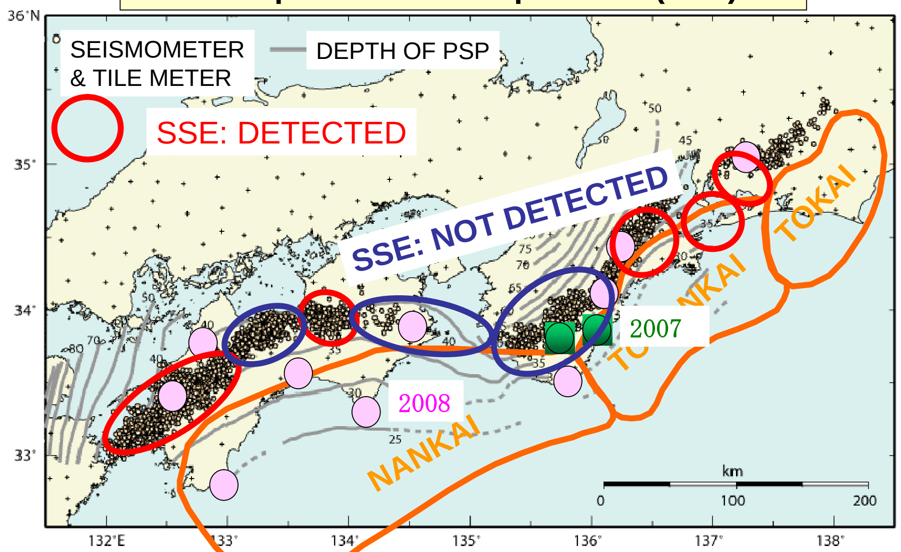

Modified From Obara,(2002) and Schwartz and Rokosky (2007)

4-1) Detection of SSE in the Southern Part of the Kii Peninsula

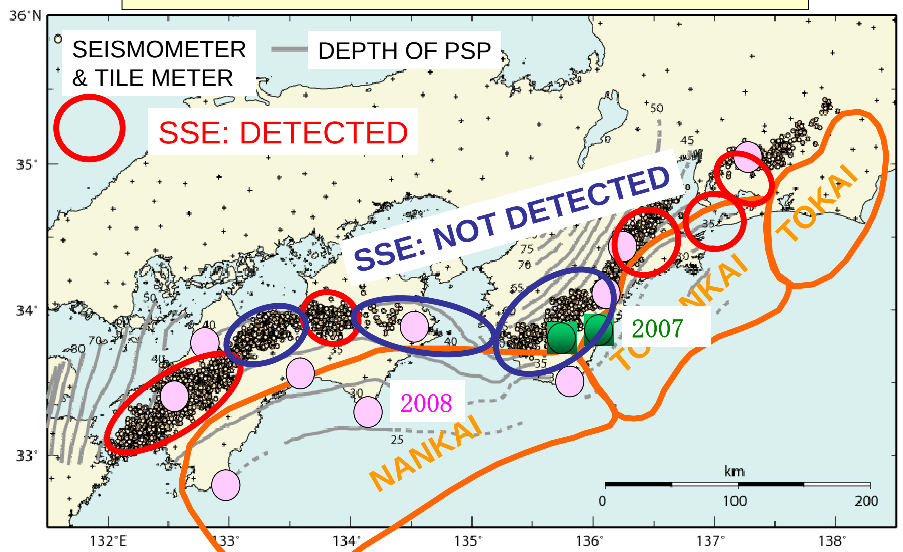

Modified From Obara,(2002) and Schwartz and Rokosky (2007)

Detection of SSE with Tremors in Jun. 2008

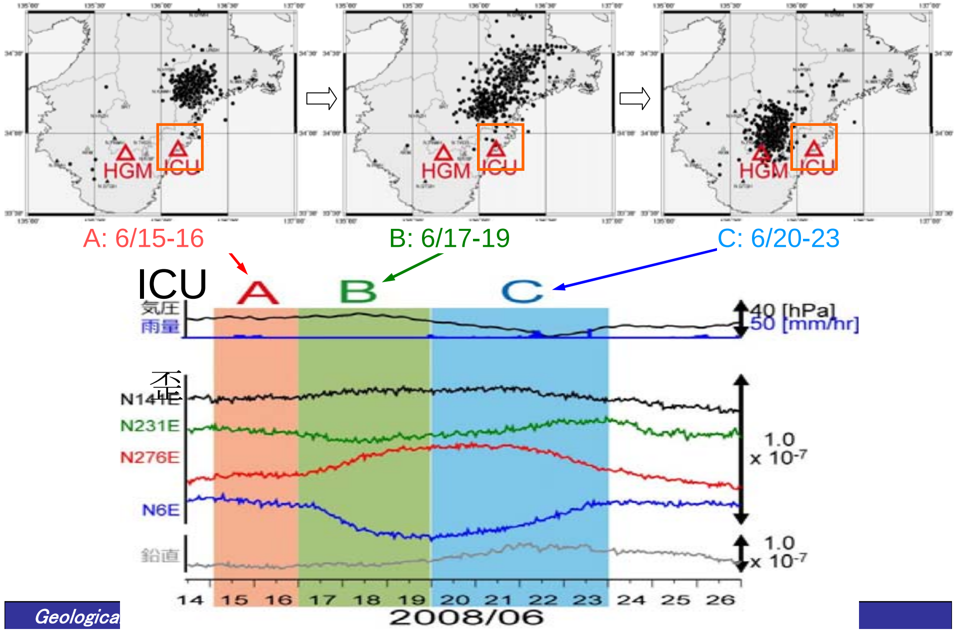

4-2)Anomalous Changes in Strain and Groundwater Level Just After the Earthquake off Muroto on July 22,2009

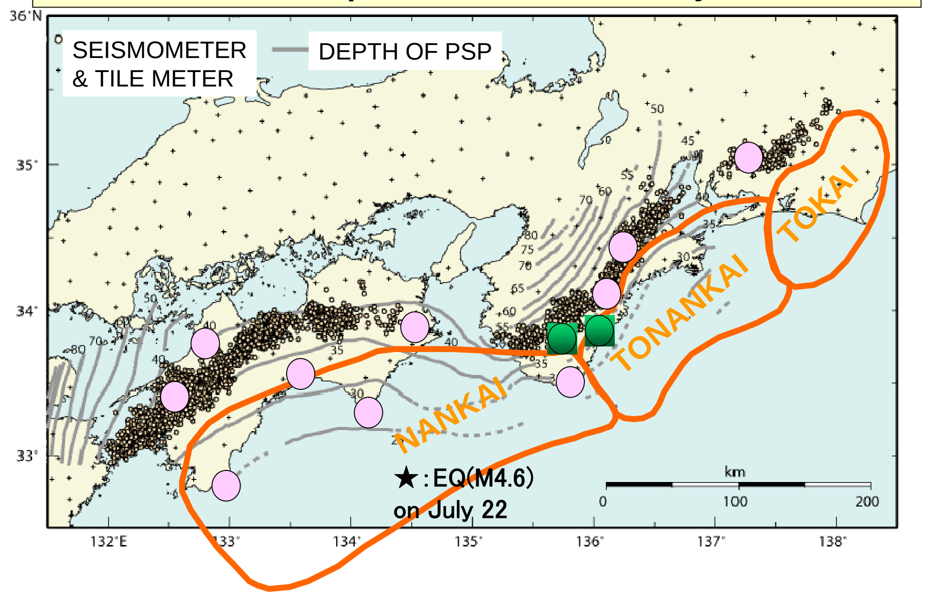

Estimation of the Fault Slip Model

Position: Tremor Area on the Plate Boundary

Slip ←→ Observed Strain Change

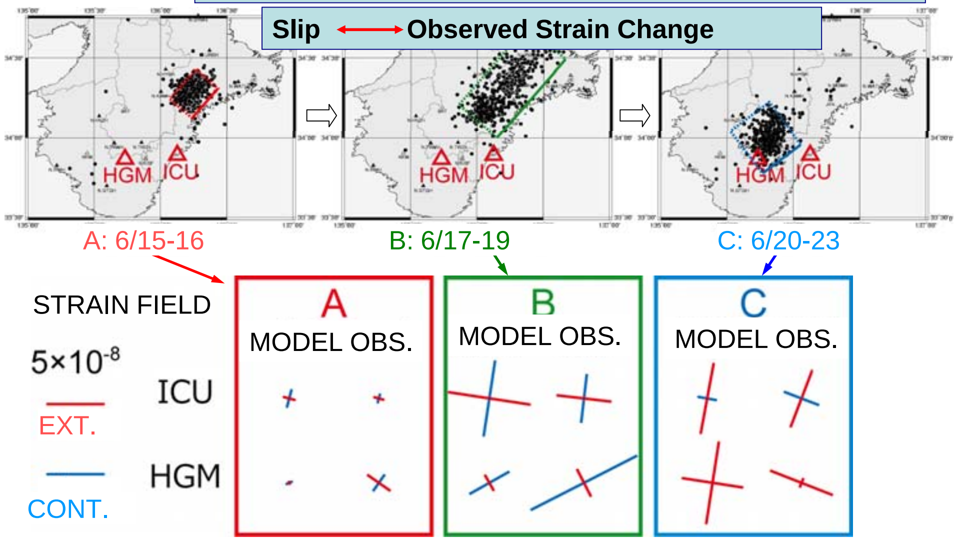

Itaba et al.(2009) PAGEOPH in Press

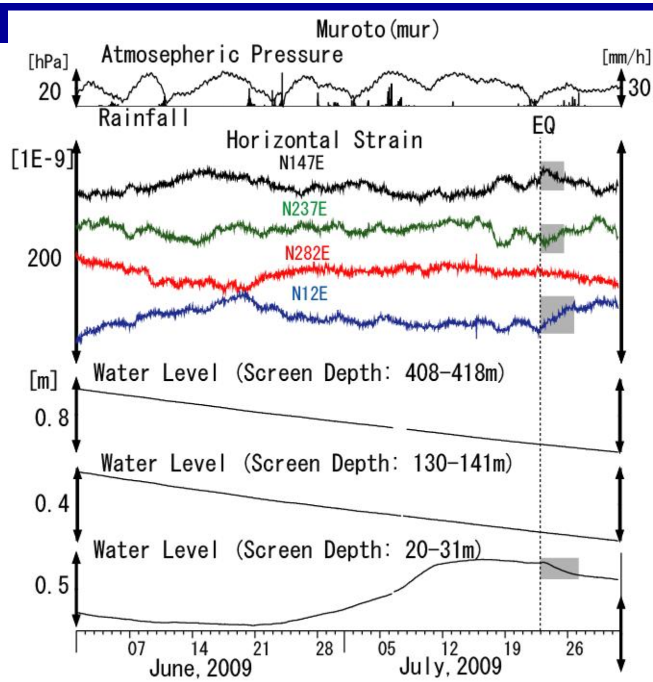

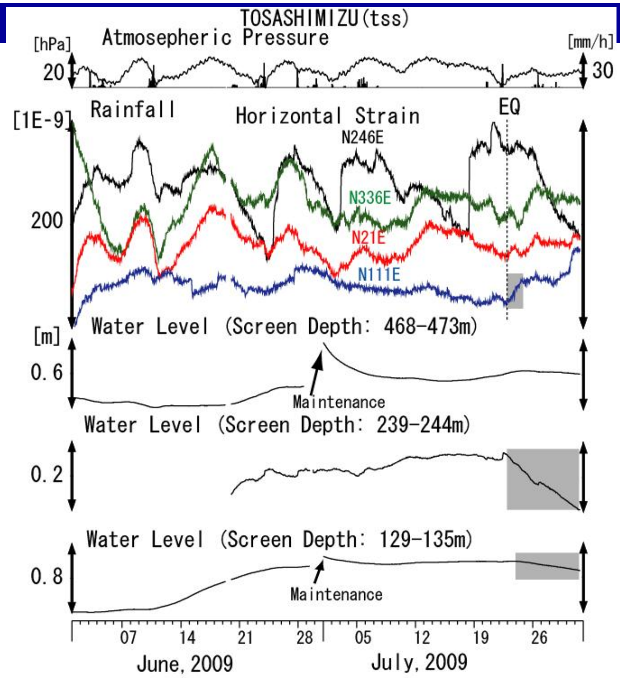

4-2)Anomalous Changes in Strain and Groundwater Level Just After the Earthquake off Muroto on July 22,2009

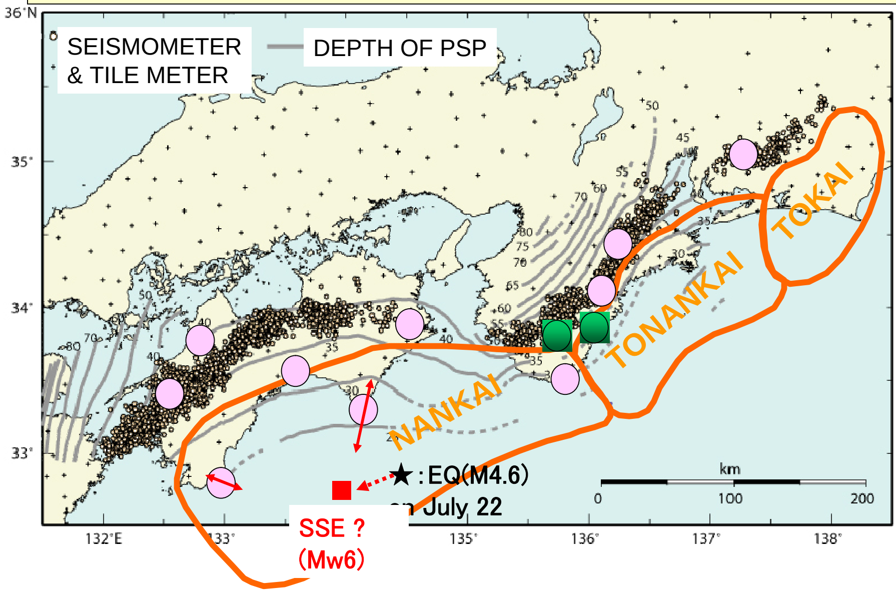

CONCLUSIONS

1)The Groundwater Level Decrease Before the Past Nankai Earthquakes Can Be Explained by Preseismic Small Crustal Deformation and Local Groundwater System Amplifying the small Crustal Deformation.

2)Based on the Past Earthquake-Related Groundwater Changes and Recent Detection of Deep Low-Frequency Tremors and Episodic Slow Slip Event (SSE), We Designed and Constructed 12 Integrated Groundwater Observatories for Forecasting the Tonankai & Nankai Earthquakes.

3)Using the Strain Data of New Observatories, We Have Found SSEs in the Southern Part of the Kii Peninsula. We Also Found the Anomalous Changes in Strain and Groundwater Level Just After the Earthquake off Muroto on July 22,2009, Which Can Be Partly Explained by SSE induced by the Earthquake.

Thank You

Precursory Swarms of Moderate-sized Earthquakes in Eastern Taiwan

Ruey-Juin Rau and Shih-Hung Hsu
Department of Earth Sciences, National Cheng Kung University, Tainan, Taiwan

Abstract

We investigated the correlation between swarm and large earthquakes for the events occurred in an area near the transition corner from subduction to collision in eastern Taiwan between January 1991 and March 2009. We systematically identified twenty swarms that have more than twenty earthquakes (M < 4.3) occurring within one month interval and found that eight out of twenty earthquake swarms located at a similar area and formed a specific seismic zone, which is twelve kilometers long, three kilometers wide and having a depth range between eight to twelve kilometers in the northern end of the Taiwan collision plate boundary. Eight swarms occurred 1-48 days preceding eight nearby moderate-sized earthquakes (5.5 < M < 6.3) within a radius of 40 kilometers. The accumulated moments of the preceding, seven out of eight, swarms are inversely related to the time-separation between the precursory swarms and the M > 5.5 earthquakes. A multiple asperity model may explain the earthquake preparatory processes observed from the precursory swarms-mainshock sequences found at the collision corner of eastern Taiwan. In this model, the Hualien space is composed of several asperities of similar size but with different stress level, in which the precursory-swarm is located within one of the asperities. As the tectonic stress increases, the smaller faults in the surrounding weaker zone start to break as background small earthquakes. When the stresses continue to increase, at some point, the swarms within the certain asperity start to break and in the mean time, turn on the switch for the "stress-meter" approaching the strength of one of the asperities. Following the empirical relationship between the accumulated seismic moments of the preceding swarms and the time-separation between the precursory swarms and the M > 5.5 earthquakes, the more the seismic moment accumulated by the earthquake swarm, the shorter the time we need to wait for the forthcoming M > 5.5 earthquake. Eventually one of the asperities breaks as the tectonic stress continuing to increase. This ends one earthquake cycle and starts a new one.

Precursory swarms of moderate-sized earthquakes in eastern Taiwan

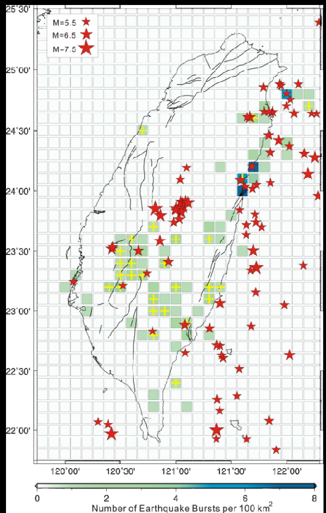

Ruey-Juin Rau and Shih-Hung Hsu
Department of Earth Sciences, National Cheng Kung University, Taiwan

Sequence of seismicity pattern predicted by the asperity model

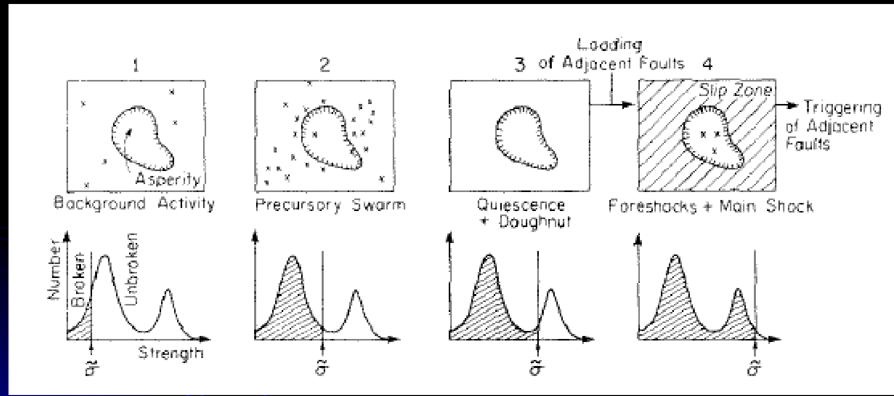

Kanamori, 1981

Space-time plot of seismicity for the Kurile Island regions

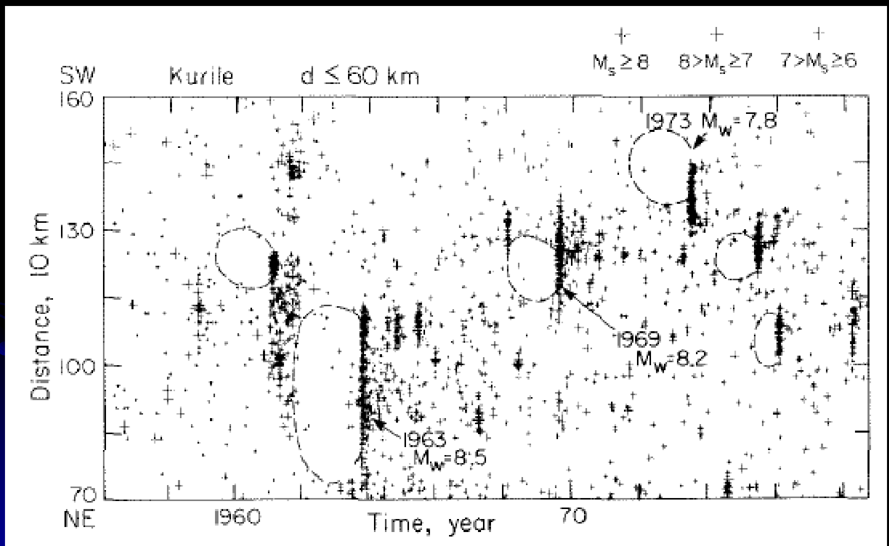

Kanamori, 1981

Where do we expect for having precursory swarms for large earthquakes in Taiwan?

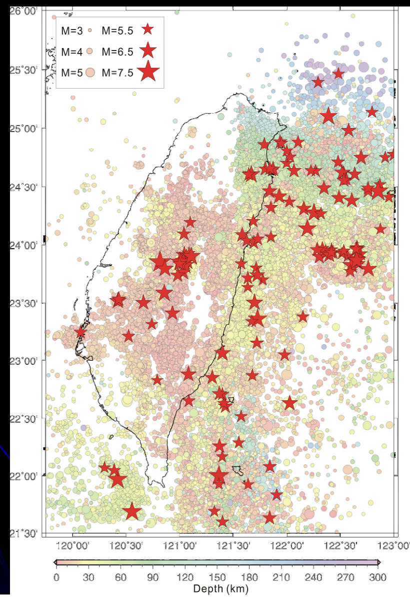

Is there any?

Earthquake bursts in Taiwan

* At least 40 events within a radius of 6 km in 14 days.

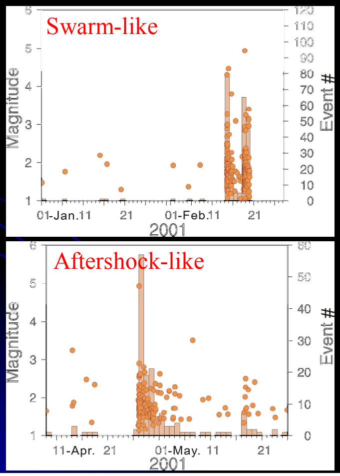

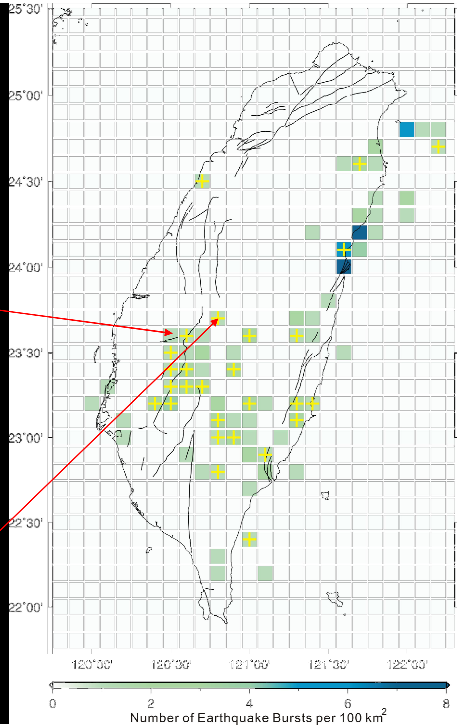

2006 NE Taiwan earthquake sequence

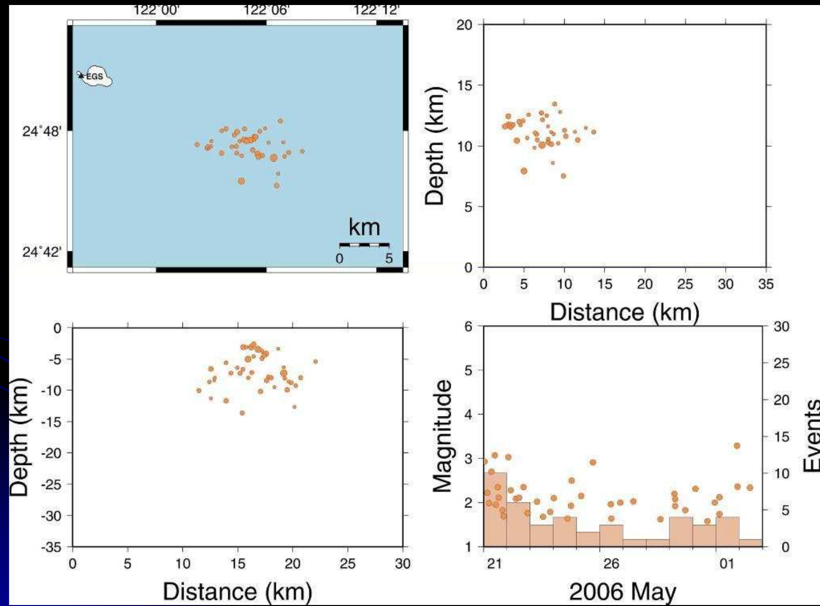

2008 Taoyuan earthquake sequence

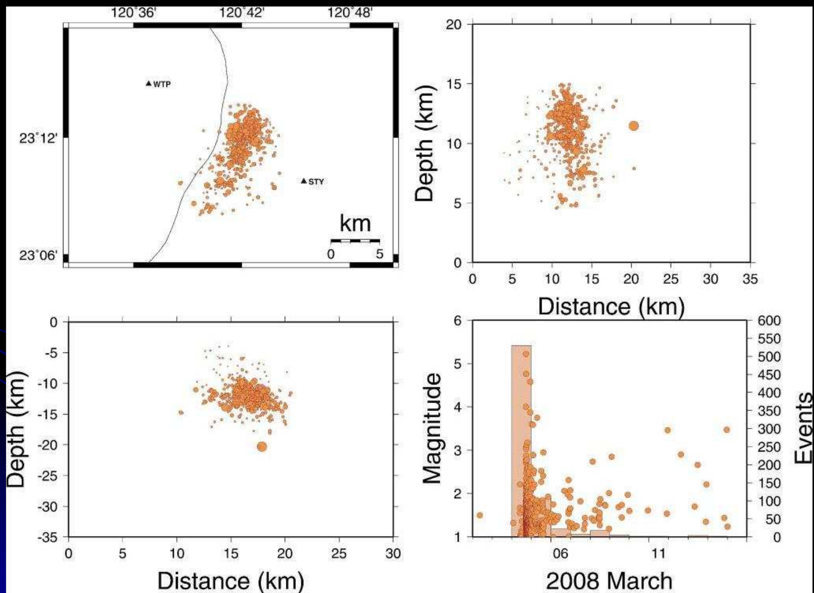

Mechanisms driving earthquake bursts

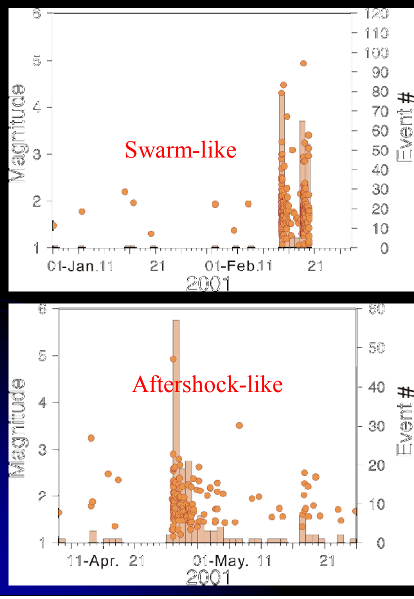

Pore fluid pressure fluctuations and/or episodic aseismic slip as drivers (*Vidale and Shearer*, 2006)

Earthquake bursts distribution overlap with large earthquakes

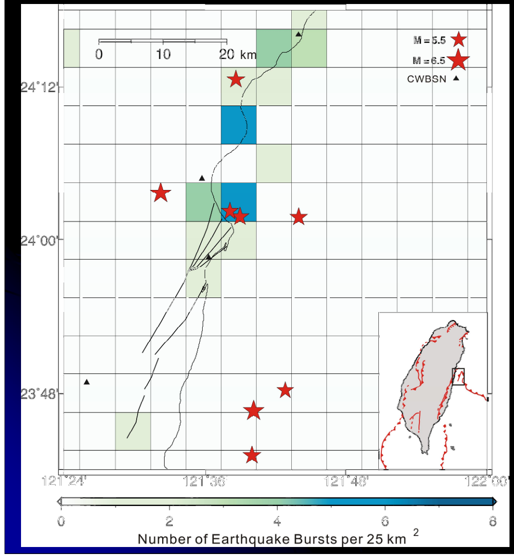

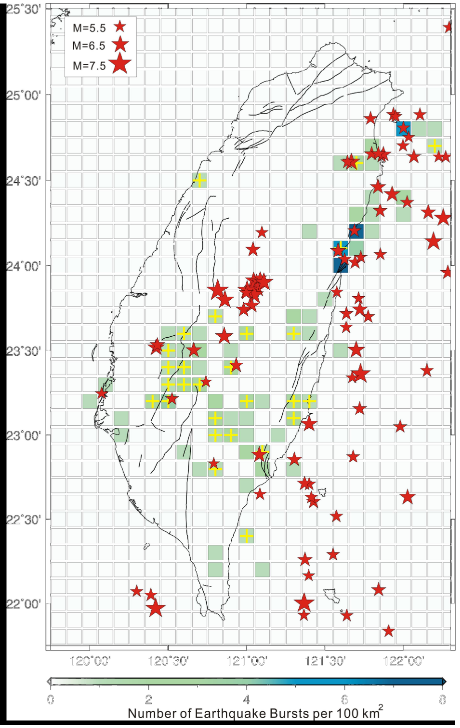

Seismicity in Hualien Area

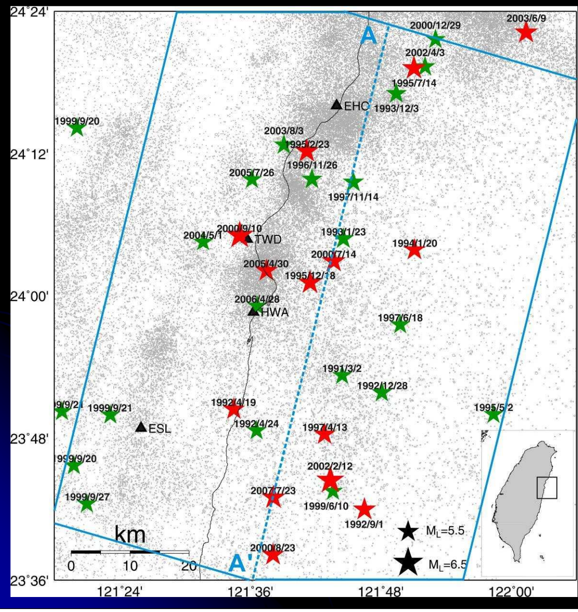

★ Green Stars
5.5 > M >= 5.2

★ Red Stars
6.3 > M >= 5.5

1991-2009

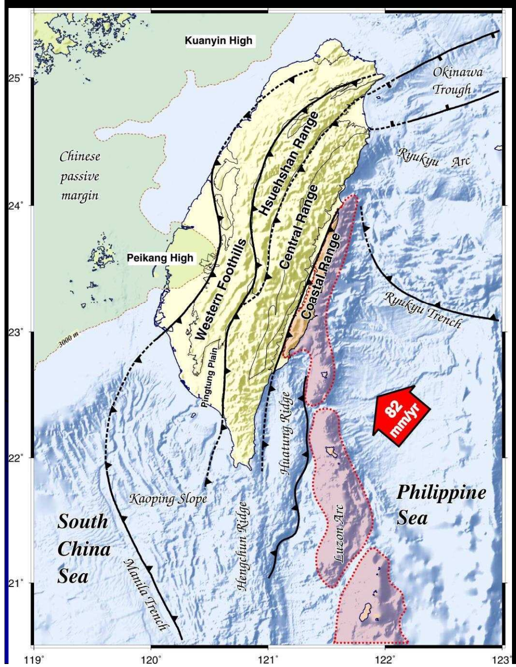

Hualien as the Subduction-Collision Edge Propagator

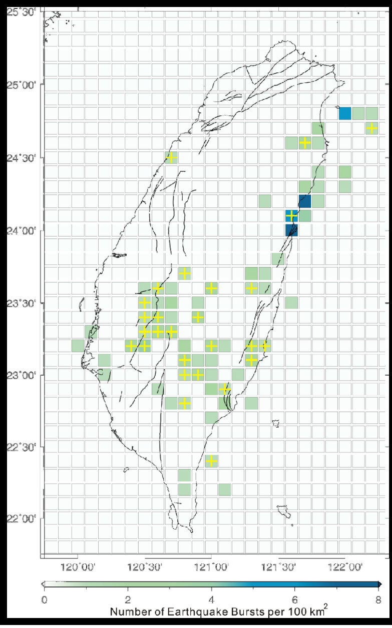

Earthquake magnitude completeness for Hualien area

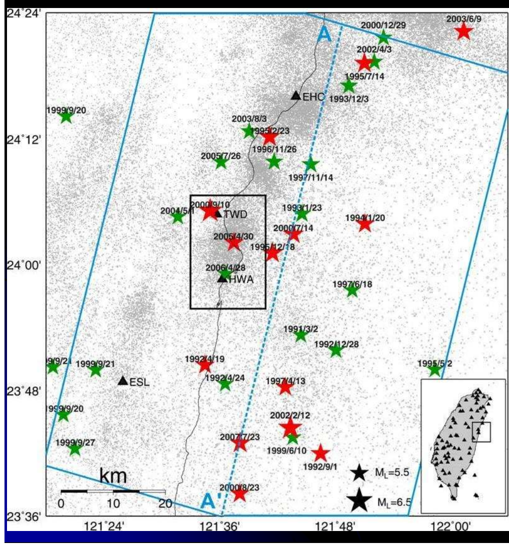

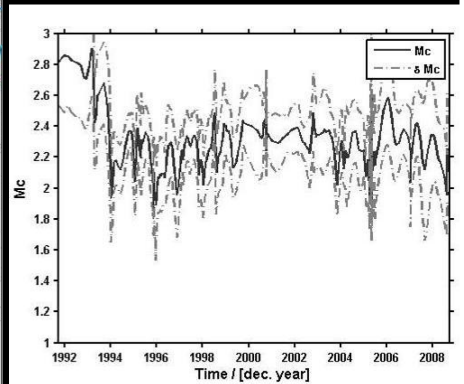

1991-2009

Mc and event statistics for EQ in Hualien area

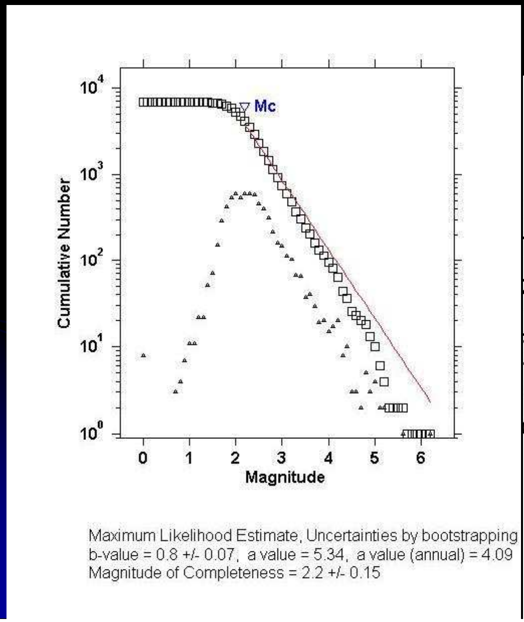

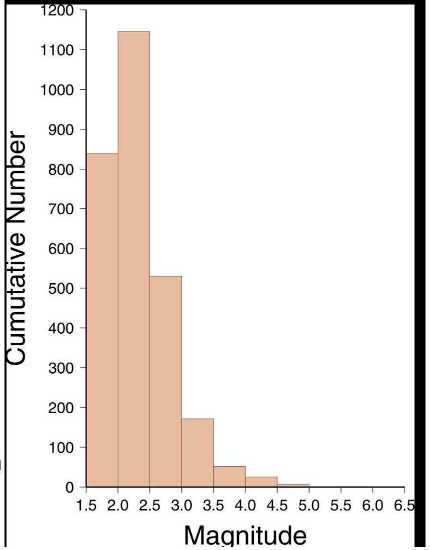

Space-time plot of seismicity in Hualien area

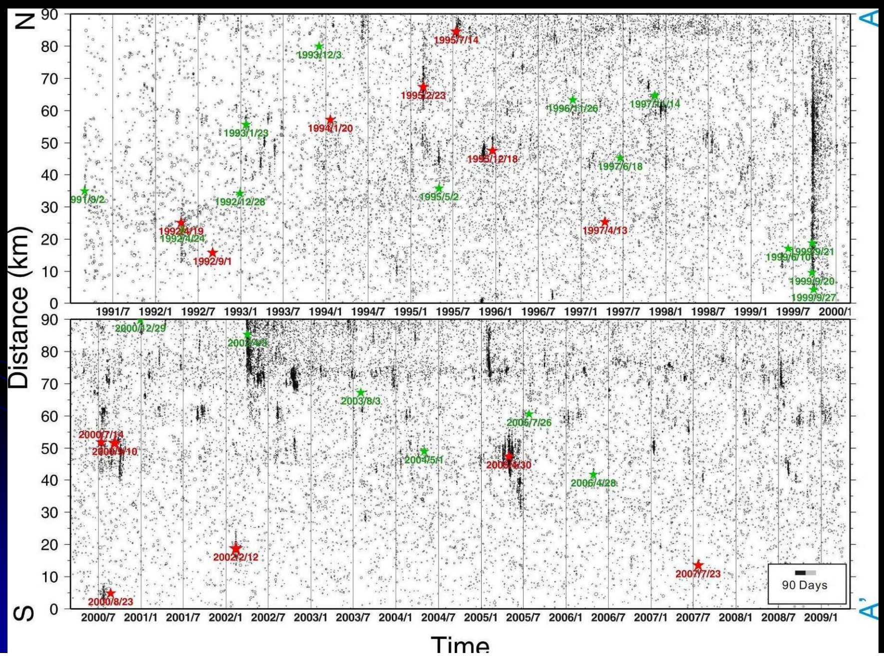

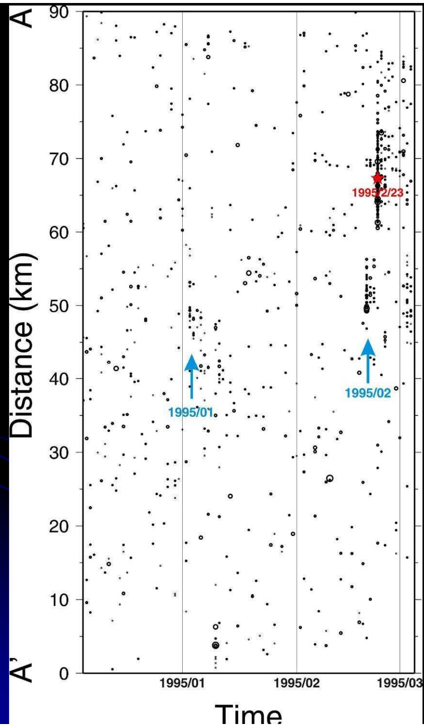

Which one is the precursor?

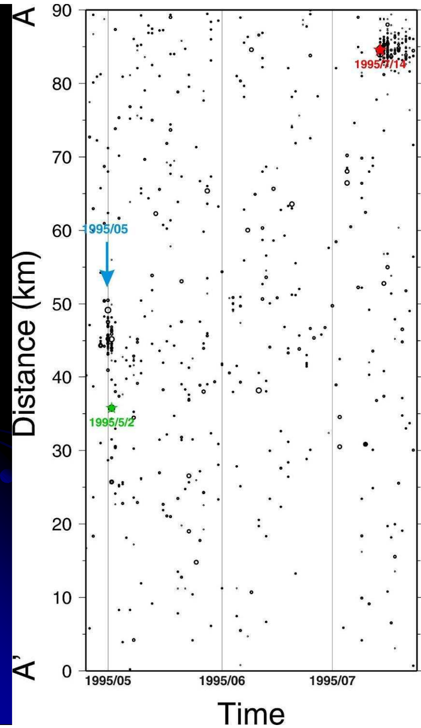

Precursor to the 1995 May event or the July event?

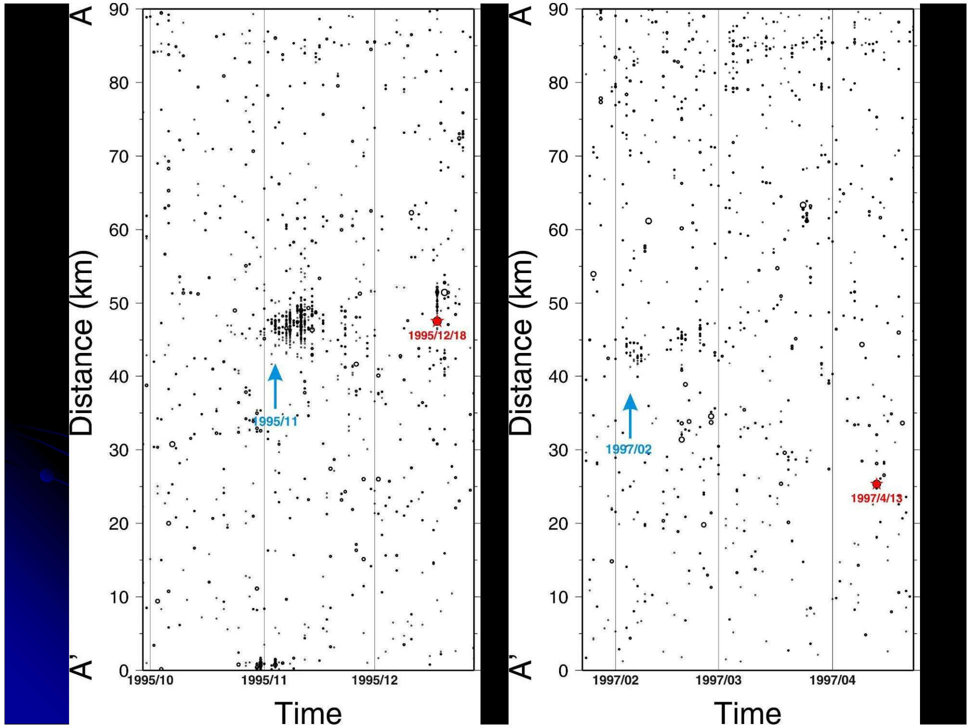

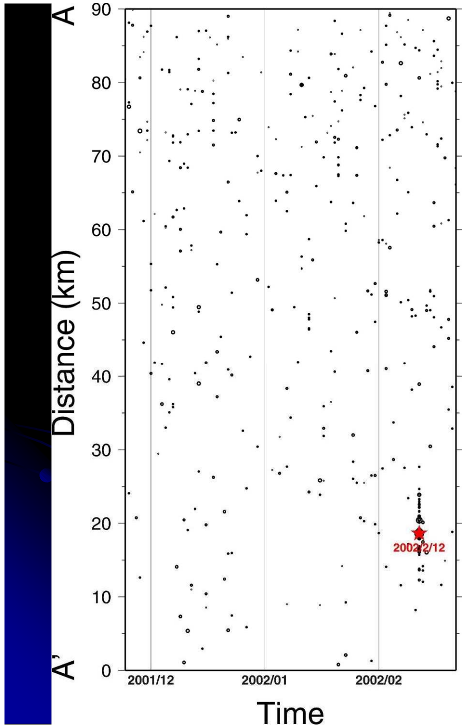

No precursory swarm?

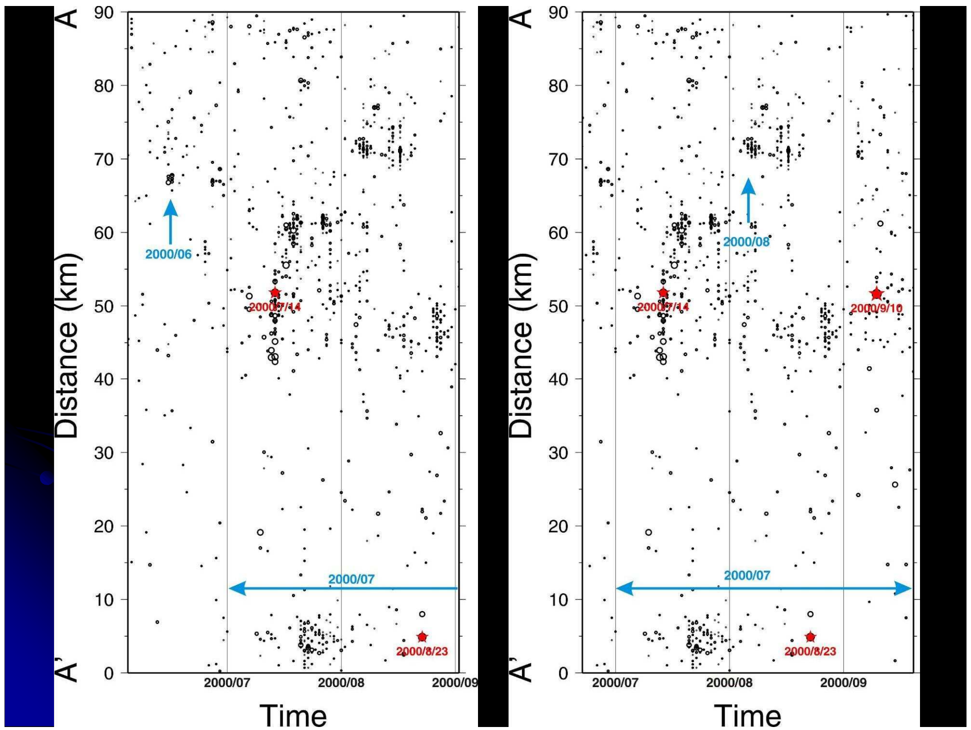

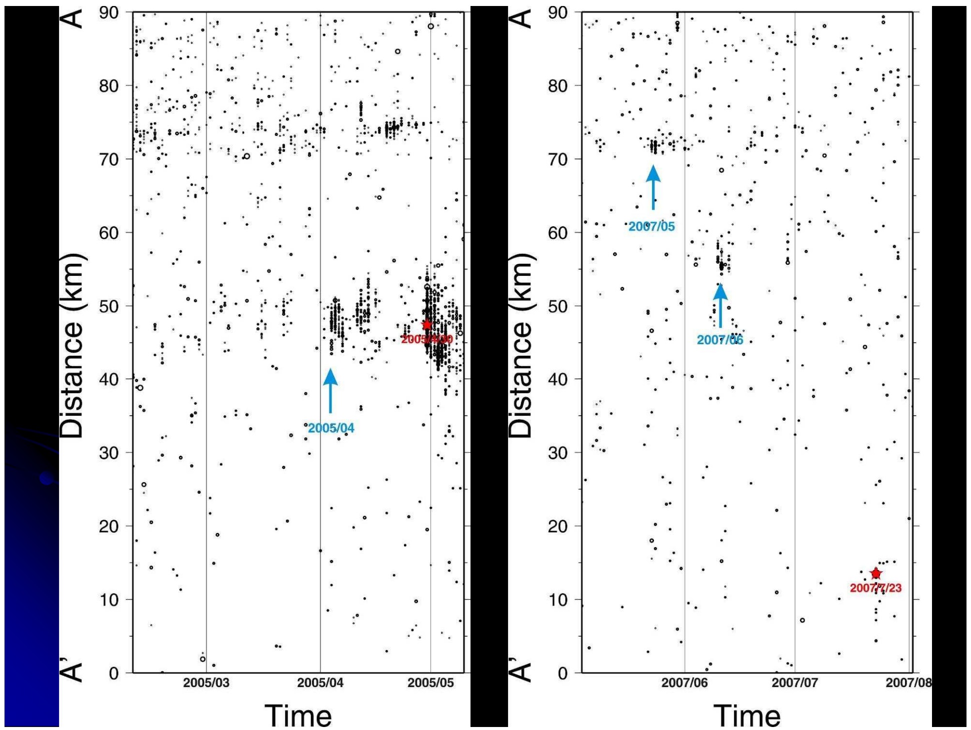

Time series for earthquake swarms in Hualien area

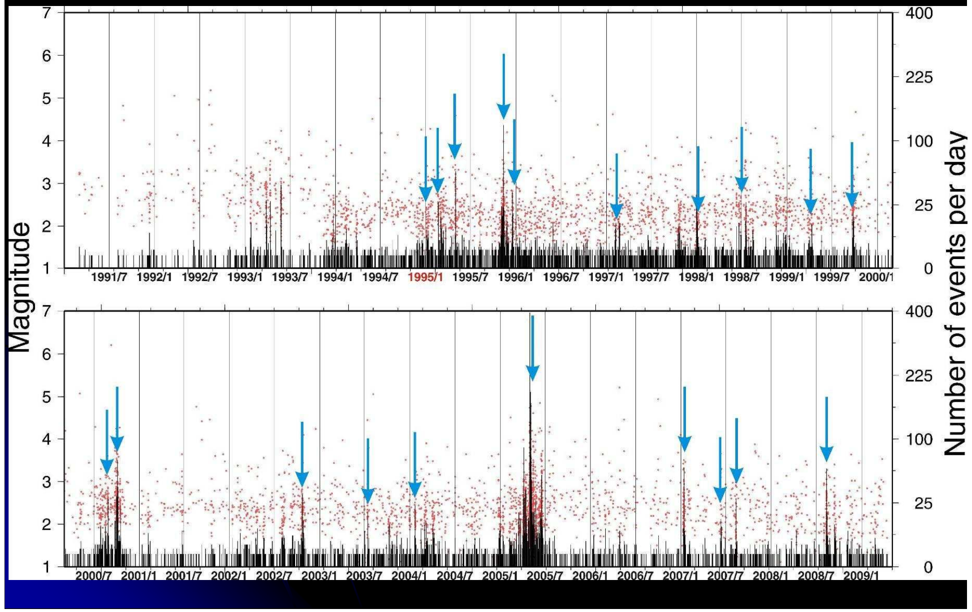

Swarm relocations

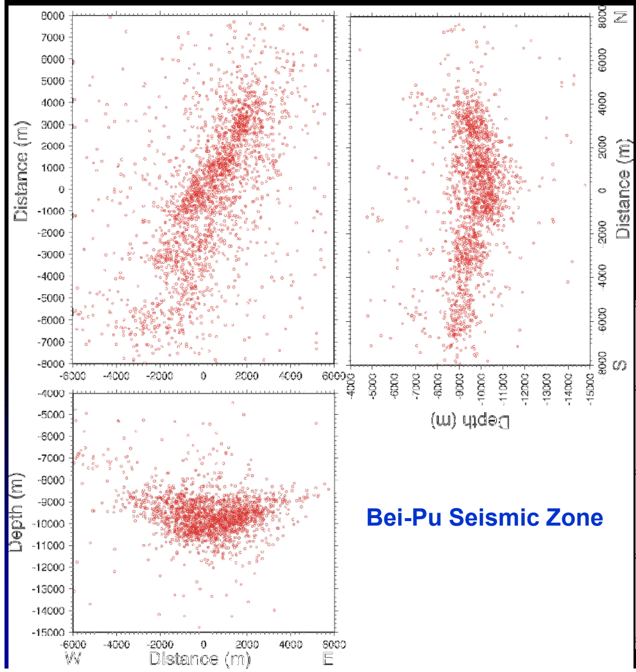

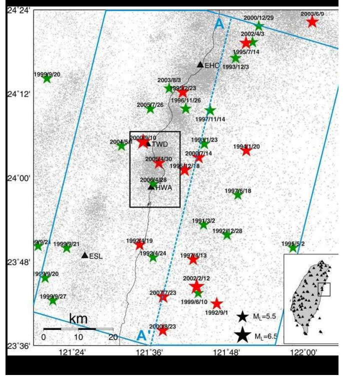

Temporal relationship between precursory swarms and moderate-sized earthquakes

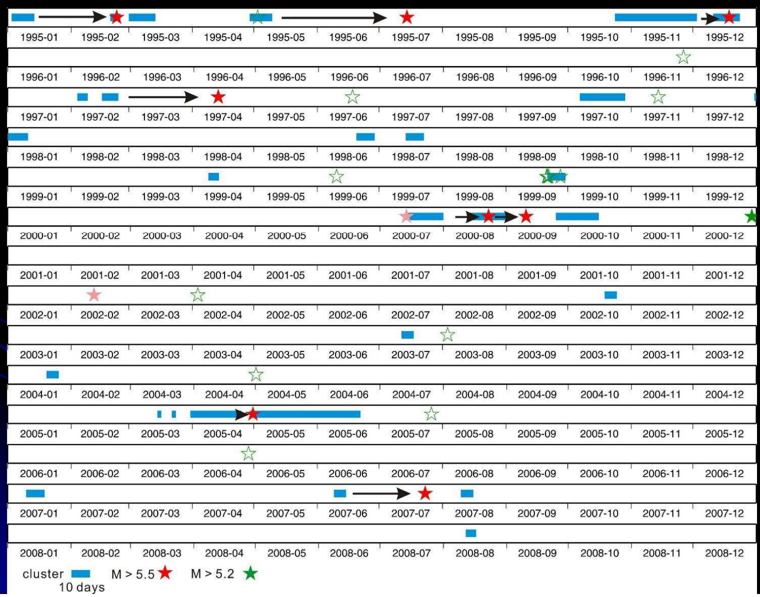

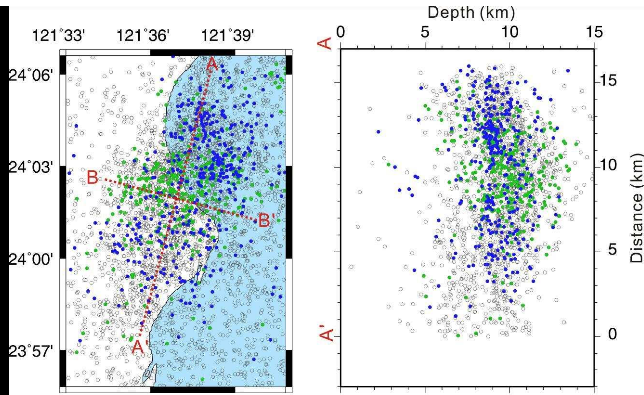

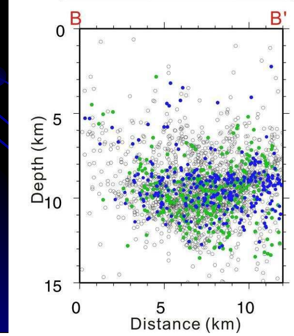

Earthquake Catalogue

Green: Swarms followed by M > 5.5 earthquakes

Blue: Swarms not followed by M > 5.5 earthquakes

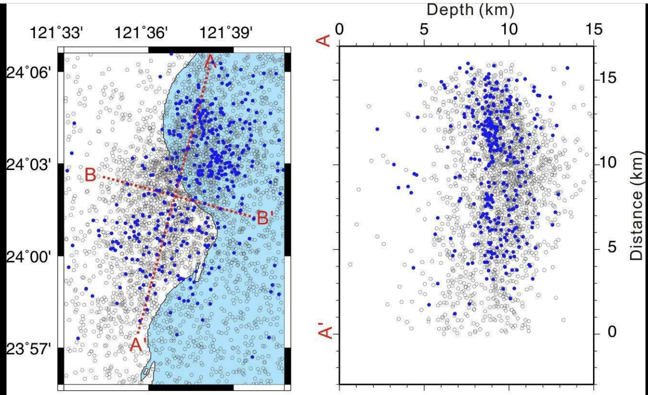

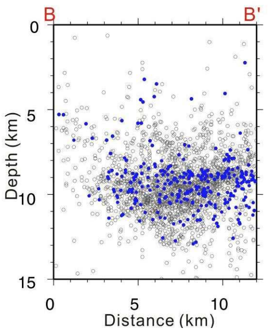

Earthquake Catalogue

Green: Swarms followed by M > 5.5 earthquakes

Blue: Swarms not followed by M > 5.5 earthquakes

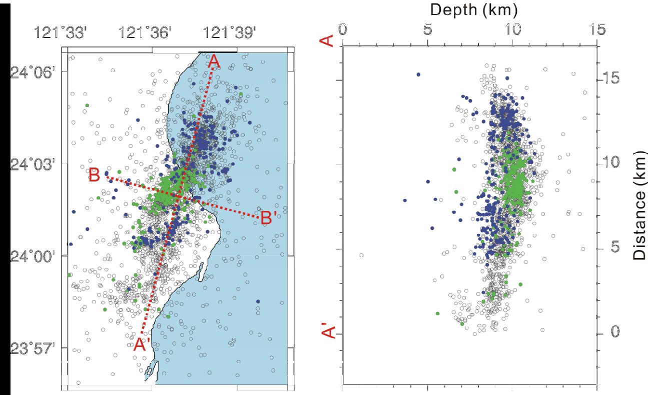

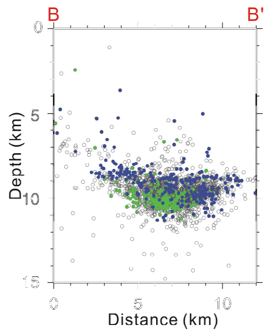

Earthquake Relocation

Green: Swarms followed by M > 5.5 earthquakes

Blue: Swarms not followed by M > 5.5 earthquakes

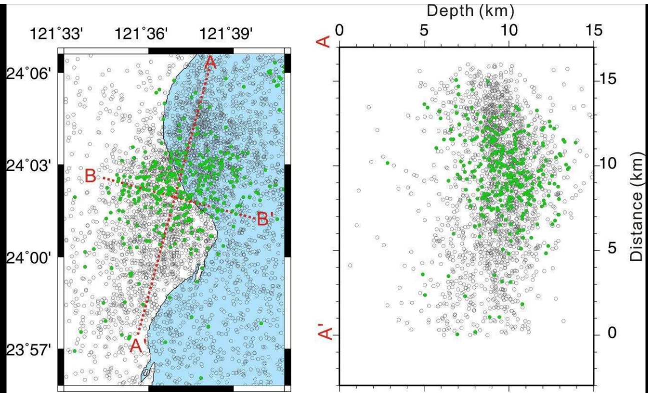

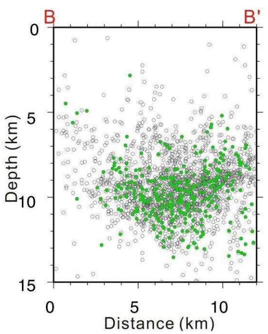

Earthquake Catalogue

Green: Swarms followed by M > 5.5 earthquakes

Blue: Swarms not followed by M > 5.5 earthquakes

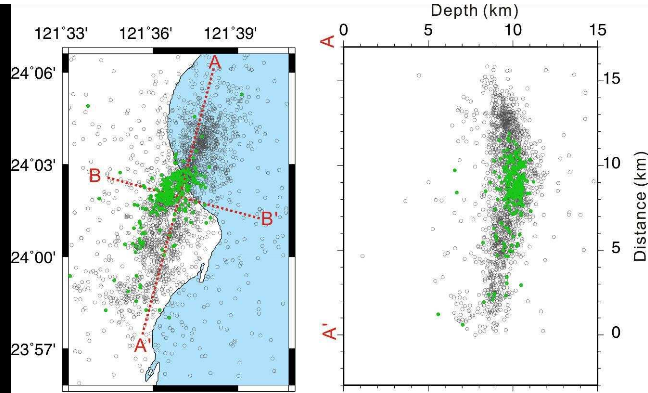

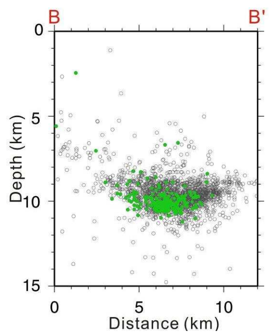

Earthquake Relocation

Green: Swarms followed by M > 5.5 earthquakes

Blue: Swarms not followed by M > 5.5 earthquakes

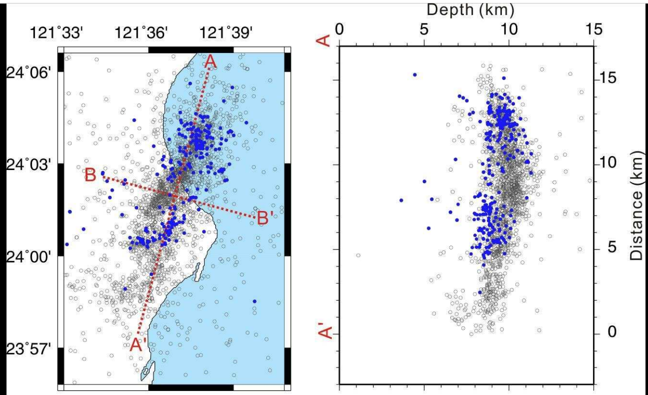

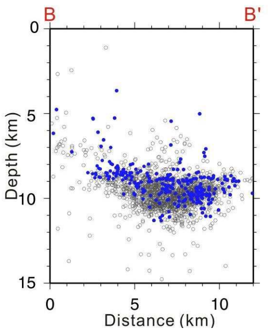

Earthquake Relocation

Green: Swarms followed by M > 5.5 earthquakes

Blue: Swarms not followed by M > 5.5 earthquakes

Distance-Moment and Time-Moment relationships between the precursory swarms and the M > 5.5 earthquakes

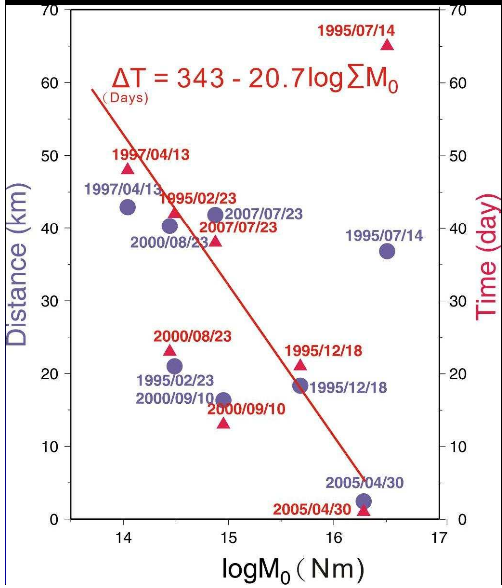

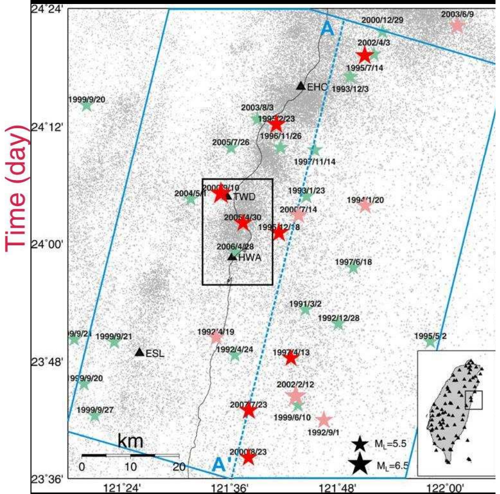

Distance-Moment and Time-Moment relationships between the precursory swarms and the M > 5.5 earthquakes

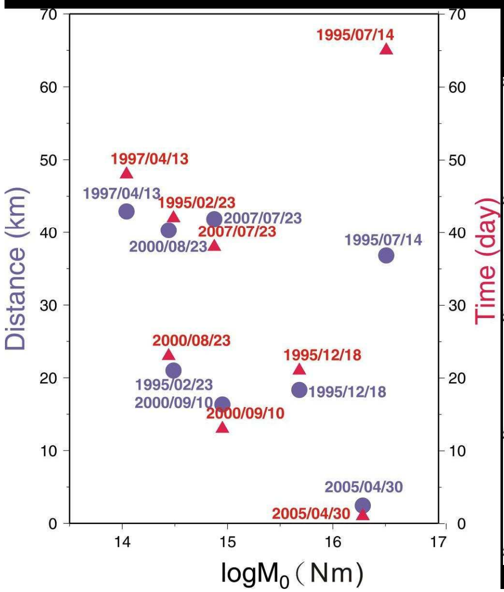

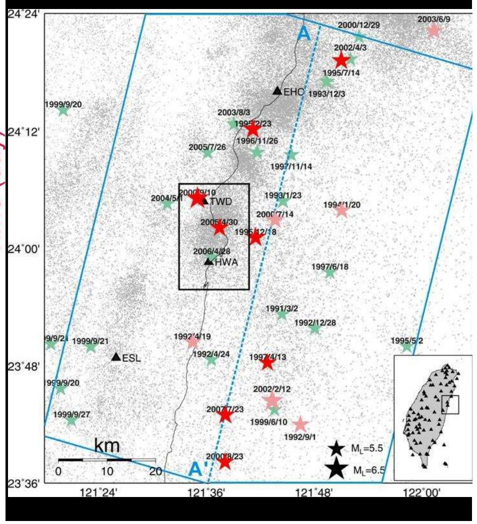

Seismicity in North of Hualien

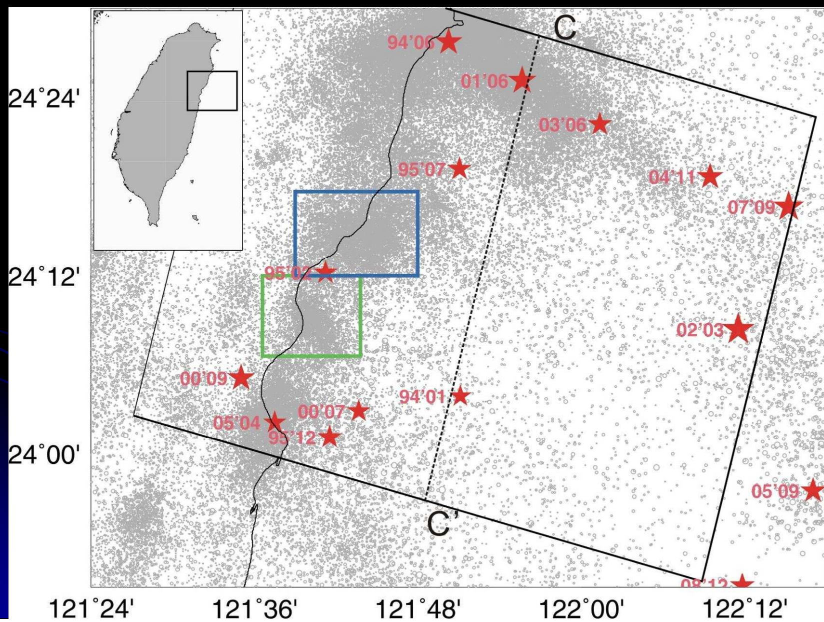

Space-time plot of seismicity in north of Hualien

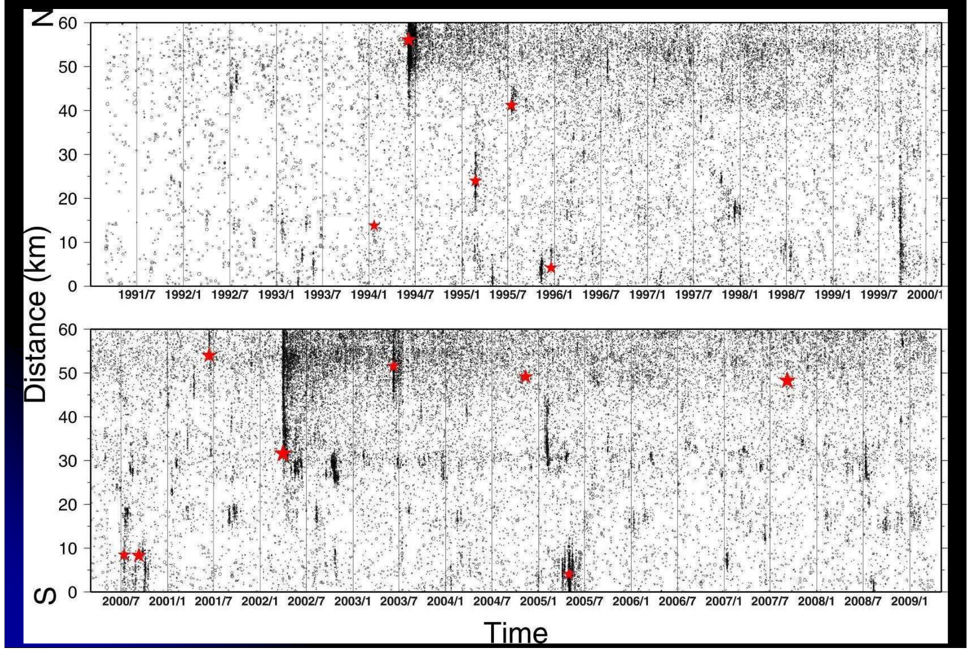

Time series for EQ swarms in N of Hualien

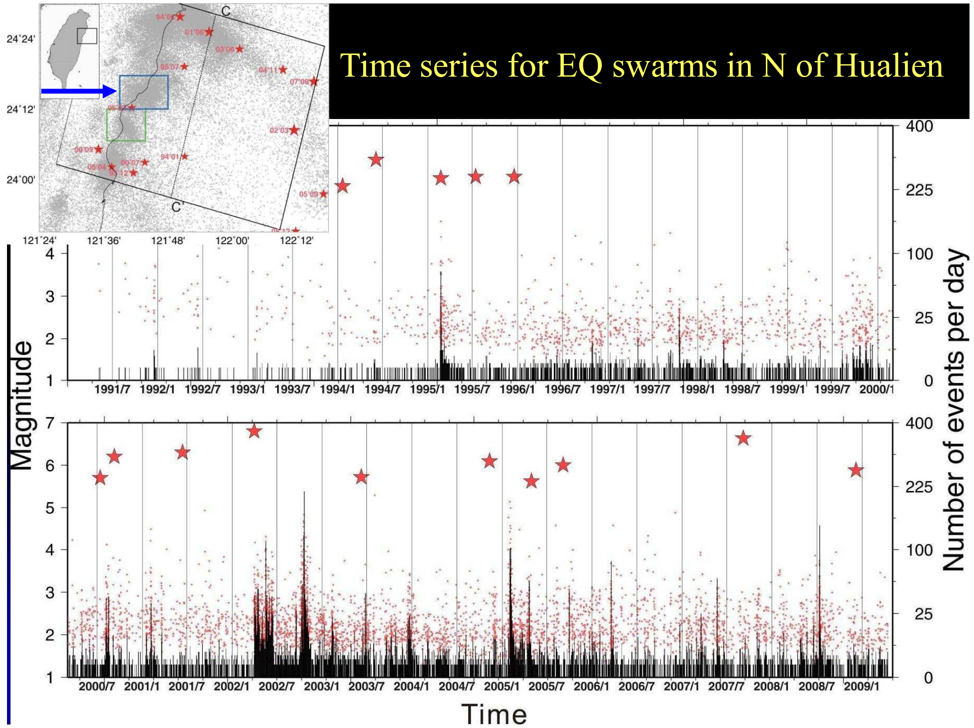

Time series for EQ swarms in N of Hualien

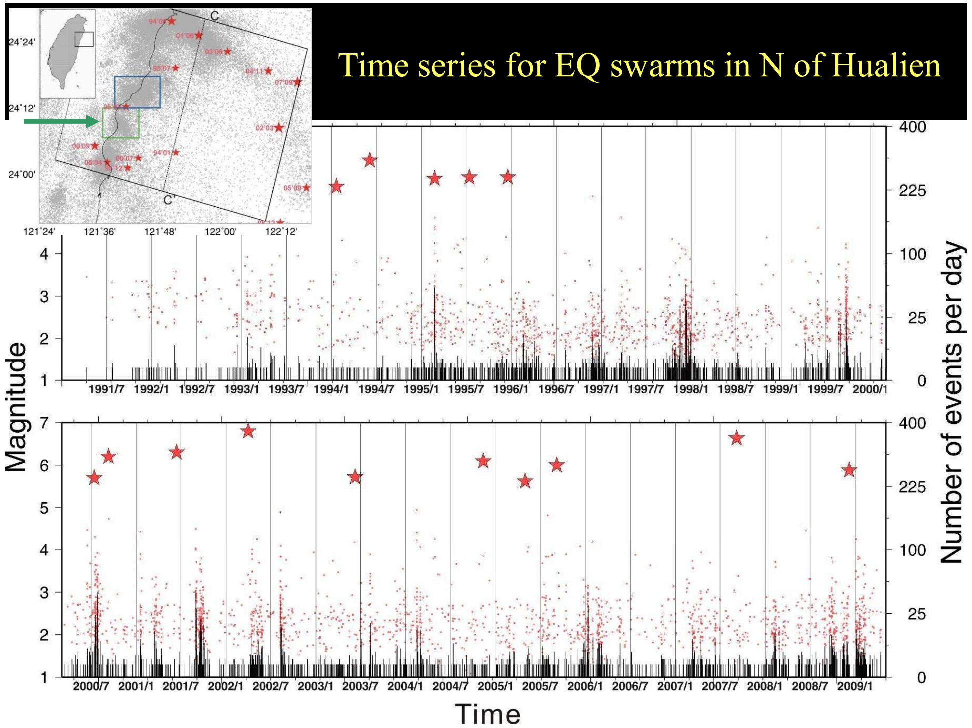

Sequence of seismicity pattern predicted by the asperity model

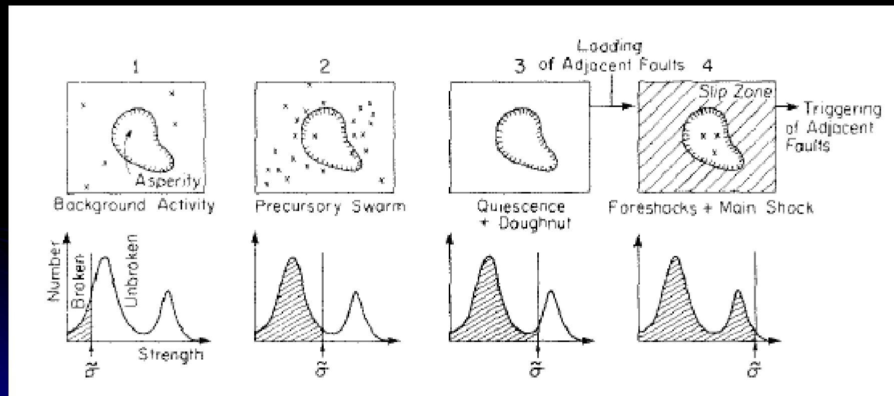

Kanamori, 1981

Temporal variation of stress at a subfault

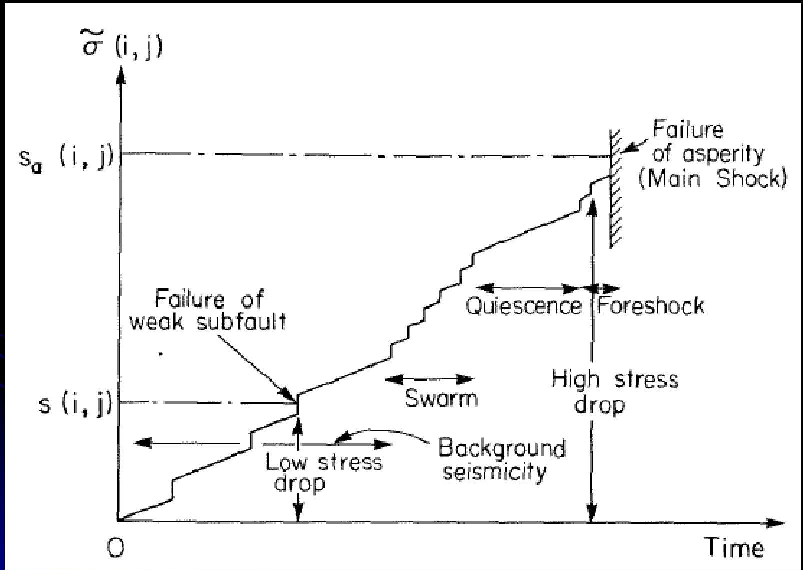

Kanamori, 1981

A multiple asperity model for precursory swarm in eastern Taiwan

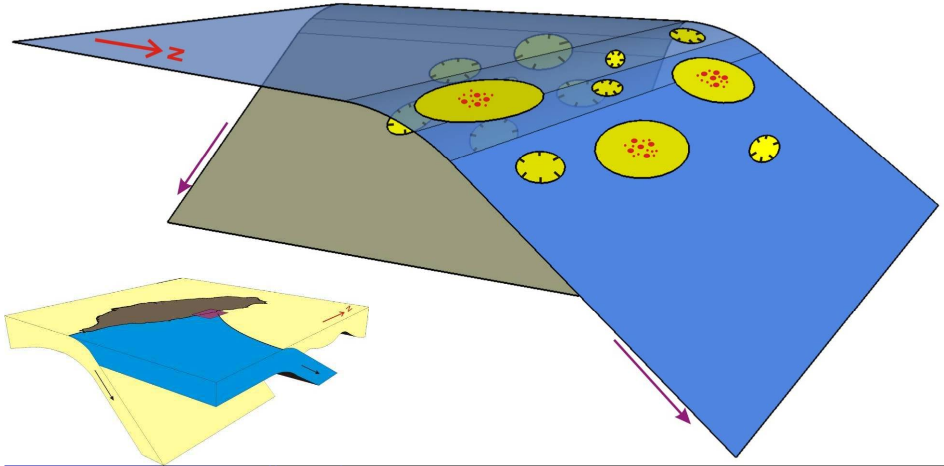

Summary

•Eight clusters of M < 4.3 earthquake swarms (duration of 7-32 days) occurred 1-48 days preceding 5.5 < M < 6.3 earthquakes within a distance of ~40 km at the subduction-collision corner in eastern Taiwan between 1991 and 2009

•The accumulated moments of the preceding, seven out of eight, swarms are inversely related to the time-separation between the precursory swarms and the M > 5.5 earthquakes

•The precursory swarms occurred in a clustered seismic zone corresponding to the Bei-Pu structure mapped at the surface

•A multiple-asperity model may explain the earthquake preparatory processes observed from the precursory swarms-mainshock sequences found at the collision corner of eastern Taiwan

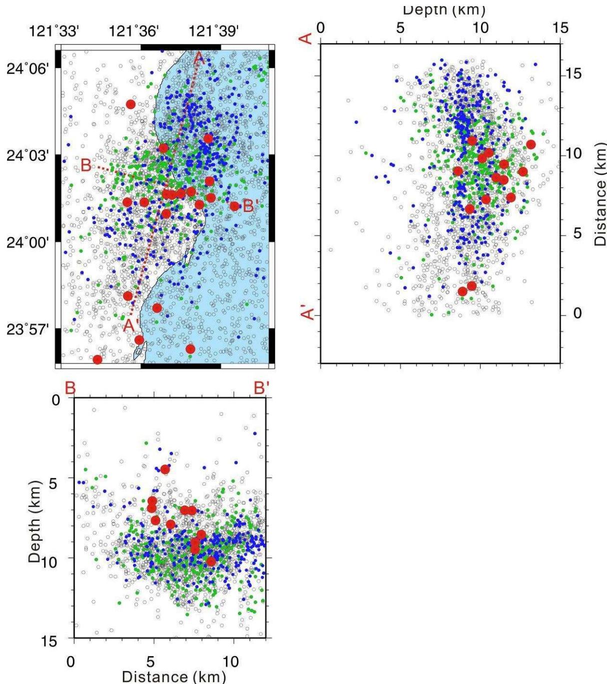

- 2009/9/4~9/9
- Total M_0=1.8E+15
- T = 27.2 days

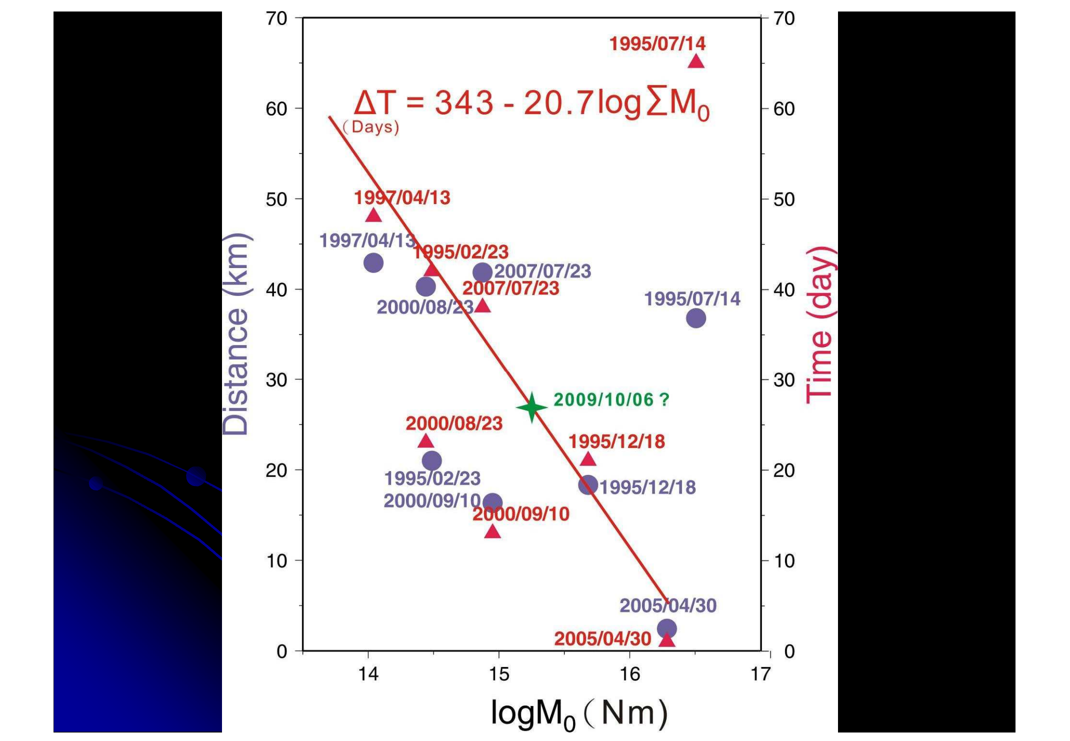

ΔT = 343 - 20.7logΣM0
(Days)
1995/07/14
1997/04/13
1997/04/13
1995/02/23
2007/07/23
2007/07/23
2000/08/23
1995/07/14
2009/10/06 ?
2000/08/23
1995/12/18
1995/02/23
2000/09/10
1995/12/18
2000/09/10
2005/04/30
2005/04/30
Distance (km)
Time (day)
logM0 (Nm)

Dynamic strain variations and co-seismic groundwater level changes associated with the August 2009 Suruga-bay earthquake (M6.5) observed at the Tono area, Central Japan

Yasuhiro Asai and Hiroshi Ishii

Tono Research Institute of Earthquake Science, Association for the Development of Earthquake Prediction

Abstract

A moderate-size earthquake (MJMA 6.5) occurred at the Suruga-bay, central Japan at 05:07 (JST) on August 11, 2009. The dynamic strain variations and co-seismic groundwater level changes associated with this earthquake were observed at Togari crustal activity borehole observation (TGR350) site and Shizubora crustal activity borehole observation site (97FT-01, SN-1 and SN-3) at Tono area, central Japan. The distance between two sites is approximately 3 km. The epicentral distance is 110 km.

We investigated the dynamic strain variations and the co-seismic groundwater level changes observed at each observatory. The following results were obtained: At the TGR350, observed co-seismic groundwater level change was caused by dynamic strain variations with peak-to-peak amplitude of order of 10^{-6} strain, which exceeds the threshold value in TGR350 (Asai, 2008). The co-seismic groundwater level change is approximately a 3.8 m “increase”. The increase is the same as earlier observation results (Asai, 2008). Unfortunately, the co-seismic groundwater level changes after the peak is undergoing enormous hydrological disturbance due to the excavation of Mizunami Underground Research Laboratory. At the SN-3, at first, the approximately 0.4 m sudden decrease in groundwater level was observed, and after the eleven hours, groundwater level decrease stopped and is increasing afterward. At the SN-1, approximately 1 m slow decrease in groundwater level was observed, and after the eight days, groundwater level started to increase. The observed co-seismic groundwater level changes in SN-1 and SN-3 were also caused by dynamic strain variations in 97FT-01 with peak-to-peak amplitude of order of 10^{-6} strain.

References

Asai, Y., 2008, Trigger and Mechanism of Co-seismic Groundwater Level Changes in the Togari350 well, central Japan, in Proceedings of 6th Japan-Taiwan International Workshop on Hydrological and Geochemical Research for Earthqauke Predicion, GSJ Openfile Report, no.484, 1 CD-ROM, Geol. Surv. Japan, AIST.

Dynamic strain variations and co-seismic groundwater level changes associated with the August 2009 Suruga-bay earthquake (M6.5) observed at the Tono area, Central Japan

Yasuhiro Asai and Hiroshi Ishii

Tono Research Institute of Earthquake Science,
Association for the Development of Earthquake Prediction

Eighth Taiwan - Japan International Workshop on Hydrological and Geochemical Research for Earthquake Prediction
29 September, 2009, Tainan, Taiwan

Table of Contents

- **Observations:**
  - a) Dynamic strain variations and co-seismic groundwater level changes associated with the August 2009 Suruga-bay earthquake (M6.5) observed at Tono region.
  - b) In case of other earthquakes: Earthquake (M6-7) which occurred before and after Suruga-Bay earthquake, and the 2008 Sichuan, China Earthquake (Mw7.9) etc.

Goal: To clarify whether the threshold values which cause the co-seismic groundwater level changes in SN-1 and SN-3 exist or not.

- **Summary**

Borehole Array Observation System operated by TRIES

Shizubora site (SZB)

Modified from Azuma et al.,(2007)

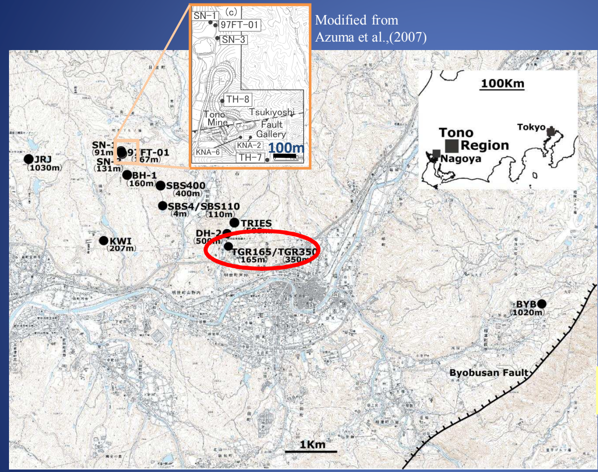

Modified from Asai et al., (2009, in press)

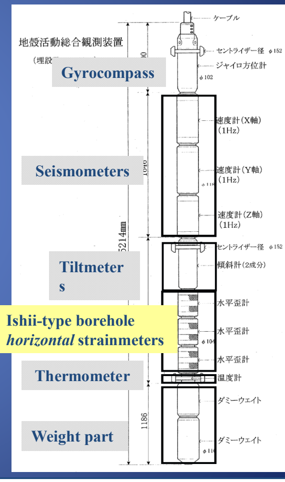

SN-1 and SN-3 are located within a distance of 100m.
TGR350 is located about 3 km southeast of Shizubora site.

The multi-component borehole instrument installed at the bottom of TGR350 and 97FT-01

Co-seismic groundwater level (GWL) changes associated with the Suruga Bay Earthquake (M_{JMA}6.5) observed at TGR350 SN-1, and SN-3

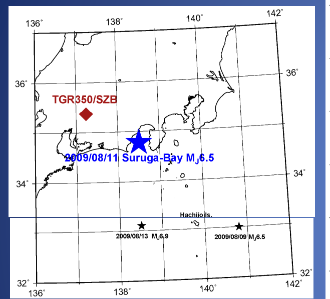

Location map of the epicenters (by JMA) and observation sites.
The epicentral distance is 110km.

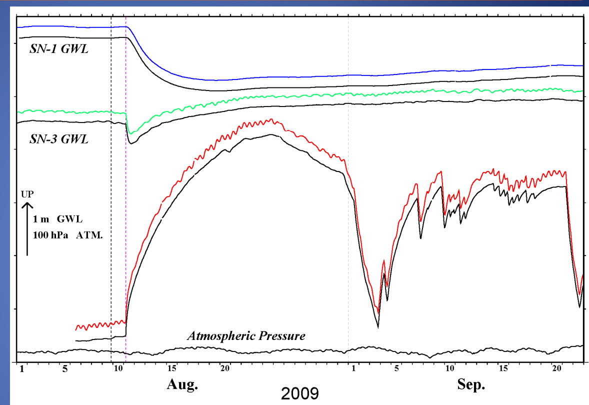

- TGR350: The co-seismic GWL change (increase to 3.8 m) was observed, but this changes is undergoing enormous hydrological disturbance due to the excavation of Mizunami Underground Research Laboratory which is located about 400m north of TGR350.
- SN-3: Sudden decrease to 0.4 m during 11 hours and increase afterward.
- SN-1: Slow decrease to 1 m during 8 days and increase afterward

Hydroseismogram (Upper) and Dynamic strain variations (lower) associated with the August 11, 2009 Suruga-bay earthquake (M_{JMA}6.5; depth=23km) observed at TGR350(left) and Shizubora (97FT-01, SN-1, SN-3; right)

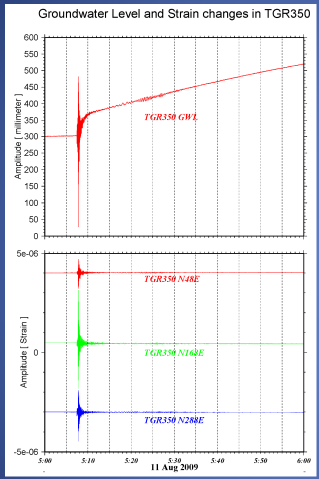

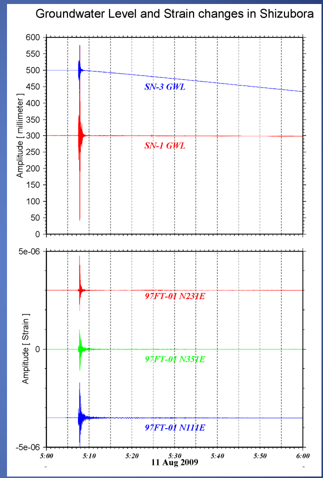

⇒ Assuming plane strain, Areal, Max. Shear, and Principal strains were calculated from the independent three-component strain data-set.

We focus on only the peak-to-peak amplitude of dynamic strain variations.

Dynamic strain variations (lower) and Hydroseismogram (upper) associated with the August 9, 2009 earthquake (M_{JMA}6.9; depth=340km)

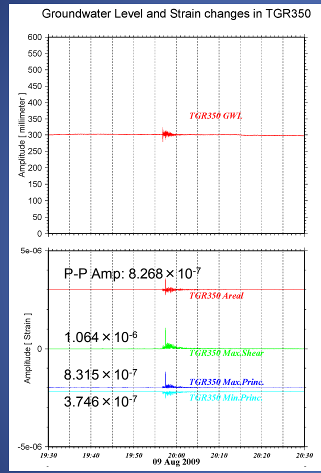

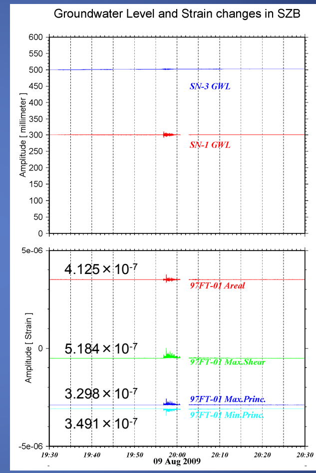

・TGR350: Co-seismic GWL change (increase of 5 cm) was caused by dynamic strain variations (Areal and Max. Shear) with peak -to-peak amplitude of approximately 10^{-6} strain.
・SN-3: Co-seismic GWL change (increase of 5 cm) was cause by dynamic strain variations with peak -to-peak amplitude of approximately 4-5 $\times 10^{-7}$ strain.
・SN-1: Co-seismic GWL change was not cause by dynamic strain variations.

Comparison of Dynamic strain variations (lower) and Hydroseismogram (upper) on August 11, 2009 Suruga-Bay earthquake (M_{JMA}6.5; depth=23km)

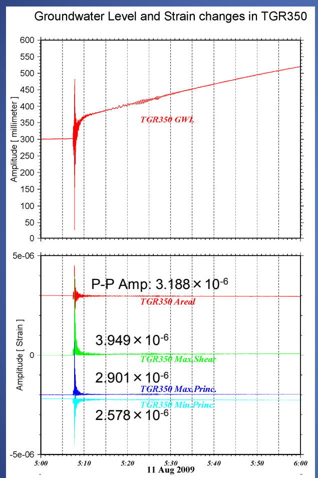

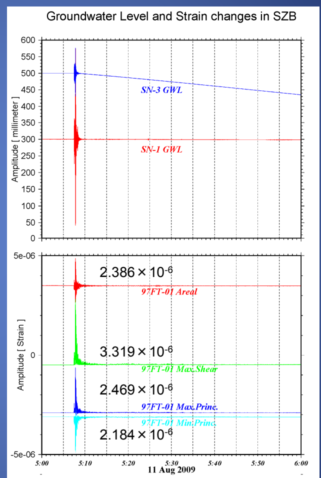

・Co-seismic GWL change was caused by dynamic strain variations (Areal and Max. Shear) with peak -to-peak amplitude of order of 10^{-6} strain.
・ For the TGR350, these amplitudes exceeds the threshold value (3×10^{-7} strain; Asai et al., 2008).

Dynamic strain variations (lower) and Hydroseismogram (upper) associated with the August 13, 2009 earthquake (M_{JMA}6.5; depth=440km)

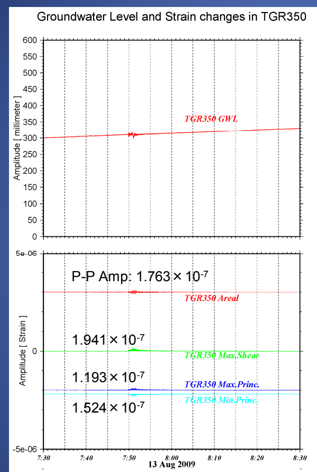

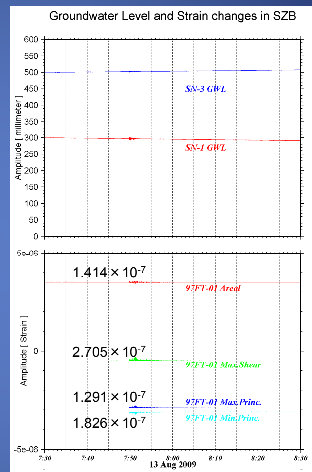

・TGR350: Although dynamic strain variations with peak -to-peak amplitude of approximately 2×10^{7}strain, which exceeds the threshold value , no co-seismic GWL change was observed.
・SN-3 and SN-1: No co-seismic GWL change were observed.

For the TGR350, The case of during the co-seismic changes after the peak, we know dynamic strain variations above threshold do not affect (Asai ,2008).

Co-seismic GWL changes associated with the May 8, 2008 off Ibaraki Earthquake (Mw6.8 ;USGS) and May, 12, 2008 Sichuan, China Earthquake (Mw7.9) observed at TGR350 SN-1, and SN-3

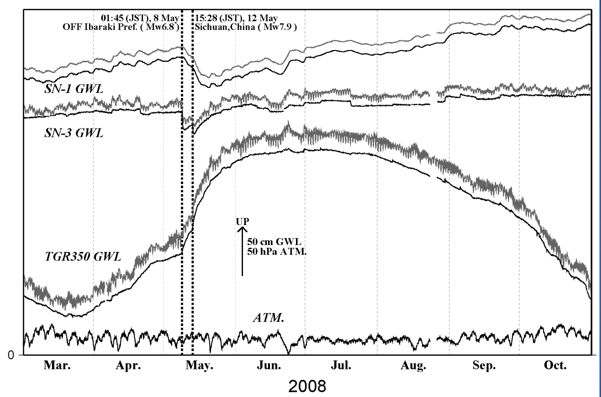

(Asai et al, 2009)

- TGR350: The co-seismic GWL change (increase of 0.25m for off Ibaraki Eq. and 0.84 m for Sichuan Eq.) was observed.
- SN-3: Sudden decrease of 0.18 m during 24 hours for off Ibaraki Eq. and 0.08m during 16 hours for Sichuan Eq., respectively, and slow increases afterward.
- SN-1: Slow decrease of 0.11 m during 4 days (to the Sichuan Eq.) for off Ibaraki Eq. and 0.20m during 165 hours for Sichuan Eq., respectively, and slow increase afterward .

Dynamic strain variations (lower) and Hydroseismogram (upper) associated with the May 8, 2008 off Ibaraki earthquake (Mw6.8).

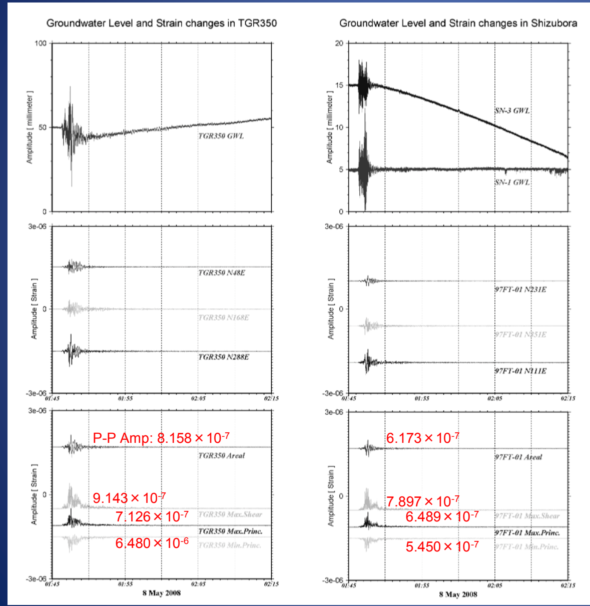

Co-seismic GWL change was caused by dynamic strain variations with peak -to-peak amplitude of $8\text{-}9 \times 10^{-7}$ strain for TGR350 and $6\text{-}9 \times 10^{-7}$ strain for SN-1/SN-3.

Modified from Asai et al., (2009)

Dynamic strain variations (lower) and Hydroseismogram (upper) associated with the Sichuan, China Earthquake (Mw7.9)

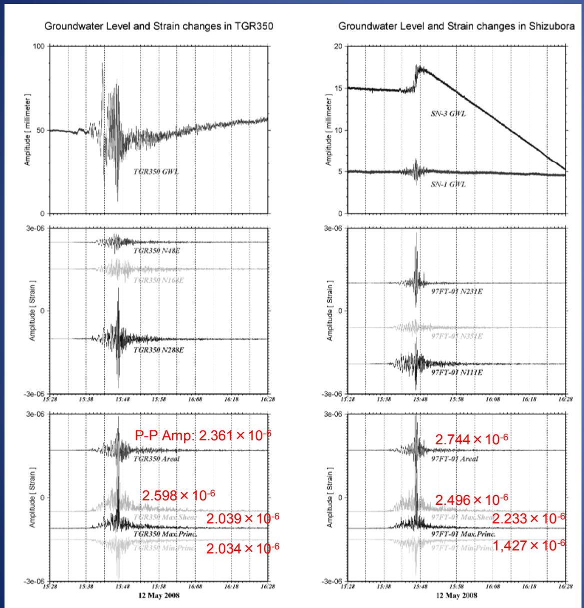

Co-seismic GWL change was caused by the dynamic strain variations with peak -to-peak amplitude of $2\text{-}3 \times 10^{-6}$ strain.

Modified from Asai et al., (2009)

At the SN-1 and SN-3, co-seismic GWL changes were caused by p-to-p Amp. above 6×10^{-7} strain for Areal strain and 9×10^{-7} strain for Max.Shear strain

Does threshold value exist for SN-1 and SN-3 ?

In the case of the Sep. 11, 2008 off Tokachi earthquake (M_{JMA}7.1).

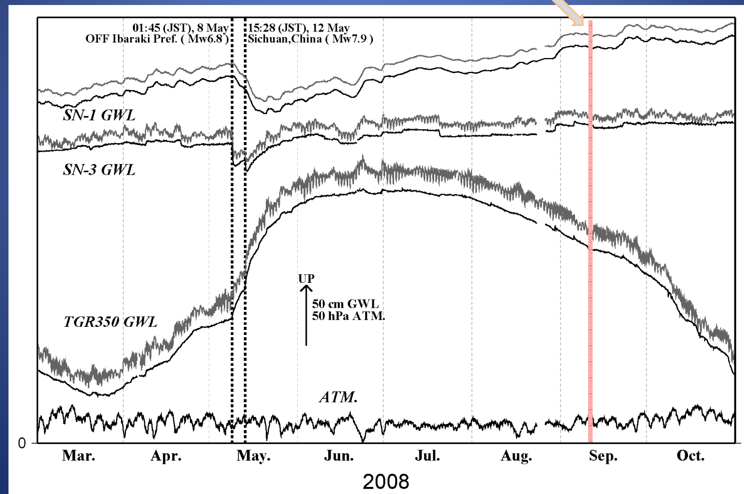

Dynamic strain variations (lower) associated with Sep. 11, 2008 off Tokachi earthquake (M_{JMA}7.1).

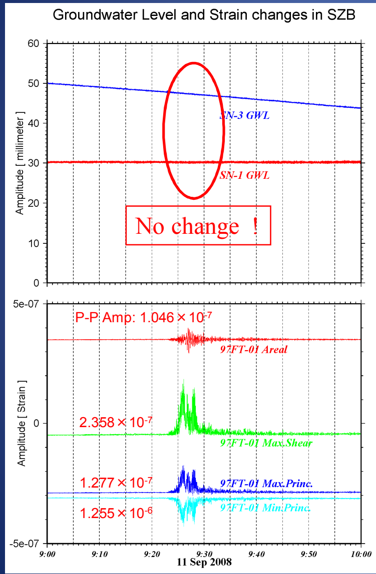

SN-1 and SN-3:
No co-seismic GWL change were cause by dynamic strain variations with peak-to-peak amplitude of approximately 1-2 $\times 10^{-7}$ strain.

In case of the May 8, 2008 off Ibaraki earthquake (Mw6.8), co-seismic GWL change were caused by dynamic strain variations with peak -to-peak amplitude of 6-9$\times 10^{-7}$ strain for SN-1 and SN-3.

Does threshold value exist between 1-2 $\times 10^{-7}$ strain and 6-9$\times 10^{-7}$ strain ?

However, we haven't investigated of all data.
The detailed investigation of the threshold value is await s future studies.

Summary

1. Co-seismic groundwater level changes and dynamic strain variations associated with the August 8 Suruga-bay earthquake (M_{JMA}6.5) were observed at TGR350 site and Shizubora site (97FT-01, SN-1 and SN-3) at Tono area, central Japan.

2. We investigated the dynamic strain variations and the co-seismic groundwater level changes observed at each observatory. The following results were obtained:

   a) At the TGR350, observed co-seismic groundwater level change was caused by dynamic strain variations with peak-to-peak amplitude of order of 10^{-6} strain, which exceeds the threshold value in TGR350 (Asai, 2008).

   b) The observed co-seismic groundwater level changes in SN-1 and SN-3 were also caused by dynamic strain variations in 97FT-01 with peak-to-peak amplitude of order of 10^{-6} strain.

   c) Preliminary investigation shows that the threshold value exist between approximately 2 $\times 10^{-7}$ and 6$\times 10^{-7}$ strain .

Geological, seismological, tsunami and folklore studies related to giant earthquakes along the Ryukyu trench

Masataka Ando, Cheng-Horng Lin and Yoko Tu
Institute of Earth Sciences, Academia Sinica, Taiwan

Abstract

The size of subduction earthquakes has been considered to be mainly dependent on convergence rate and age of the subducting lithosphere. Giant earthquakes with a magnitude over 9.0 can occur at a high convergence rate and young oceanic lithosphere. Regarding the subduction zone along Ryukyu Islands, it is widely believed that a giant earthquake is implausible to occur in this region because it does not have the above characteristics. In addition, the rifting along the Okinawa trough located behind the Ryukyu trench, implies that this subduction boundary can be aseismic without any significant earthquakes.

However, a possible simultaneous uplift of the coastal terraces along the subduction zone of the Ryukyu trench could be associated with giant or large earthquakes. Based on the age of uplifted terraces, the simultaneous uplift could have occurred 3000 BP over the entire subduction zone of a length 1,500km and maybe associated with an extraordinary earthquake of Mw>9.0 (Furumoto and Ando, 2009). Study of tsunami sediment can yield evidence if a giant earthquake had affected this region.

On the other hand, a large tsunami has never been considered to strike the east cost of Taiwan due to its surrounding tectonics and bathymetries, despite its proximity to Ryukyu trench. Moreover, it is worthy to note that there is a place called “Marauro” located at the center of the present Chengong city on Taiwan’s east coast. In one of Ami tribe’s folklores indicated “big sea waves struck the area, plants and trees all perished, and the place was named Marauro”, which means withered place. To check if such folklore has a basis, collection of soil samples and numerical simulation for tsunamis would be required to estimate both the location and fault mechanism of the tsunami source in conjunction with giant earthquakes along the Ryukyu trench.

In the western Ryukyu subduction, very low frequency earthquakes (M2.5-M4.5) have been found near the trench axis with thrust mechanisms (Tu et al., 2009). In addition, slow slips have been also found at depths around 40-50 km (Heki and Kataoka, 2008; Nakamura, 2009). These features are quite similar to the Nankai trough where large thrust earthquakes have occurred in history.

With the possibility of giant earthquakes in Ryukyu region as indicated by scientific evidence coupled with legends, this study highlights the importance of integrated studies of emergent marine terraces, seismological information, tsunami numerical simulation, and together with folklores that could most probably been based on real episode.

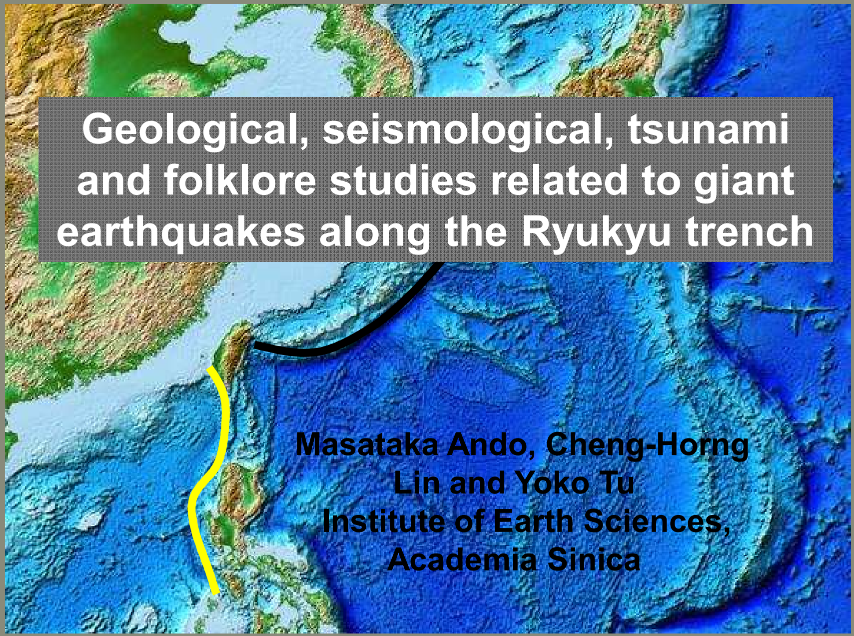

A question on the Ryukyu subduction:

Are the two plates coupled?

↓

Potential site for future large earthquakes.?

Mode of subduction

Is the Ryukyu subduction of the Mariana type？

Marian type **Chilean type**

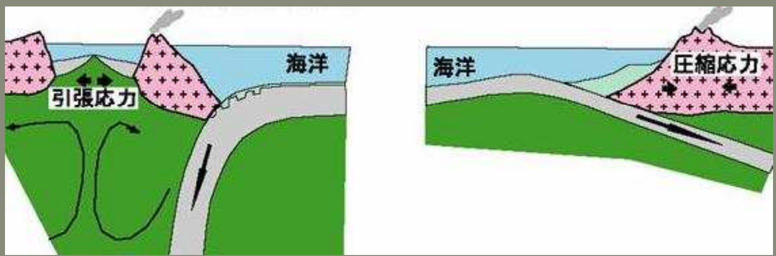

Uyeda and Kanamori (1979)

Contents

1. Low frequency earthquakes
2. Slow slips
3. Seafloor geodetic survey
4. Emerged coastal terraces
5. Folklores and tsunami sediments

2. Low frequency earthquakes

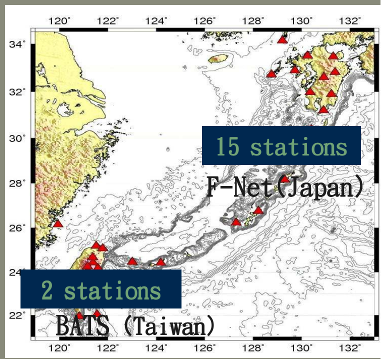

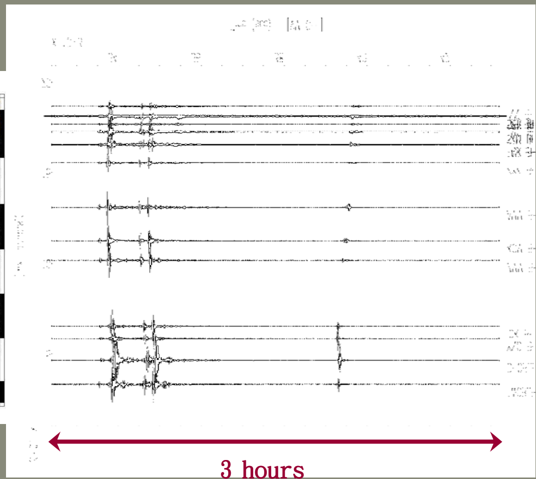

Tu et al. (2009)

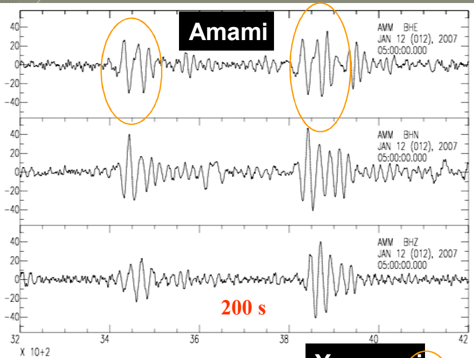

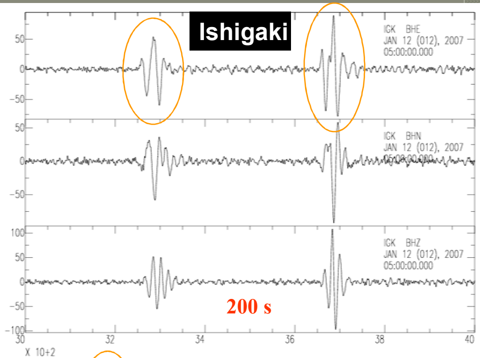

Band-pass filter 20-50s

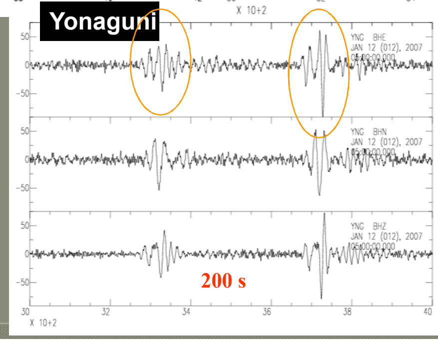

Tu et al. (2009)

Very low frequency earthquakes

High-pass filter at 1

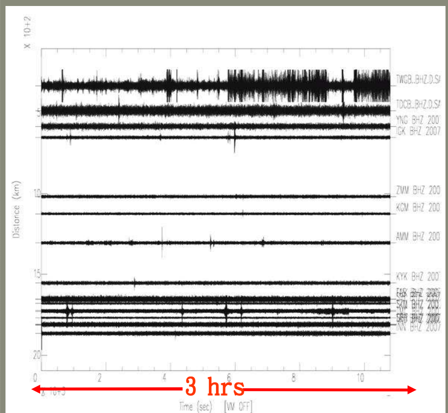

Band-pass filter between 20-50

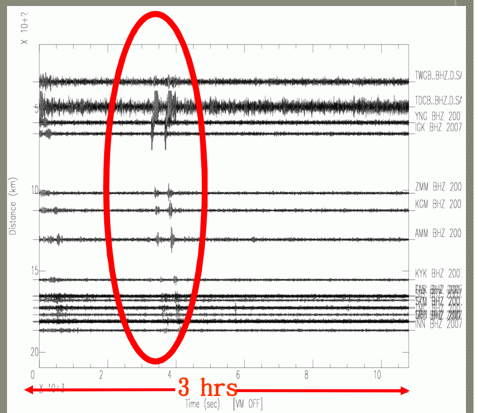

2007/01/12 05:00~08:00 (UT)

Tu et al. (2009)

Hypocenter and focal mechanism

Inversion Technique

(Nakano and Kumagai, 2008)

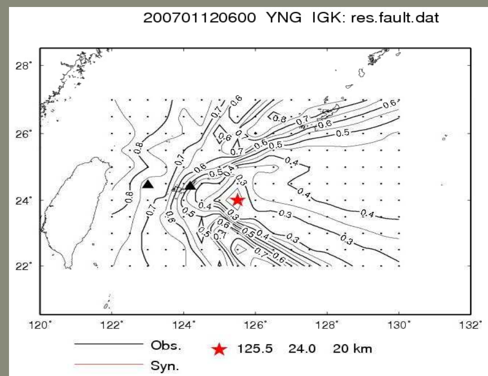

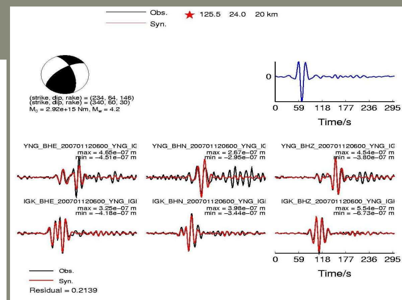

Tu et al. (2009)

Very low frequency earthquakes along the Ryukyu trench

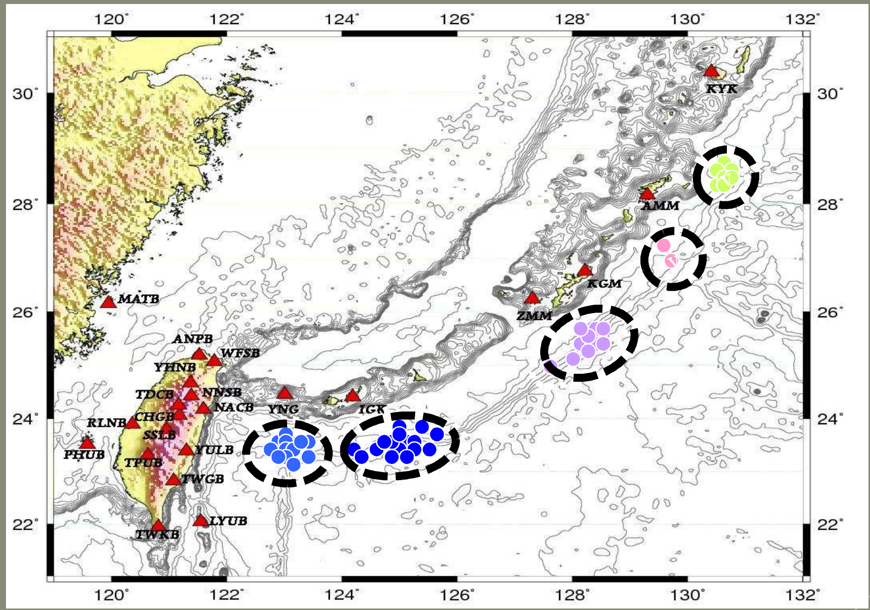

Tu et al. (2009)

Variation of baselines(1996-2007)

Semiannual intervals

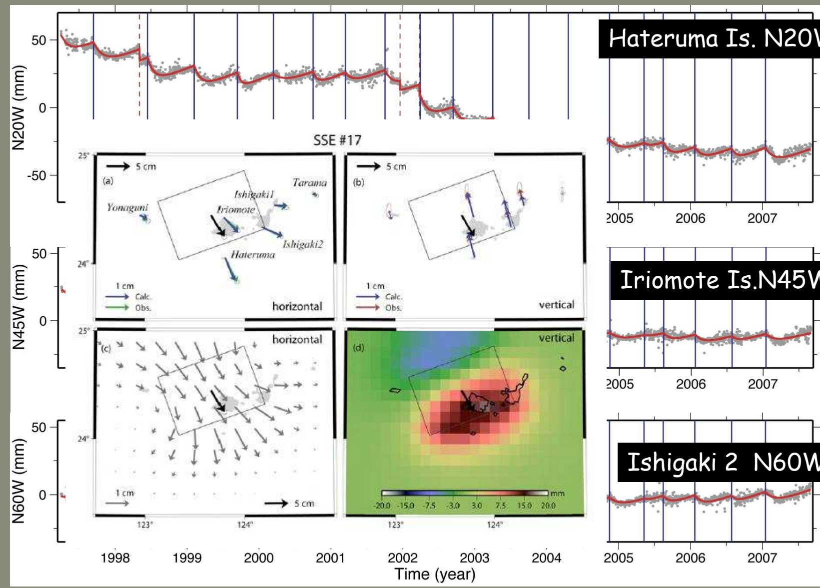

Heki and Kataoka, JGR (2008)

3. Slow slips in western Ryukyu

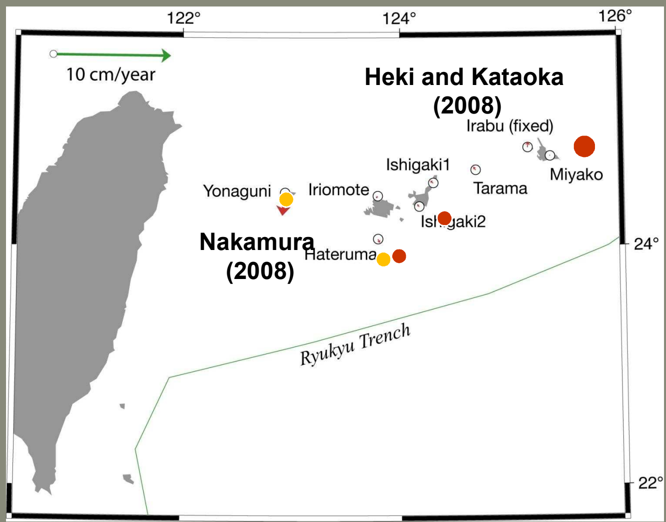

Yonaguni slow slip event

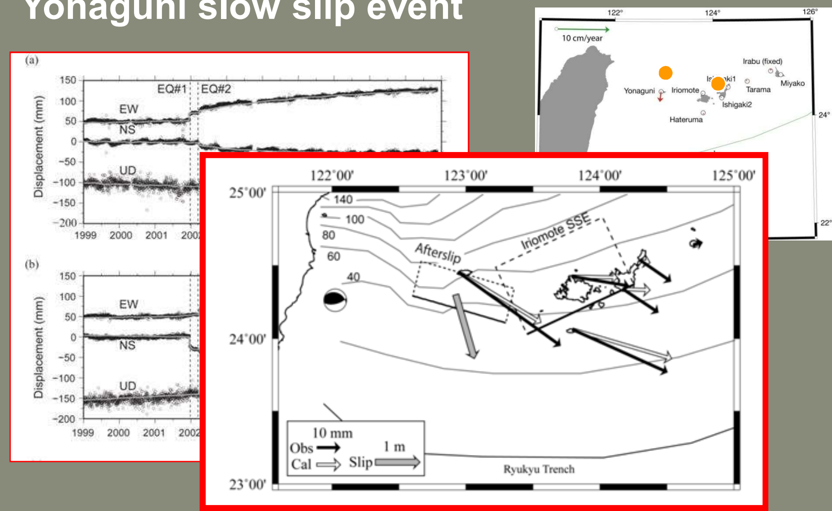

Nakamura, GRL (2009)

Summary of slow slips and very low frequency earthquakes

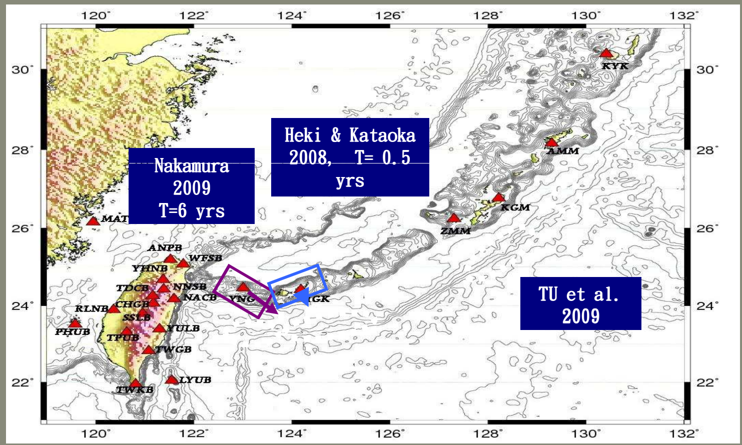

Tu et al. (2009)

3. Seafloor geodetic survey

Unlocked (aseismic, decoupled)?

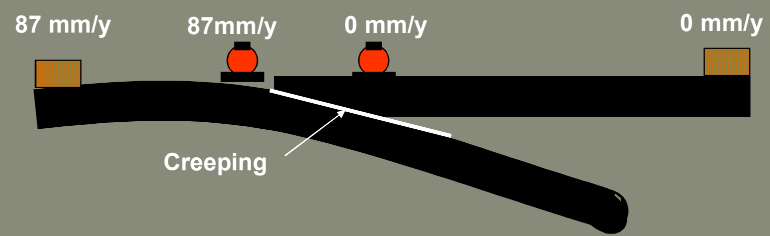

Locked (seismic, coupled)?

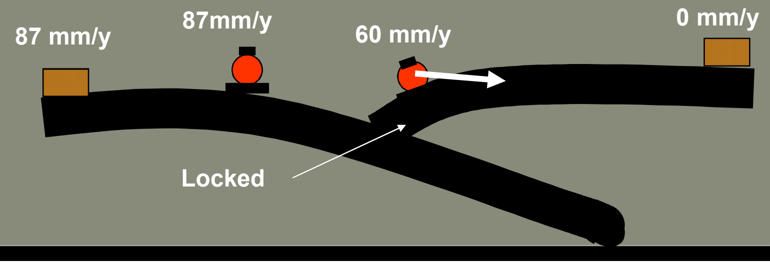

Slow earthquake or slow events

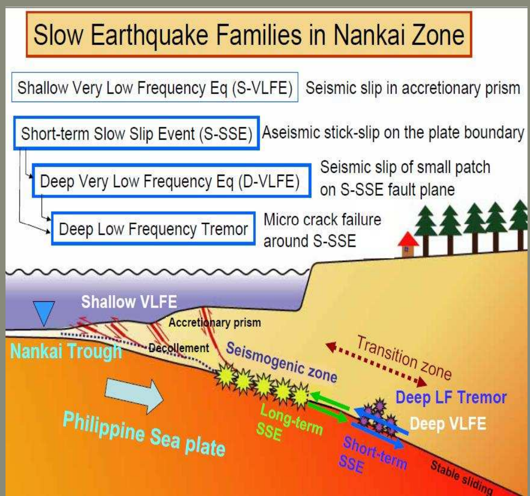

Ultra-low frequency earthquakes near the convergence boundary

Obara (2005)

Location of seafloor geodetic off Ryukyu

Benchmark: 35km from the trench axis

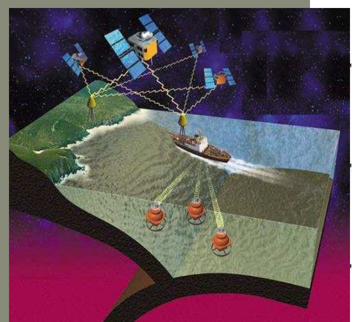

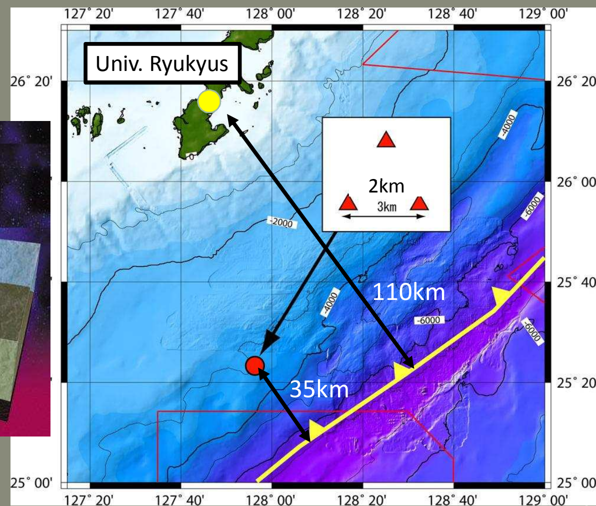

Seafloor horizontal displacements between Jan 2008 and July 2009

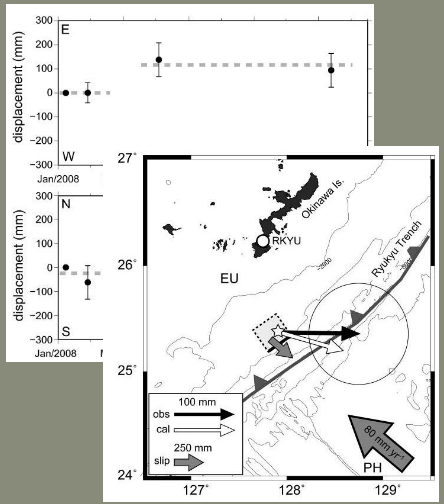

We need more seafloor geodetic sites!

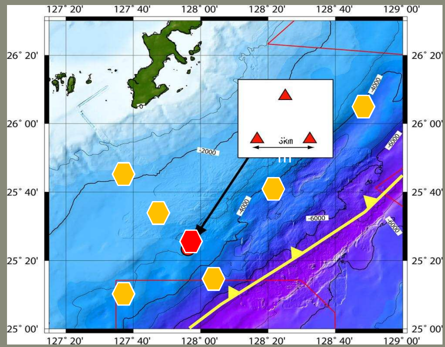

Nakamura et al. (2009)

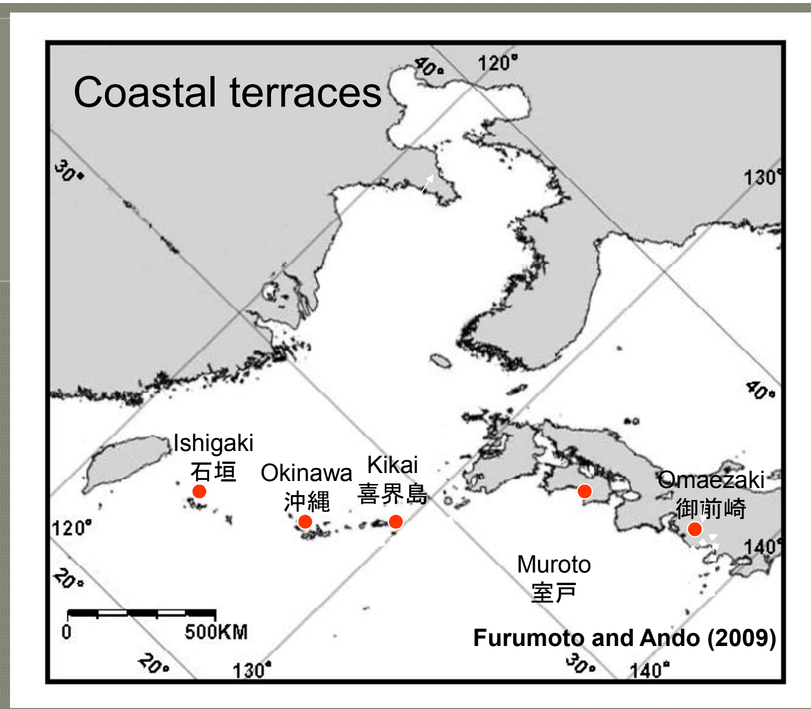

4. Emerged coastal terraces

Emerged notches and uplift terraces
- Evidence for giant or large earthquakes?

- Omaezaki
- Muroto
- Kikai Island
- Okinawa Island
- Ishigaki Island

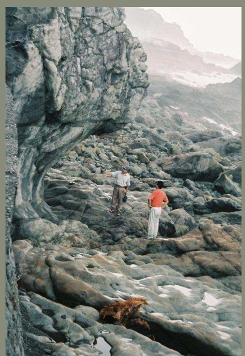

At Chinen, Yonabara

http://www001.upp.so-net.ne.jp/fl-fg/08_sea/08-06_notch.htm

Estimated ranges of times of uplift events

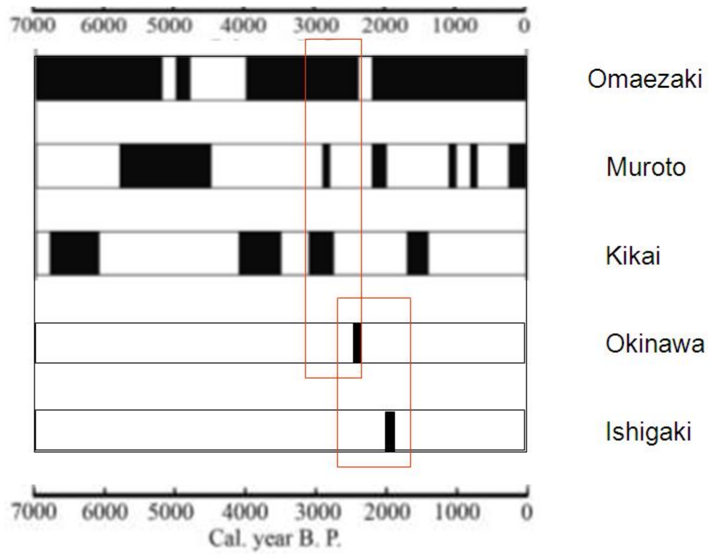

Furumoto and Ando (2009)

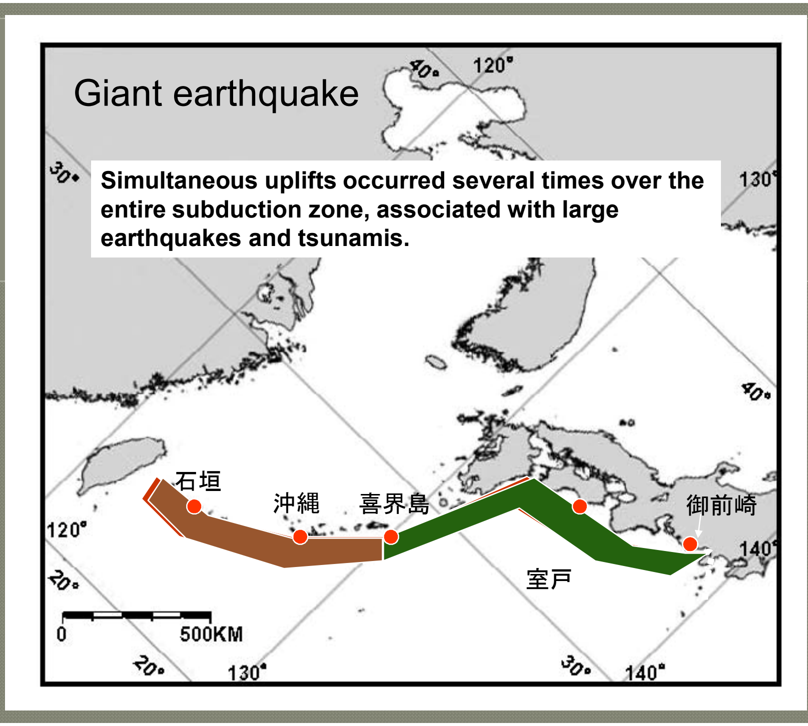

Did tsunamis struck the east coast of Taiwan in the past?

Another example is found in Chenggong County (成功鎮)

麻荖漏(Marauro)= Wither in Ami tribe's language

A legend of Ami tribe says that "rice plants and trees were all died by the struck of big waves in 1850's". If it was really a tsunami, its height would have been >20-30m.

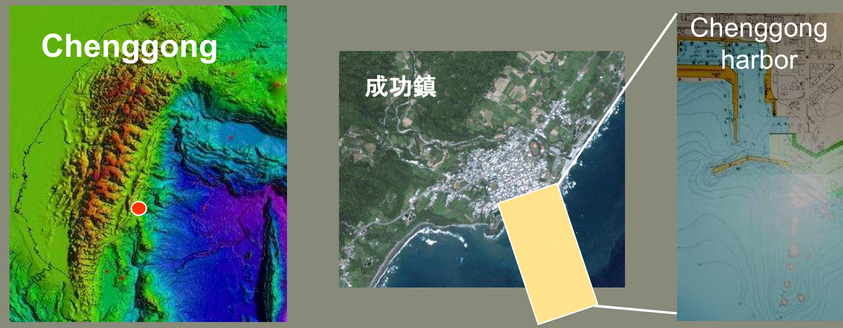

5. Folklore and tsunami sediments

Propagation of tsunami from a source in the westernmost part of the Ryukyu trench

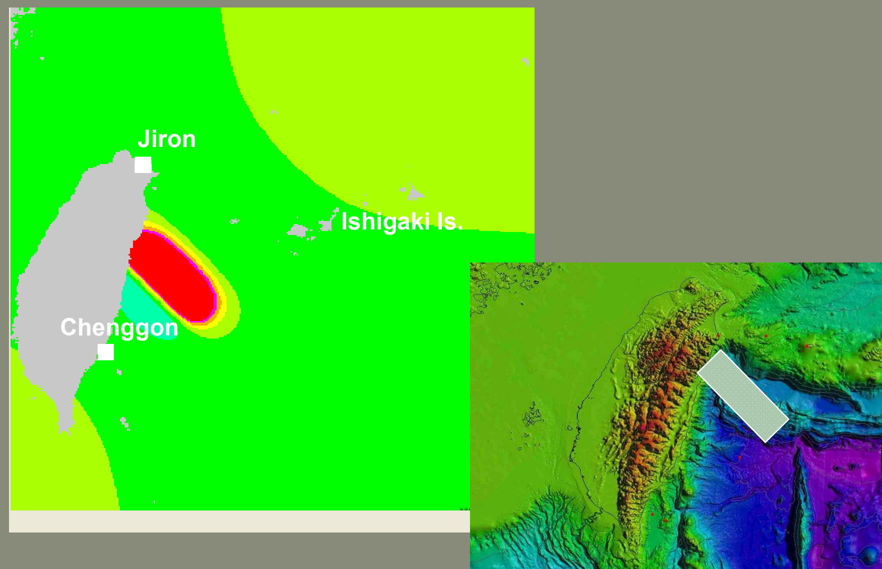

Auguring for finding tsunami sediments at Chenggong Sep. 26, 2009

Subduction zone east of Coastal Range

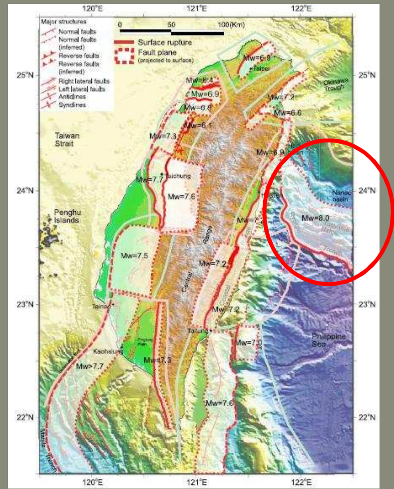

Bruce et al. (2005) JGR, 110

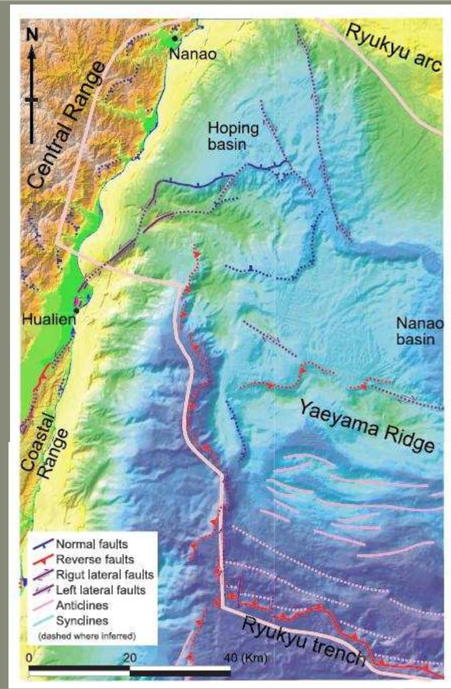

Summary

- In the western Ryukyu subduction, **very low frequency earthquakes** (M2.5-M4.5) were found near the trench axis with thrust mechanisms.
- **Slow slips** were found at depths around 40-50 km.
- A possible **simultaneous uplift** of the coastal could have been associated with giant or large earthquakes.
- Further extensive **geodetic surveys** are necessary over the entire Ryukyu trench.
- Study of **tsunami sediments** can yield evidence if a giant earthquake had affected this region.
- The importance of **integrated studies** of emergent marine terraces, seismological information, geodetic survey, tsunami numerical simulation, and together with **folklores** were shown in this study.

Yonaguni slow slip event

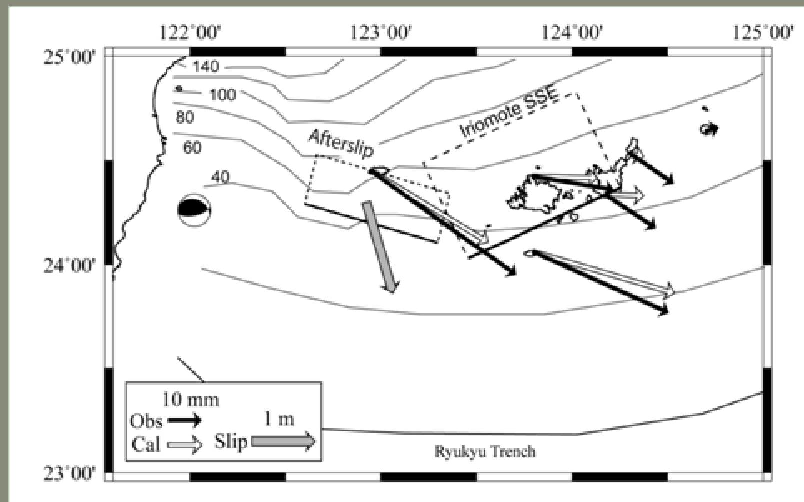

Nakamura, GRL (2009)

Ryukyu trench

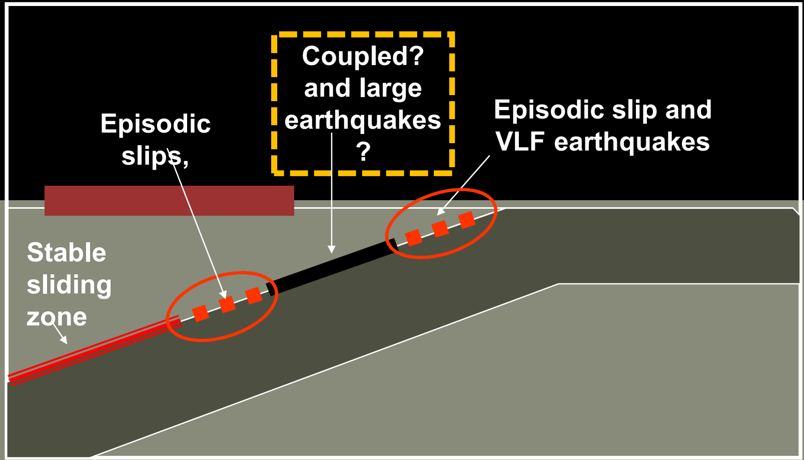

Map of slow slips and non-volcanic tremors along the subduction boundaries

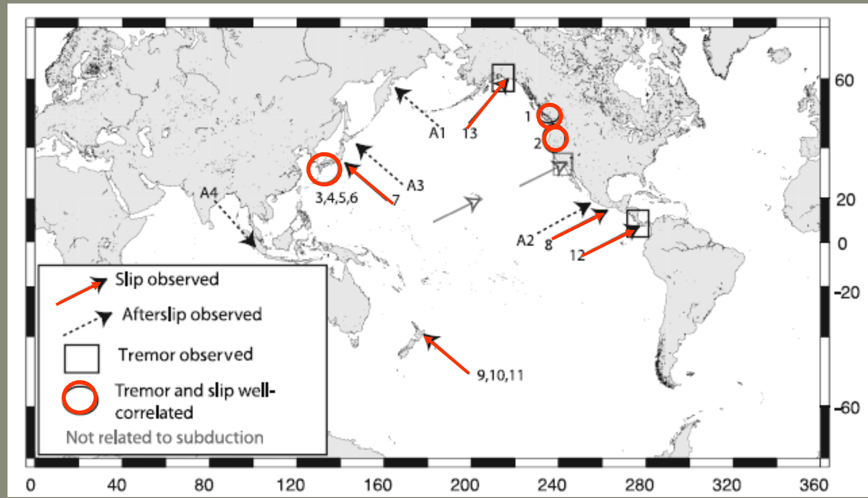

Schwartz and Rokosky (2007)

An example of the slow slip events

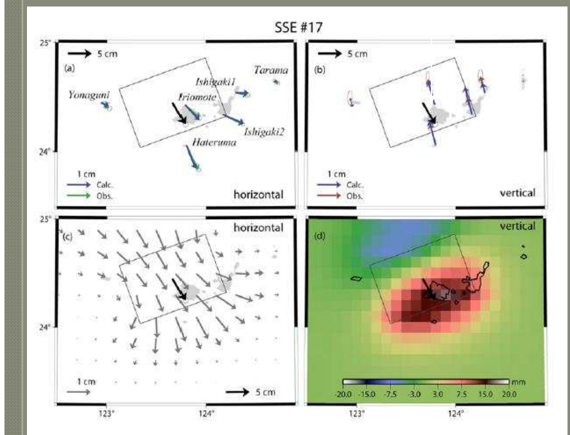

Mw=6.6

- Slow-slip events in SW Ryukyu
- Depth: 30km, Mw6.6
- Recurrence interval: 0.5 y

Heki & Kataoka, JGR (2008)

Modeling and Scaling of Earthquakes in Taiwan region

Kuo-Fong Ma and Ying-Tung Yen
Institute of Geophysics, National Central University, Taiwan

Abstract

We investigated the finite-fault source model inferred from waveform inversion to explore the scaling relations between moment and source parameters, which include fault length, fault width, mean slip. The spatial slip distributions of 19 events derived from the dense strong motion stations in Taiwan and the Global Seismographic Network were determined to give the finite-fault solution for the moment ranged from 7.8×10^{15} to 3.8×10^{20} N-m. In addition to the 1999 Chi-Chi Mw7.6 earthquake, there are 10 blind thrust events, one normal event and seven strike-slip events. Among them, there are three subduction zone events. The M8.0 2008 Wenchuan earthquake, M9.1 2004 Sumatra earthquake and M7.6 2001 Bhuj earthquake were also included as the reference events in the scaling to provide broader scales for large earthquakes. The asperities in a finite-fault were lack of quantitative definition, and the dimensions of the finite-fault geometry were often overestimated due to the slip heterogeneity. The subjective definition of asperity for earthquakes leads to a less accurate scaling relationship for the source models. A mathematic method in which the autocorrelation function defined from quantifying spatial slips was utilized to evaluate the effective fault dimensions to systemically redefine the characteristics of the source parameters, including effective fault length (Le), width (We) and average slip (De). Our analysis shows two scaling relationships for $M0 \propto Le{\sim}2$ and $M0 \propto We{\sim}2.5$. Effective length to width scaling behavior has a slope of $Le \propto We$. This relationship might reflect the character for collision zone earthquakes, which events commonly from blind thrusts with deeper focal depths. Thus, this source scaling might provide additional information for further studies on the simulation of ground motion for earthquakes from the tectonic collision zone. This scaling relationship is useful for further determination for understanding of the stress pattern and investigation on the earthquake related physical process.

In addition to the earthquake mechanism and the corresponding distribution on slips, an in-situ fault zone borehole seismometers had been installed at the depth arnge from 950m to 1300m across the recent ruptured Chelungpu fault. We observed the events showing the distinct P-wave without S-wave. These distinct P-wave only events had been observed continuously through time. The events in the same group are almost identical in P-waves, but with slightly difference in pulse width. It suggests

the events in the same group have similar mechanisms, but with different source dimension and stress drop. The characteristics of the events from waveform observations suggest these events are repeatable from different locations. The modeling of the observed waveforms suggested these events are from an irotropic source in the depth range of about 1300m to 1500m, and within 150-500m horizontal to the TCDP BHS site. The modeling for the isotropic source gives the synthetics with distinct P-wave without S-wave with satisfactory explanation to the observed waveforms. It suggests that these events might be resulted from a hydraulic fracturing within the fault zone. The behavior of this fluid associated mechanism might play a role to present the status of the stress transition after a large earthquake. And, the observation of these fluid associated events provides the hint to the involvement of fluid in earthquake nucleation.

Modeling and Scaling of Earthquakes in Taiwan Region

Kuo-Fong Ma & Yin-Tung Yen

Institute of Geophysics,
National Central University, Taiwan

Kinematic Modeling

Finite fault Approximation

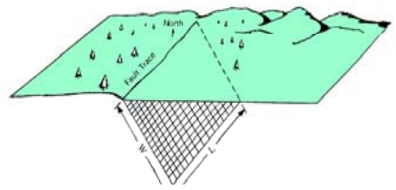

$$u(t,\vec{x}) = \sum_{j=1}^{n}\sum_{k=1}^{m} D_{jk}[\cos(\lambda_{jk})Y_{jk}^{1}(t,t',\vec{x}) + \sin(\lambda_{jk})Y_{jk}^{2}(t,t',x)] * \dot{S}_{jk}(t)$$

D_{jk}	Slip amplitude
λ_{jk}	Rake angle
$\dot{S}_{jk}(t)$	Derivative of rise time function
t'	Rupture initiation time
$Y_{jk}^{i}(t,t',\vec{x})$	Subfault Green's functions

(Ma et al., 2002, Ji et al., 2004, Lee et al., 2006)

Inversion procedure

- *For each subfault, we invert for the slip amplitude, rake angle, rupture time, and shape of a simplified rise time.*
- *A wavelet transform method is applied to build up the objective function in order to extract more information from seismic data.*
- *A threshold least square root criteria is used for static measurements*
- *A Simulated Annealing method is applied to search for the global optimal solution.*

1999 Chi-Chi (Mw7.6) Earthquake

TSMIP (since 1993)

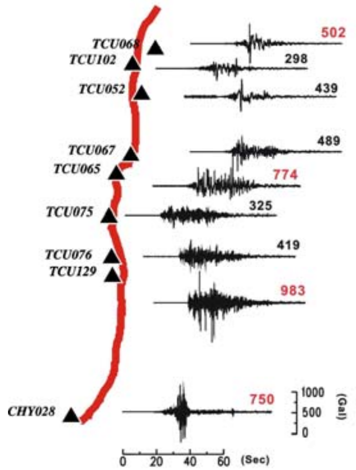

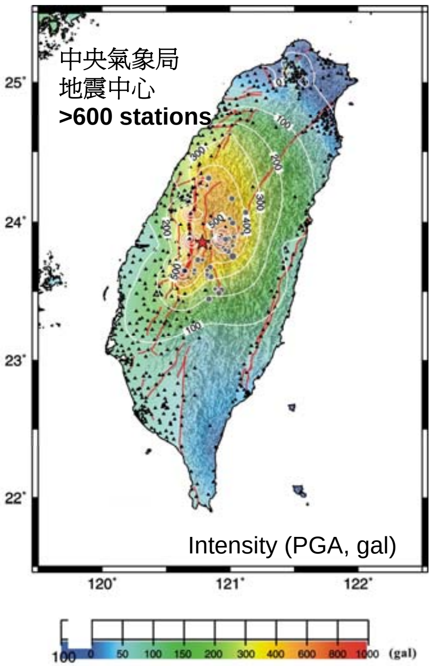

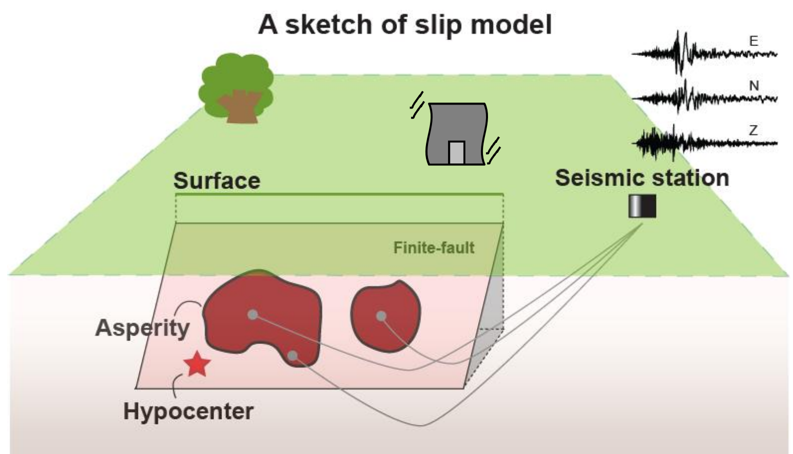

Scaling relationship of source parameters

(fault length, fault width and mean slip)

- underlying mechanics of the rupture process
- nature of tectonic setting
- implication in the seisimic-hazard analysis
- prediction of strong-ground motion

How to evaluate

- surface rupture
- aftershock distribution
- waveform inversion or geodetic modeling

For **large** strike-slip earthquakes, seismogenic layer is the constant maximum.

W-model

$$\Delta\sigma = C\mu\frac{\bar{u}}{W}$$

$$M_0 = \frac{\Delta\sigma}{C}LW^2$$

if stress drop is constant,
slip is proportional to the width
Moment is proportional to the length
(Romanowicz, 1992)

L-model

$$\Delta\sigma = C\mu\frac{\bar{u}}{L}$$

$$M_0 = \frac{\Delta\sigma}{C}L^2W$$

if stress drop is constant,
moment is proportional to the square of length

(Scholz, 1982; Pegler&Das, 1996; Wang&Ou, 1998; Stock&Smith, 2000 Shimazaki, 1986)

For **small** earthquakes

$$M_0 = \mu LWD \qquad L/W = \text{const.}, \quad \bar{D}/\tilde{L} = \text{const.} \qquad M_0 \propto L^3,\ M_0 \propto W^3,\ M_0 \propto D^3$$

(Mai&Beroza, 2000; Stock&Smith, 2000; Shimazaki, 1986)

The data in Taiwan region since 1993

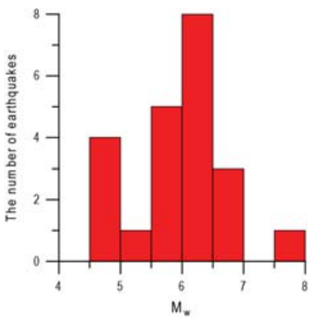

Total event number : 19

Fault type		num.	eq.
Strike		8	7
Dip	Reverse (13)	14	12
	Normal (1)		

Seismic moment range from source model :

7.75 x 10^{15} ~ 3.79 x 10^{20} N-m

M_w(4.5) M_w(7.7)

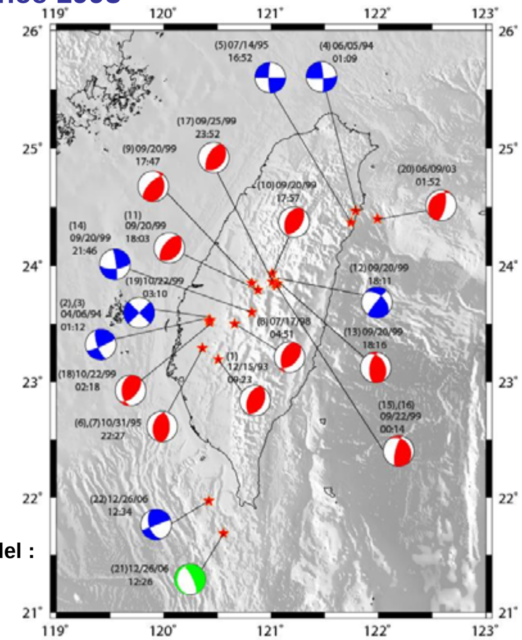

Characterizing of slip model dimension

$$f(u) = \bar{D}_u = \frac{\sum_{i=1}^{N}(D_{ui}\times W_s)}{W}$$

$$f * f = \int_{-\infty}^{\infty} f(u)\cdot f(u-x)du$$

$$L_e = \frac{\int_{-\infty}^{\infty} f * f\,dx}{f * f\big|_{x=0}}$$

u : the order of grids along strike direction
D : the slip of each grid
N : the number of grids along dip direction
W_s : subfault length
W : fault width

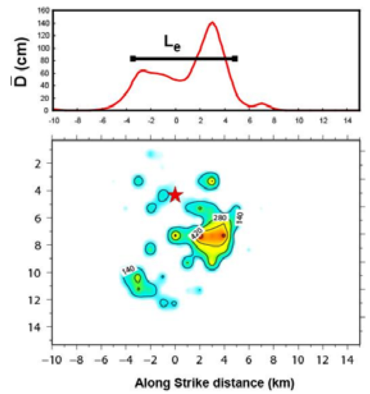

(Bracewell, 1986; Mai and Beroza, 2000)

Definition of effective fault dimensions

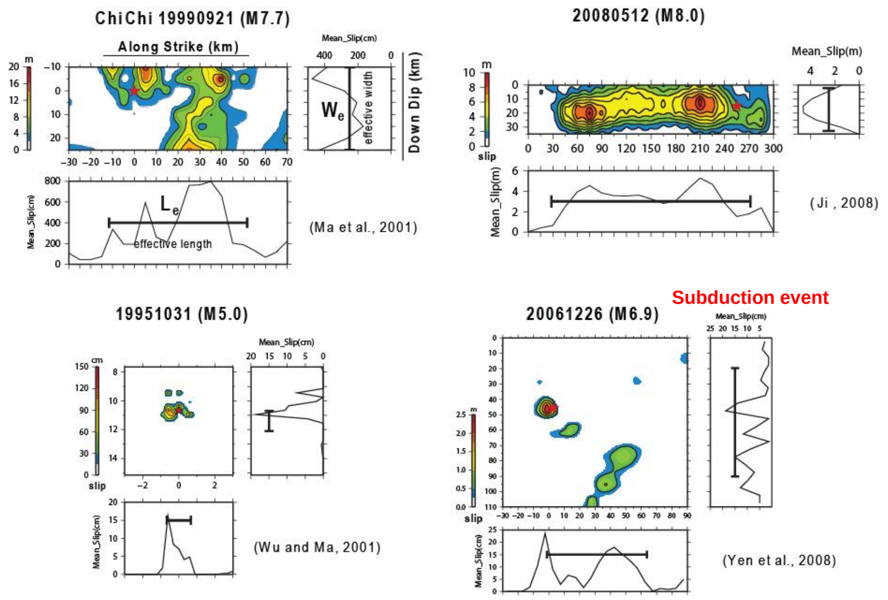

Taiwan data set + 3 constraints (Sumatra&Wenchuan&Bhuj)

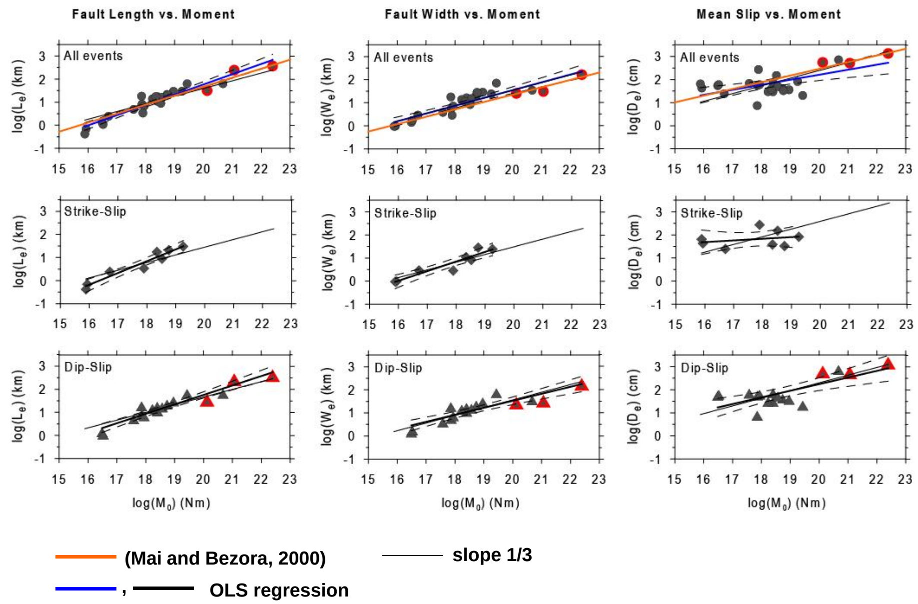

Comparison of the measurements based on original and effective dimension

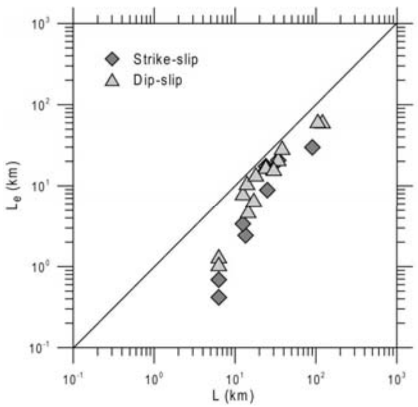

Median change : 0.53

$$\Delta L = L_e / L$$

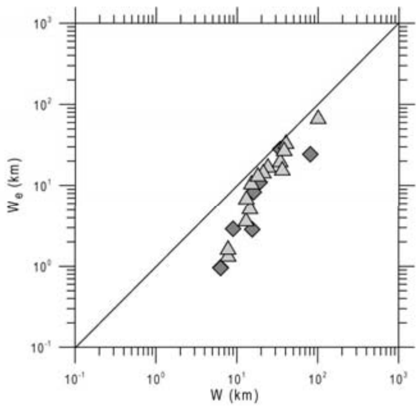

Median change : 0.53

$$\Delta W = W_e / W$$

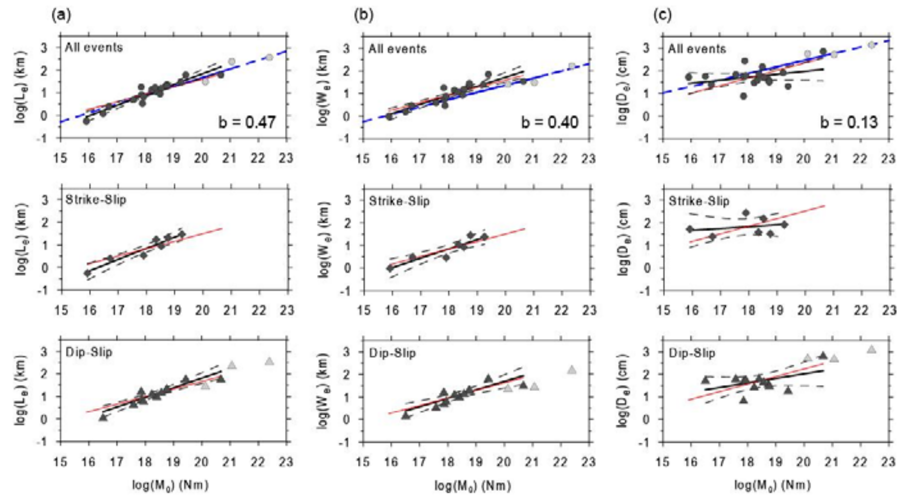

$$\log L_e = 0.47 \log M_0 - 7.46$$

$$\log W_e = 0.40 \log M_0 - 6.30$$

$$\log D_e = 0.13 \log M_0 - 0.65$$

Prediction from scaling relation

This study (just Taiwan data set)		
earthquake size	Length (km)	Width (km)
Mw7.3 (1.0E20Nm)	**70**	**64**
This study (just Taiwan data set + 3 constraints (Sumatra&Wenchuan&Bhuj)		
earthquake size	Length (km)	Width (km)
Mw7.3 (1.0E20Nm)	42	**36**
Mai and Beroza, 2000		
earthquake size	Length (km)	Width (km)
Mw7.3 (1.0E20Nm)	47	22
Wells and Coppersmith, 1994		
earthquake size	Length (km)	Width (km)
Mw7.3 (1.0E20Nm)	**91**	**22**
Wu, 2000		
earthquake size	Length (km)	Width (km)
Mw7.3 (1.0E20Nm)	76	25

Estimation from slip model

L_e: 63 km W_e: 35 km

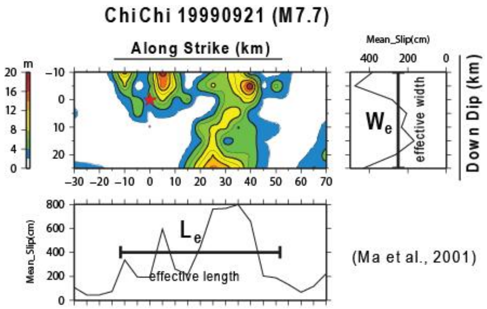

(Ma et al., 2001)

W&C: overestimated the length, and underestimated the width
Using different regression for larger events ruptured length greater than seimsogenic depth

Scaling Relationship of D_e vs. L_e & D_e vs. W_e

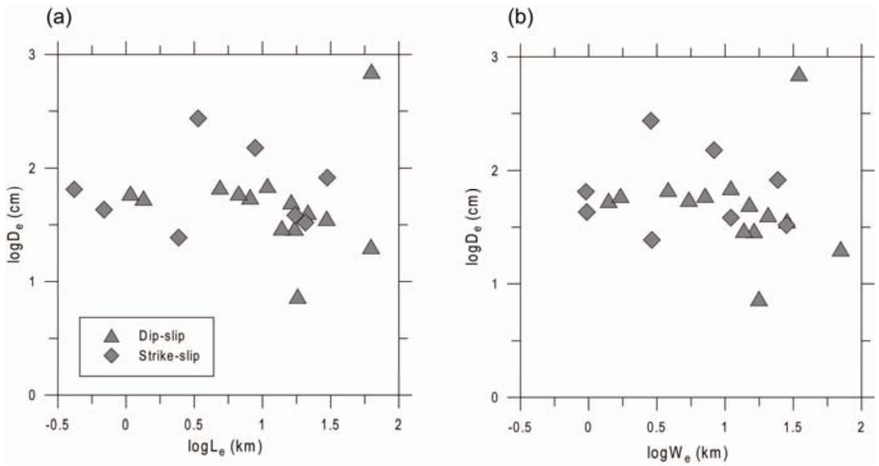

D_e~ constant, not follow self-similar scaling

Prediction from scaling relation

This study (just Taiwan data set)		
earthquake size	Length (km)	Width (km)
Mw6.1 (2.0E18Nm)	10.18	12.50
This study (just Taiwan data set + 3 constraints (Sumatra&Wenchuan&Bhuj)		
earthquake size	Length (km)	Width (km)
Mw6.1 (2.0E18Nm)	7.63	9.60
Mai and Beroza, 2000		
earthquake size	Length (km)	Width (km)
Mw6.1 (2.0E18Nm)	10.17	6.40
Wells and Coppersmith, 1994		
earthquake size	Length (km)	Width (km)
Mw6.1 (2.0E18Nm)	14.27	8.26
Wu, 2000		
earthquake size	Length (km)	Width (km)
Mw6.1 (2.0E18Nm)	9.37	7.00

Estimation from slip model

L_e: 12.05 km W_e: 10.40 km

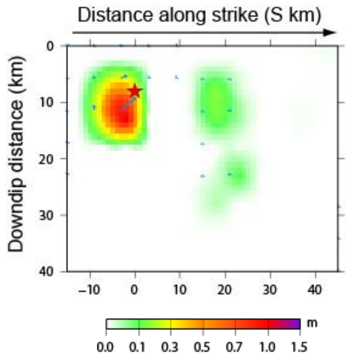

20060410 Taitung earthquake (Mw6.1)

Illustration of effective fault length against width:
A reflection related to the seismogenic thickness

Taiwan data set

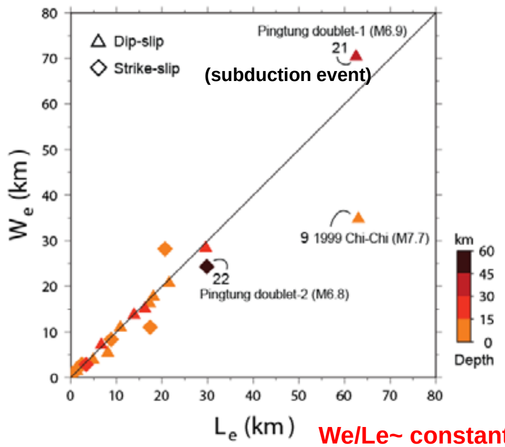

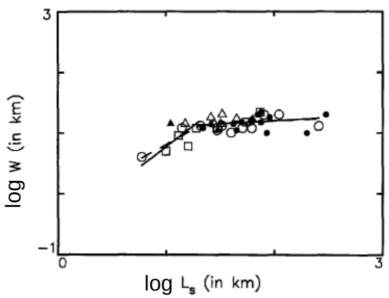

(Wang and Ou, 1998)

We/Le~ constant for small to moderate size events, similar feature for subduction zone event

Le>>We, for large event

- Uncertainty of mean slip -

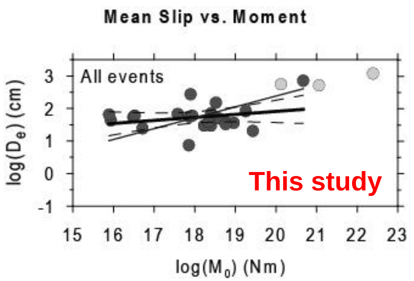

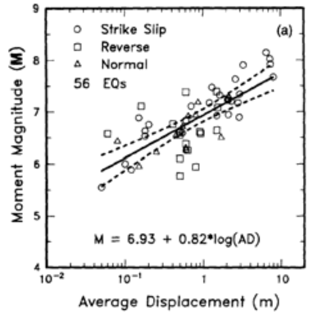

(Wells & Coppersmith, 1994)

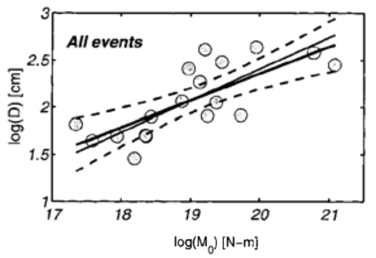

(Mai & Beroza, 2000)

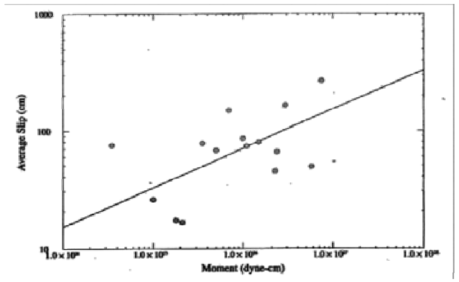

(Somverville et al., 1999)

Seismogenic layer in Taiwan collision zone

- particularly thicker seismogenic environment

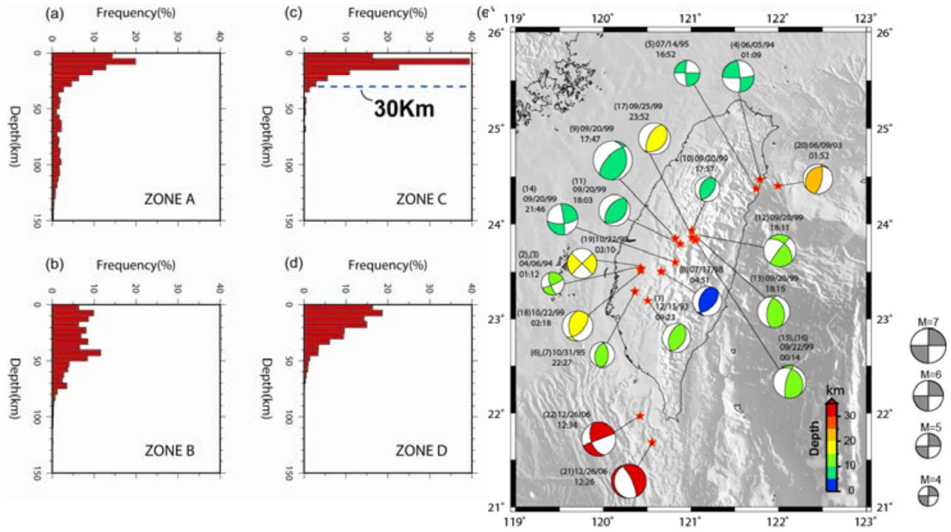

Seismogenic layer in Taiwan collision zone

- particularly thicker seismogenic environment

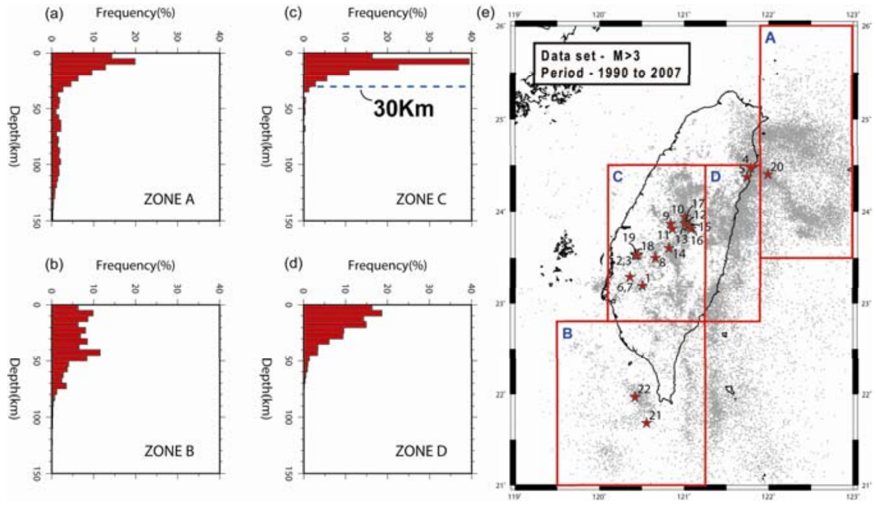

2006 Pingtung Earthquake Doublet

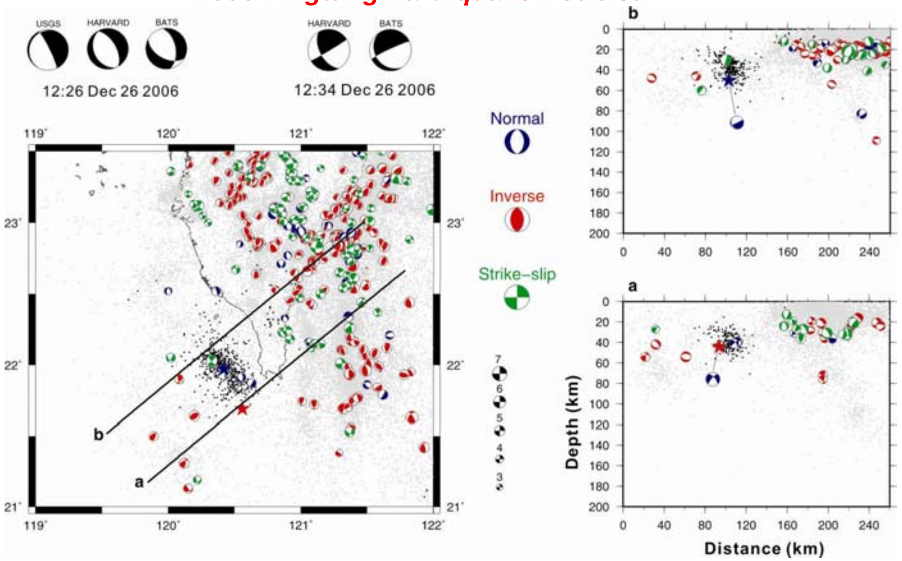

★ **1226 earthquake**
★ **1234 earthquake**

Background Seismicity(M>2.5) 1973/01 ~ 2006/12 (CWB)
Focal mechanism(Mw>3) 1995/07 ~ 2007/10 (BATS)

Asperity projection and aftershocks

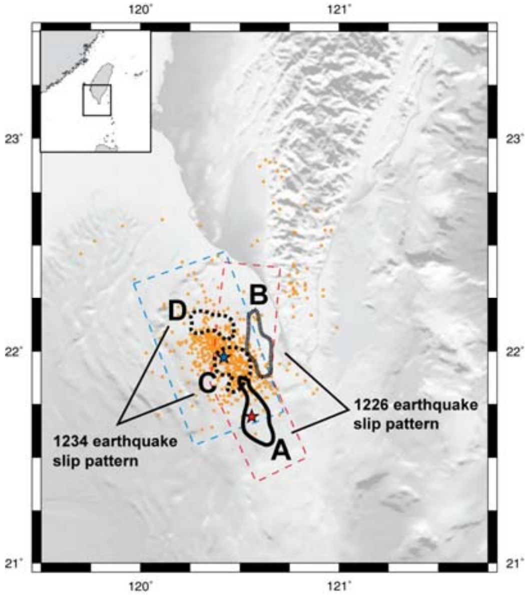

Hard to define
the rupture dimension
from aftershock distribution

Summary

1. The seismogenic depth controls the pattern of the rupture scaling. Adopting of the source scaling relationship should consider the setting of the tectonic environment.

2. Mean slip has a constant trend with increasing seismic moment in the range of 10^{16} to $10^{19.5}$ Nm. For large dip-slip events, when the ruptured length larger than the seismogenic thickness, the mean slip becomes proportional to the seismic moment.

3. The earthquake rupture could be two dimensional (Width and Length), while the ruptured was within the seismogenic depth as 30km in Taiwan collision zone.

4. For events within the seismogenic zone (M4.6 to M6.6), the stress drop is not constant, thus, is non-self-similar scaling.

5. While the large events with ruptured length greater than the seismogenic depth, the earthquake follow self-similar scaling. However, it does not apply to deeper subduction zone events, where the width can extend to deeper depth along the slab.

Stress Drops

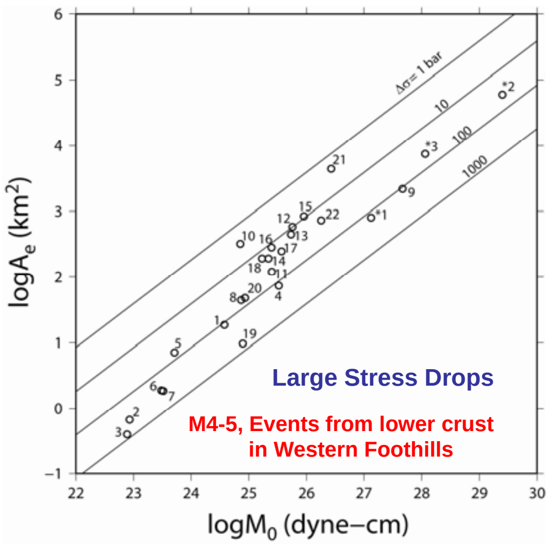

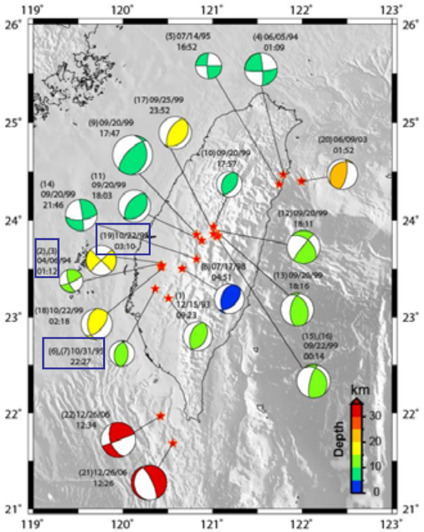

Thank you for your attention

Taiwan data set only –

The values of scaling relation using the ordinary least-squares method

log(Y) = a + b*log(X)		Slope	standard error	Intercept	standard error	Correlation coefficient	standard deviation
Y	X	b	σ_b	a	σ_a	R^2	σ_y
All event							
L_e	M_0	**0.49**	0.04	-7.95	0.64	0.91	0.19
W_e	M_0	**0.42**	0.04	-6.59	0.72	0.85	0.21
D_e	M_0	**0.09**	0.07	0.06	1.32	0.07	0.39
Dip event							
L_e	M_0	0.46	0.05	-7.25	0.90	0.88	0.19
W_e	M_0	0.40	0.06	-6.26	1.08	0.79	0.23
D_e	M_0	0.14	0.11	-0.96	1.94	0.13	0.41
Strike event							
L_e	M_0	0.51	0.05	-8.36	0.97	0.94	0.19
W_e	M_0	0.42	0.06	-6.65	1.04	0.90	0.20
D_e	M_0	0.07	0.11	0.54	1.89	0.07	0.37

Taiwan data set only –

Scaling relation

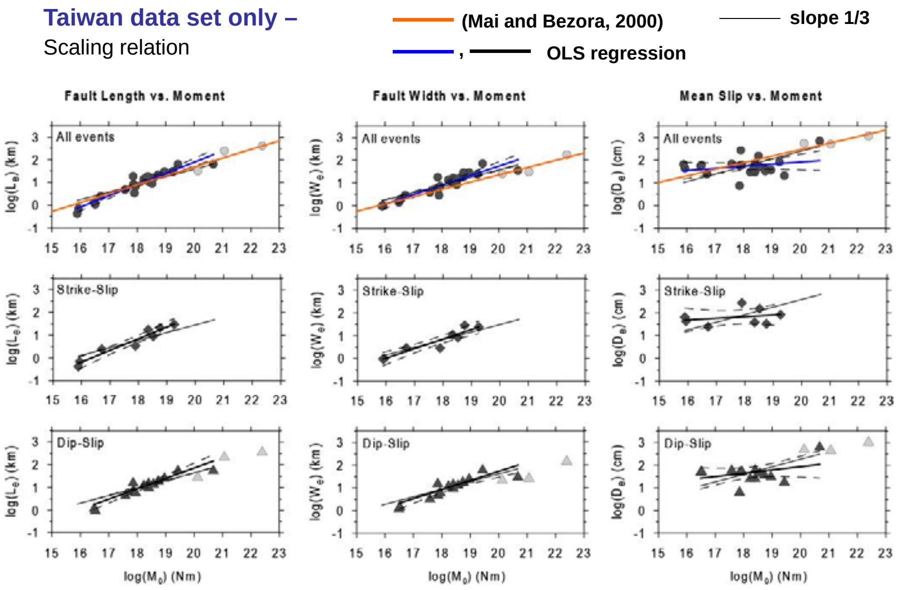

Dip-slip (reverse, normal and oblique)

Interplate coupling and slow slip events in the Ryukyu Trench

Mamoru Nakamura
University of the Ryukyus

Abstract

Historically, interplate earthquakes have not been observed and the interplate coupling is assumed to be weak in the Ryukyu Trench. However, numerical simulation of tsunami, global positioning system (GPS) measurement, and observation of ocean-bottom crustal movement inform the state of inter-plate coupling in the Ryukyu trench. These results provide that the interplate coupling is locally strong at the shallower and deeper part of the Ryukyu subduction zone.

Slow slip event beneath Yonaguni Island. Anomalous crustal deformation following the Mw = 7.1, March 31, 2002, Hualien earthquake was observed over 5 years using the GPS network in the south Ryukyu Islands. The analysis showed an afterslip event at a depth of 30 km on the subducting Philippine Sea plate. The magnitude of the cumulative moment reached 7.4. The afterslip promoted Coulomb failure stress on the fault of the repeating slow slip events (SSEs) in the vicinity of the afterslip, which accelerated the slip rate of the SSEs after the earthquake.

Interplate coupling in the shallow part of the Ryukyu Trench. The 1771 Yaeyama earthquake generated a large tsunami with a maximum runup of 30 m, causing significant damage in south Ryukyu, Japan, despite the weak ground shaking. The result of numerical simulation indicates that the source fault of the tsunami is very close to the Ryukyu Trench. The 1771 Yaeyama tsunami was caused by a tsunami earthquake (Mw = 8.0) that occurred in the subducted sediments beneath the accretionary wedge. Thus suggests that the shallow part of the south Ryukyu Trench is coupled.

Anomalous crustal movement in the central Ryukyu Trench. Ocean bottom benchmark system was set at about 35 km landward from the axis of the central Ryukyu trench to detect the crustal deformation by the interplate coupling between the Philippine Sea plate and the Eurasian plate. A set of three acoustic transponders has been installed on the seafloor, at a depth of about 2900m. Four campaign observations were carried out for the period from January 2008 to May 2009. The RMS of the travel time residuals for each campaign analysis is about 60 micro-seconds. For two years observation, difference of positions between February

2008 and July 2008 epochs indicates an easterly movement of about 11 cm. We assumed that the 25 cm thrust-slip occurred on the subducted Philippine Sea plate beneath the benchmark. The shallow part of the interplate boundary near the Ryukyu Trench axis is locally coupled, and causes the aseismic slip event.

Interplate coupling and slow slip events along the Ryukyu Trench

Mamoru Nakamura (Univ. Ryukyus)

GPS velocity field in the Ryukyu arc

Southward movement of Ryukyu Islands:

Weak inter-seismic coupling (?)

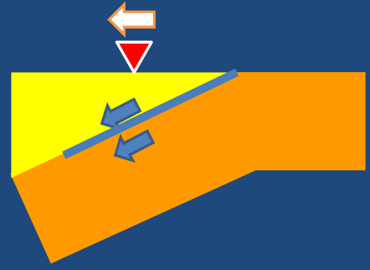

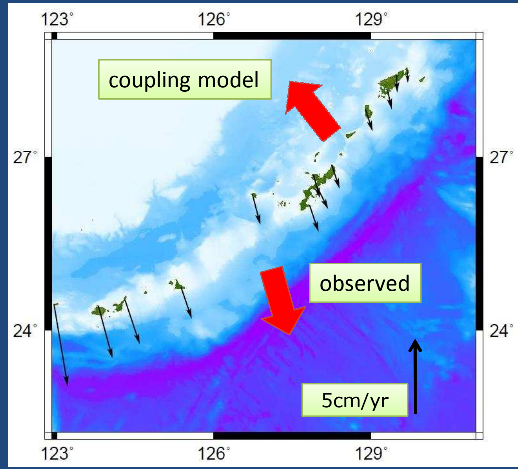

GPS horizontal velocity
(GSI, 1997-2006)
Tsushima is fixed

Historical large earthquakes in the Ryukyu trench (1700-2007)

Thrust-type large earthquakes:

no records for 300 years (?)

Damaged earthquakes in Ryukyu

1771 Yaeyama tsunami (M7.4)
1911 Kikaijima earthquake (M8.0)
(Philippine Sea plate: intra-plate)

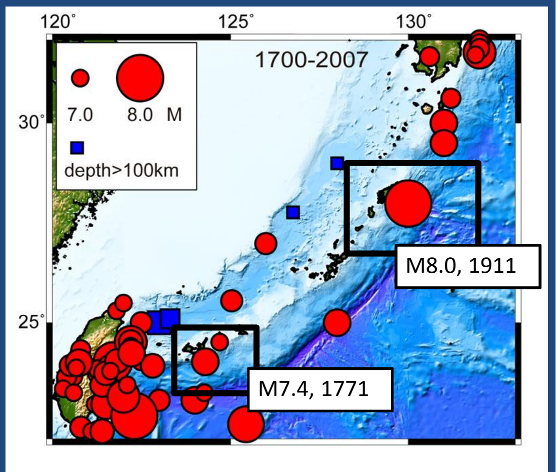

Afterslip (or slow slip event) beneath the Yonaguni Island

(Nakamura, 2009a)

Two large earthquakes (Mw>7.0) from Dec. 2001 to Mar. 2002.

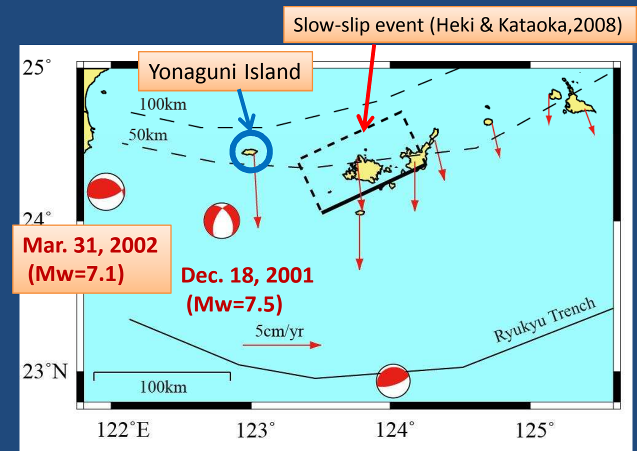

De-trended GPS (GSI) data

Subtract linear, annual, and coseismic components
Anomalous trend after Apr. 2002
Duration of SSE: 5 years

$$y = A + Bt + \sum_{i=1}^{2}\left(C_i \sin\left(\frac{2\pi it}{T}\right) + D_i \cos\left(\frac{2\pi it}{T}\right)\right) + \sum_{j=1}^{N}\left(Y_j^{cos} + Y_j^{post}\left(1 - \exp\frac{-(t-T_j)}{\tau_j}\right)\right)H(t-T_j)$$

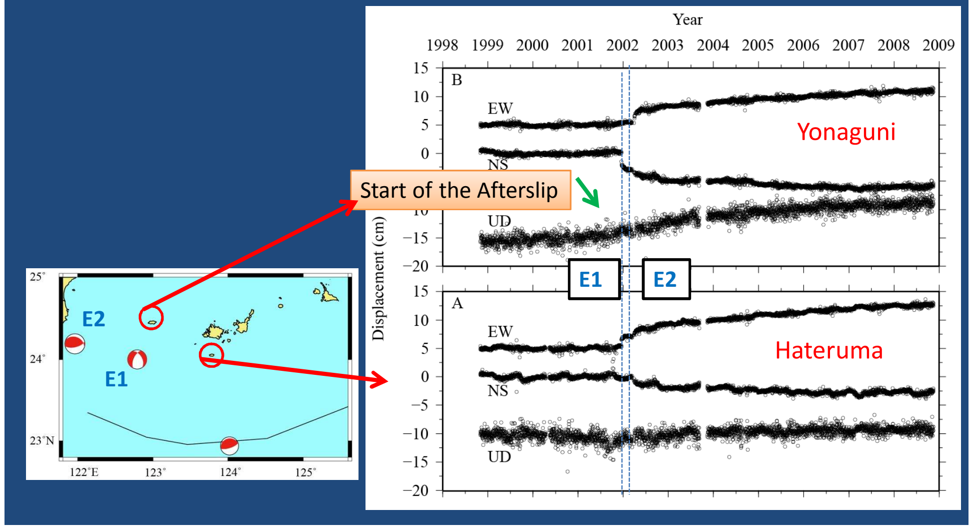

Fault model of the Yonaguni afterslip

Grid-search method

Period: Jul. 2002-Jul.2008
Horizontal and vertical displacements

Fault Parameter

Depth:35km
L:80km
W:30km
slip:140cm
Mw:7.4

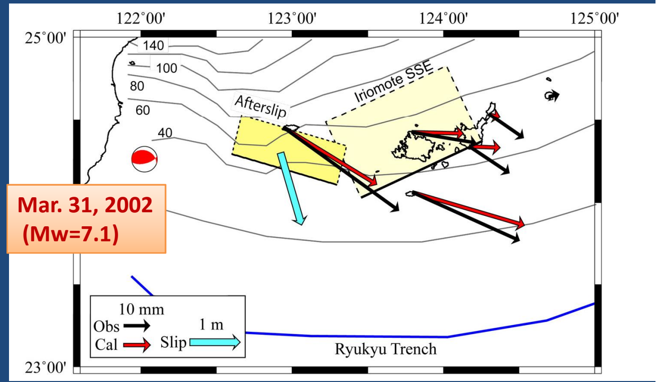

Horizontal motion of the Yaeyama region

(Jul.2002-Jul.2008)

Total Horizontal displacement

max. 5cm (ESE direction) at Yonaguni and Hateruma

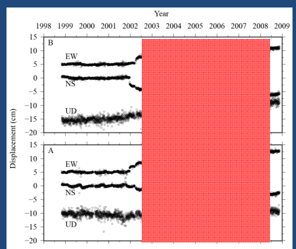

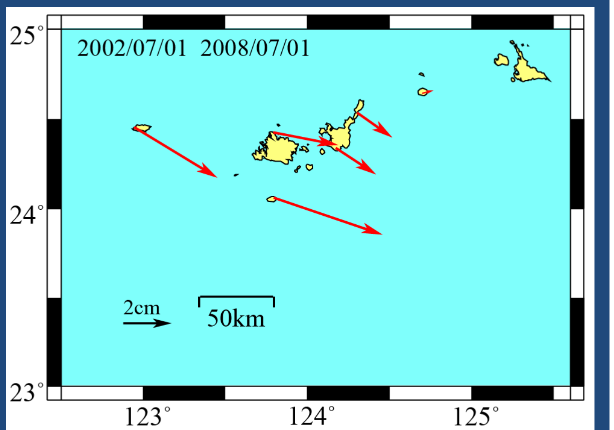

Yonaguni Afterslip

1. Long duration (5 years)
2. Cumulative moment exceeds that of the mainshock.
3. The fault of the afterslip is far from the mainshock fault.

Different from usual afterslips
duration: ~1 year
close to the mainshock fault.

The afterslip changed the slip rate of the Iriomote SSE.

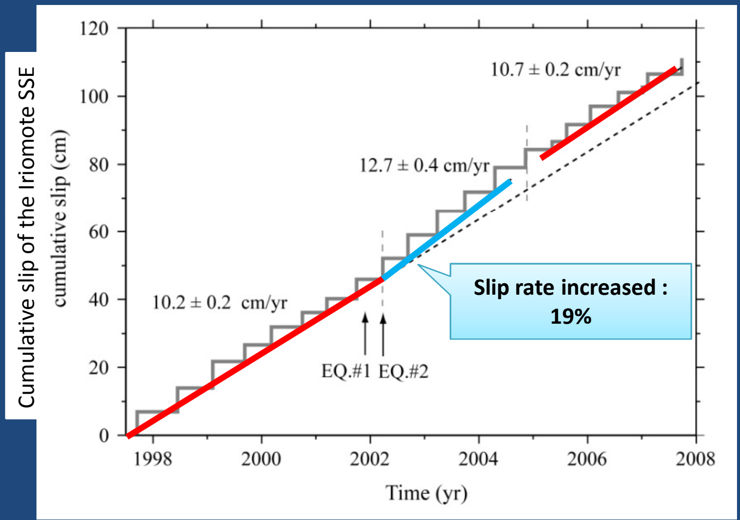

Observation of Ocean Bottom Crustal Deformation in the central Ryukyu trench

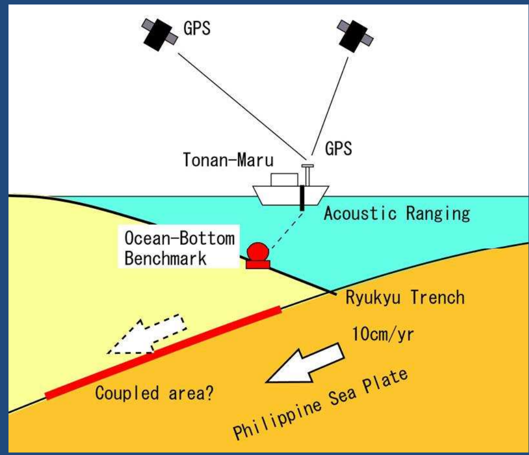

Combination of

(1) Kinematic GPS (5Hz sampling)

(2) Acoustic ranging system

Position determination of ocean-bottom benchmarks

Members of the project

Univ. Ryukyus : M. Nakamura, T. Matsumoto, M. Furukawa,

Nagoya Univ. : K. Tadokoro, T. Okuda, T. Watanabe, K. Miyata, S. Sugimoto

IES, Taiwan : M. Ando

Okinawa Prefectural Fisheries and Ocean Research Center

Estimation of slip rate change through Coulomb failure stress model

Stress drop of the Iriomote SSE: 34 kPa

Average Coulomb failure stress change: 45 kPa (=9 kPa/yr)

13% increase in slip rate

= (9 kPa/yr)/(34 kPa*2)

Observed increase in slip rate : 19%

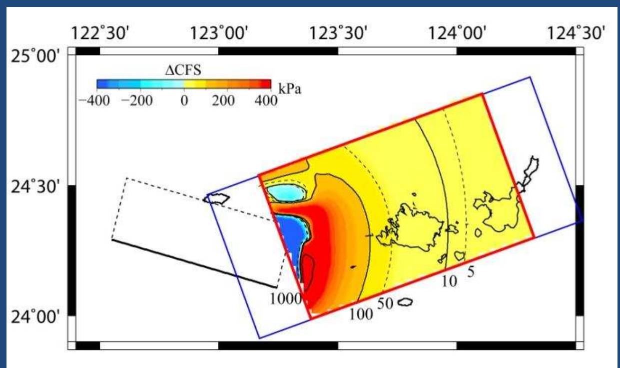

Tonan-Maru (176t)

(Okinawa Prefectural Fisheries and Ocean Research Center)

Ocean-bottom crustal deformation measurement in the central Ryukyu trench

Benchmarks
35km land-side from Ryukyu Trench
interval: 2km

Reference of GPS
Univ. Ryukyus

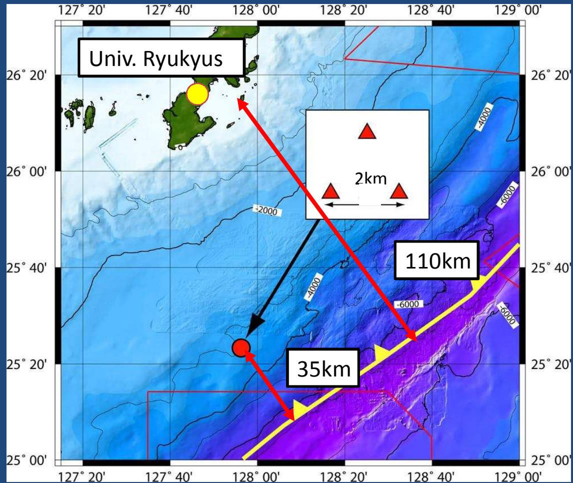

Vertical cross-section of the central Ryukyu Trench

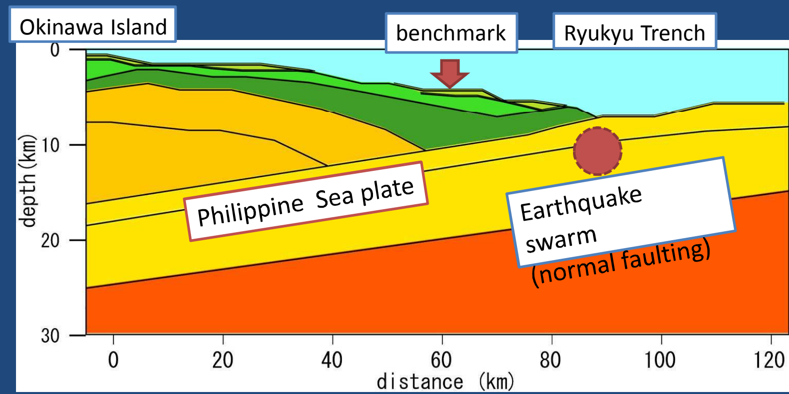

Kodaira et al. (1996)

Result of the observations

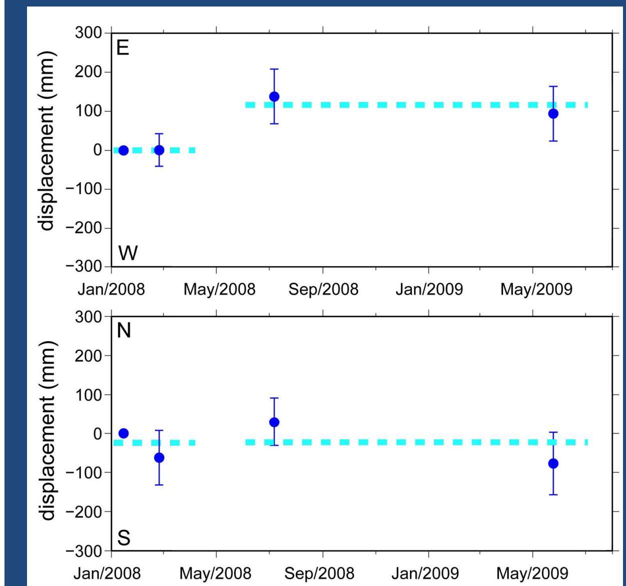

110 mm movement to east direction

Fault model of the aseismic slip

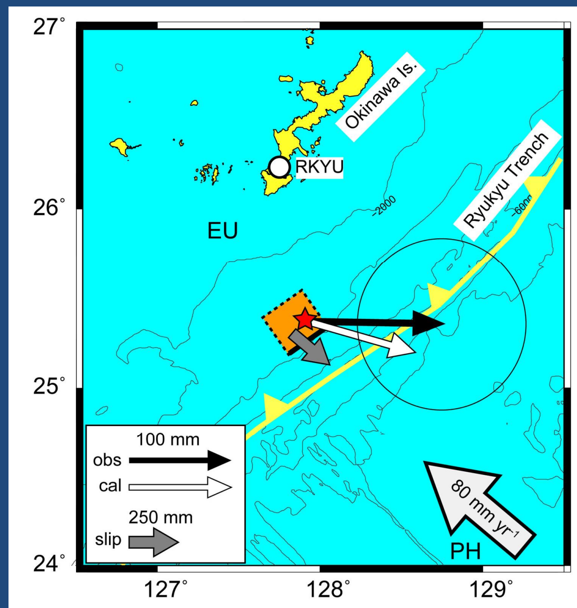

Fault
L = W = 30 km
Depth = 5 km
Dip = 6 °
Rake = 110 °
Slip = 250 mm
Mw = 6.5

Induced earthquake swarm by the aseismic slip

ΔCFS by the aseismic slip

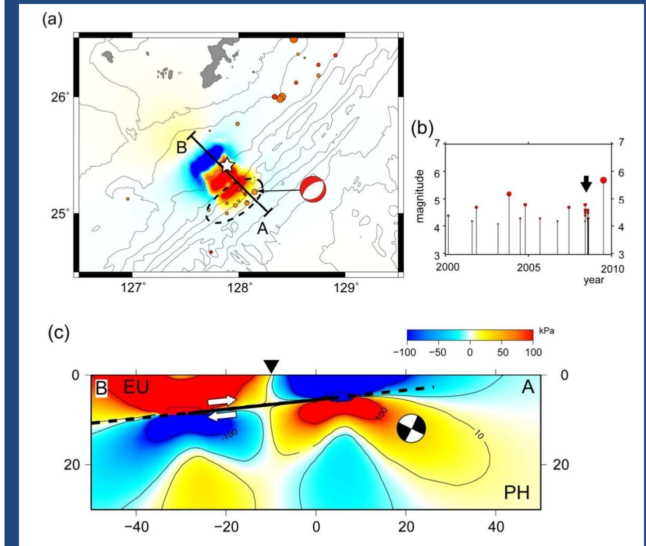

Fault model of the 1771 Yaeyama earthquake

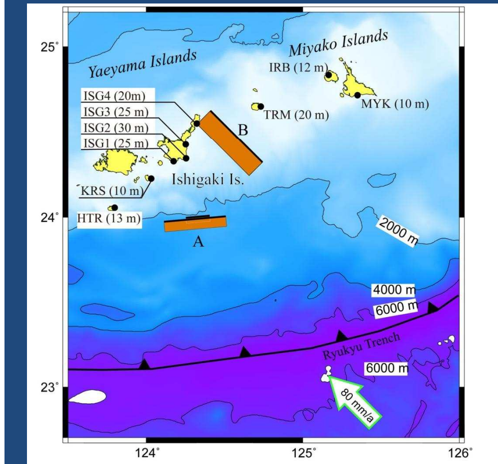

Previous source model of the 1771 Yaeyama earthquake

A: Intraplate Eq. & landslide (Imamura et al., 2001)

B: Intraplate Eq. (Nakamura, 2006)

Possibility of interplate earthquake?

The 1771 Yaeyama earthquake was a tsunami earthquake

(Nakamura, 2009b)

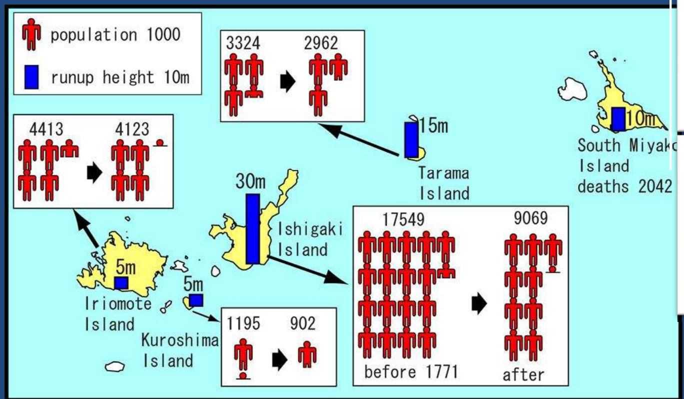

Tsunami runup heights (bars) and population change between before and after the Yaeyama Tsunami.

Result of Numerical simulation Tsunami Source model

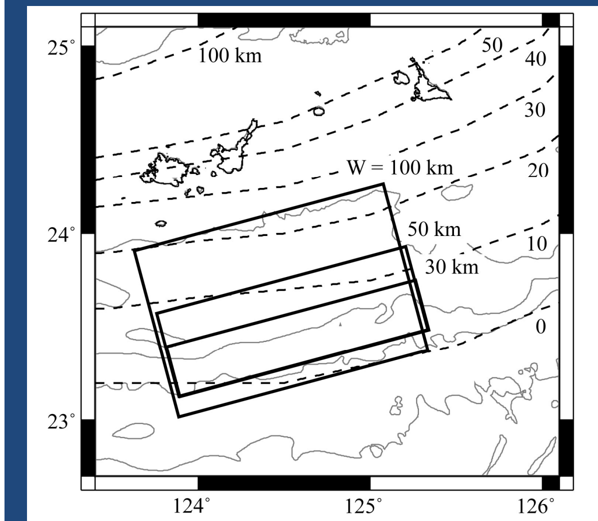

Fault length: 150km
Fault width: 30, 50, 100 km

Calculate maximum runup

Compare the observed runup heights with calculated heights at coast.

Observed runup heights and calculated wave heights

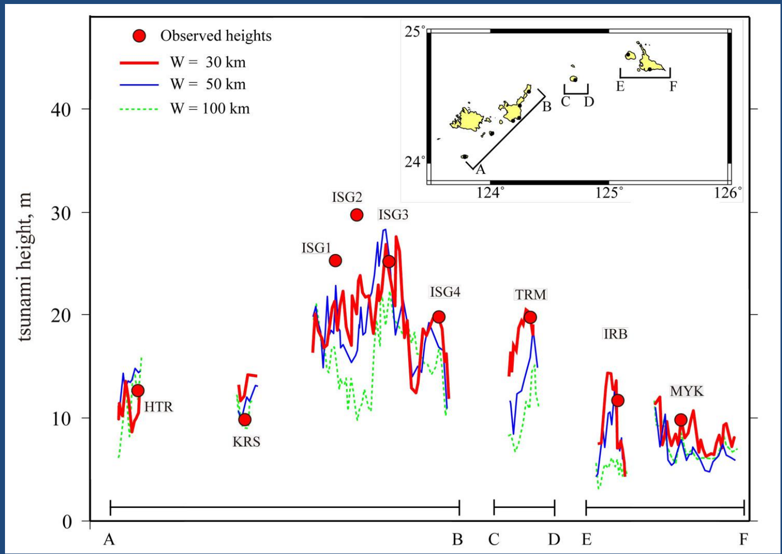

Tsunami earthquakes in the world

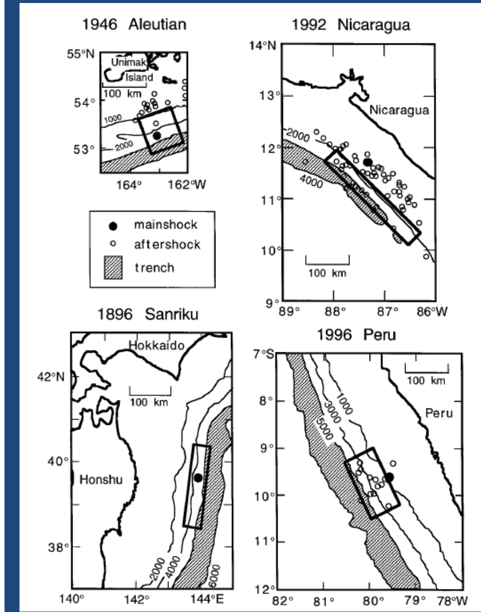

Satake & Tanioka (1999)

1771 Yaeyama

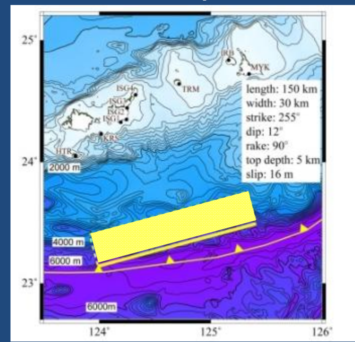

Fault model of the Yaeyama earthquake

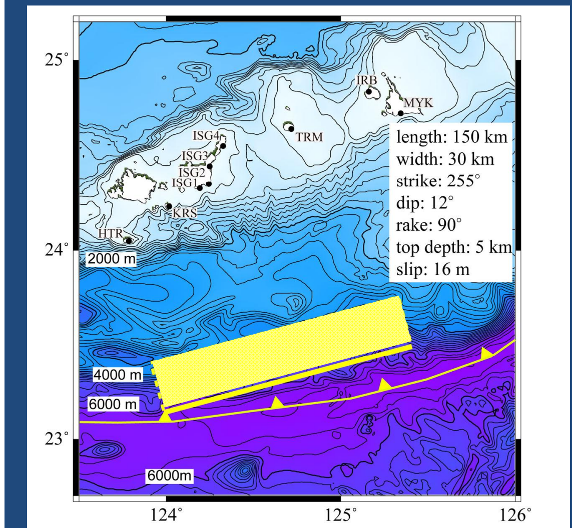

Source fault:
near the Ryukyu Trench

Seismic intensity:
weak (< 5 in JMA scale)

Tsunami earthquake

Conclusions: Interplate coupling along the Ryukyu subduction zone

Deep part of the Ryukyu Trench: Slow-slip events and afterslip
- A: Heki & Kataoka (2008, JGR)
- B: Nakamura (2009a, GRL)

Shallow part of the Ryukyu Trench: Slow-slip event and Tsunami earthquake
- C: Nakamura et al. (2009)
- D: Nakamura (2009b, GRL)

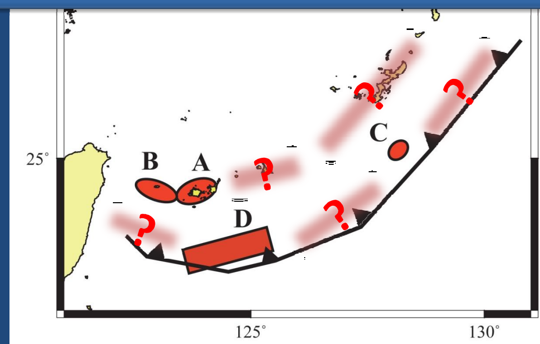

Comparison of the deformation between geological term and geodetic term across the Yuli fault by Precise Leveling Survey, eastern Taiwan

Nobuhisa Mathuta[1], Masayuki Murase[2], Jui-Jen Lin[3], Hsin-Chieh Pu[4], MD ABDUL MATIN[3], Wen-shan Chen[1], Cheng-Horng Lin[3]

1: Department of Geosciences, ***National Taiwan University, Taiwan***

2: Department of Geosystem Sciences, College of Humanities and Sciences, Nihon University, Japan

3**:** Institute of Earth Sciences, Academia Sinica, Taiwan

4: Institute of Geophysics, National Central University, Taiwan

Abstract

The Longitudinal Valley fault (LVF) displays both creeping and locked segments and has produced moderate to large earthquakes. Because, the boundary between creeping and locked segments accumulates strain, it is the asperity on the fault. In this area, it is important to comprehend the slip deficit rate distribution on the fault at depth. And long term deformation which consists of interseismic and coseismic deformation is estimate by tectonic geomorphology. We can probably predict the behavior of the huge earthquake by the comparison of the estimated deformation by Leveling survey with the long term deformation pattern. Yuli is located around the boundary between creeping and locked segments. We had a leveling survey to focus to deform the surface across the LVF around Yuli.

Large earthquake commonly occur in eastern Taiwan along the Longitudinal Valley due to the vigorous arc-continental collision between Philippine Sea Plate and Eurasian Plate with a converging rate 85 mm/yr (Yu et al., 1997). The 150 km long, NNE-SSW trending, Longitudinal Valley in eastern Taiwan separates two quite different geologic provinces: the Central Range which is composed of the pre-Tertiary metamorphic to the west and the Coastal Range which consists of Neogene andesitic volcanic units, turbidite sediments and mélange to the east. A major discontinuity of about 35 mm/yr on the rate of crustal shortening across the Longitudinal Valley is attributed to inter seismic slip of the LVF (YU et al., 2001). The Longitudinal Valley fault (LVF) runs along the eastern rim of the valley and an east-dipping reverse fault. The Chieshan segment (south segment of the LVF) is creeping and show a horizontal shortening of 17-19 mm/yr by creepmeter (Lee et al, 2001). The LVF is east dipping reverse fault has built the Coastal Range. The long term vertical slip rate is 28 mm/yr (Chu, 2007) at western rim and 7-8 mm/yr (Hsieh and Rau, 2009) at eastern rim of the Coastal Range.

We established about 30km leveling route from Yuli to Changbin to detect the vertical deformation in detail. The installation interval of benchmarks near the fault area is about 100 m. Others were installed every about 300m along the road. The precise leveling surveys were conducted in August 2008 and August 2009, and we measured with DNA03 Digital Leveland Invar Staff with Bar Code by Leica Co. owned by Institute of earth Science, Academia Sinica.

The overview of the deformation detected in the period from 2008 to 2009 is as follows. It was detected about 2.7 cm uplift, referred to the west end of our route, at about 2km region across the fault. The vertical displacement in 200m through the LVF is 1.7 cm. Uplift was gradually-reduced with the distance from the fault, and was 1.5 cm at the east coast. In the observation period, there is no significant earthquake in Yuli fault. It suggests the detected deformation as a cause for the creep motion of the Yuli fault.

The deformation pattern for a year is characterized by a pop-up structure as the highest uplift is located near the fault on hanging wall side. I can think of two reasons. One is the slip increase on the fault with depth. Another is the fault geometry become gentle in subsurface. A lot of tectonic bulges are noted in Fuli area which is located at south of Yuli town. These bulges have been controlled by fault geometry. Therefore, we propose that the deformed surface for a year on the fault tip is also driven by changed fault geometry.

CREEPING DEFORMATION ALONG THE LONGITUDINAL VALLEY FAULT AT YULI, EASTERN TAIWAN, REVEALED BY LEVELING, 2008 - 2009

Nobuhisa Matsuta[1*], Masayuki Murase[2], Jui-Jen Lin[3], Hsin-Chieh Pu[4], MD ABDUL MATIN[3], Wen-shan Chen[1], Cheng-Horng Lin[3]

1: Department of Geosciences, ***National Taiwan University, Taiwan***
2: Department of Geosystem Sciences, College of Humanities and Sciences, Nihon University, Japan
3: Institute of Earth Sciences, Academia Sinica, Taiwan
4: Institute of Geophysics, National Central University, Taiwan

Our motivation

How will the earthquake occur?

When and Where will the earthquake occur?

Where is asperity?

How much is interseismic slip on the fault? Leveling

How is displacement distributed?

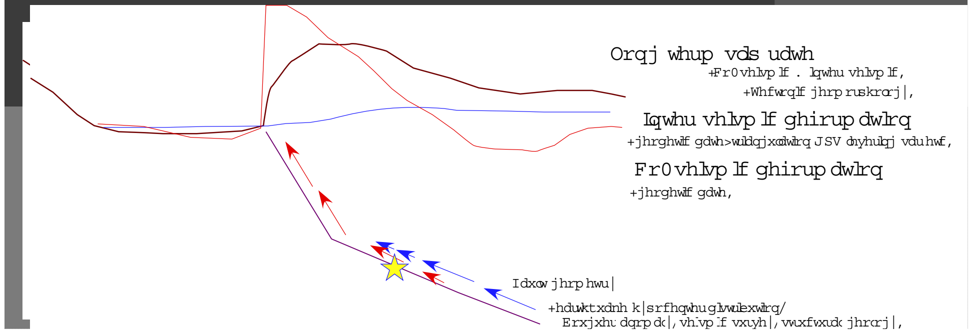

Outline of presentation

- Rxup rwlydwlrq
  - Why Yuli? Why leveling ?
    Inter seismic slip and surface deformation
- Whfwrqlf vhwwlqj
  - Taiwan
  - Longitudinal valley
- Ohyholqj vxuyh|
  - Leveling line and actually survey
  - Result
- Discussion
  - Compared surface deformation
  - Compared GPS
  - Compared hypocenter and 2003 earthquake
  - Compared long term deformation
- Frqfoxvlrqv

Why Yuli ?

- We believe that there is the boundary between creeping fault and locked fault.
- We can estimate the displacement on the fault since it is not vertical fault.
- The new road was constructed across the coastal range.
- We can draw the actually fault trace by tectonic geomorphology in the south of Yuli.

Outline of presentation

- Rxu prwlydwlrq
  - Why Yuli? Why leveling ?
    Inter seismic slip and surface deformation
- Tectonic setting
  - Taiwan
  - Longitudinal valley
- Ohyholqj vxuyhb
  - Leveling line and actually survey
  - Result
- Discussion
  - Compared surface deformation
  - Compared GPS
  - Compared hypocenter and 2003 earthquake
  - Compared long term deformation
- Frqfoxvlrq

Jhrorjlfdo vhwwlqj dorqj wkh Orqjlwxglqdo ydoohb

- Components of the Coastal range
  - Miocene volcanic rock
  - Pliocene –Pleistocene deep sea turbidites
  - tectonic melange (Lichi melange)

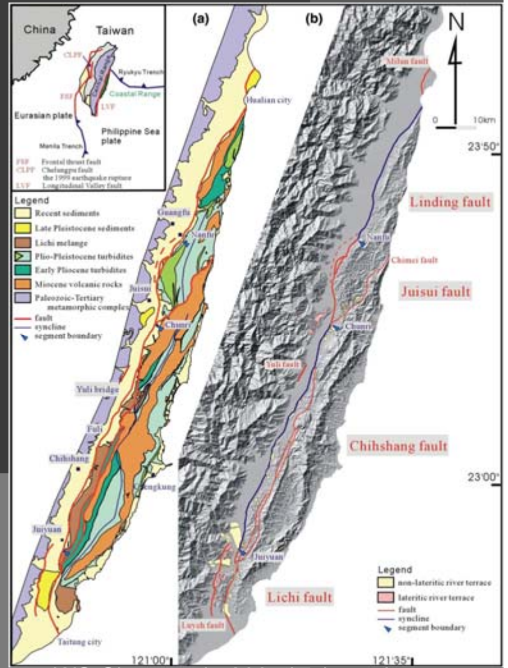

WS Chen et al., 2007the boundaryt

Taiwan tectonic setting

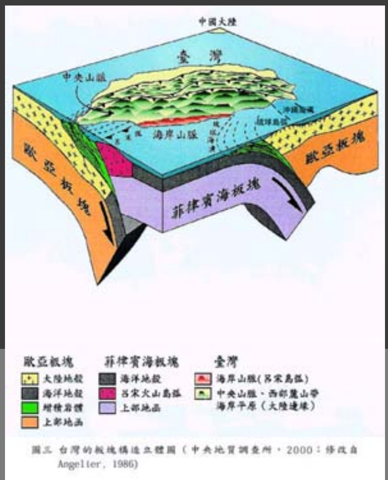

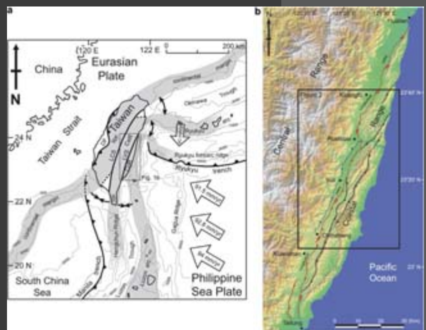

Shyu et al., 2007

- Arc-continental collision
  high speed convergent rate
- Costal range: Luzon arc
  accretionary sediments & island arc rock
- Central range: Eurasian plate
  metamorphic rock

The longitudinal valley fault (LVF)

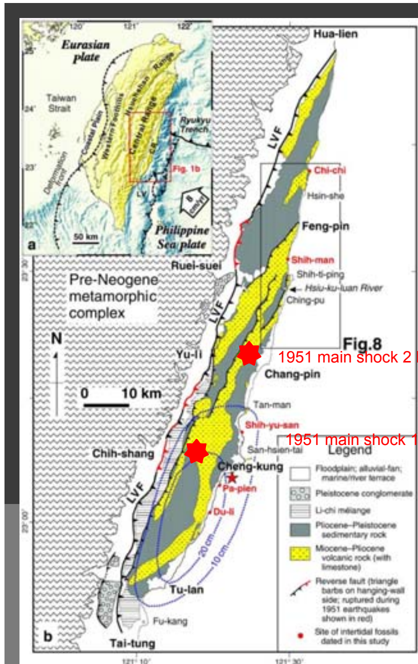

- The longitudinal valley fault
  - 1951 earthquakes
  - Creeping dominant segments
    South segments
    (Chih –shang area)
  - Recurrence interval
    North (Ruei-suei)
    170-210 yr
    South (Chih shang)
    less than 140 yr

Modified from Meng-Long Hsieh Ruey Juin Rau, 2009

Outline of presentation

- Rxup rwlydwlrq
  - Why Yuli? Why leveling ?
    Inter seismic slip and surface deformation
- Whfwrqlf vhwwlqj
  - Taiwan
  - Longitudinal valley
- Leveling survey
  - Leveling line and actually survey
  - Result
- Discussion
  - Compared surface deformation
  - Compared GPS
  - Compared hypocenter and 2003 earthquake
  - Compared long term deformation
- Frqfoxvlrq

The location of the bench mark

The interval of bench marks is
- 100 m near the longitudinal fault.
- 200 - 300 m far the longitudinal fault.


drilling in the firm concrete


Set screw by the bond


use the existing bench mark

Leveling line

The interval of bench marks
- 100 m (near the LVF)
- 200 - 300 m (far from the LVF)

Result

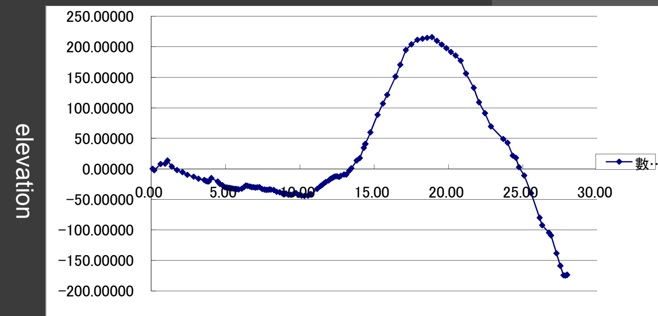

There is poor correlation between uplift and elevation.

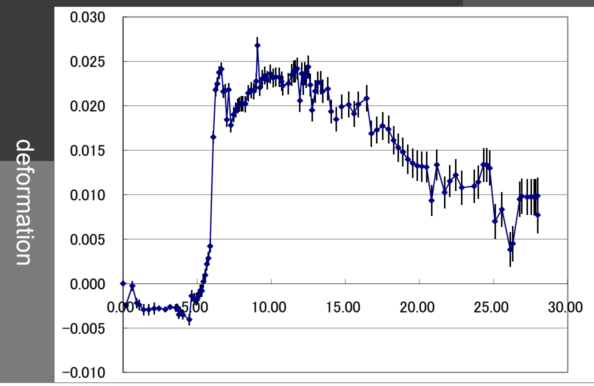

Projected deformation

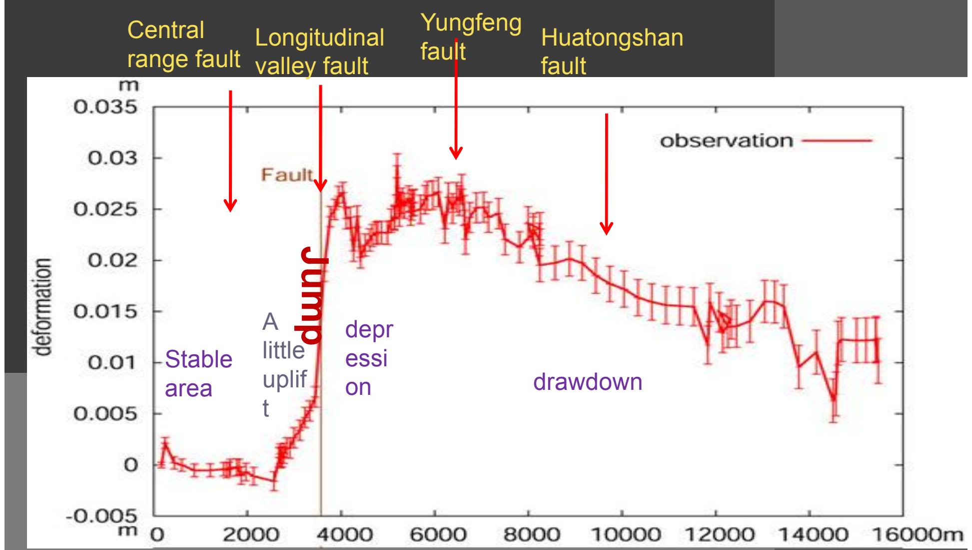

Tectonic geomorphology

- The CRF is not clear in this area
- The LVF can make a draw the trace with tectonic bulges.
- We can show cumulative offset by the LVF on the difference terraces
- On the hangingwall of the LVF, there are syncline and anticline.

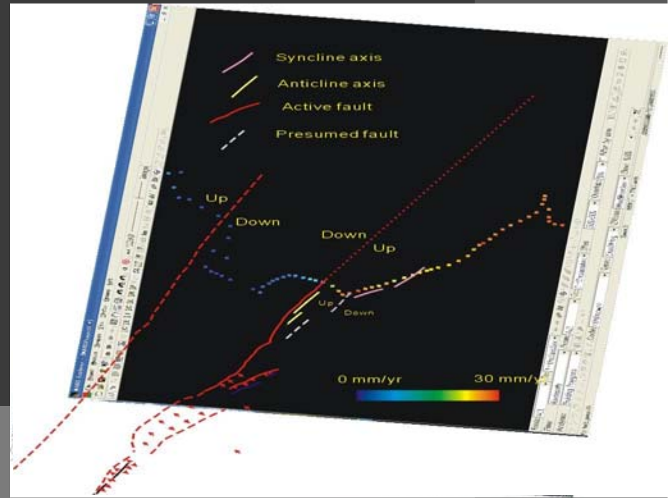

The short term deformation pattern by leveling observation fits the long term deformation pattern.

Outline of presentation

- R xup rwlydwlrq
  - Why Yuli? Why leveling ?
  - Inter seismic slip and surface deformation
- Whfwrqlf vhwwlqj
  - Taiwan
  - Longitudinal valley
- Ohyholqj vxuyh|
  - Leveling line and actually survey
  - Result
- Discussion
  - Compared surface deformation
  - Compared GPS
  - Compared hypocenter and 2003 earthquake
  - Compared long term deformation
- F rqfoxvlrq

K rz wr p dnh wkh vxuidfh ghirup dwlrq B

Fault geometry model

Slip disribution model

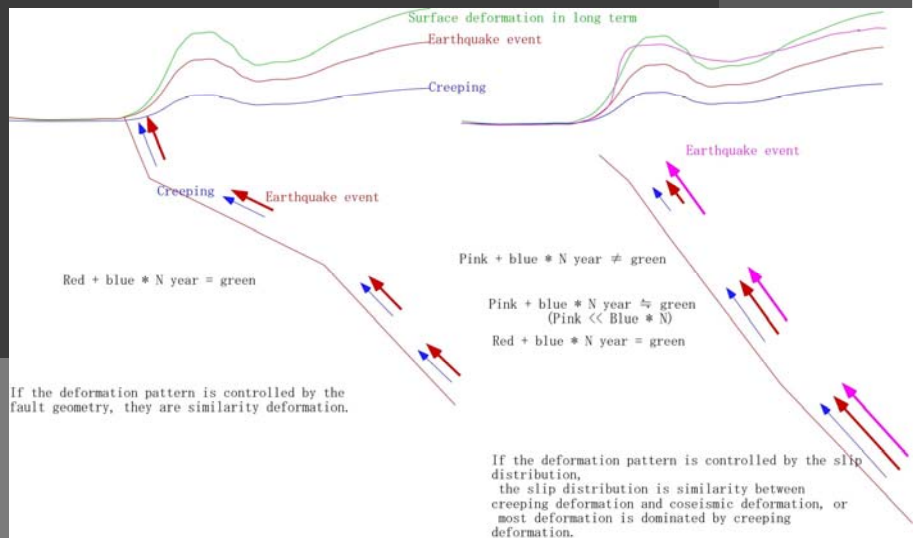

Outline of presentation

- Rxup rwlydwlrq
  - Why Yuli? Why leveling ? Inter seismic slip and surface deformation
- Whfwrqlf vhwwlqj
  - Taiwan
  - Longitudinal valley
- Ohyhdqj vxuyh|
  - Leveling line and actually survey
  - Result
- Discussion
  - Compared surface deformation
  - Compared GPS
  - Compared hypocenter and 2003 earthquake
  - Compared long term deformation
- F rqfoxvlrq

Vrxwkhuq vhjphqw

Horng-yue Chen et al., 2004

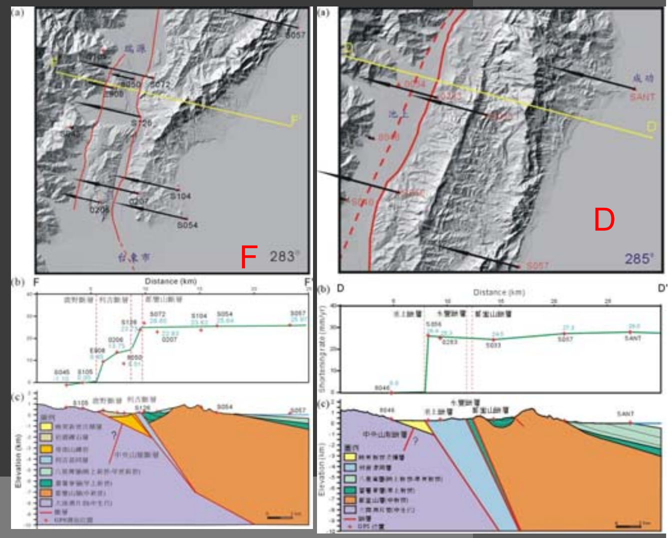

1992-1999

Wen-shan Chen et al., 2007)

We can show the gap across the fault trace and the uniformly uplift on the hangingwall

GPS data

We focus the deformation along the coastal line

Solid line: the station is Penghu island in the Chinese continental margin

Dashed arrow: respect to the Central range

Solid line is parallel → convergent rate is similarity

Compared coastal line to the east margin of longitudinal valley

- Chih-shan area : similar → creeping
- Yuli: decrees → locked ?_
- North: ?

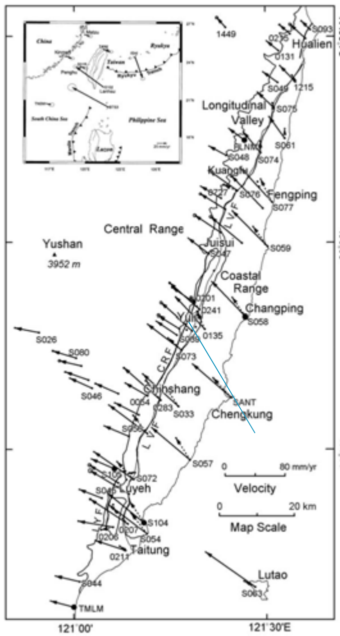

1992-1999

Horng-yue Chen et al., 2004

Q ruwkhuq vhjphqw

Horng-yue Chen et al., 2004

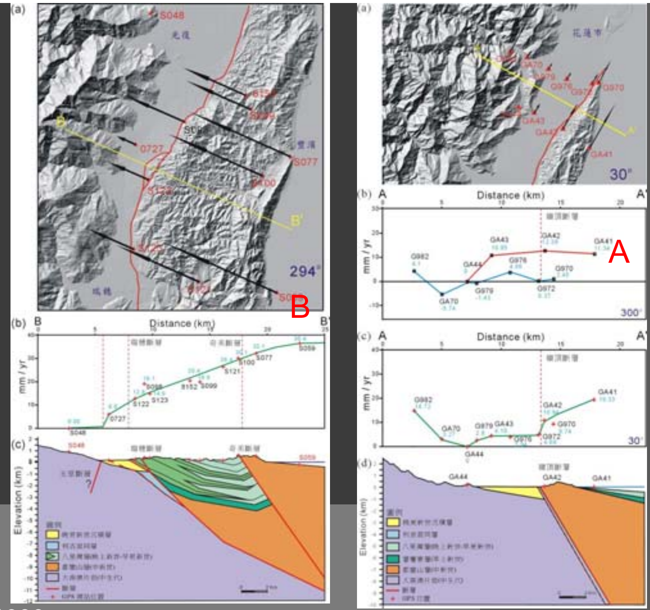

1992-1999

Wen-shan Chen et al., 2007)

We are shown the increased uplift to the east on the hangingwall.

Jhrghwlf
ghirupdwlrq

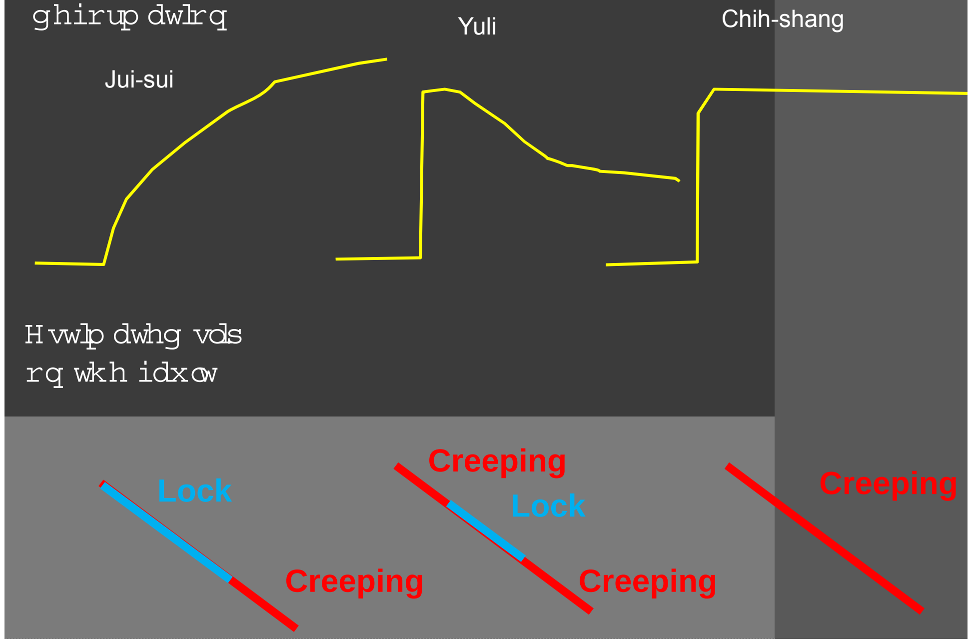

Hvwlp dwhg vds
rq wkh idxow

Outline of presentation

- Rxuprwlydwlrq
  - Why Yuli? Why leveling ? Inter seismic slip and surface deformation
- Whfwrqlf vhwwlqj
  - Taiwan
  - Longitudinal valley
- Ohyhdqj vxuyh|
  - Leveling line and actually survey
  - Result
- Discussion
  - Compared surface deformation
  - Compared GPS
  - Compared hypocenter and 2003 earthquake
  - Compared long term deformation
- Frqfoxvlrq

The creeping in Yuli area

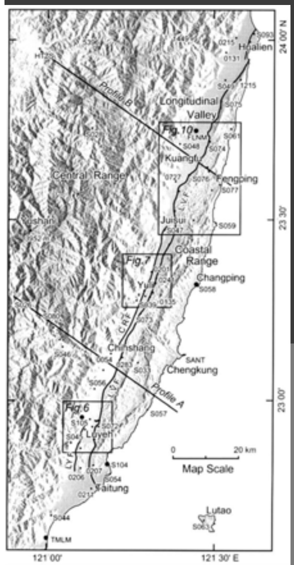

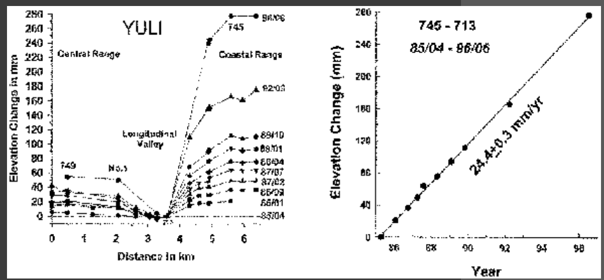

1985-1996

Shui Beih Yu and Long-Chen Kuo, 2001

The uplift rate is 24.4+- 0.3 mm/yr

This data supports to our data

J. Angelier et al., 1997

5336 fkhqj0nxqj hduwktxdnh

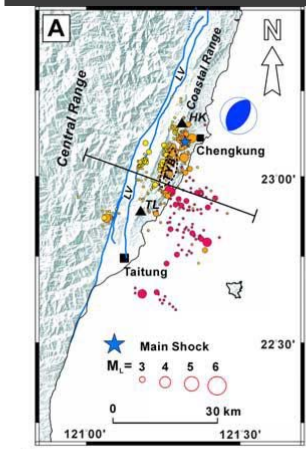

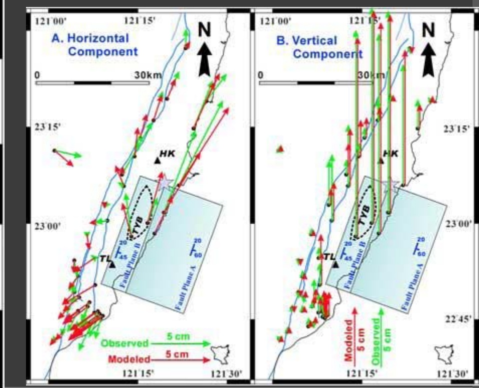

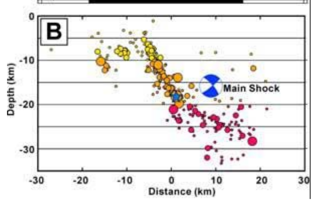

We can estimate the geometry of the fault

Y.M. Wu et al., 2006

Hypocenter

Where is the tip on the LVF ?

➢North segment
a few EQ in shallow
The tip is 20 km depth?

➢Yuli segment
The tip is 10 km depth

➢Sourth segment
The tip is shallow

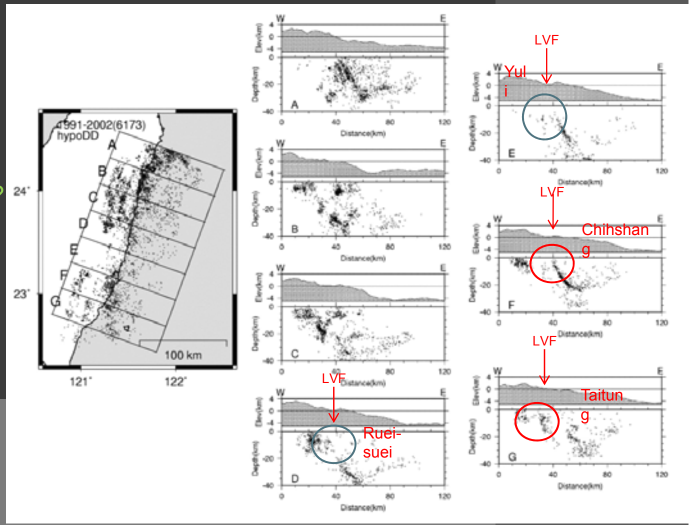

Kuochen et al.,2004

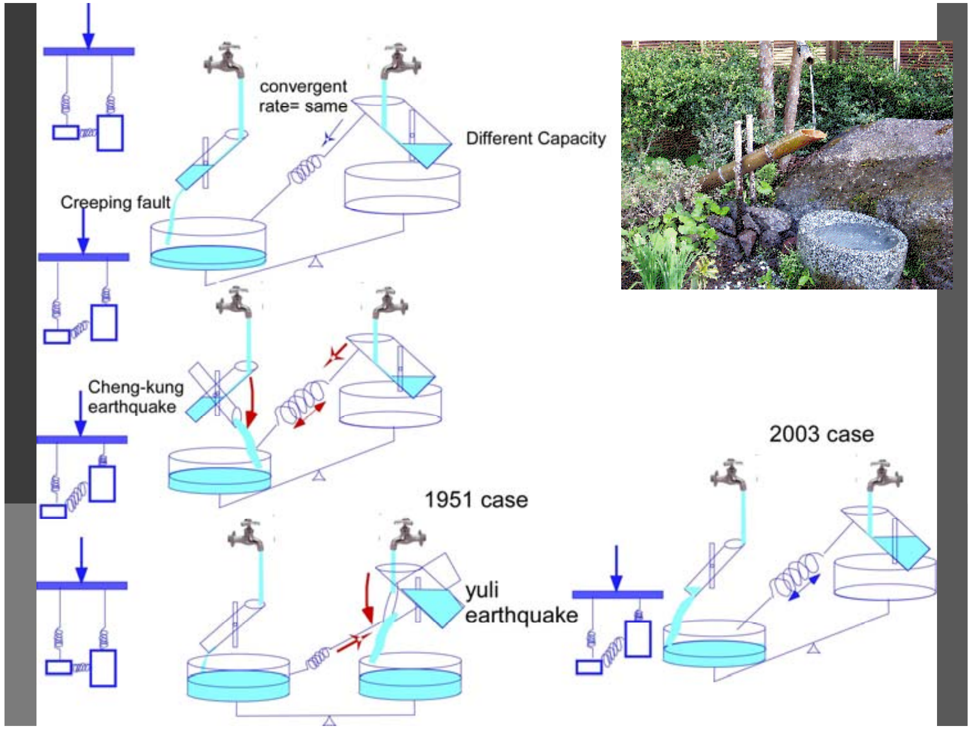

X sdiw udwh dqg sdwhuq dqj wkh frdvwdodqh

Long term (over 1 ka) deformation by the marine terrace
Meng-Long Hsieh Ruey Juin Rau, 2009

4- 10 mm/yr ?

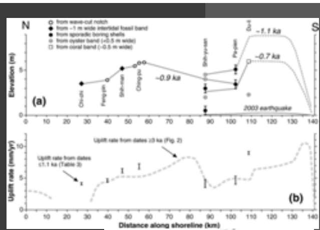

Long term deformation

≈

Coseismic deformation

+

Inter seismic deformation

1- 5 mm/yr ?

2003 Cheng-kung earthquake (co-seismic deformation)

Horng-Yue Chen et al., 2004

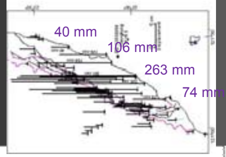

1984-1987 Leveling along the highway 11

Yuan His Lee et al., 2008 (Based on Liu and Yu, 1990)

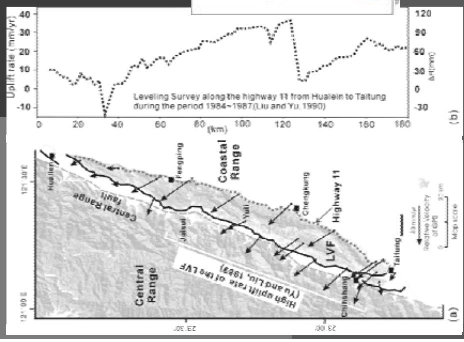

Conclusions

- The vertical deformation of 2.7cm/year were detected by the precise leveling survey during 2008-2009.
- The deformation pattern near the LVF surface trace is similar to the long-term deformation.
- The LVF is locked in deep area and creeping in shallow in Yuli area. Yuli has a asperity. Sometimes the Chengkung (Chihshan) EQ triggers the Yuli EQ

Creeping distribution on the Longitudinal valley fault at Yuli area estimated by precise leveling survey, Southeast Taiwan

Masayuki Murase[1], Nobuhisa Mathuta[2], Jui-Jen Lin[3], Hsin-Chieh Pu[4],
MD ABDUL MATIN[3], Wen-shan Chen[2], Cheng-Horng Lin[3]

1: Department of Geosystem Sciences, College of Humanities and Sciences, Nihon University, Japan
2: Department of Geosciences, National Taiwan University, Taiwan
3: Institute of Earth Sciences, Academia Sinica, Taiwan
4: Institute of Geophysics, National Central University, Taiwan

Abstract

Longitudinal valley faults in eastern Taiwan are commonly considered collision boundary between the Eurasian plate and Philippine sea plate. Yuili fault, one of the active segments of the longitudinal valley faults, is reverse fault with east dip.

We established about 30km leveling route from Yuli to Changbin to detect the vertical deformation in detail (Murase et al. 2009). The installation interval of benchmarks near the fault area is about 100 m. Others were installed every about 300m. Compared to the 2km installation interval of the Geological Survey Institute, Japan for making the map, installation interval of our survey is dense. The precise leveling surveys were conducted in August 2008 and August 2009.

The overview of the deformation detected in the period from 2008 to 2009 is as follows. It was detected about 2.7 cm uplift, referred to the west end of our route, at about 2km region across the fault. Uplift was gradually-reduced with the distance from the fault, and was 1.5 cm at the east coast. In the observation period, there is no significant earthquake in Yuli fault. It suggests the detected deformation as a cause for the creep motion of the Yuli fault.

Mathuta et al. (2009, this WS) will discuss the comparison of the deformation between geological term and geodetic term across the Yuli fault using the dense leveling data. It's an object of this survey to understand not only this but the overall behavior of the Yuli fault. In this presentation, we discuss the creep distribution of Yuli fault.

We adopted a two-dimensional reverse fault model to estimate the creep distribution. As candidates for the source models, we assumed a model with four types of fault model. The geometry of the faults was optimized using the genetic algorithm in order to conform to the leveling data. The goodness of the fit of the four examined models is determined on the basis of Akaike's information criteria (AIC).

The model with two faults was selected as the optimal model from the candidate models.

From our result, it is suggested that the creeping area is shallower than about 10km.

Reference

M. Murase, N. Matsuta, J. J. Lin，H. C. Pu，W. S. Chen and C. H. Lin (2009), Precise Leveling Survey at the Yuli fault, Southeast Taiwan, Proceedings of the institute of natural sciences, Nihon university, 44, 159-166 (in Japanese with English abstract).

Creeping distribution on the Longitudinal valley fault at Yuli area estimated by precise leveling survey, Southeast Taiwan

Masayuki Murase*, Nobuhisa Mathuta, Jui-Jen Lin, Hsin-Chieh Pu,
MD ABDUL MATIN, Wen-shan Chen,
Cheng-Horng Lin

* Department of Geosystem Sciences,
College of Humanities and Sciences,
Nihon University, Japan

Previous leveling survey at Yuli

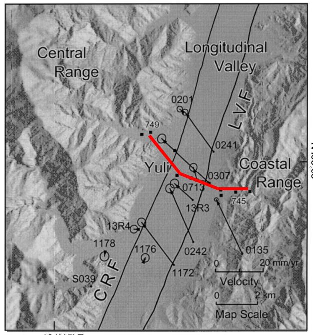

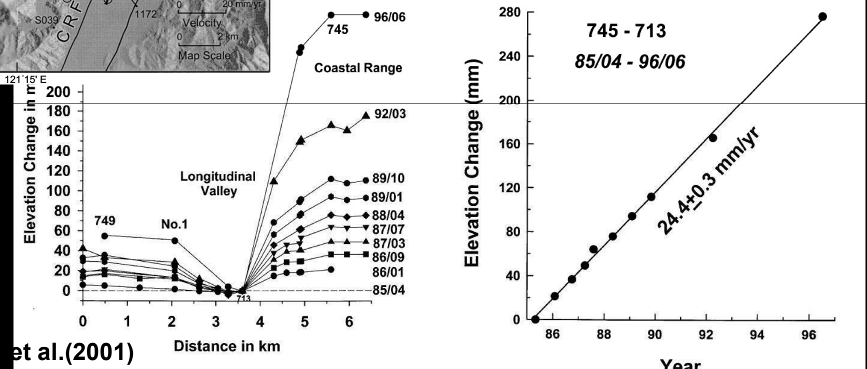

et al.(2001)

Fig. 8. Elevation changes of benchmarks relative to BM 713 in the

6 km route is too short to discuss the creeping at Yuli fault in detail

purpose of our research

- Yuli fault has a potential of earthquake occurrence?

purpose of our research

- Yuli fault has a potential of earthquake occurrence?

Leveling route in Yuli area

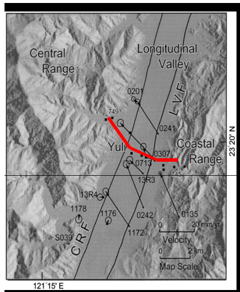

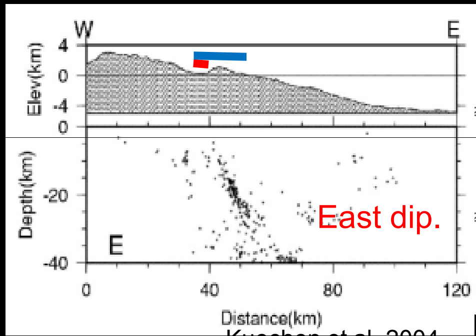

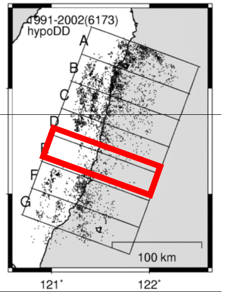

[redacted]

Projection on a single plane of N70W

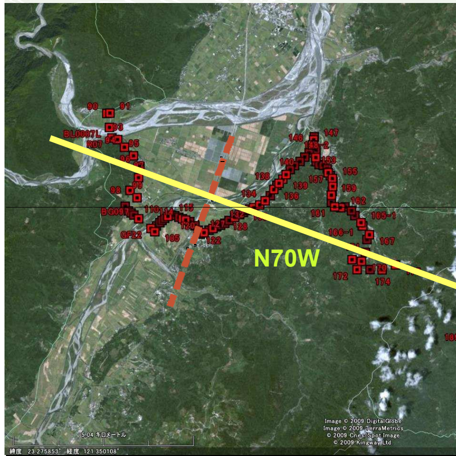

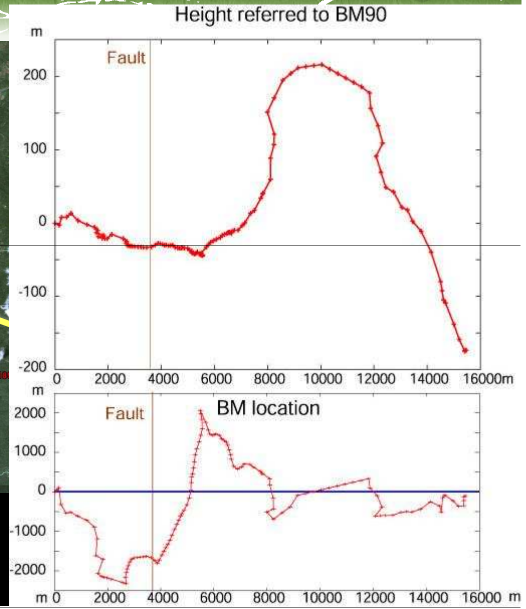

Leveling route in Yuli area

[redacted]

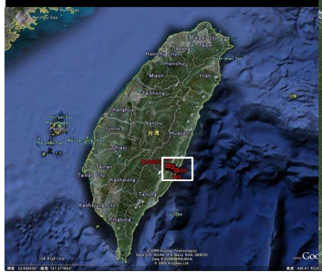

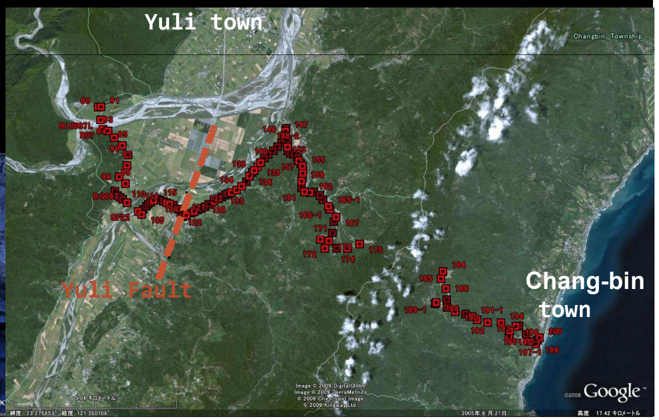

Vertical deformation (Aug. 2008–Aug. 2009)

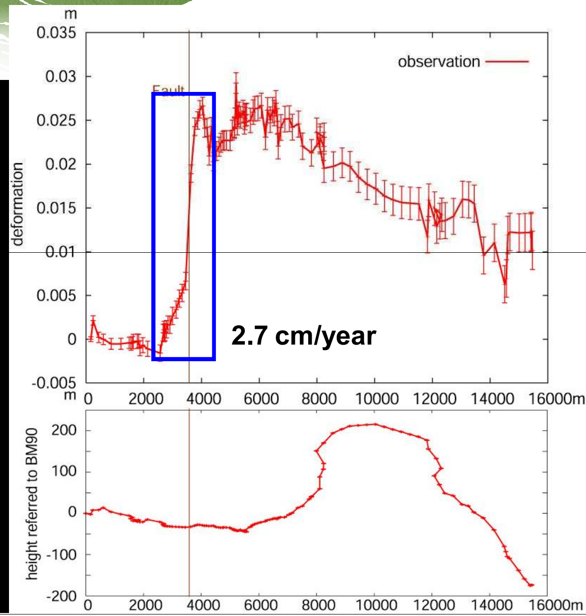

Closing error

Leveling route was measured two times

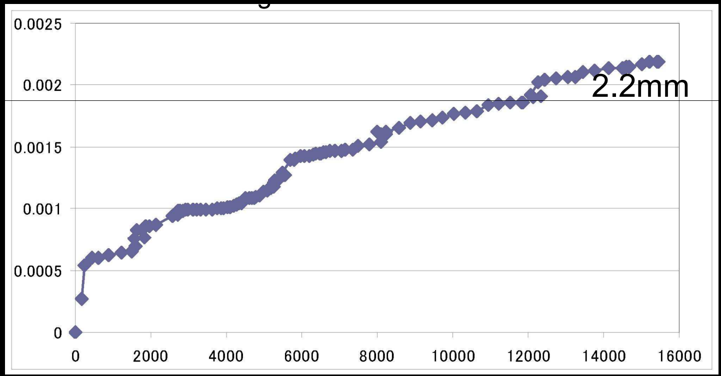

Comparison with the previous study

Aug. 2008-Aug. 2009

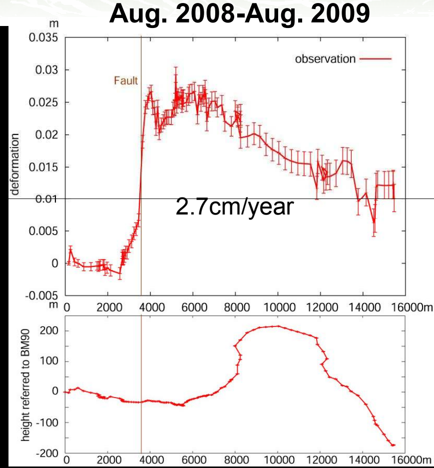

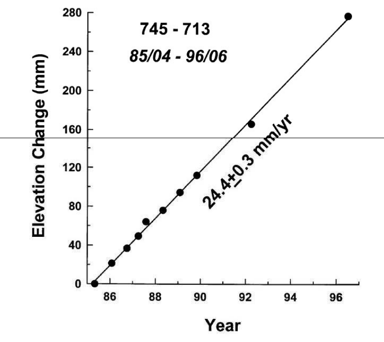

Fig. 9. Time variation plot for elevation changes between BM 745 and BM 713 from 1985 to 1996.

Checking the influence of refraction

Refraction error increases in proportion to the observed height

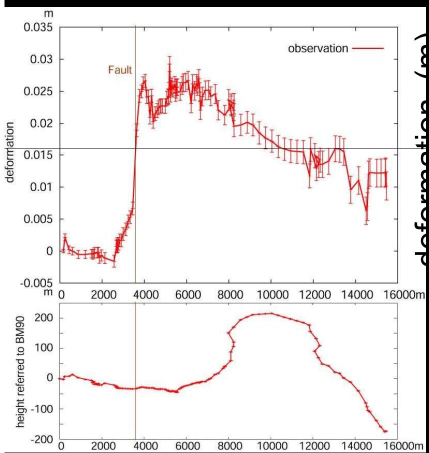

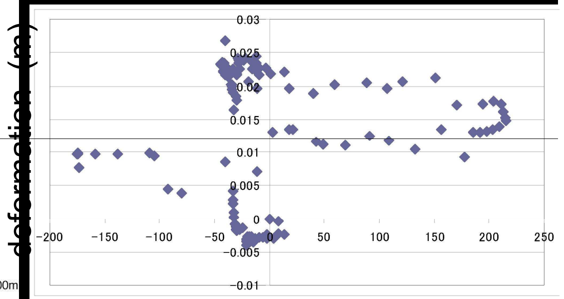

Model selection

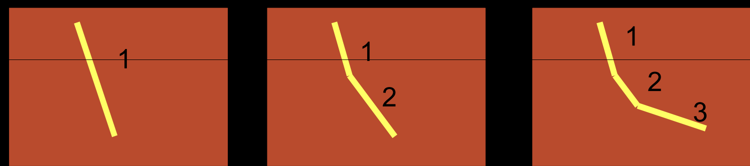

Model selection

We estimated following parameters.

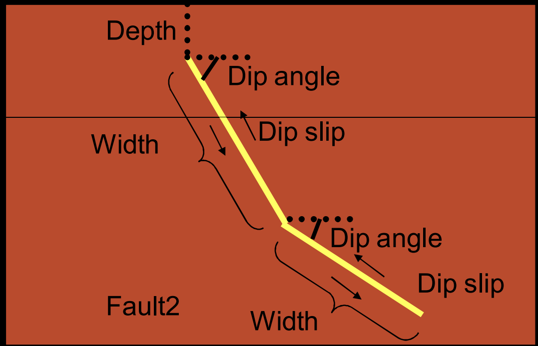

Two faults model

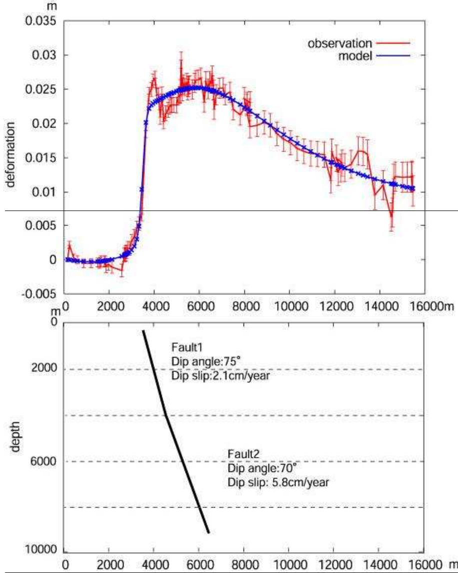

Creeping area shallower than 10 km

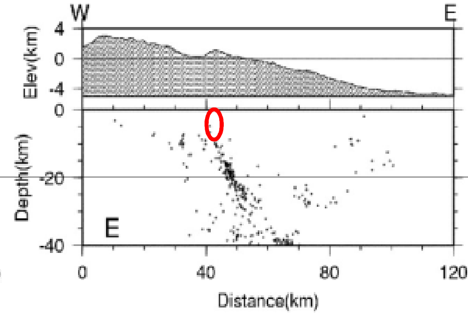

Yuli fault deeper than 10 km may be accumulating the strain?

We should check the resolution of our model.

Modeling of the creeping distribution

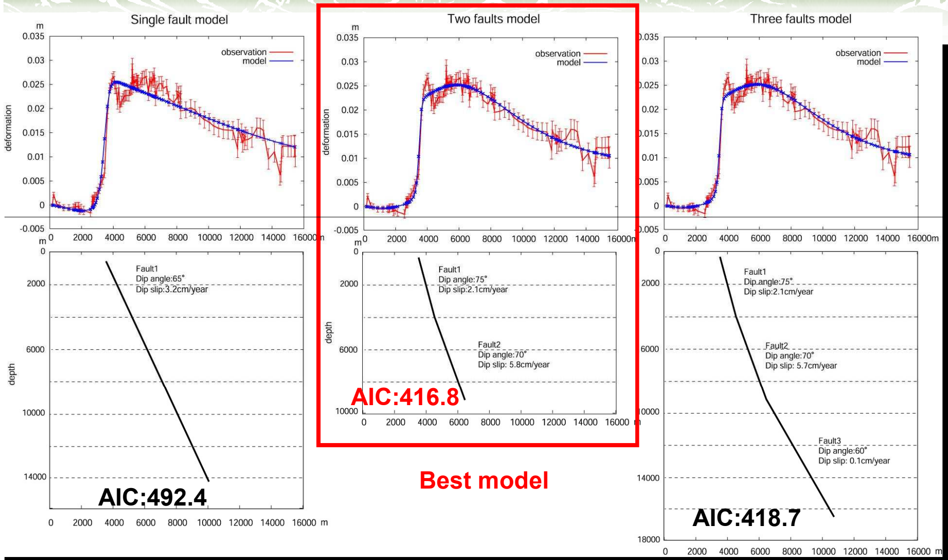

Best model

Resolution check

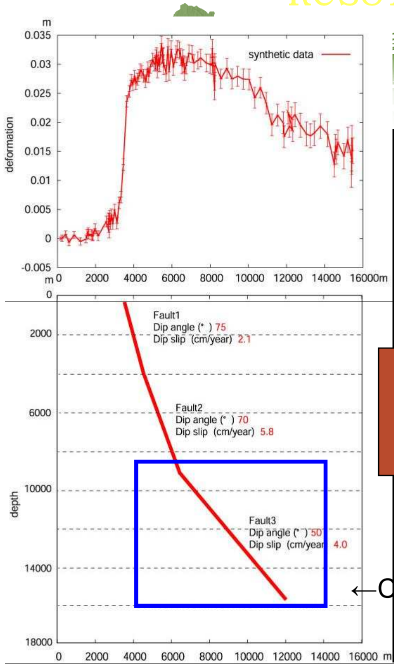

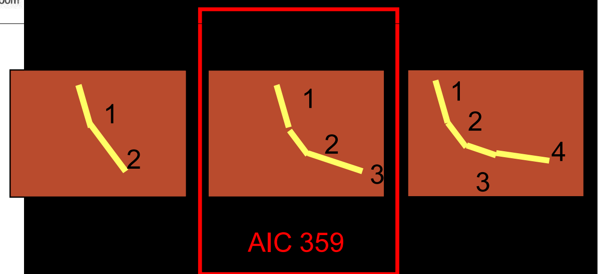

Resolution check

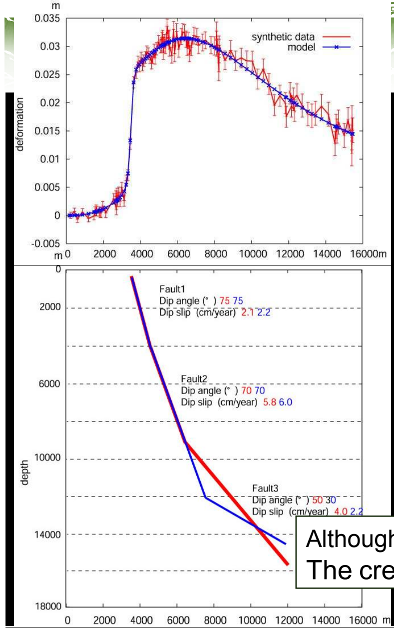

		assumption	estimation
	Location (m)	3500	3500

Although it is difficult to estimate fault parameter in detail,
The creeping deeper than 10km can be detected.

P-wave tomography at SAF

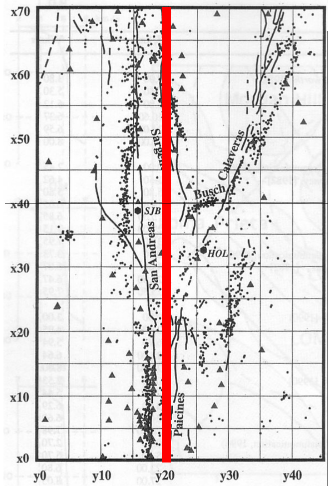

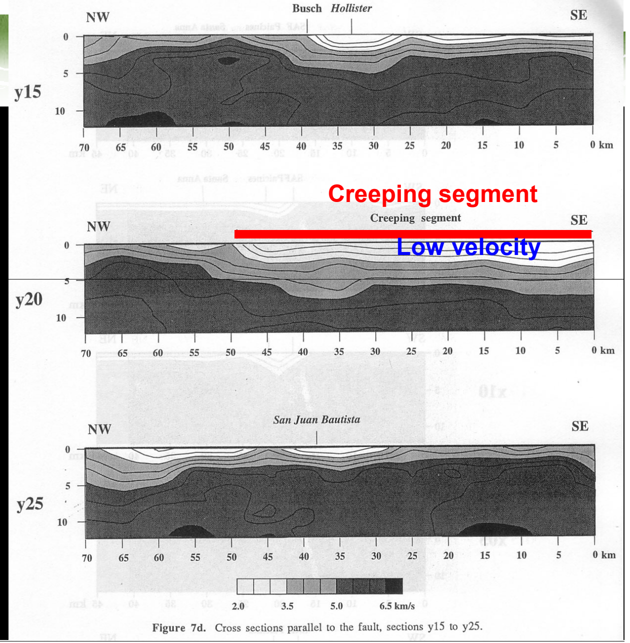

Comparison with P-wave tomography

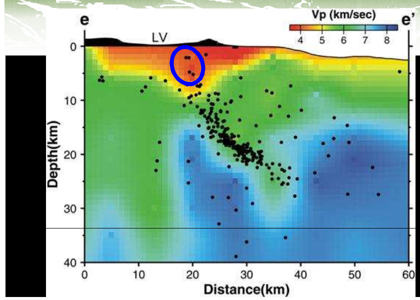

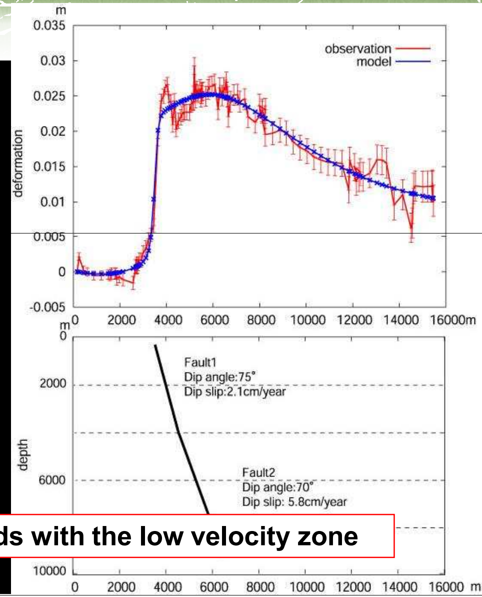

- Low P velocity zone shallower than 10km (Wu et al.,2007)
- Creeping area estimated the leveling is also shallower than 10km.

Creeping area corresponds with the low velocity zone

P-wave tomography at Atotsugawa fault

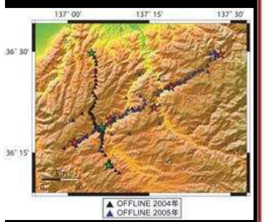

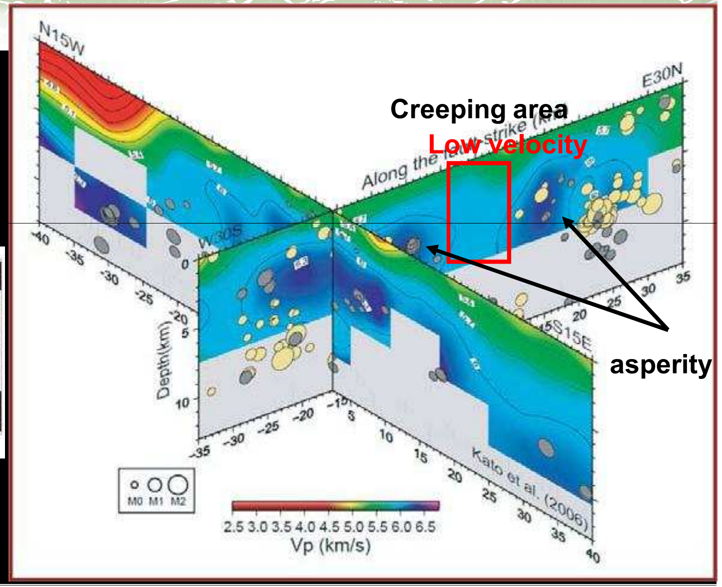

Creeping area shallower than 10 km

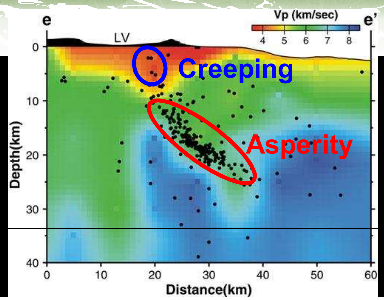

(Wu et al.,2007)

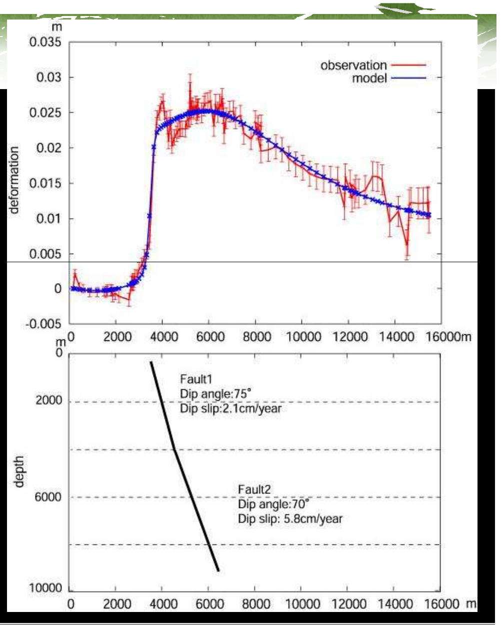

•Creeping area estimated the leveling is also shallower than 10km.

•Yuli fault deeper than 10km may be fixe and have an ability of earthquake occurrence.

Summary

[redacted]

lateral variation of creeping velocity.

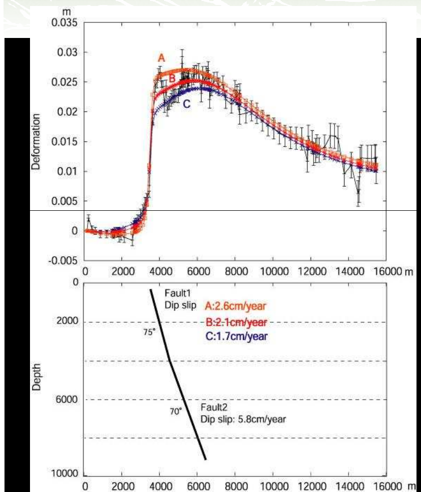

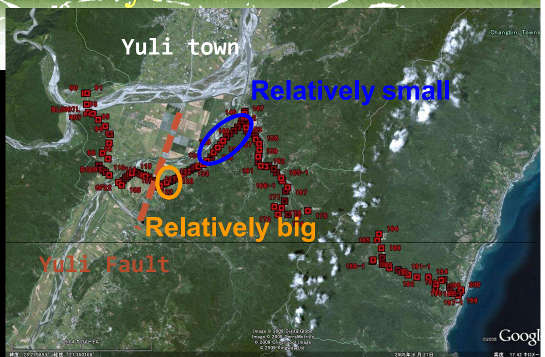

Is the creeping area really shallower than 10km?

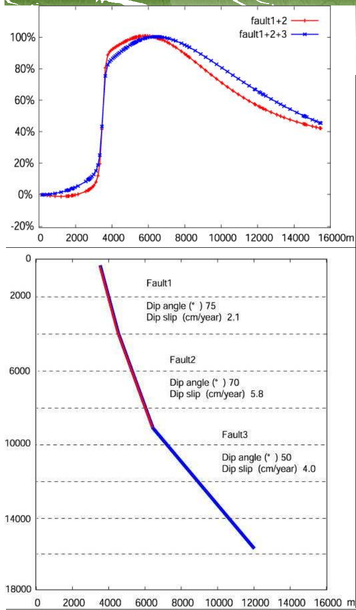

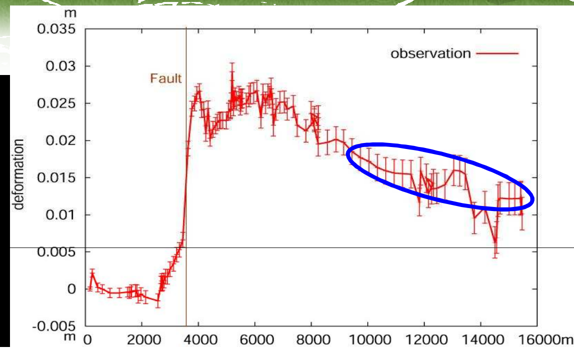

The deformation near the coast area is important to discuss if the creeping area deeper than 10km is present.

Chengkung earthquake ruptured Chihshang Fault

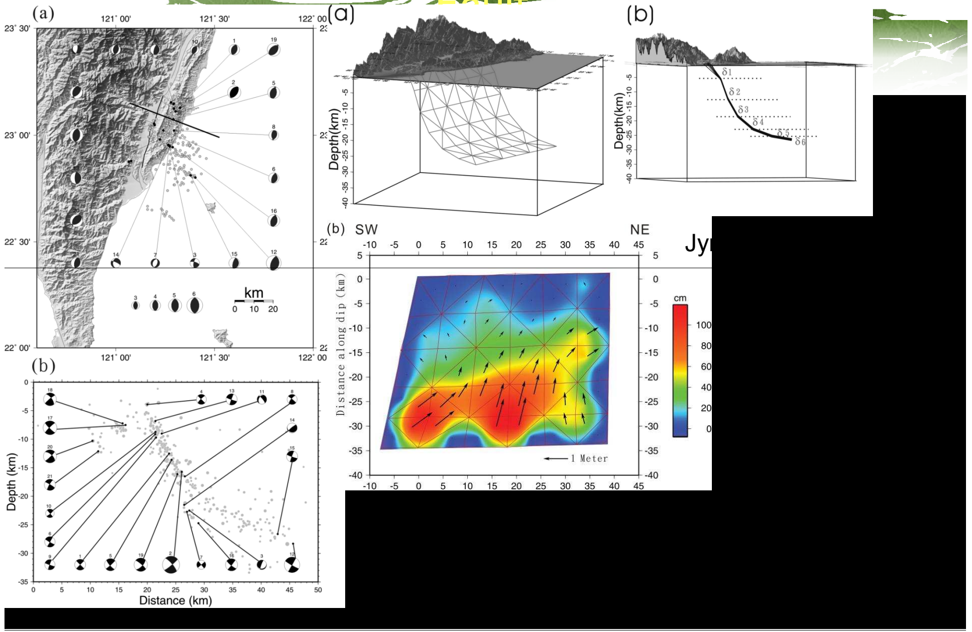

BOREHOLE STRAIN AND GPS STRAIN IN EASTERN TAIWAN

Chiching Liu
Inst. Earth Sciences, Academia Sinica

Abstract

Dense deployed borehole strainmeter networks have been setup in some fast deformed areas in Taiwan; some of them have been stabilized and get rid of the borehole relaxation effects. Tectonic related signals in strainmeter data can be interpreted with other geophysical observations, especially with GPS. Baseline changes and relative site displacements from GPS observations usually interpreted as local crustal strain based on the uniform strain or locked-fault deformation assumption. Fault patch creeping, silent earthquakes, slow earthquake and some micro- earthquakes can break this assumption, and mislead to a false interpretation. Borehole strainmeter data among GPS network can help to identify the real strain accumulation or just a block motion displacement between GPS sites. These two different cases can lead to completely opposite interpretation – increasing or decreasing in seismic risk.

For a strainmeter network (3 stations, RNT, RST and ECT) near a reservoir in southern-west Taiwan, the orientations of major strain axis of all 3 sites keep stable during 2004 and 2006.5 ~ 2007.5, but experienced a rotation of 90 degree during 2005 ~ 2006.5. These occurred on all 3 stations, and probably a process of the exchange of the direction of major and minor strain axis.

Permanent GPS observations over the same area are used to perform the strain daily time series, either in linear strain, areal strain and orientation of principal strain axes format, can be compared with the borehole strainmeter observations. Strainmeter data showed slower strain accumulation than the GPS strain during 2004 while several slow events occurred, and keep similar accumulating rate during 2005-2007. GPS strain shows consistency and inconsistency with borehole strain. The slow events showed in borehole strainmeter data may play an important role.

Strainmeter data at several sites in west Taiwan also experience a train drop during the surface wave arrival of Wen Chuan earthquake (M=7.9) in May 12, 2008. Areal strain in these sites were increased up to 0.1 μstrain during surface wave passage. We are still looking for some proper interpretations.

Borehole Strain and GPS Strain in Eastern Taiwan

8th Taiwan-Japan Joint Workshop on Hydrological Research for Earthquake Prediction

Chiching Liu

Inst. Earth Sci., Academia Sinica

Sept. 29, 2009

GPS & Strainmeter networks

- ● = GPS sites
- ★ = Borehole strainmeter sites
- \+ = Planned Borehole strainmeter sites

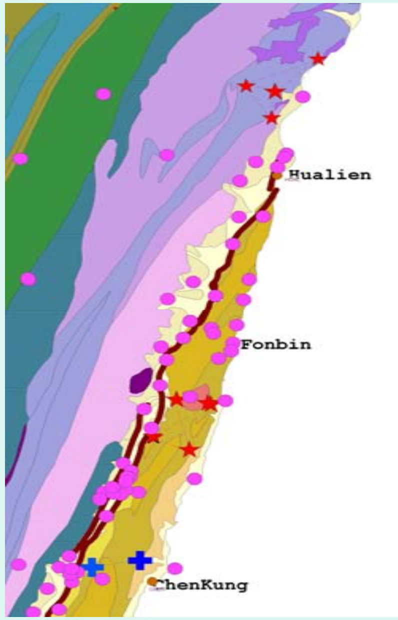

Borehole Strainmeter

Borehole strainmeter :

- PBOT: Integrated Geodetic Networks
- Slow Events: minutes to days
- Tremors
- Principal strain axes rotation
- Detection of Pre- and post-seismic stress redistribution
- Abrupt change of strain —— local or neighbor seismic event
- Strain Seismometer
- Rotational Seismometer

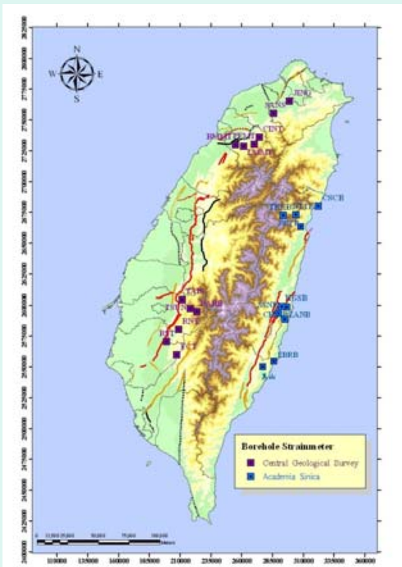

GPS Site Velocities

GPS LAB by L.C. Kuo
http://gps.earth.sinica.edu.tw/images/ppt/horizontal_velocity_s01r_2007-2008.gif

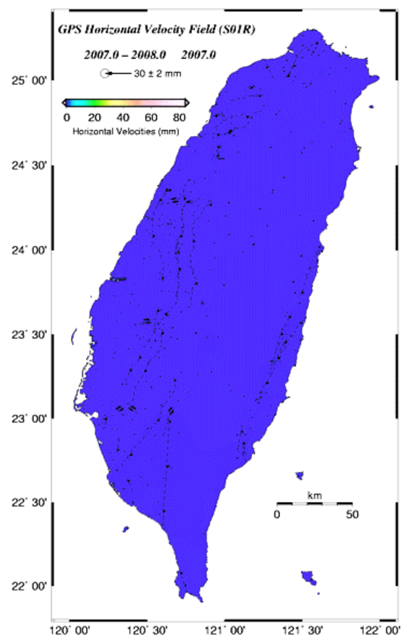

Velocity Gap

- 8cm/yr Overall
- 2cm/yr Over Coastal Range
- Integrated Geodetic Networks for over 20 years
- Low Seismicity on Costal Range

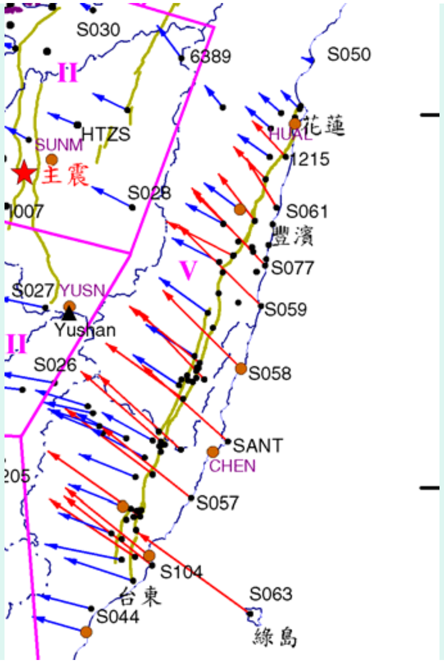

Chimei Strainmeter Network

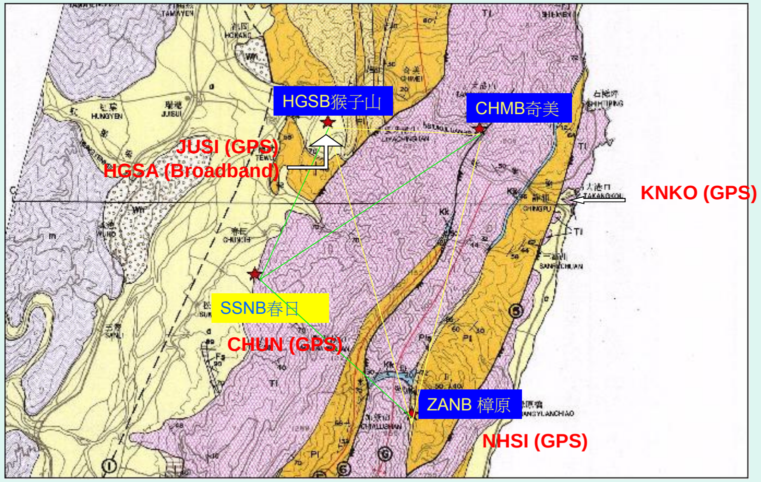

Local Seismicity

•Max. M_L < 7.5 During 1900-2009

•At Nakai, Japan; 3 M≥ 8.0 Earthquakes in 20th Century

•Seismicity Gap in this region

2004年12月3日Slow Earthquake

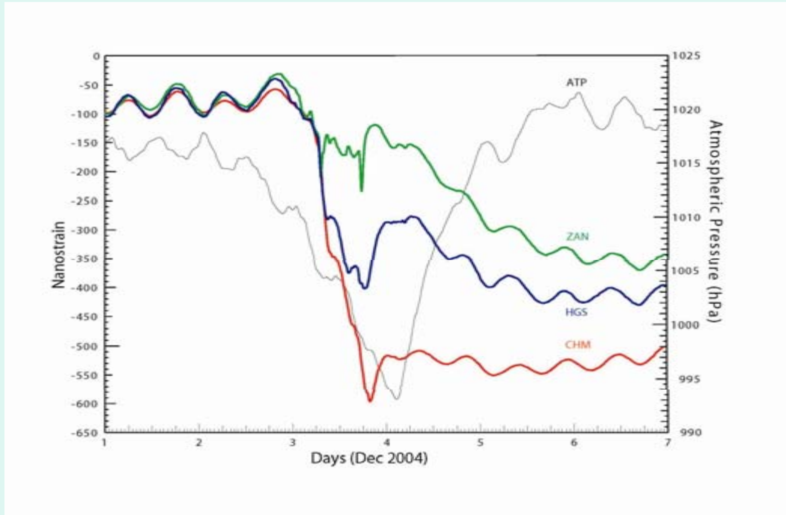

Dislocation Modeling

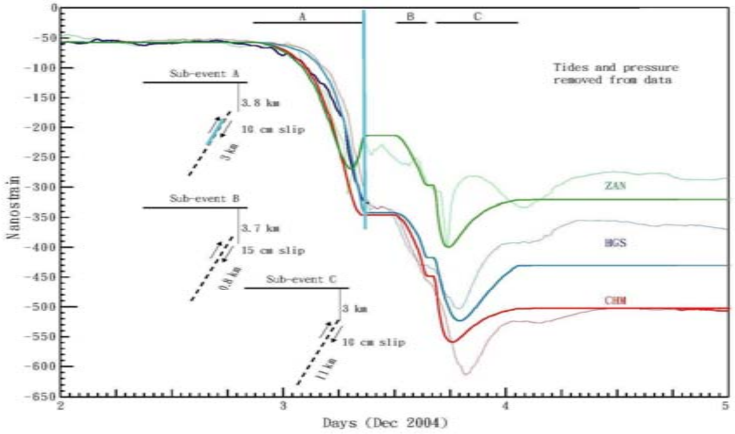

Dislocation Modeling

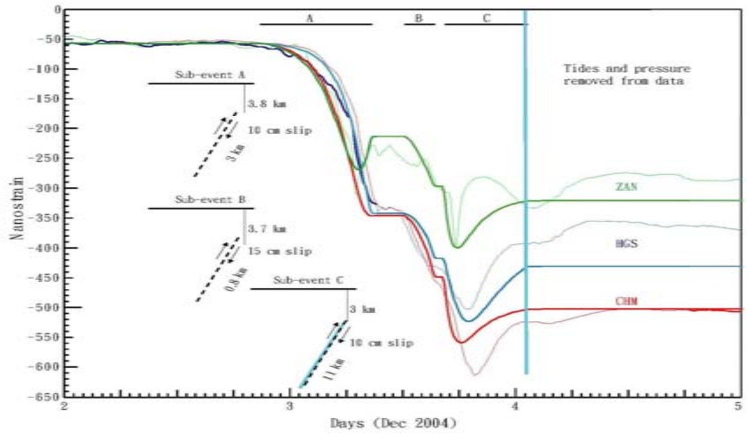

Dislocation Modeling

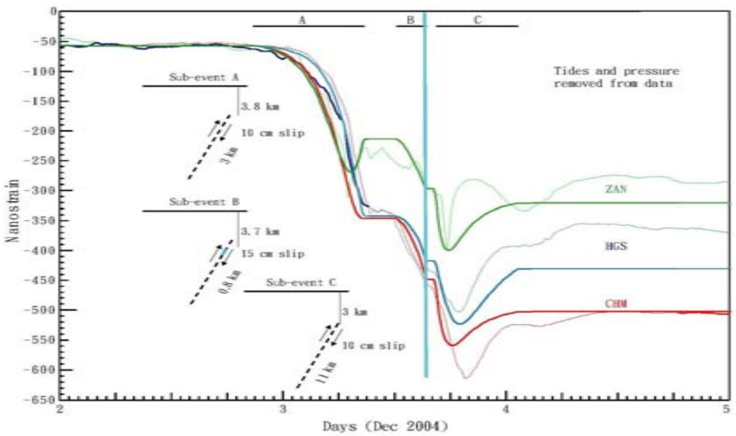

Borehole Strain 2003~2007

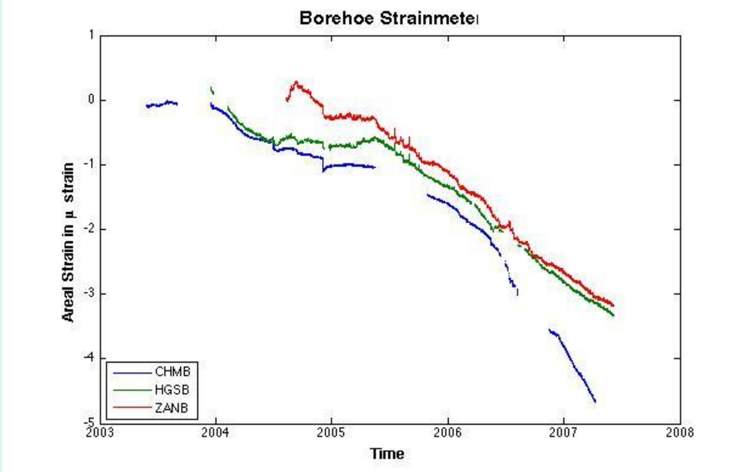

N
E
T
W
O
R
K

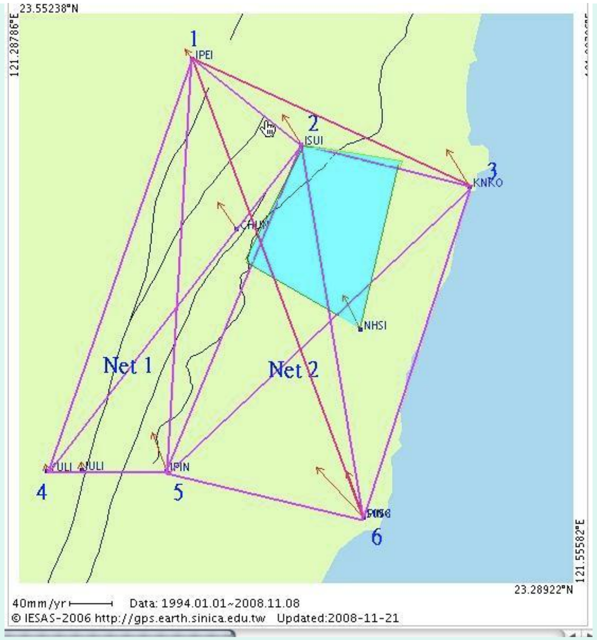

GPS Baseline Strain JPEI-KNKO

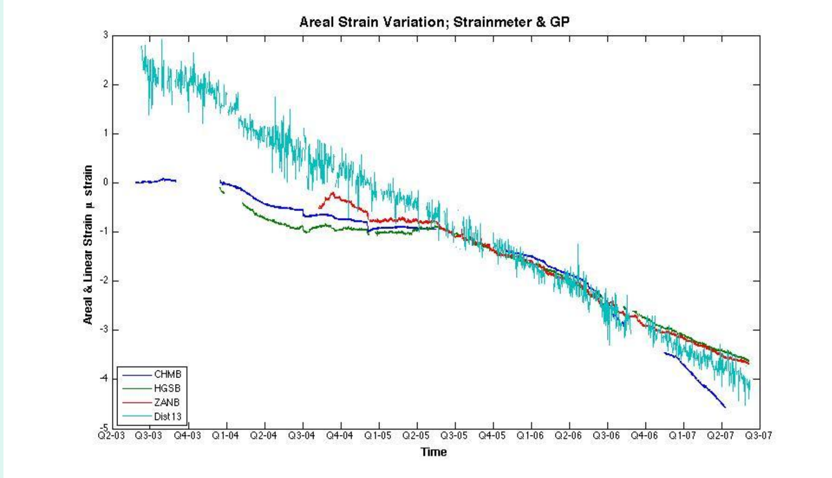

Areal Strain All Sites

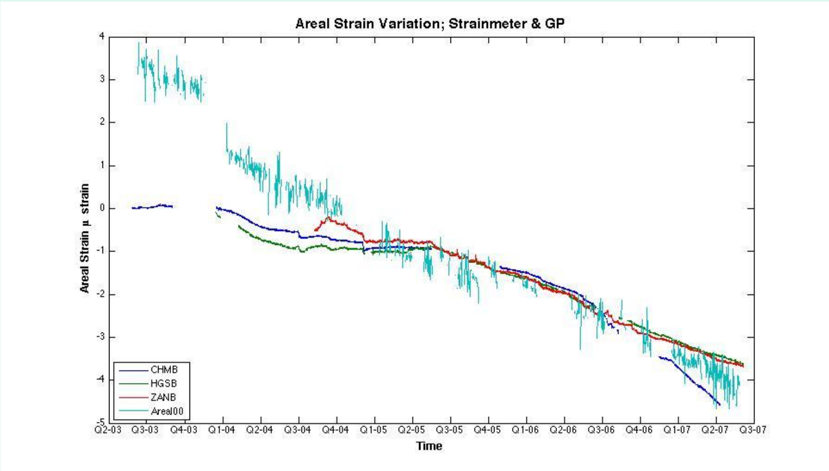

Strain Sites in S. Western Taiwan

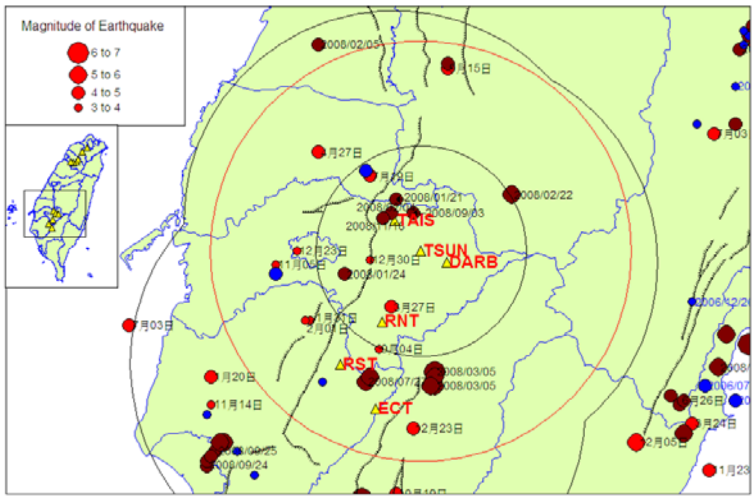

Areal Strain in Eastern Taiwan

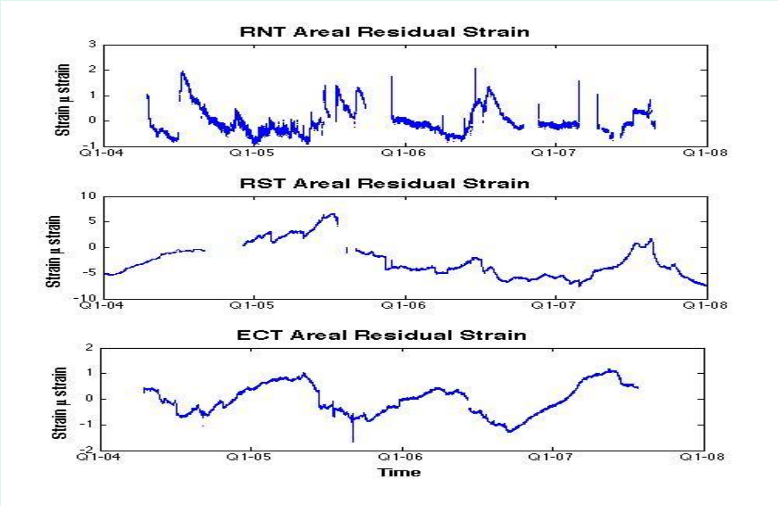

Orientation of Principal Strain Axis

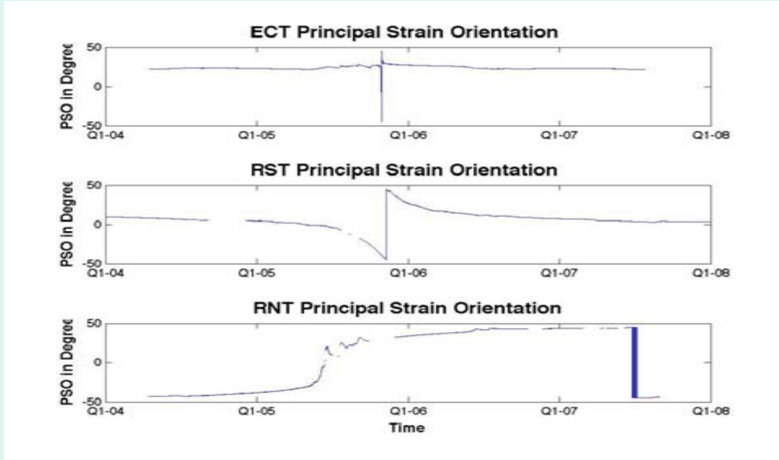

Engineer Shear Strain γ_1 & γ_2

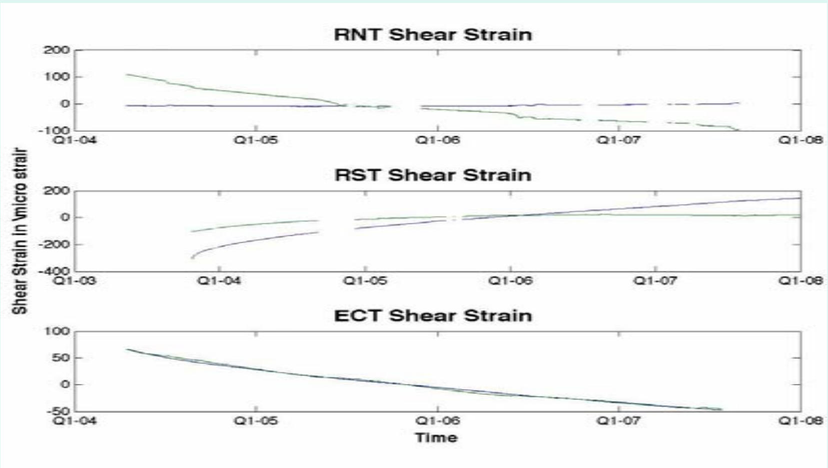

- γ_1 ; γ_2

Strain seismography

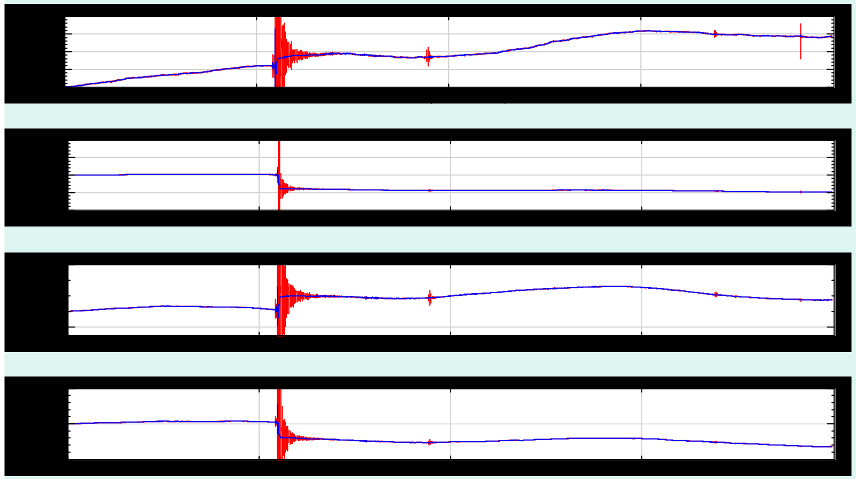

Chen et al., 2009, will be submitted to GRL

512 Wenchuan earthquake

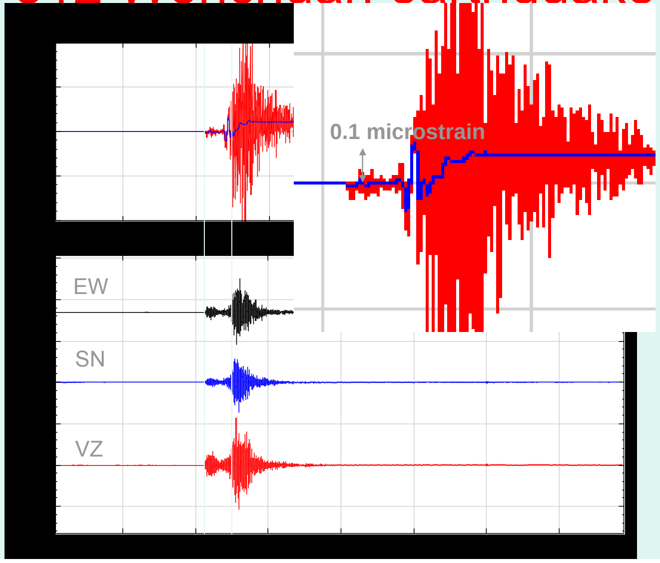

FIN

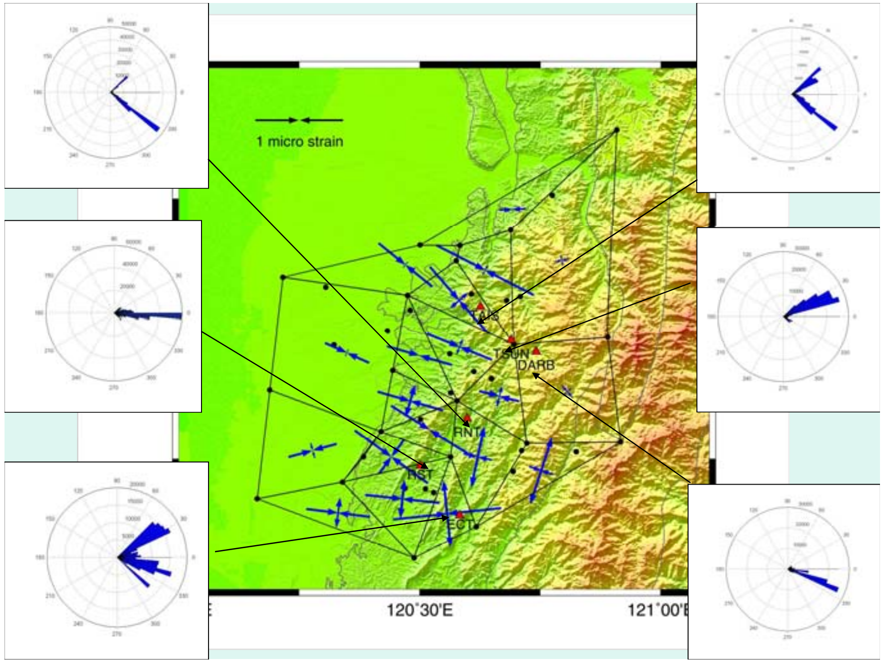

Structure of long-term sealing in the fault zone during aseismic period – examples from the Chelungpu fault in Taiwan

Kuniyo Kawabata and Kuo Fong Ma
National Central University

Abstract

Earthquakes occur repeatedly with certain time intervals on same fault. Such earthquake recurrence is explained by the strain buildup and release hypothesis (Reid, 1910), which leads to the concept of seismic cycle. To buildup the stain, it is required that fault zones strengthen between earthquakes. The strength of fault is recovered with porosity decrease by mechano-chemical processes: (i) Rapid deposition of minerals in cracks and pores; (ii) Mineral sealing in cracks and pores; and (iii) Pressure solution (e.g. Boullier et al 2004; Tanaka et al., 2007; Kawabata et al., 2007). It appears that rapid deposition occurs simultaneously with slip/fracture of rock, which are inferred by the texture of floating fragments suggesting that fragments were supported by surround depositional minerals before it were sank. Mineral sealing occurs mainly in a breccia zone by fluid infiltration through aseismic period. Pressure solution is the creep mechanisms consist of three basic processes of dissolution, transfer and deposition, and occurs through aseismic period. These processes are promoted under presence of water and cause mass transfer. These processes change properties in fault zone by mass transfer as well as healing fault zone. Healing and the relevant material changes in fault zone play a key role in evolution of a fault and estimating the earthquake cycle.

Chelungpu fault is the active fault occurred big earthquake (magnitude 7.7) in Chi-Chi Taiwan, in 1999. Taiwan Chelungpu fault Drilling project (TCDP) drilled two vertical holes (hole A and B) and one side-track hole from hole B (hole C). Pressure solution has been observed in drilled samples from hole B through the Chelungpu fault (Boullier et al 2004; Gratier and Gueydan, 2007). Rapid deposition of nano-scaled quartz grains has reported in samples recovered from drilled hole C penetrated to Chelungpu fault (Ma et al., 2006; Tanaka and Ma, 2007 AGU abstract). This sample from hole C keep whole structures including a primary slip zone and other old slip zones. The observation of each slip zone enables us to infer history of faulting and healing of the Chelungpu fault. We will present the evolution of the Chelungpu fault by micro structural observation focusing on sealing structures using the samples from hole C.

Structure of long-term sealing in the fault zone during aseismic period – examples from the Chelungpu fault in Taiwan

Kuniyo Kawabata

Kuo Fong Ma

National Central University

Earthquake cycle

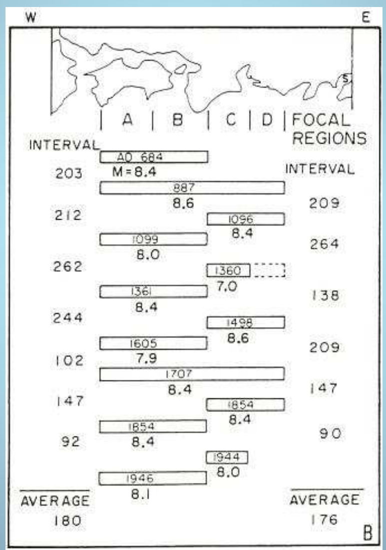

[Scholz 1990 (based on Ando 1975)]

Earthquake cycle hypothesis

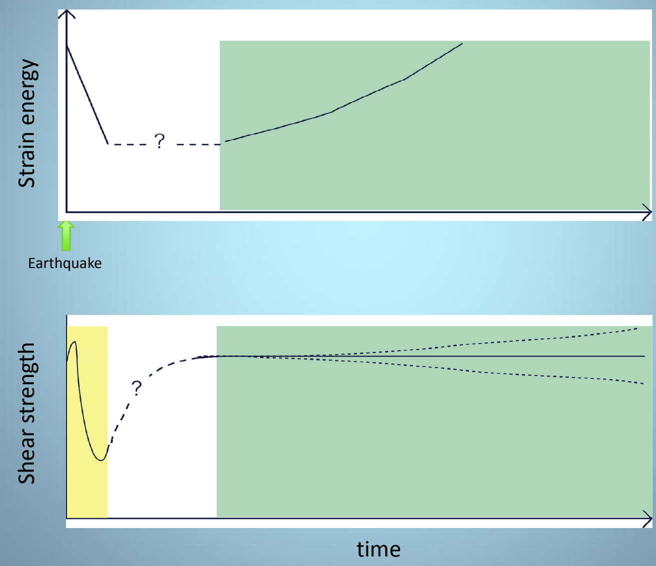

Sealing of fault zones

- Sealing
  - Mechanical compaction
  - Rapid mineral deposition
  - Mineral sealing in cracks and pores
  - Pressure solution

Rapid mineral deposition

[Sakaguchi, 2004] From OST in Okitsu mélange of Shimanto accretionary complex

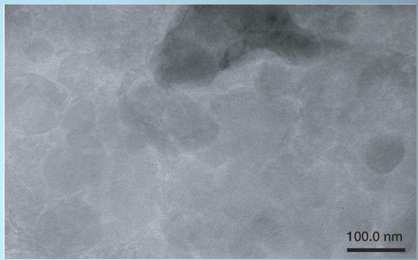

[Ma et al., 2006] from Chelungpu fault

Pressure solution

From Shimanto accretionary complex

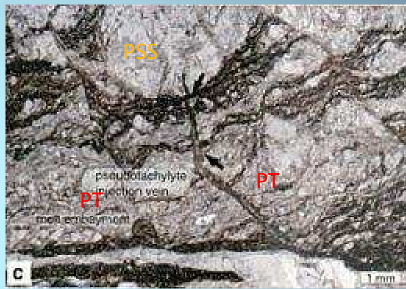

[Sakaguchi, 2004] From OST in Okitsu melange of Shimanto accretionary complex

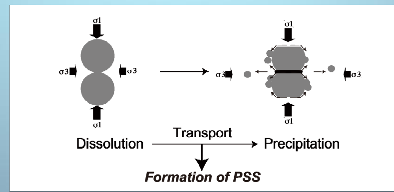

[Kawabata et al., in press]

Mineral sealing

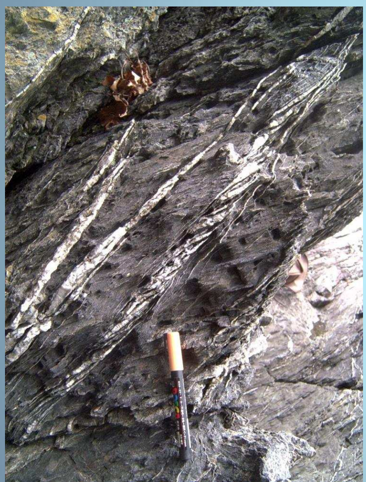

From near Nobeoka fault in Shimanto accretionary complex

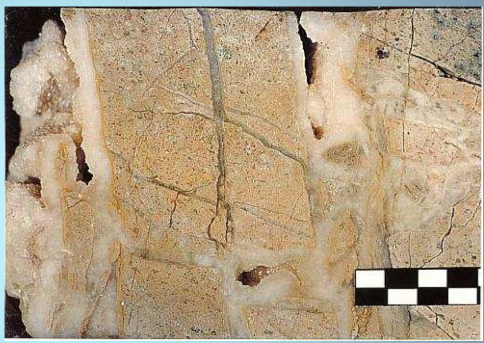

[Tanaka et al., 2001] From Nojima fault

Sealing of fault zones

- Sealing
  Mechanical compaction, Rapid mineral deposition --- short time
  Mineral sealing in cracks and pores, Pressure solution--- long time

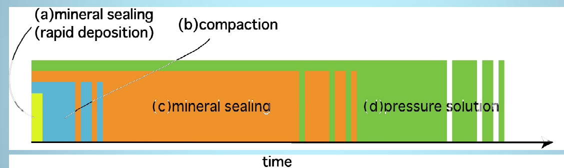

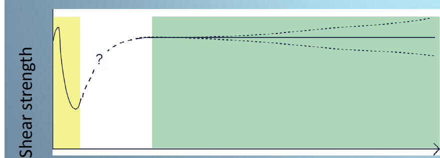

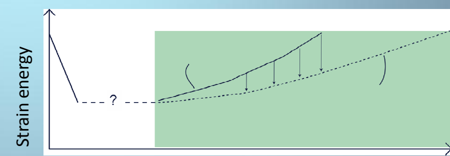

TCDP drill hole

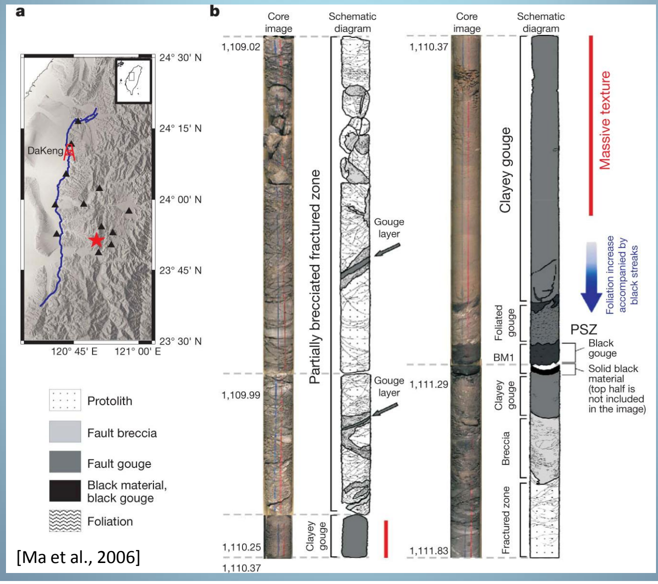

Microscopic observation 1

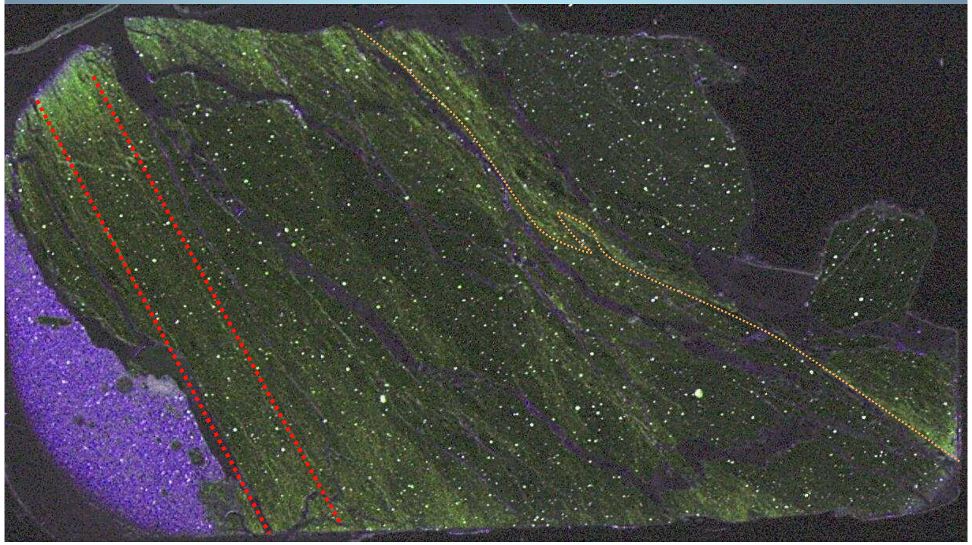

TCDP hole C

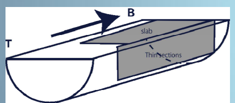

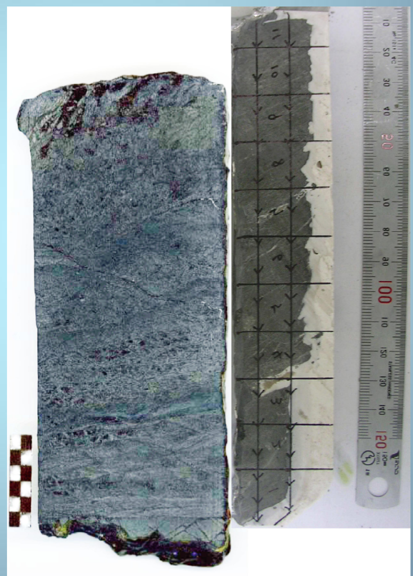

Microscopic observation 2

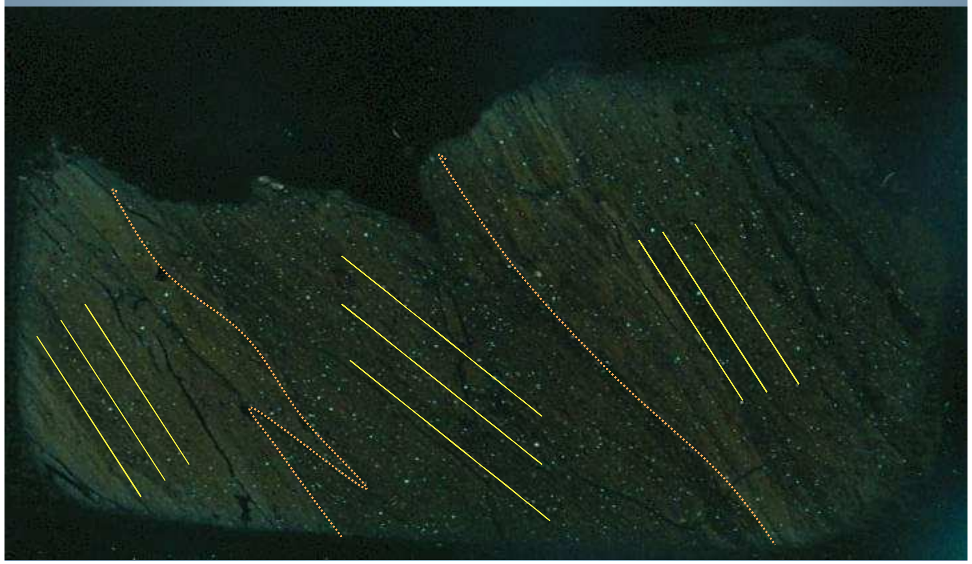

Microscopic observation 3

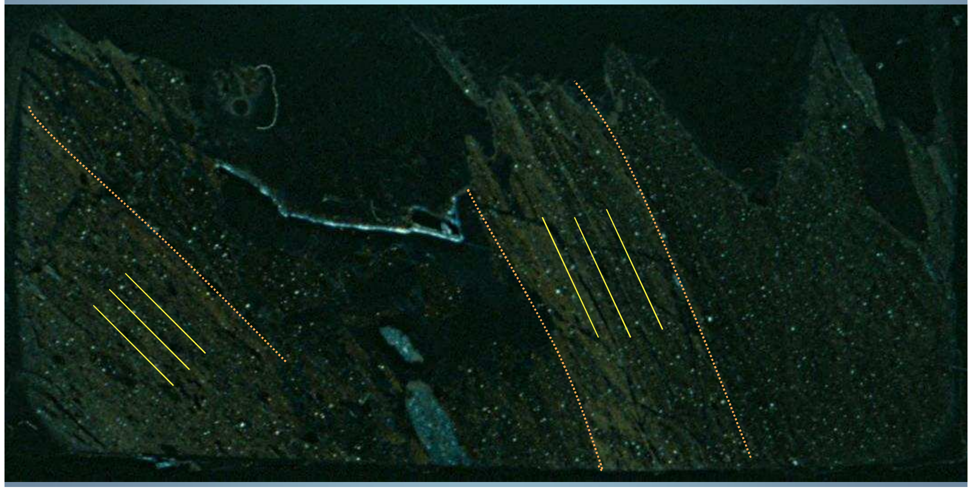

Microscopic observation 4

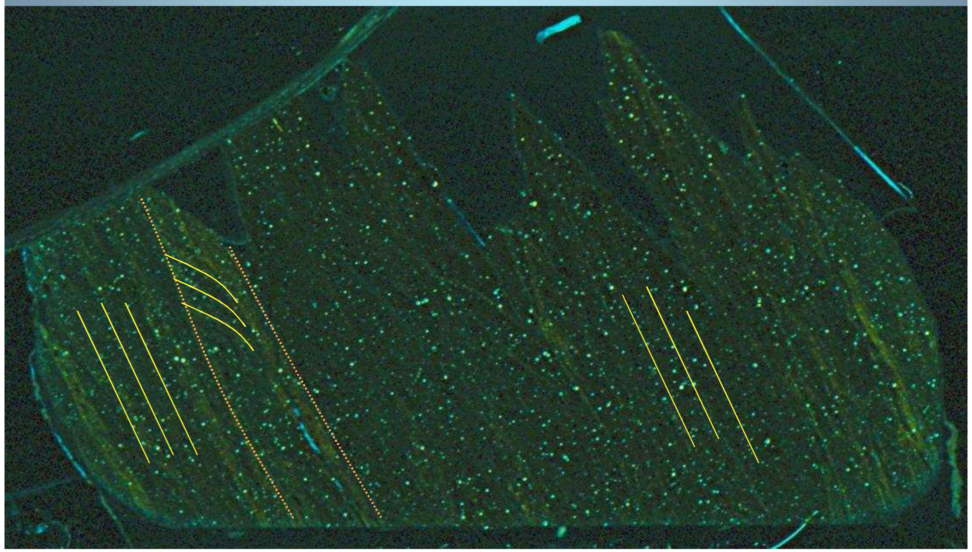

Summary of observation

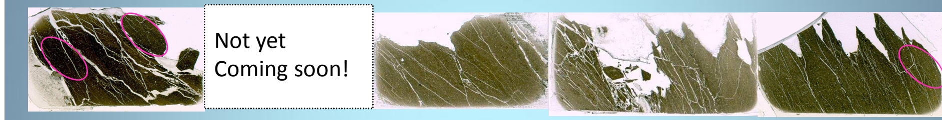

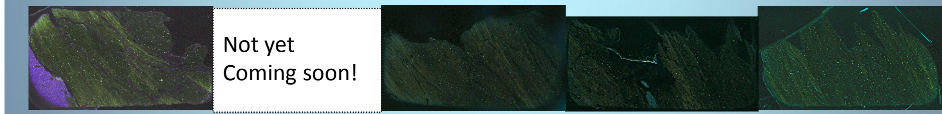

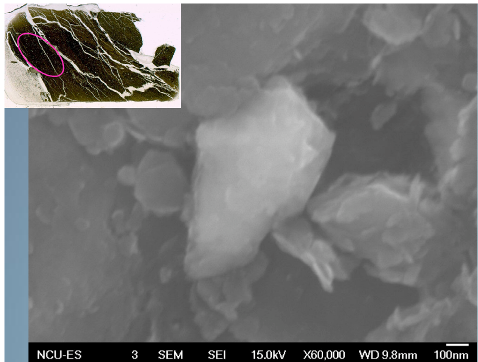

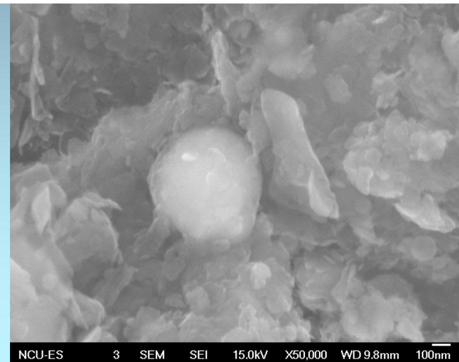

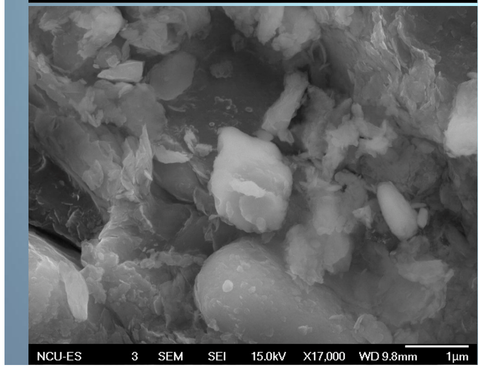

Zircon ($ZrSiO_4$)

Fine grained by comminution?
Rounded by comminution?

My first impression
A lot of accessory minerals are included in slip zone

Need to compare it between fault zone and host rock

Interpretations of history

- Slip
- Rapid quartz precipitation in slip zone
- Alternation (clay mineralization) by fluid infiltration in slip zone and along the cracks
- Calcite precipitation in small cracks
- Pressure solution in brecca zones
- Mass transfer (SiO_2) by pressure solution

No less than 3 times

Semi-continuous groundwater gas monitoring system at Kashima observatory

F. Tsunomori
Laboratory of Earthquake Chemistry, Graduate School of Science, The University of Tokyo

Abstract

Dissolved gas concentration in groundwater must be an indicator of stress state of a fractured aquifer adjacent to an active fault. Radon and methane concentration are especially important species, and it is essential to compare gas concentration changes with permeability changes for reliable development of geochemical earthquake prediction. We propose a semi-continuous groundwater gas monitoring system in order to record absolute values of gas concentration with the permeability of the aquifer. In addition, preliminary results measured at Kashima and Kamakura observatories are presented.

Semi-continuous groundwater gas monitoring system at Kashima observatory and Kamakura observatory

F. Tsunomori[1] and M.C. Kuo[2]

[1] Laboratory of Earthquake Chemistry, Graduate School of Science, The University of Tokyo
[2] Department of Mineral and Petroleum Engineering, National Cheng Kung University

Background and Approach

Cape No.7, the best movie of 2008

Outline

- Background and Approach
- Hypotheses and Requirements
- Groundwater Sampling
- Gas Analysis by QMS
- Chemical Monitoring Project in Taiwan
- Summaries

Izu-Oshima Kinkai EQ, 1978

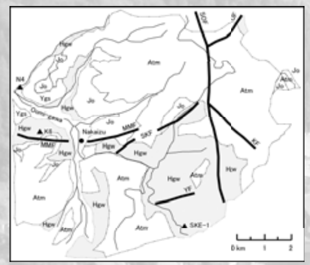

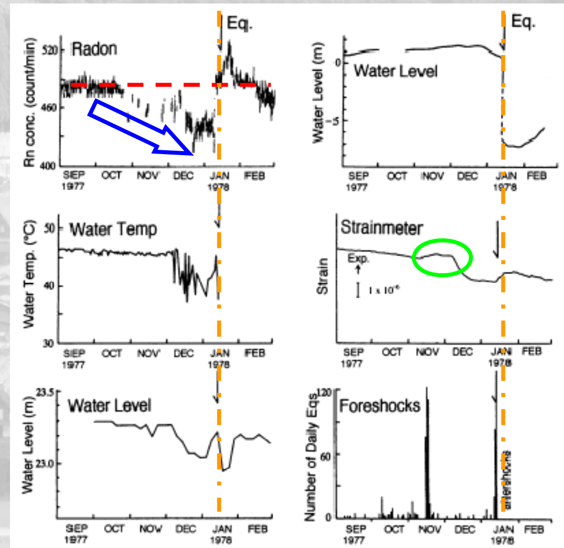

$$C_w = \frac{1}{HS_g + 1} C_0$$

Kuo et al. (2006)

Wakita et al. (1980,1996)

Radon Partitioning Experiment

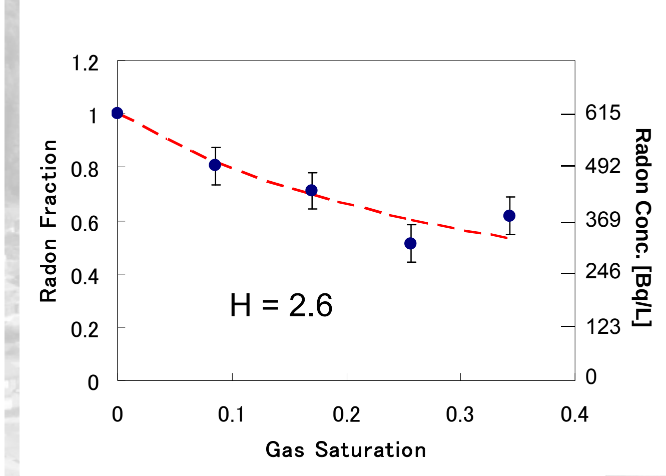

$$C_w = \frac{C_0}{HS_g + 1}$$

S_g	Cw	Fraction
0	615	1
0.085	495	0.804
0.170	437	0.711
0.256	315	0.512
0.342	379	0.617

Tsunomori and Kuo (in press)

Hypotheses and Requirements

Lao-Shi gate

Result

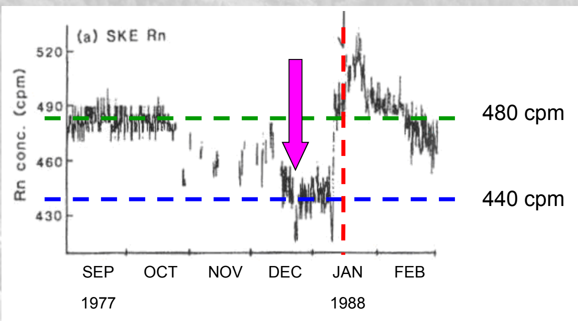

$$C_w = \frac{C_0}{HS_g + 1}$$

$S_g = 0.035$

Wakita et al., 1988

The 3.5 % vapor phase volume relative to initial pore volume was induced by volumetric strain change before the earthquake.

Radon anomaly was well-explained by the vapor-liquid partitioning model.

Hypotheses and Tasks

- A brittle block in a ductile region near a fault might be a potential field for seismo-chemical monitoring.
  - A sensitive point "Tsubo" might be a borehole drilled in such a potential field.
- Corroborative data of the vapor-liquid partitioning of radon should be acquired by a parallel monitoring at a sensitive filed.
  - Hydraulic conductivity (transmissibility)
    - provides direct information of pore volume.
  - Helium, argon, methane and nitrogen
    - behave in the same way as radon.
  - Electric conductivity (ion concentration)
    - indicates direct information of microcrack generation

Challenges in Chemical Monitoring

- Groundwater must be pumped for sampling in most wells.
  - Pumping changes groundwater level.
  - It is difficult to pump groundwater in a precise and low rate by a common pump.
- Gas analyzer must be customized for a long-running monitoring.
  - Gas extraction efficiency should get high to get exact concentration.
  - Automated calibration system must be required because sensitivity of a detector gradually decreases.

Pumping Test at Kashima (KSM)

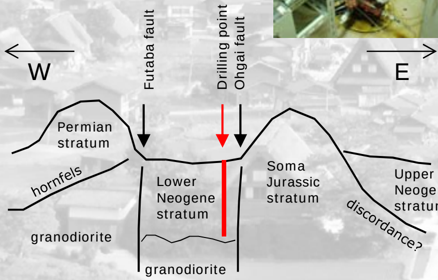

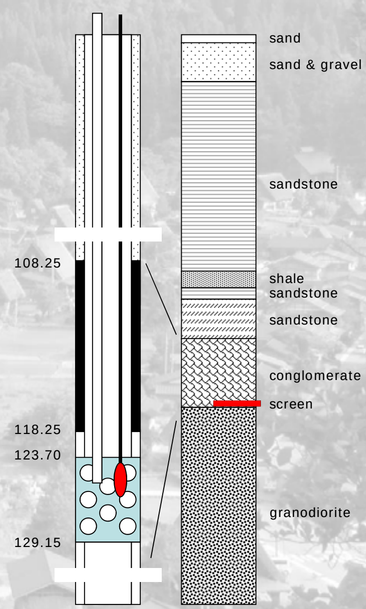

Water head is 50cm above the ground level.

Continuous and Intermittent Sampling

Birds in a salt field

Water Level Monitoring at KSM

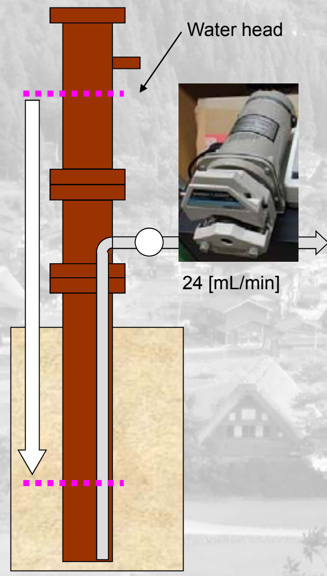

Radon counter

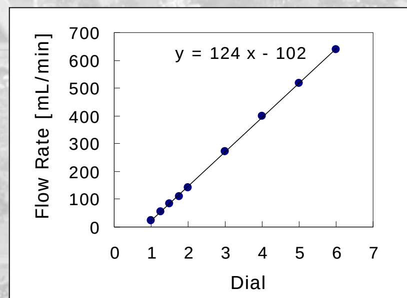

Water Level Change

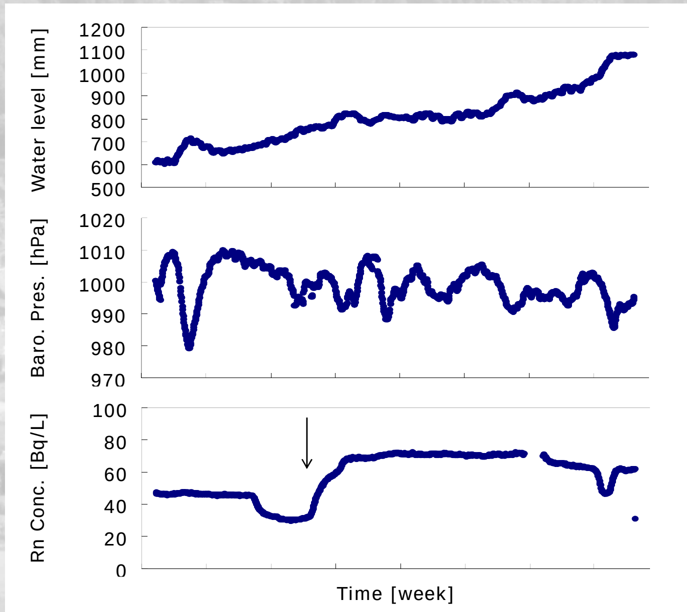

Recovery Test at Kamakura (KMK)

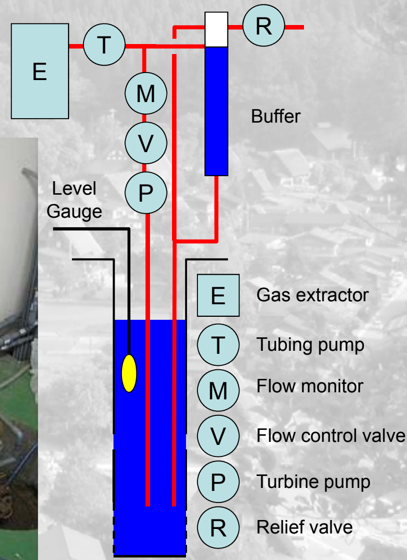

Results for Continuous Pumping

- Continuous pumping …
  - does not disturb a tidal response of groundwater level according to FFT analysis.
  - It is difficult to discriminate an effect of slight misalignment of the pumping rate from a trend change of groundwater level.
- An actual lifetime of a tube is about 1.5 months.
  - It is shorter than guaranteed lifetime of 3 months.

Water Level Change

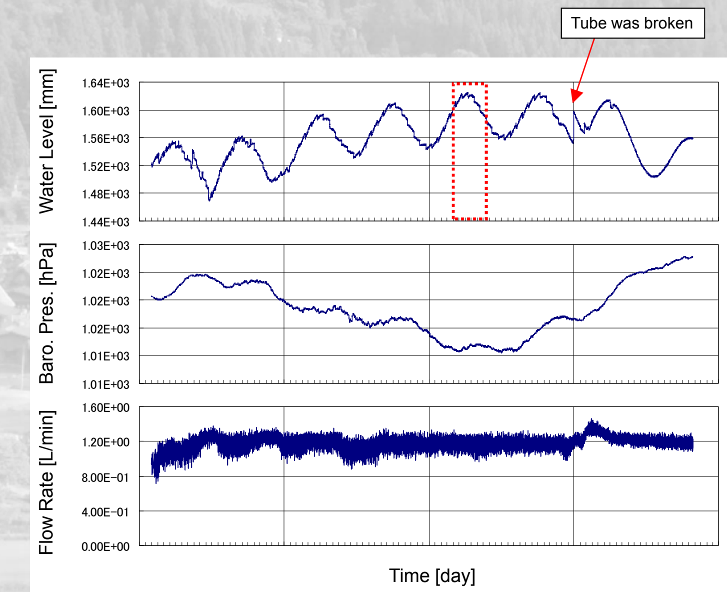

Water Level Recovery

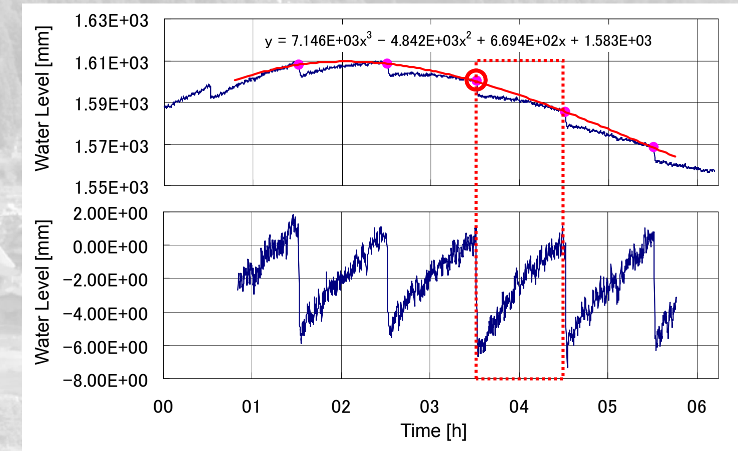

Hydraulic conductivity is calculated on the basis of Jacob analysis

Results for Intermittent Sampling

- Intermittent sampling …
  - realizes hourly monitoring of hydraulic conductivity.
  - provides an enough water volume (1184 mL/min) for a dissolved gas analysis by a QMS.
- A tube of a tubing pump was broken in 3 days.
  - A tubing pump is useful only for a laboratory experiment. No commercial s for our purpose.
  - We are going to apply an imr pumping and sampling.

Active Monitoring of Hydraulic Conductivity

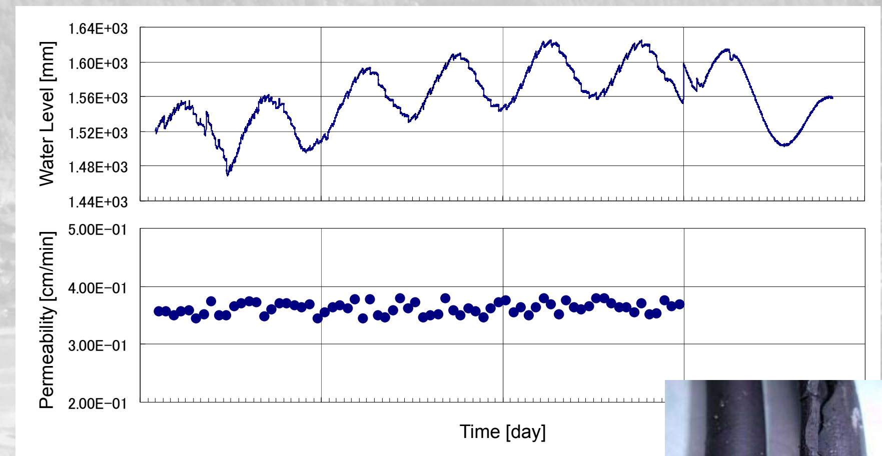

Gas Analysis by QMS

Sunset in Tainan

Automated Calibration and Purification

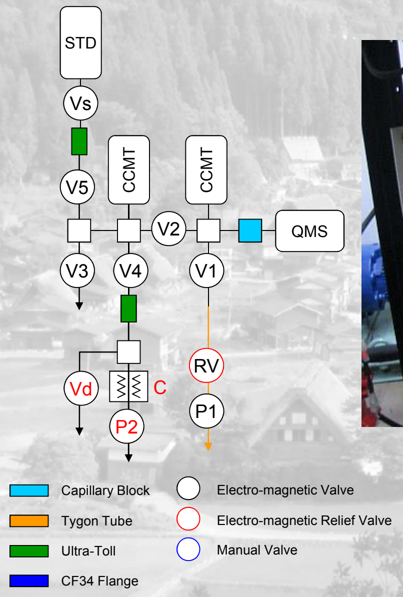

Chemical Monitoring Project in Taiwan

My best friends

Preliminary Records at KMK

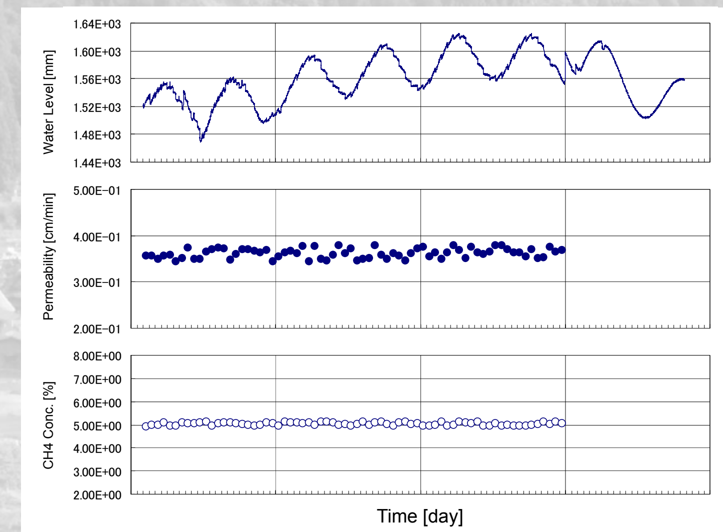

Crustal Movement in Taiwan

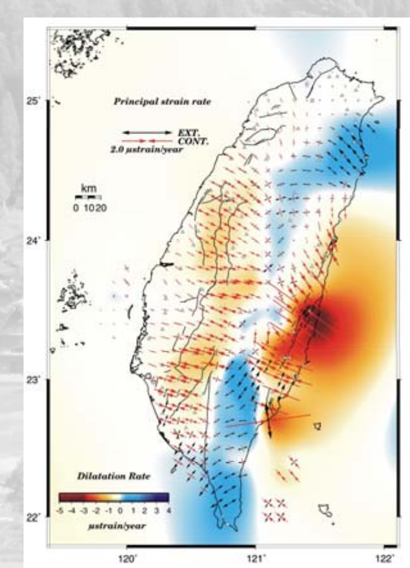

(Lin et al., 2008)

1995-2005

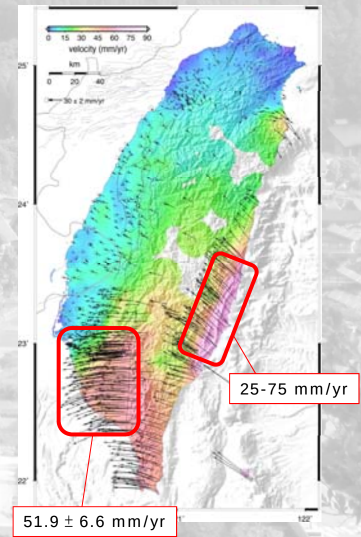

(Prof. Hu presented, in 2008 WS @ GSJ)

Summaries

- The vapor-liquid partitioning model is the most qualified candidate for explaining seismo-chemical anomalies.
- The intermittent sampling enables us to monitor the hydraulic conductivity of an aquifer with gas concentration changes dissolved in groundwater.
- Southwest region, especially Tainan area, is the most adequate field for the seismo-chemical groundwater monitoring in Taiwan.

Thank you very much for your attention!

I'm absent from nursery school because of flu! Ha ha ha ….

Jacob Analysis

Theis Solution

$$h(u) = \frac{Q}{4\pi T}\left(-0.5772 - \ln u + \sum_{i=1}^{\infty}(-1)^{i+1}\frac{u^i}{i \cdot i!}\right) \qquad u = \frac{r^2 S}{4Lkt}$$

Jacob Solution

$$\begin{aligned}\Delta h &= h(u) - h(u') \\ &= \frac{Q}{4\pi T}\left(\ln\left[\frac{4Lkt}{r^2 S}\right] - \ln\left[\frac{4Lkt'}{r^2 S}\right]\right) \\ &= \frac{2.30Q}{4\pi Lk}\log\left(\frac{t}{t'}\right)\end{aligned}$$

Δh = 0.601 [cm]
Q = 1184 [cm^3/min]
L = 1000 [cm]

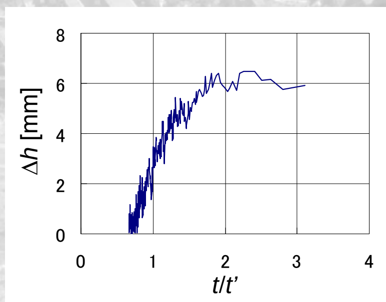

k = 3.61x10^{-1} [cm/min]

Power Spectrum Density

FFT

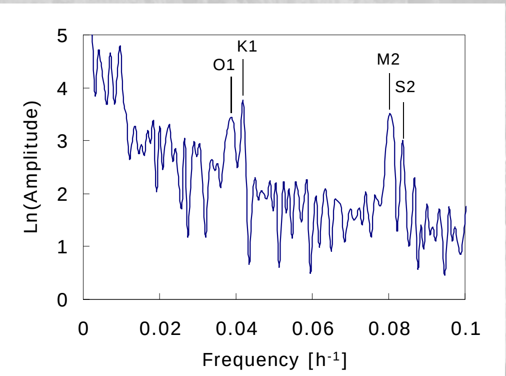

MEM

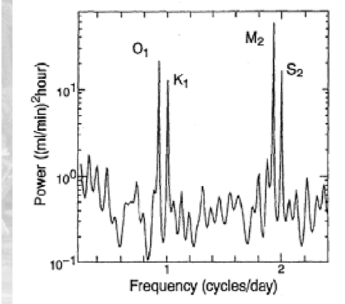

Tohjima et al. (1994)

	O1	K1	M2	S2
Interval [h]	25.82	23.93	12.42	12.00
KSM	25.92	23.92	12.44	11.96

Cheng-Kung EQ, 2003

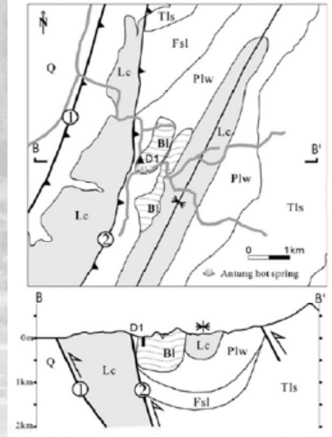

Figure 3. Geological map and cross section near the radon-monitoring well in the area of Antung hot spring (Q: Holocene deposits, Lc: Lichi mélange, Plw: Paliwan Formation, Fsl: Fanshuliao Formation, Tls: Tuluanshan Formation, Bl: tuffaceous fault block, D1: radon-monitoring well, ① Chihshang or Longitudinal Valley fault, ② Yongfeng fault). See Figure 1 for map location.

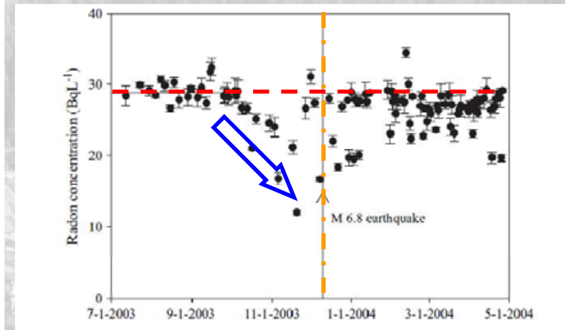

Fig. 3. Radon concentration data at the monitoring well (D1) in the Antung hot spring.

$$C_w = \frac{1}{HS_g + 1} C_0$$

Kuo et al. (2006)

Challenges in Chemical Monitoring

- An appropriate volume of groundwater must be sampled for a dissolved gas analysis.
  - For mass spectrometry, a few cm^3 water is enough. On the other hand, 1000 cm^3 water is required for gas chromatography.
    - Gas concentration in saturated water is about 0.05 cm^3・STP/cm^3.
    - 0.001 cm^3・STP gas is needed for a mass spectrometry, and 50 cm^3・STP for a gas chromatography.

Tidal Response of Flow Rate

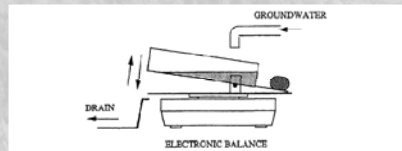

Fig. 3. Schematic diagram of the flow rate measuring apparatus. The groundwater is introduced into a vessel on an electronic balance and is weighed every minute. When the vessel becomes filled with water, it tips around a fulcrum.

24 mL/min

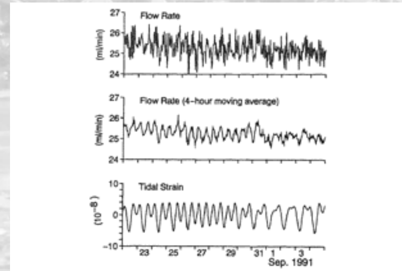

Fig. 5. Temporal variation in flow rate at the KSM well: hourly averaged data (top) and 4-h moving averaged data (middle) together with theoretical tidal volumetric strain changes (bottom).

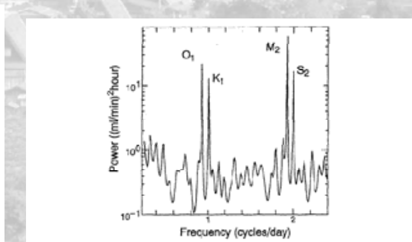

Fig. 6. Power spectra of the flow rate calculated by the Maximum Entropy Method (MEM). The flow rate have power for M_2 and O_1 tidal constituents as well as S_2 and K_1 tidal constituents.

Tohjima et al. (1994)

Faults and Tectonic Model of Taiwan

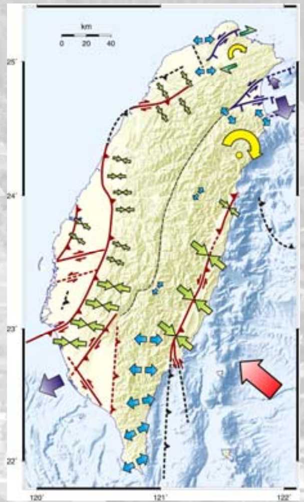

(Prof. Hu presented, in 2008 WS @ GSJ)

Uranium Decay Series

	Element	Decay	Half Life	Energy /MeV
1	^{238}U	α	4.468×10^{9} y	
2	^{234}Th	β^-	24.10 d	
3	^{234m}Pa	β^-	1.17 m	
4	^{234}U	α	2.455×10^{5} y	
5	^{230}Th	α	7.538×10^{4} y	
6	^{226}Ra	α	1.600×10^{3} y	
7	^{222}Rn	α	3.824 d	
8	^{218}Po (RaA)	α	3.10 m	
9	^{214}Pb (RaB)	β^-	26.8 m	
10	^{214}Bi (RaC)	β^-	19.9 m	
11	^{214}Po (RaC')	α	1.643×10^{-4} s	
12	^{210}Pb (RaD)	β^-	22.3 y	
13	^{210}Bi (RaE)	β^-	5.013 d	
14	^{210}Po (RaF)	α	138.4 d	
15	^{206}Pb (RaG)		∞	

Vapor-Liquid Partitioning Model

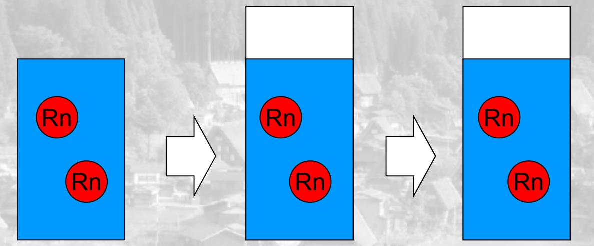

Rn concentration in groundwater declines

Gas phase is generated by the pore volume increase due to new micro-crack generation.

Radon gas must move to gas phase according to Henry's law.

Parameters for Radon

Production Rate of ^{222}Rn in Pore Space	1.14×10^{-5} kBqm^{-3}s^{-1}	
Henry's Constant	4.4	Wilhelm et al. (1977)
Solid–Water Partitioning Coefficient	1.4×10^{-5} m^{3}kg^{-1}	Nazaroff (1992)
Diffusion Coefficient	~ 10^{9} m^{2}s^{-1}	
Half-life	3.3×10^{5} s	
Boiling Temperature	211.3 K	
Melting Temperature	202 K	
Solubility	22 cm^3/100gH_2O	20ºC, 1atm
Recoil Length	20 ~ 70 nm	

Radon from Rocks

- ^{222}Rn is generated by α decay of ^{226}Ra existing in rock subsurface.

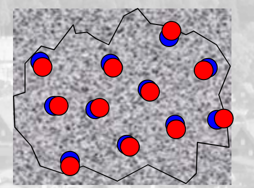

- Radon emanation power governing the amount of radon gas released from a rock is regarded as constant because the half-life of ^{226}Ra is 1600y.
- The radon supply is proportional to surface area of a rock.

Radon Supply into Groundwater

- In a fractured aquifer
  - Radon emanation power E is constant.
  - Radon supply is proportional to surface area S.

- Radon generation rate from crack surfaces into pore volume is written as,

$$R \propto ES$$

Radon in Aquifer

- Aquifer has many fractures retaining groundwater.

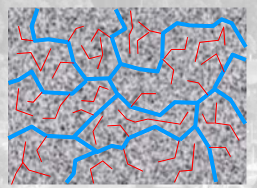

Effective Porosity

$$\phi_e = \frac{V_{p,all} - V_{p,stag}}{V_t} = \frac{V_{p,flow}}{V_t}$$

- Radon is supplied from fracture surfaces contacting with groundwater.
- The radon supply is proportional to surface area of cracks S.

Radon Concentration

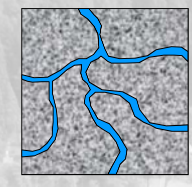

- ✓ Groundwater flow is stable.
- ✓ Rn diffusion coefficient is same as that in normal water.

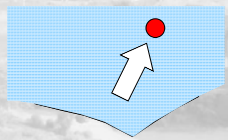

Number of radon is written as,

$$\frac{d}{dt}N = R - \frac{1}{\tau}N \qquad (1)$$

R : Radon generation rate in pore space (Bq s^{-1})

τ : Decay time of radon (s)

$$N = D\exp\left(-\frac{t}{\tau}\right) + \tau R \qquad (2)$$

Under the steady state,

$$N_0 = \tau R \qquad (3)$$

$R \rightarrow R'$ at t=0,

$$N = (N_0 - \tau R')\exp\left(-\frac{t}{\tau}\right) + \tau R' \qquad (4)$$

Radon Decline

$$N = \tau R = \tau E S$$

$$C = \frac{N}{V_p} = \tau E \frac{S}{V_p}$$

τ : Decay time of radon (s)

R : Radon generation rate in pore space (Bq s^{-1})

E : Radon emanation power (Bq m^{-2} s^{-1})

S : Effective surface area (m^2)

V_p : Effective pore volume (m^3)

Decrease of a radon concentration can be induced by S to be decreased, V_p to be increased, or S/V_p ratio to be decreased.

Possible Cases

- Dilation rate of rock mass ≤ Recharge rate

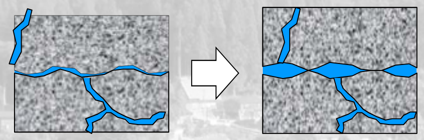

All micro-cracks are filled with water.

- Dilation rate of rock mass > Recharge rate

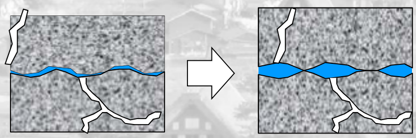

Gas phase is produced in new micro-cracks.

Scenarios for Pore Volume Change

- Without increase of surface area

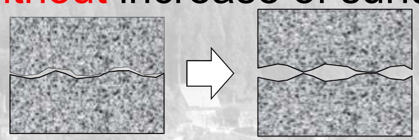

No additional fracture is generated.

- With increase of surface area

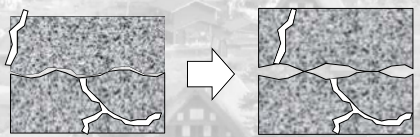

New micro fractures will be generated.

Kashima (KSM) Observatory

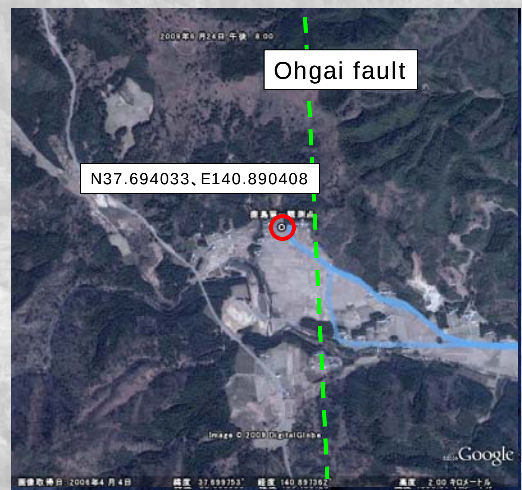

264km, 4 hrs drive

N37.694033, E140.890408

Pumping Test at KSM

A pumping test at the Kashima well.

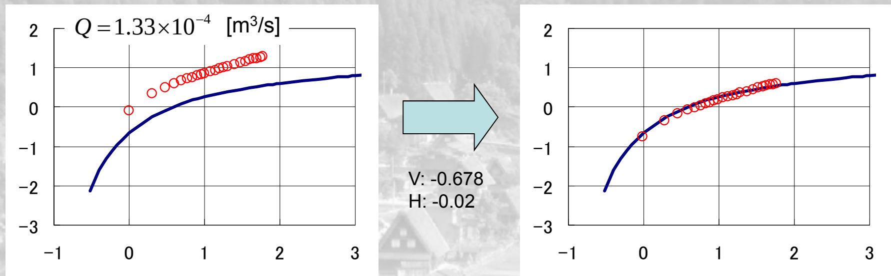

$$\ln\left(\frac{Q}{4\pi T}\right) = -0.678$$

$$T = 2.09\times10^{-6} \quad \text{[m²/s]}$$

$$k = 3.84\times10^{-7} \quad \text{[m/s]}$$

4.12×10^{-8} Initial value (1980)

$$\ln\left(\frac{4T}{S}\right) = -0.02$$

$$S = 8.53\times10^{-6}$$

where, $r = 1.0$

Theis Analysis

$$\frac{\partial^2 h}{(\partial r)^2} + \frac{1}{r}\frac{\partial h}{\partial r} = \frac{S}{T}\frac{\partial h}{\partial t}$$

S Storage coefficient

$T = kL$ Transmissivity

Q Pumping rate

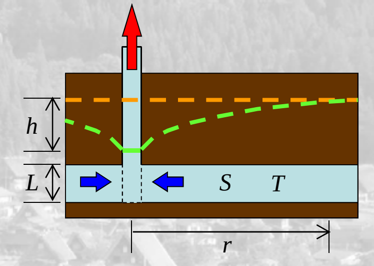

$$h(u) = \frac{Q}{4\pi T}W(u)$$

$$u = \frac{r^2 S}{4Tt}$$

$$W(u) = -\gamma - \ln u + \sum_{i=1}^{\infty}(-1)^{i+1}\frac{u^i}{i \cdot i!}$$

γ Euler's constant ~0.577

$$\ln\left(\frac{Q}{4\pi T}\right) = \ln(h) - \ln(W)$$

A gap between log values of water head change and that of well function indicates transmissivity of an aquifer.

$$\ln\left(\frac{4T}{S}\right) = \ln\left(\frac{1}{u}\right) - \ln\left(\frac{t}{r^2}\right)$$

A gap between log values of $1/u$ and that of time indicates S storage coefficient of an aquifer. Where, r (a radius of an influenced area by pumping) should be assumed to estimate the storage coefficient.

Parameters of Porous Material

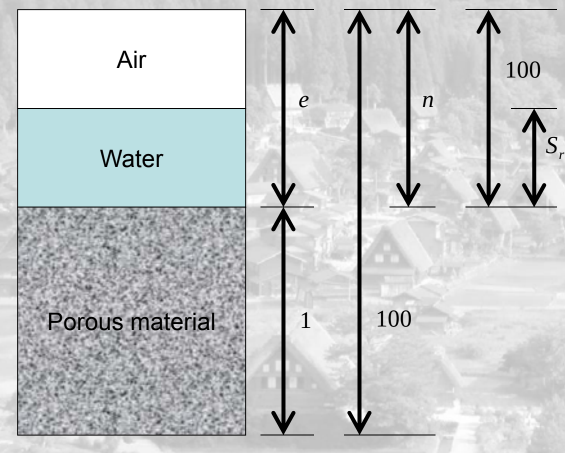

e Void ratio

n Porosity

S_r Saturation ratio

$$n = \frac{e}{1+e}\times100$$

Theis Analysis (1)

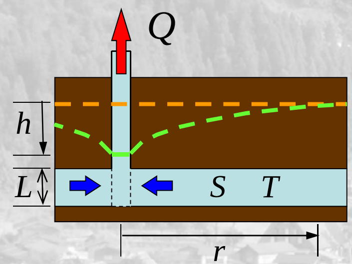

$$\frac{\partial^2 h}{(\partial r)^2} + \frac{1}{r}\frac{\partial h}{\partial r} = \frac{S}{T}\frac{\partial h}{\partial t}$$

S Storage coefficient

$T = kL$ Transmissivity

$$u = \frac{r^2 S}{4Tt}$$

$$\frac{\partial h}{\partial t} = -\frac{dh}{du}\frac{u}{t} \qquad \frac{\partial h}{\partial r} = \frac{dh}{du}\frac{rS}{2Tt}$$

$$\frac{\partial^2 h}{(\partial r)^2} = \frac{\partial^2 h}{(du)^2}\frac{uS}{Tt} + \frac{dh}{du}\frac{S}{2Tt}$$

Theis Analysis (2)

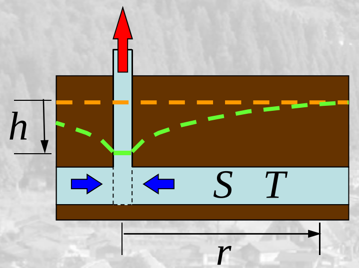

$$\frac{\partial^2 h}{(\partial u)^2}+\left(\frac{1}{u}+1\right)\frac{dh}{du}=0$$

$$u=\frac{r^2 S}{4Tt}$$

$$\frac{dh}{du}=\frac{\exp(C-u)}{u}$$

$$h(u)=-\exp(C)\int_u^\infty \frac{\exp(-u)}{u}du$$

Theis Analysis (3)

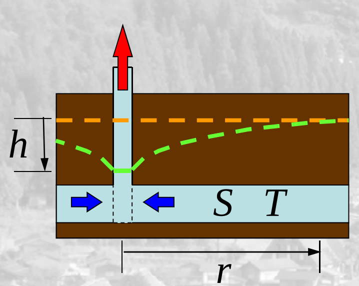

$$Q_w=-2\pi rT\frac{\partial h}{\partial r}$$

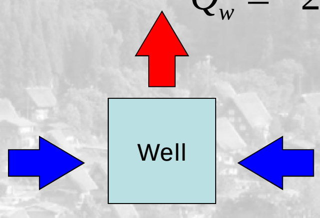

$$\frac{dh}{du}=\frac{\exp(C-u)}{u}$$

$$Q=\lim_{r\to 0}(-2\pi rT)\frac{\partial h}{\partial r}$$

$$-\exp(C)=\frac{Q}{4\pi T}$$

Theis Analysis (4)

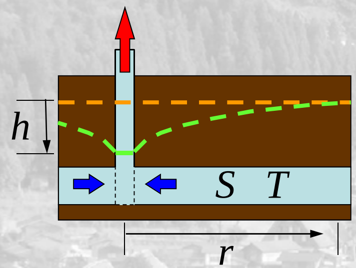

$$h(u)=-\exp(C)\int_u^\infty \frac{\exp(-u)}{u}du$$

$$h(u)=\frac{Q}{4\pi T}\int_u^\infty \frac{\exp(-u)}{u}du$$

$$h(u)=\frac{Q}{4\pi T}W(u)$$

$$W(u)=-\gamma-\ln u+\sum_{i=1}^{\infty}(-1)^{i+1}\frac{u^i}{i\cdot i!}$$

γ Euler's constant ~0.577215665

Theis Analysis (5)

$$W(u)=-\gamma-\ln u+\sum_{i=1}^{\infty}(-1)^{i+1}\frac{u^i}{i\cdot i!}$$

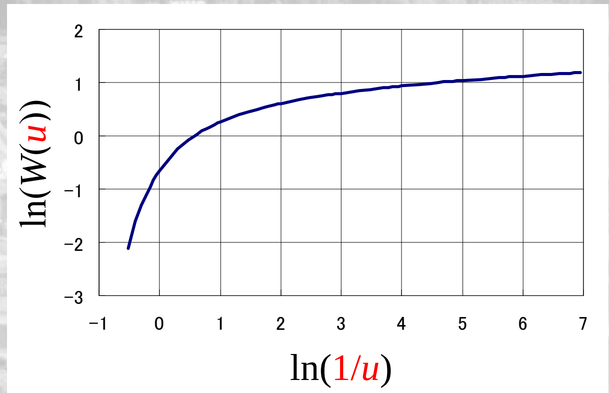

Estimation of fracture porosity using radon as a tracer

T. Kuo [1] and F. Tsunomori [2]

1: Department of Mineral and Petroleum Engineering, National Cheng Kung University, Tainan, Taiwan
2: Laboratory of Earthquake Chemistry, Faculty of Science, The University of Tokyo, Tokyo, Japan

Abstract

In fractured aquifers of limited recharge, the in-situ volatilization of dissolved radon could cause a decline of radon in ground water precursory to an earthquake. Based on the mechanism of in-situ radon volatilization, a mathematical model was developed to correlate the radon decline with fracture porosity and volumetric strain change in the aquifer rocks. In this paper, a quantitative method using the precursory radon decline as a tracer to estimate fracture porosity is presented with the help of a case study.

Hvwlpdwlrq ri iudfwxuh srurvlw| xvlqj udgrq dv d wudfhu

T. Kuo, National Cheng Kung University
F. Tsunomoro, University of Tokyo

- Zkroh fruh dqdo|vlv dqg grzqkroh fdphudv surylgh gluhfw vrxufhv ri lqirupdwlrq iru hydoxdwlqj iudfwxuh srurvlw|1
- Rwkhu lqgluhfw vrxufhv ri lqirupdwlrq iru hydoxdwlqj iudfwxuh srurvlw| dqg shuphdelolw| lqfoxgh gulcolqj klvwru|/ orj dqdo|vlv/ zhoo whvwlqj/ lqiodwdeoh sdfnhuv/ dqg surgxfwlrq klvwru|1

Introduction

- Qdwxudoo| iudfwxuhg uhvhuyrluv krog odujh jurxqg zdwhu/ jhrwkhupdo/ dqg k|gurfduerq uhvrxufhv1
- Iudfwxuh srurvlw| lv dq lpsruwdqw sdudphwhu iru hydoxdwlqj qdwxudoo| iudfwxuhg uhvhuyrluv1

Objective

- Wklv sdshu lqyhvwljdwhv wkh srvvleoh xvh ri jurxqgzdwhu udgrq ghfolqh suhfxuvru| wr dq hduwktxdnh dv d wudfhu wr ghwhuplqh wkh iudfwxuh srurvlw|1

Fig. 1.

- P ds ri wkh L}x Shqlqvxod dqg wkh vxuurxqglqj duhd +dgdswhg iurp Z dnlwd hw do/ 4<;3,1

Fig. 2.

- Suhfxuvru| fkdqjhv ri wkh 4<:; L}x0Rvklp d0 Nlqndlhduwktxdnh +Z dnlwd/ 4<<9,1
- +d, Udgrq frqfhqwudwlrq fkdqjhv revhuyhg dw wkh VNH04 z hoo+683 p ghhs, z lwk d glvwdqfh iurp wkh hslfhqwhu +G, @ 58 np 1
- +e, Uhfrug ri wkh yroxp hwulf vwudlqp hwhu dw Lur}dnl z lwk G @ 83 np 1
- +f, Z dwhu ohyhofkdqjhv revhuyhg dw wkh Nlvkl z hoo+833 p ghhs, z lwk G @ 63 np 1

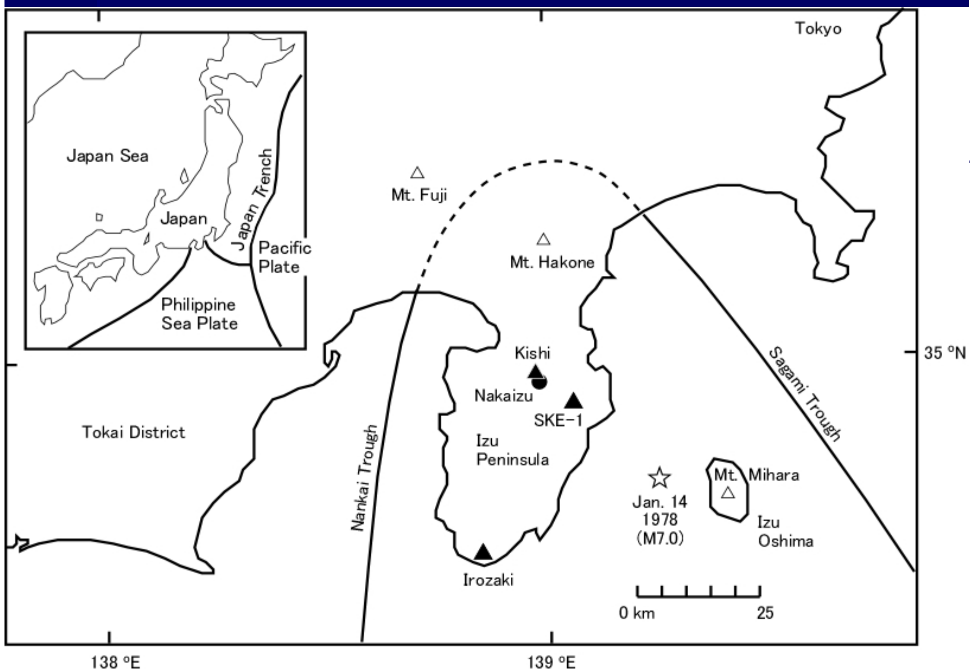

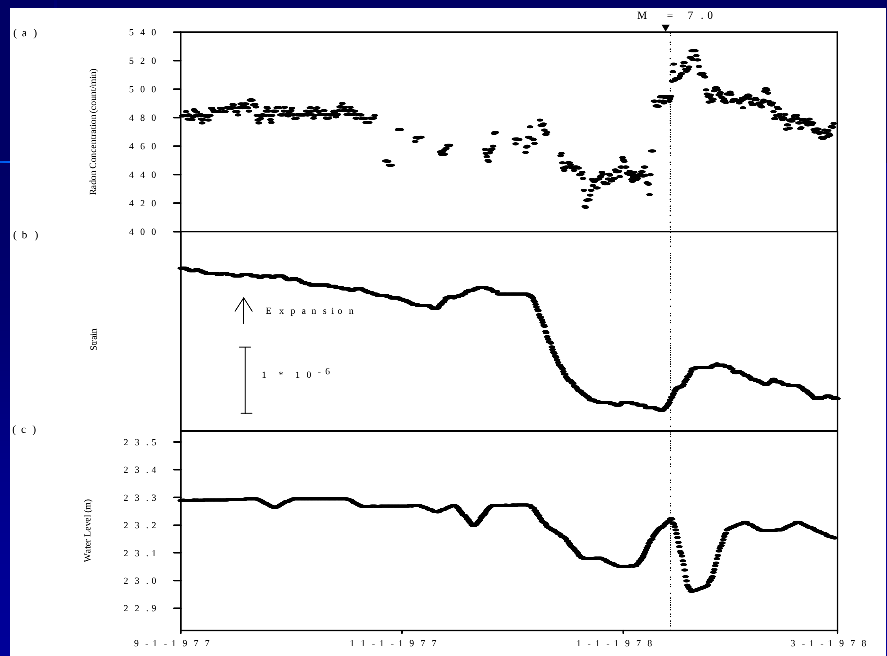

- D p dwkhp dwlfdop rghoz dv ghyhorshg wr fruhodwh wkh udgrq ghfdqh z lwk wkh jdv vdwxudwlrq/ iudfwxuh srurvlw|/ dqg yroxp hwulf vwudlq fkdqjh lq wkh dtxlihu urfnv1
- 41 udgrq0yrodwlo}dwlrq p rgho
- 51 urfn0gldwdqf| p rgho

Conclusions

- Vshfliifdo|/ udgrq ghfuhdvhg iurp d edfnjurxqg dyhori 7;3 ± 43 fsp wr d p lqlp xp ri 763 ± 48 fsp sulru wr wkh 4<:; P :13 L}x0R vklp d0nlqndlhduwktxdnh1
- Wkh p hdvxuhg fuxvwdo0vwudlq dwwkh L}x Shqlqvxod sulru wr wkh P :13 hduwktxdnh z dv derxw4 ssp 1
- Wkh iudfwxuh srurvlw| ri 313333759 z dv hvwlp dwhg iru VNH04 dtxlihu xvlqj wkh udgrq0yrodwlo}dwlrq p rghodqg wkh urfn0 gldwdqf| p rghd1

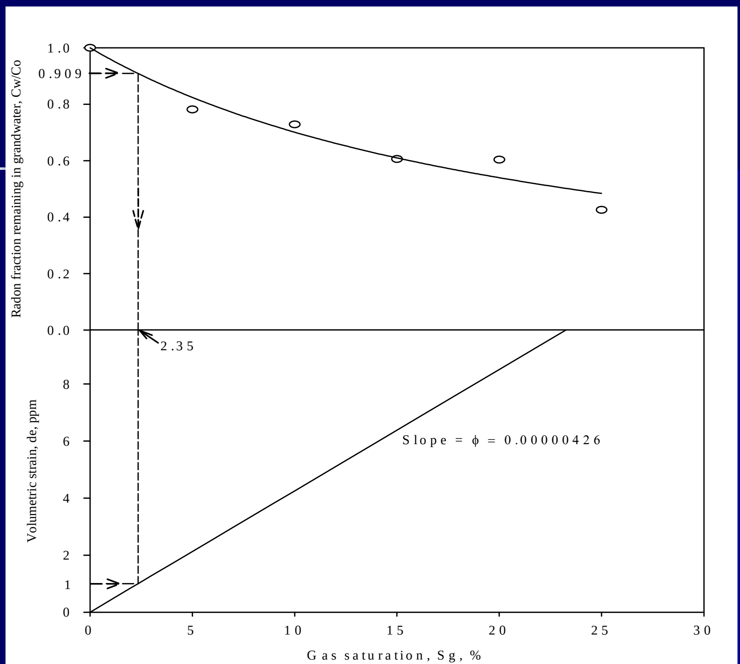

Conclusions

- D txdqwlwdwlyh p hwkrg lv suhvhqwhg wr hvwlp dwh iudfwxuh srurvlw| xvlqj jurxqgz dwhu udgrq ghfdqh dqg dvhlvp lf fuxvwdo0vwudlq vljqdov suhfxuvru| wr dq hduwktxdnh1

Underground Water Observation in Hot Spring, Central Part of Japan

**Shigeki Tasaka[1], Masaya Matsubara[1],Yoshimi Sasaki[2],
Norio Matsumoto[3] and Akito Araya[4]**

1: IMC, Gifu Univ.
2: Faculty of Education, Gifu Univ.,
3: Geological Survey of Japan, AIST,
4: Earthquake Research Institute, Univ. Tokyo

Abstract

Wari-ishi hot spring is located on the Atotsugawa active fault in Central Part of Japan, is an artificial well which emits water at about 30 liter/min from the depth of 850 meters. The managers of the hot spring had started to measure the water flow rate using a water bucket, on every Monday from 1977(1st period). The monitoring networks were started by using the electromagnetic flow meter with the accuracy of 0.25%, in the 10 minute interva1 from 1998 to 2004(2nd period), and in 1 Hz sampling from 2004(3rd period). The 1Hz data logger was supported by AIST, GSJ. Broadband area strain observation was carried out from 2004, by the laser strain meters in Kamioka Mine of the distance left from Wari-ishi hot spring at 5km, by Earthquake Research Institute of The University of Tokyo.

There have been 27 co-seismic and pre-seismic events associated with seismic activity over last 32 years. The observed results of water change were related to the crust distortion accompanying with the earth tide or the occurrence of an earthquake through the change of the pore pressure of a stagnant water layer.

Analysis for the water flow was performed in the following viewpoints:

1) The variations of the tidal M_2 and O_1 amplitudes of the earth tide by the BAYTAP-G program, and the tidal response on the tidal strain calculated by GOTIC-2.
2) The comparison of the step-like increase of discharge water with the volumetric strain calculated by MICAP-G from the earthquake fault model.
3) The comparison the water changes with the area strain in the seismic dynamical waveform with the 1Hz sampling data.
4) The dynamical sensitivity by use of the FFT analysis of discharge water and area strain waveform.
5) The comparison the initial movement of the water waveform with the

dynamical area strain data.

6) The characteristic pre-seismic phenomena of water waveform in the amplitude and cycle of the irregular component, before Off Noto Peninsula earthquake (Mar-2007).

Underground Water Observations in Hot Spring, Central Part of Japan

Shigeki Tasaka[1]; Masaya Matsubara[2];Yoshimi Sasaki[3]; Norio Matsumoto[4]; Akito Araya[5]

[1], [2] IMC, Gifu Univ.; [3] Faculty of Education, Gifu Univ.;

[4] Geological Survey of Japan, AIST;

[5] Earthquake Research Institute, Univ. Tokyo

8th Taiwan-Japan International Workshop on Hydrological and Geochemical Research for Earthquake Prediction

Date:Sep.29, 2009

Place: National Cheng Kung University, Tainan, Taiwan

Observation Method

(1)Discharge Water were observed in Wari-ishi Hot Spring, 1977-2009.

- 1st period :1977-1998(4 EarthQuakes)

Observed by Bucket and Stopwatch(±10%) on every Monday

- 2nd period :1998-2004(4 EQ) Electromagnetic Flow Meter(±0.25%) at 10 min interval
- 3rd period :2004-2009(19 EQ) Electromagnetic Flow Meter in 1 Hz sampling, data logger system was supported by AIST,GSJ

(2)Broadband Observation with Laser Strain Meters:2004-2009(7 EQ) Data taking of 200Hz sampling, in KAMIOKA-Mine by Earthquake Research Institute, Univ. of Tokyo

Observation Site: Wari-ishi Hot Spring and Kamioka Mine

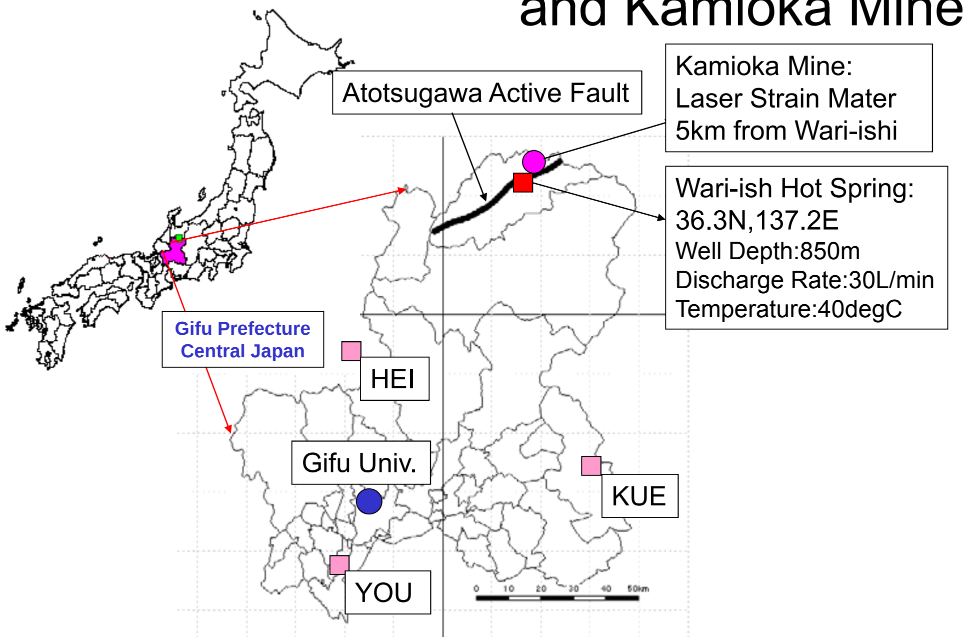

Seismic Changes of Water in Wari-ishi (2004-2009:19EQ)

Earthquake	date	Distance(km)	Mw	Mechanism	Water Flow (L/min)	
● 1)Off Kii Peninsula(1)	2004/09/05 19:07	377	7.2	Dilatation	+0.3(step)	+1.7-1.7(Oscil)
● 2)Off Kii Peninsula(2)	2004/09/05 23:57	363	7.5	Dilatation	+4.5(step)	+5.2-5.7(Oscil)
3)Chyuetsu(1)	2004/10/23 17:56	176	6.6	Compression	+1.9(step)	+0.8-0.8(Oscil)
4)Chyuetsu(2)	2004/10/23 18:34	179	6.3	Compression	+2.1(step)	+0.4-0.4(Oscil)
5)Off Kushiro	2004/11/29 03:32	1024	7.0	Compression	-	+0.6-0.6(Oscil)
● 6) Sumatra	2004/12/26 09:58	5609	9.3	-	-	+5.0-5.0(Oscil)
7)Gifu Hida	2005/02/25 06:27	7	3.0	-	+8.1(step)	+1.5-1.5(Oscil)
8)Western Fukuoka	2005/03/20 10:53	701	6.6	Dilatation	-	+0.4-0.3(Oscil)
9)Taiwan	2006/12/26 21:26	2285	6.7	-	-	+0.55-0.45(Oscil)
10)Far Off Chishima	2007/01/13 13:24	1804	8.3	-	-	+1.8-2.1(Oscil)
11)Noto Peninsula	2007/03/25 09:42	109	6.7	Dilatation	+34.1(step)	+0.7-1.8(Oscil)
● 12)Off Chyuetsu	2007/07/16 10:13	178	6.6	Compression	+0.5(step)	+1.5-1.2(Oscil)
● 13)Off Ibaraki	2008/05/08 01:45	391	6.8	Dilatation	-	+1.0-0.7(Oscil)
14)Sichuan(China)	2008/05/12 15:28	3077	7.9	-	-	+1.9-1.8(Oscil)
● 15)Iwate-Miyagi	2008/06/14 08:43	437	6.9	Compression	-	+1.2-0.5(Oscil)
● 16)Off Fukushima	2008/07/19 11:39	468	6.9	Dilatation	-	+0.6-1.2(Oscil)
17)Off Tokachi	2008/09/11 09:20	867	6.8	Dilatation	-	+0.7-0.6(Oscil)
18)Papua(Indonesia)	2009/01/04 04:44	4125	7.6	-	-	+0.8-0.8(Oscil)
19)Shizuoka	2009/08/11 05:07	207	6.5	Dilatation	+5.0(step)	

● Laser Strain Data: 2004-2009(7EQ): 1),2),6),12),13),15),16)

Observations of Discharge Water (3rd period:2004-2009)

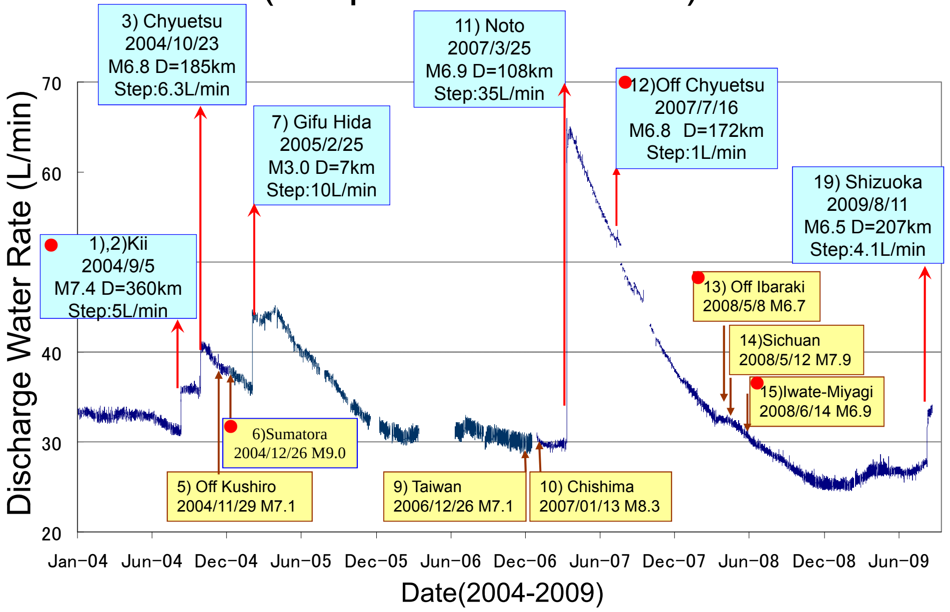

FFT Analysis of Discharge Water and Area strain

2)KII Earthquake(2)
Frequency: 0.01-0.05Hz
Amplitude Ratio (Response)
0.13±0.05(L/min)/(E-08strain)

6)Sumatra
Frequency: 0.003-0.05Hz
Amplitude Ratio (Response)
0.17±0.07(L/min)/(E-08strain)

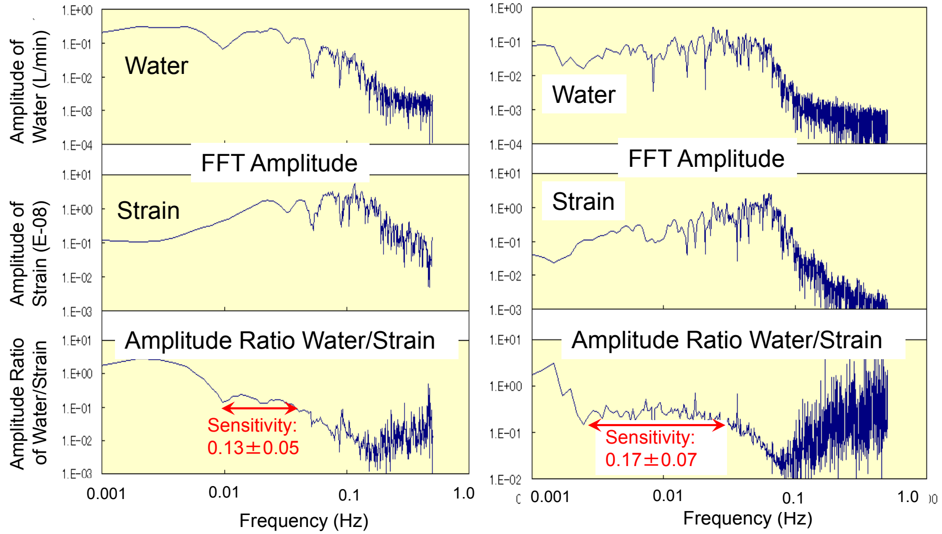

Tidal O1 and M2 Amplitude(1998-2009)

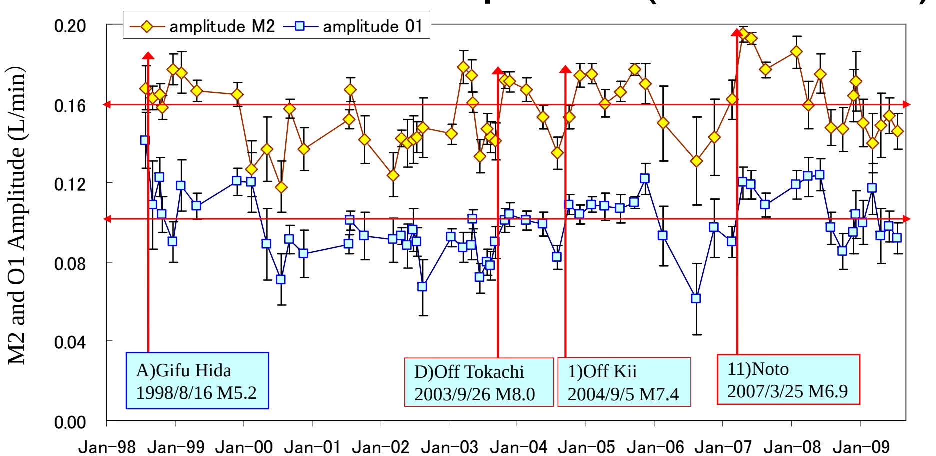

Tidal Response of Discharge Water by BAYTAP-G

M2(12.4h): 0.158±0.017 and O1(25.8h): 0.100±0.015(L/min)

Tidal Strain M2:0.997, O1:0.671(E-08 strain) by GOTIC-2

Response for the Tidal Strain M2:0.16, O1:0.15(L/min)/(E-08 strain)

Initial Movement of Discharge Water and Area Strain in Five EQ

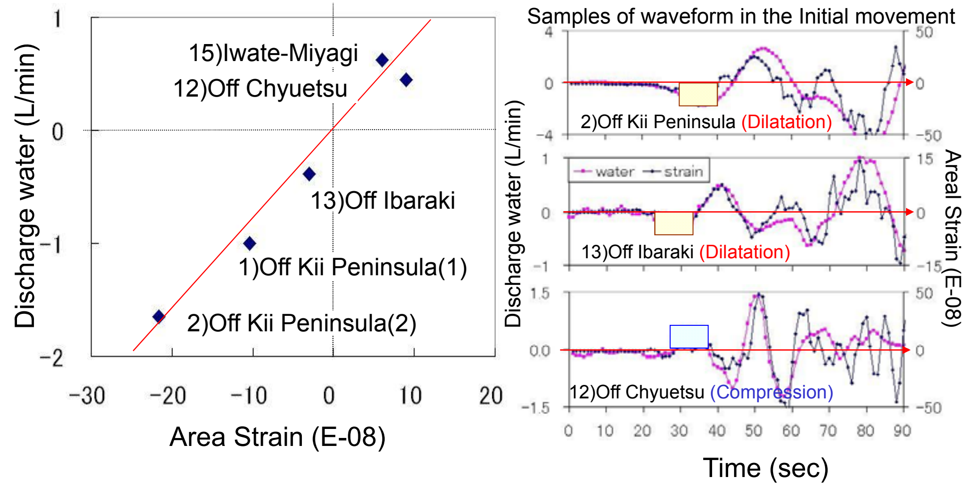

Response for area strain in Frequency 0.1-0.5(Hz)
Sensitivity: 0.079±0.015(L/min)/(E-08 strain)

Response of Discharge Water for Strain in Frequency of 10^{-5} to 10^{-1}(Hz)

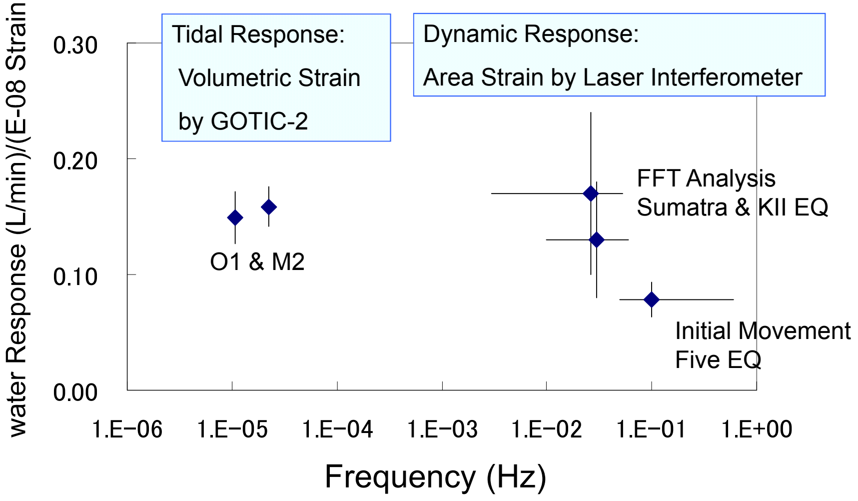

Changes of Discharge Water were explained as the Poro-Elastic Response of a Confined Aquifer

Step-like Increase of Discharge Water and Static Volumetric Strain by MICAP-G

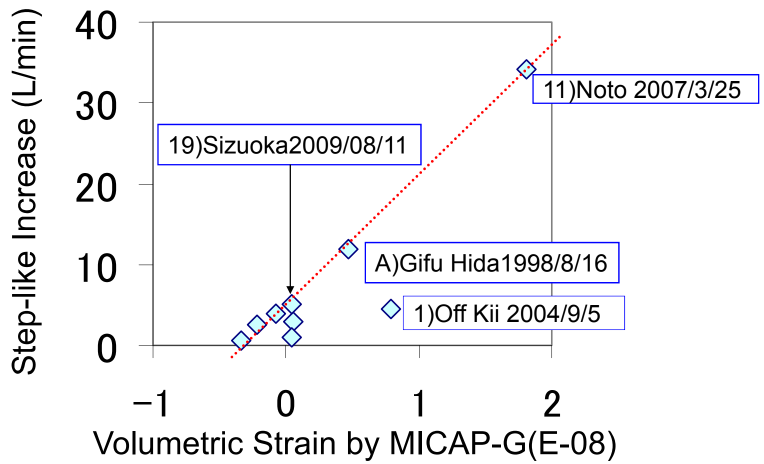

Step-like Increase:100 times larger than Volumetric Strain by MICAP-G from EQ Fault Model >>Sensitivity 0.15(L/min)/(E-08 strain)

Hydro-seismic Waveform with Step-like Increase

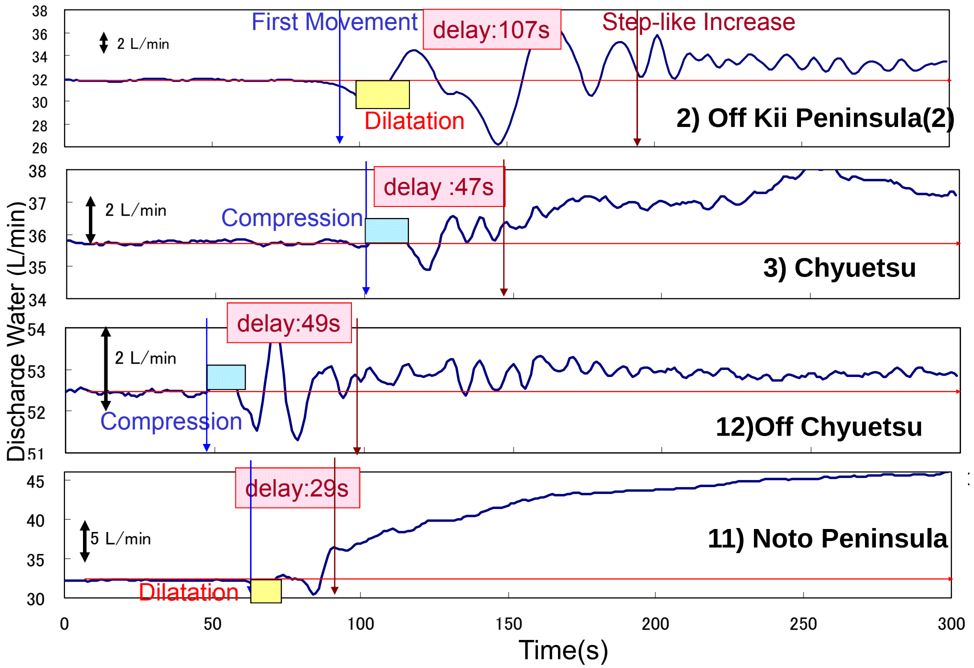

Delay Time of Step-like Water Increase from First Movement

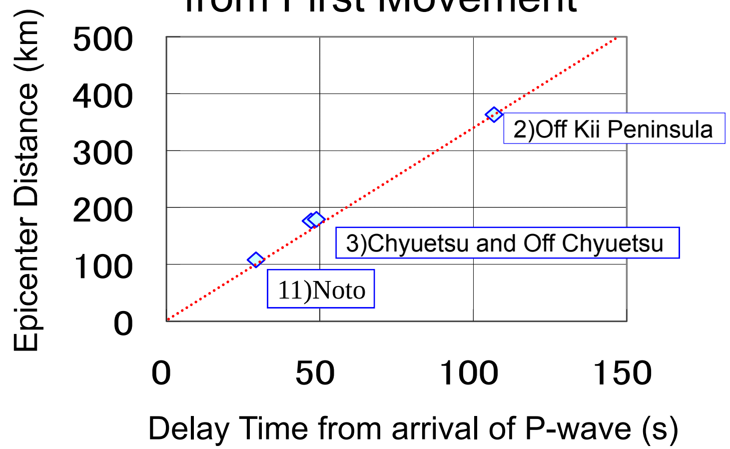

Scatter Plots of Epicenter distance and Delay Time
Delay of Velocity by 3.5(km/s)
Step-like Phenomena would be triggered with the Rayleigh Waves

Triggering Mechanism of the Step-like Increase

Earthquake	D(km)	Mw	MAX-Amp-Water (L/min)	MAX-Amp-Strain (E-08)	Step-like Water Increase (L/min)
1)Kii Peninsula(1)(2004)	377	7.2	3.3	121	0.6
2)Kii Peninsula(2)(2004)	363	7.5	10.6	263	1.2
12)Off Chyuetsu(2007)	178	6.6	2.6	107	0.3
13)Off Ibaraki(2008)	391	6.8	1.7	28	None step
15)Iwate-Miyagi(2008)	437	6.9	1.8	30	None step
6) Sumatra(2004)	5609	9.3	9.2	156	None step

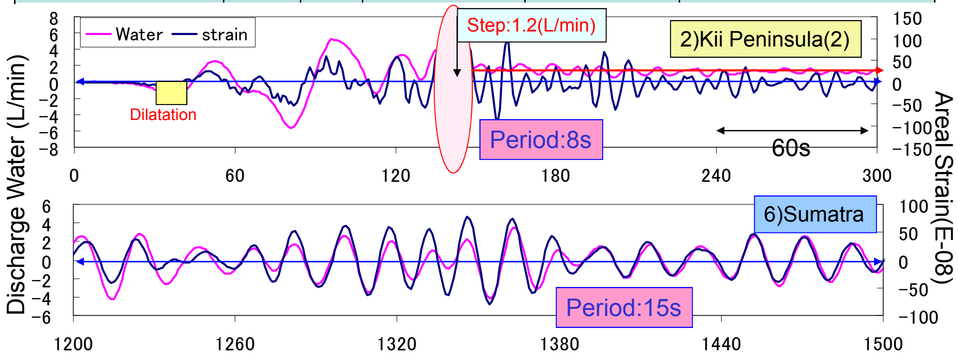

Triggered Threshold for changes of Confined Aquifer
Strain >100(E-08strain) & Period of Oscillation<8(sec)

Pre-seismic Change of Irregular Oscillation

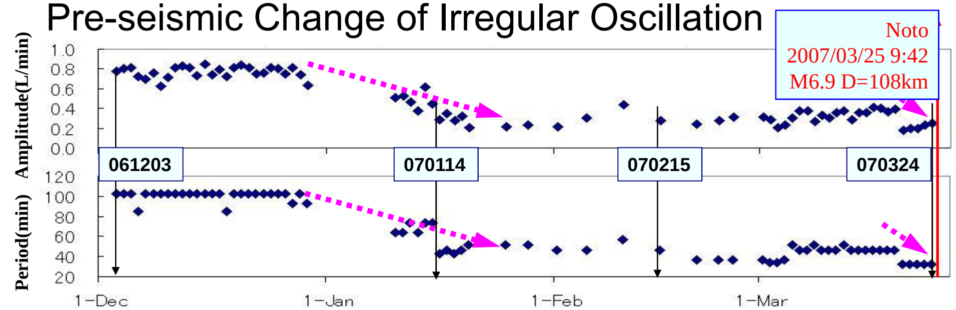

FFT-Analysis for Waveform by day
Period & Amplitude of Irregular Comp.

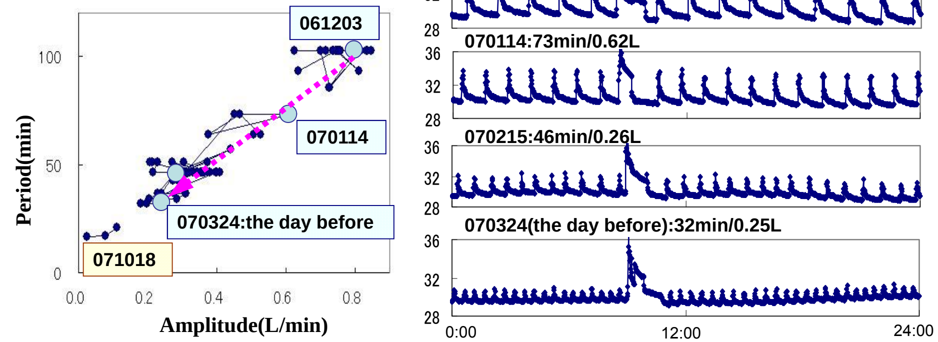

Pre-seismic and Post-seismic Change of Irregular Component in Noto Peninsula EQ

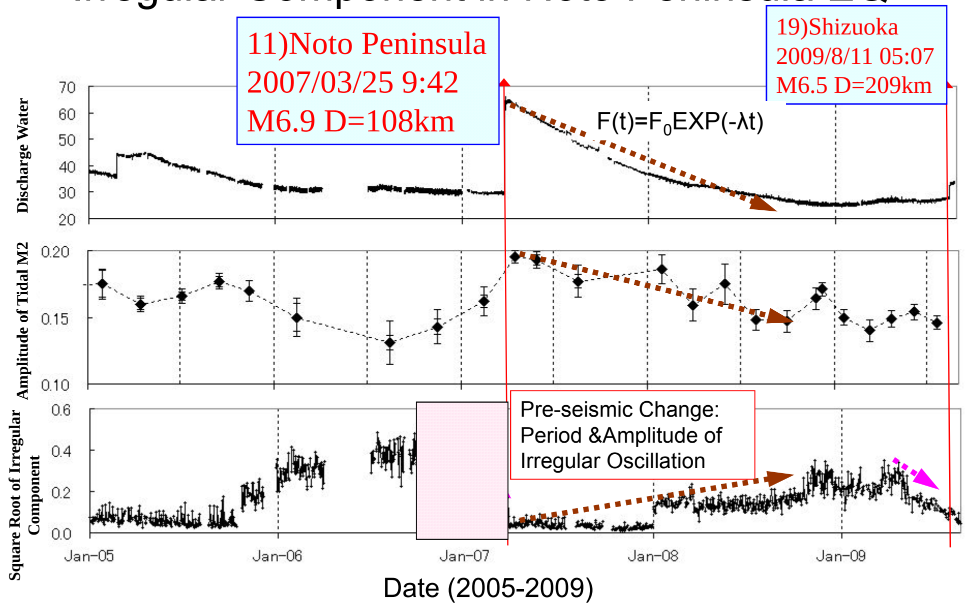

Summary

1) Seismic Change of Discharge Water in Wari-ishi Hot spring, 27 Earthquakes last 32 years.
2) Tidal Analysis of O1 and M2 Amplitude(1998-2009).
   Sensitivity for Tidal Strain :
   0.15 (L/min)/(E-08 strain)
3) FFT Analysis of Discharge Water and Area Strain.
   Sensitivity in the Frequency 0.003Hz-0.05Hz :
   0.15 (L/min)/(E-08 strain)
4) Initial Water Movement Linearly Response from the Dynamical Area Strain.
5) Step-like Water Increase was triggered with Dynamical Strain changes from 8 seconds Rayleigh-Wave of Strain Amplitude Threshold Larger than 100(E-08 strain).
6) Pre-seismic Post-seismic Change in Noto Peninsula EQ(Mar-2007): Irregular Component of Waveform changed from Three Months before and just before 5days.

RESPONSES OF WELL WATER-LEVEL CHANGES TO THE STRESS WAVE DUE TO WENCHUAN MS 8.0 STRONG EARTHQUAKEON

Yang Duoxing[1,2] , Sun Xiaolong[1,2]
1) *Institute of Crustal Dynamics, CEA, BeiJing, 100085, China.*
2) *Laboratory of Underground Fluid Dynamics, CEA, Beijing 100085, China.*

Wechuan 8.0 strong earthquake related water-level/pore pressure changes recorded at different monitoring sites showed different features, with water-level changes distribution demonstrating the heterogenous patterns in spatial scales,as shown in Fig.1. Such changes, especially those observed at large epicentral distances (about 2000km), can not be explained by the static strain field, illustrated in Fig.2 calculated on the base of the elastic dislocation model, the changes require the dominant effect of earthquake-related stress wave on water level changes.

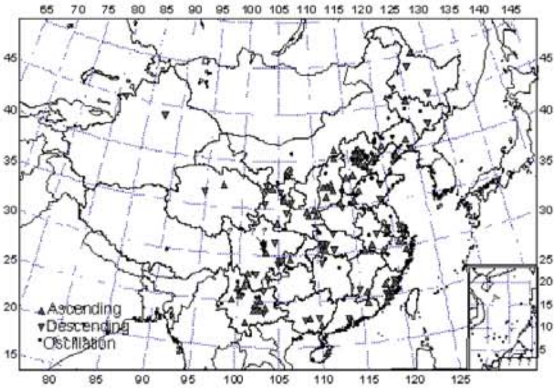

Fig. 1 Earthquake-related water level changes distribution demonstrating the heterogenous patterns in spatial scales(Liu et al., 2009).

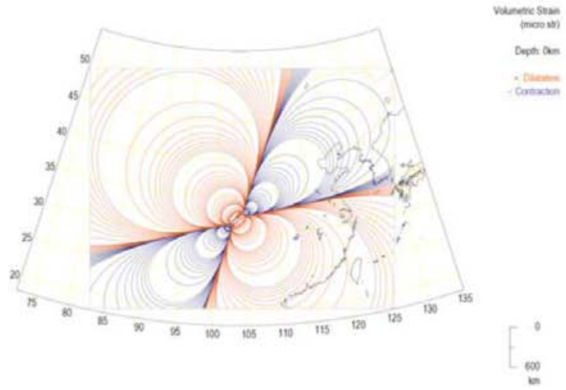

Fig.2 Strain distribution calculated on the base of the elastic dislocation model(Lai wenji et al., 2008)

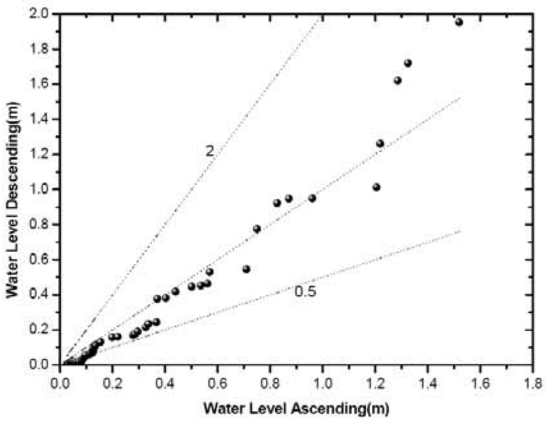

Fig. 3 QQ plots between Water level ascending and descending data

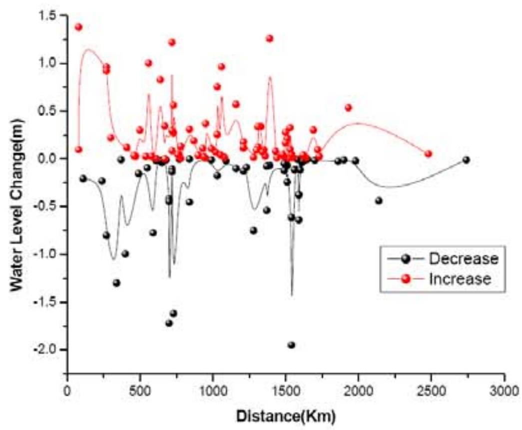

Fig. 4 Water level changes and related envelopes

After investigation of the quantile-quantile (QQ) plots of a set of water-level increase versus water-level decrease data, it is inferred that cosesmic responses of water-level increase and decrease are controlled by an analogous mechanism. The related envelopes ,as shown in Fig.4, implied the potential impact of the stress wave to water-level changes induced by Wenchuan strong earthquake.

The improved CE/SE scheme

Elastic-plastic flows model based on CE/SE (Space and time conservation element and solution element) method was applied to estimate the relationship between the stress wave and water-level changes.

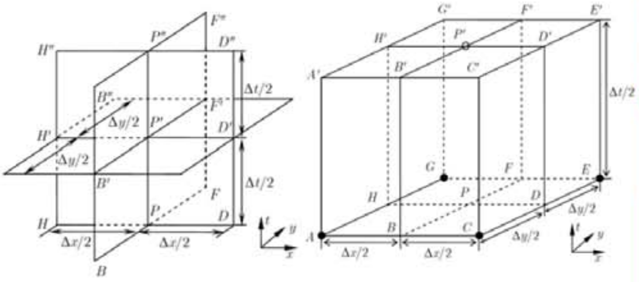

Solution element SE   Conservation element CE

Fig. 5 Mesh construction of the improved CE/SE method

Governing equations

2 D multimaterial elastic-plastic flows model based on fluid dynamical equations, obeying the Hook's law and the plasticity flow model. **The** Mie-Cruneisen equation of state and Johnson-Cook constitutive model applied.

Model validation and evaluation

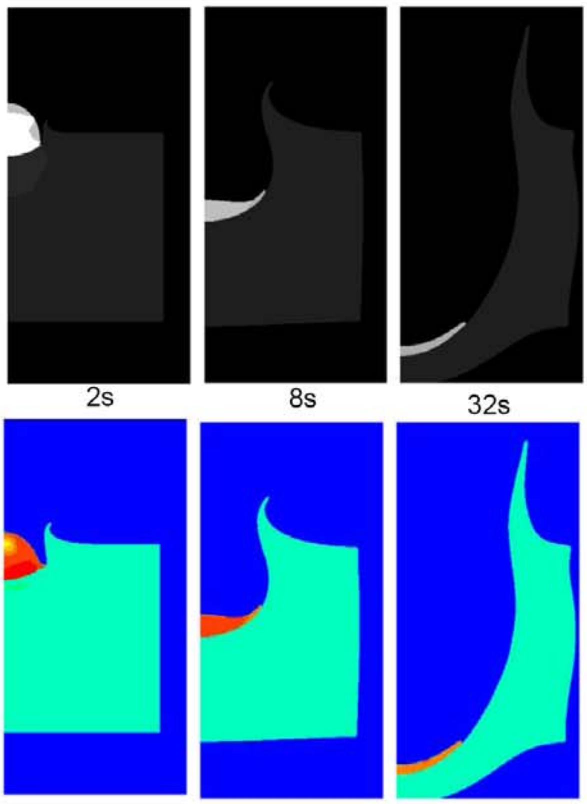

Fig. 6 Deformation of a steel ball impacting on aluminium (t=2,8,16,32s) . Experiment (gray),CE/SE calculated results (color)

Stress wave propagation

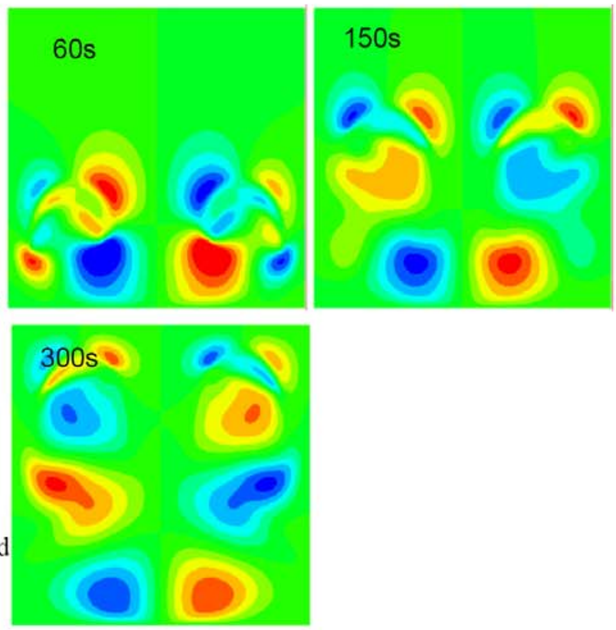

Fig. 8. Stress wave propagation, calculated by CE/SE, through a rectangular domain at time 60,150 and 300s

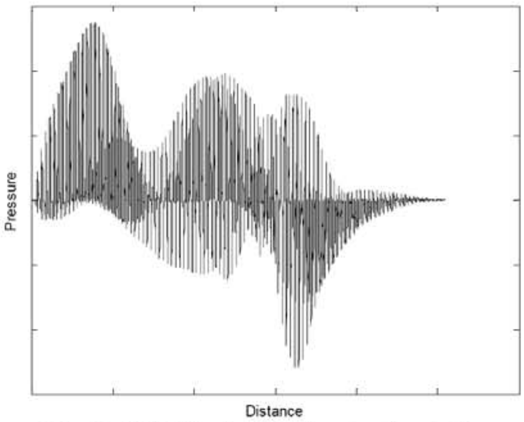

Fig. 9 CE/SE calculated water level changes and related envelopes at different monitoring sites

Results show that the model performed well in predicting water-levels changes in spatial macro-scales, which were mainly controlled by the Wenchuan 8.0 earthquke related stress wave. It implied that earthquake related stress waves result in the fluctuation of local pore pressures, which alters the surrounding pore pressure gradients , leading groundwater flow in the local scale.

RESPONSES OF WELL WATER-LEVEL CHANGES TO THE STRESS WAVE DUE TO WENCHUAN MS 8.0 STRONG EARTHQUAKEON

Yang Duoxing[1,2] , Sun Xiaolong[1,2]

1) *Institute of Crustal Dynamics, CEA, BeiJing, 100085, China.*

2) *Laboratory of Underground Fluid Dynamics, CEA, Beijing 100085, China.*

Wechuan 8.0 strong earthquake related water-level/pore pressure changes recorded at different monitoring sites showed different features, with water-level changes distribution demonstrating the heterogenous patterns in spatial scales,as shown in Fig.1. Such changes, especially those observed at large epicentral distances (about 2000km), can not be explained by the static strain field, illustrated in Fig.2 calculated on the base of the elastic dislocation model, the changes require the dominant effect of earthquake-related stress wave on water level changes.

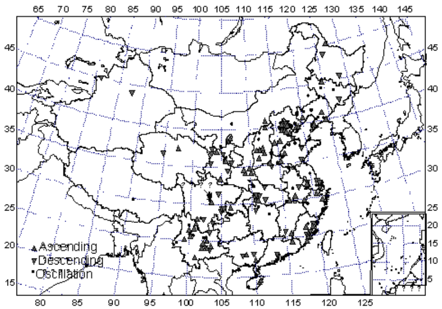

Fig. 1 Earthquake-related water level changes distribution demonstrating the heterogenous patterns in spatial scales(Liu et al., 2009).

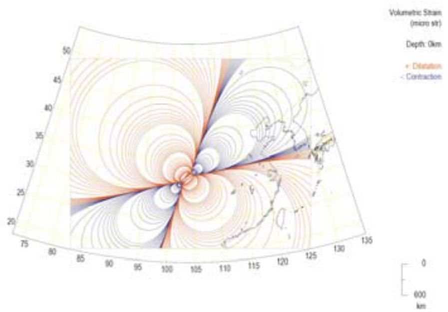

Fig.2 Strain distribution calculated on the base of the elastic dislocation model(Lai wenji et al., 2008)

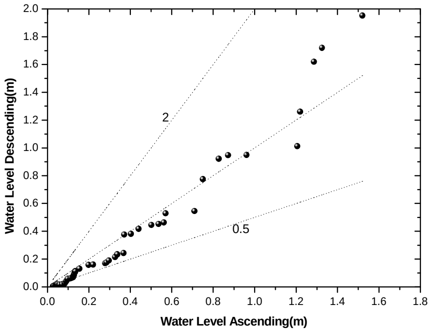

Fig. 3 QQ plots between Water level ascending and descending data

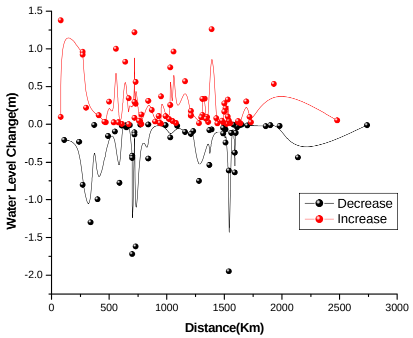

Fig. 4 Water level changes and related envelopes

After investigation of the quantile-quantile (QQ) plots of a set of water-level increase versus water-level decrease data, it is inferred that cosesmic responses of water-level increase and decrease are controlled by an analogous mechanism. The related envelopes ,as shown in Fig.4, implied the potential impact of the stress wave to water-level changes induced by Wenchuan strong earthquake.

The improved CE/SE scheme

Elastic-plastic flows model based on CE/SE (Space and time conservation element and solution element) method was applied to estimate the relationship between the stress wave and water-level changes.

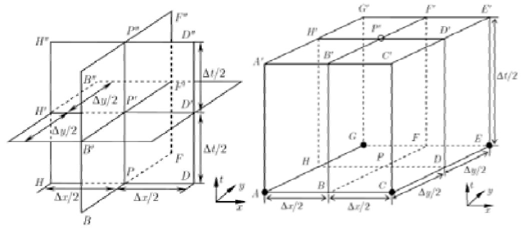

Solution element SE Conservation element CE

Fig. 5 Mesh construction of the improved CE/SE method

Governing equations

2 D multimaterial elastic-plastic flows model based on fluid dynamical equations, obeying the Hook's law and the plasticity flow model. **The** Mie-Cruneisen equation of state and Johnson-Cook constitutive model applied.

Model validation and evaluation

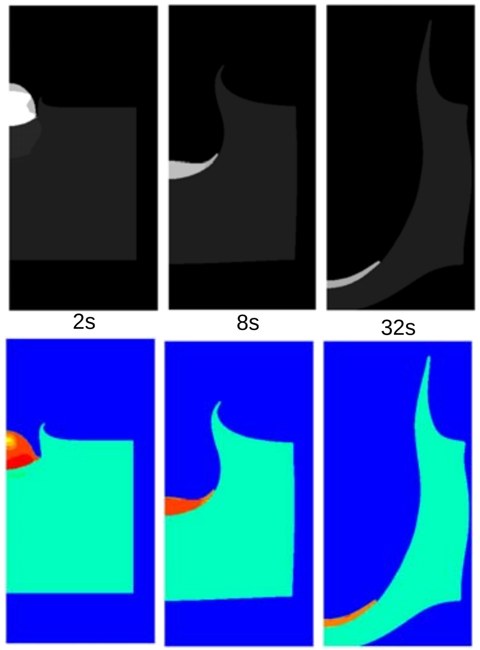

Fig. 6 Deformation of a steel ball impacting on aluminium (t=2,8,16,32s) . Experiment (gray),CE/SE calculated results (color)

Stress wave propagation

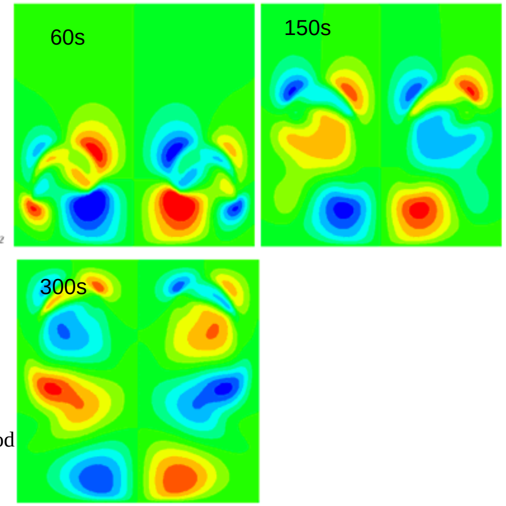

Fig. 8. Stress wave propagation, calculated by CE/SE, through a rectangular domain at time 60,150 and 300s

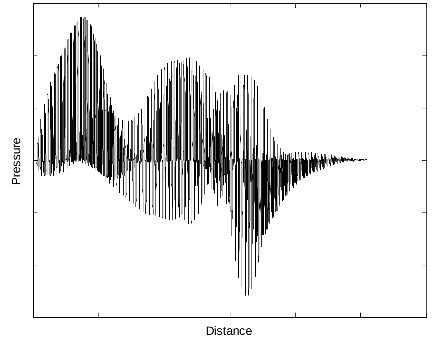

Fig. 9 CE/SE calculated water level changes and related envelopes at different monitoring sites

Results show that the model performed well in predicting water-levels changes in spatial macro-scales, which were mainly controlled by the Wenchuan 8.0 earthquake related stress wave. It implied that earthquake related stress waves result in the fluctuation of local pore pressures, which alters the surrounding pore pressure gradients , leading groundwater flow in the local scale.

Characterization of earthquake-induced water level fluctuation using data mining techniques

Kuo-Chin Hsu, Feng-Sheng Chiu,

Department of Resources Engineering, National Cheng-Kung University, Taiwan

Abstract

Recognition of groundwater anomaly pattern is important to earthquake hydrology. Recently, independent components analysis (ICA) has been emerging as an efficient tool in signal analysis. The ICA is able to recognize independent sources from complex received signals. However, the water level is recorded in few monitoring wells. To apply the technique to the earthquake-induced water level signal, wavelet independent component analysis (WICA) is introduced. The effectiveness of WICA is demonstrated by applying WICA to both synthetic signals and field groundwater levels signals. The results show that the WICA method is an efficient tool which has potential to recognize the groundwater anomaly pattern caused by earthquake.

8th Taiwan - Japan Joint Workshop on Hydrological Research for Earthquake Prediction

Characterization of earthquake-induced water level fluctuation using data mining techniques

Kuo-Chin Hsu and Feng-Sheng Chiu

Department of Resources Engineering, National Cheng-Kung University , Tainan, Taiwan, ROC

Statement of problem

How to separate sources from received data?

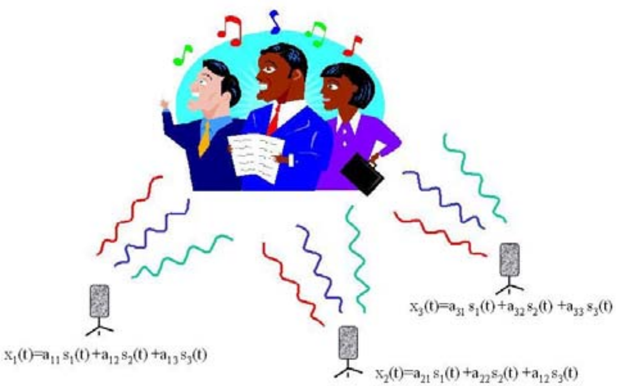

Hyvärinen et al., 2001

Independent Component Analysis (ICA)

- Three source signals s_1(t), s_2(t) and s_3(t)
- Three received mixed signals x_1(t), x_2(t) and x_3(t):
- ICA has the capability to separate source signals from the mixed signals.

$$x_1(t) = a_{11}S_1 + a_{12}S_2 + a_{13}S_3 \ldots\text{.(1)}$$
$$x_2(t) = a_{21}S_1 + a_{22}S_2 + a_{23}S_3 \ldots\text{.(2)}$$
$$x_3(t) = a_{31}S_1 + a_{32}S_2 + a_{33}S_3 \ldots\text{.(3)}$$

How ICA work?

$$x(t) = \begin{bmatrix} x_1 \\ x_2 \\ \vdots \\ x_m \end{bmatrix} = \begin{bmatrix} a_{11} & a_{12} & \cdots & a_{1n} \\ a_{21} & a_{22} & \cdots & a_{2n} \\ \vdots & \vdots & \ddots & \vdots \\ a_{m1} & a_{m2} & \cdots & a_{mn} \end{bmatrix} \begin{bmatrix} S_1 \\ S_2 \\ \vdots \\ S_n \end{bmatrix} = AS$$

With given vector x and knowing components s are independent, ICA solve matrix such that vector s is with most non-Gaussian structure that is with lowest entropy.

Why ICA not PCA?

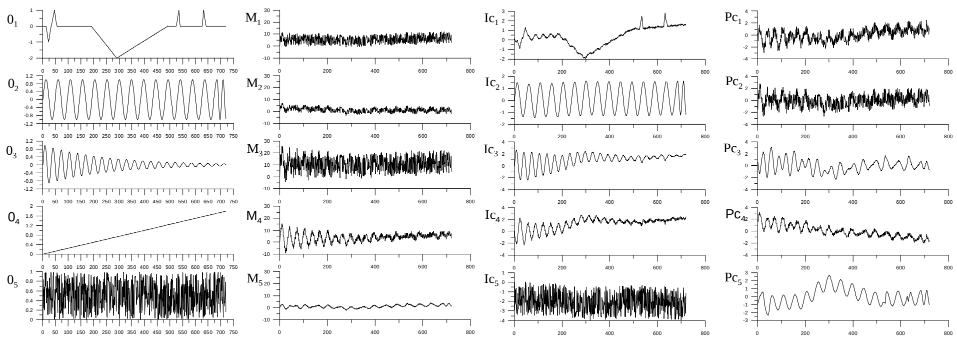

O_1 : *Rand impulses*
O_2 : *Frequency changes*
O_3 : *Amplitude changes*
O_4 : *Linear equation*
O_5 : *White noise*

$$M_1 = O_1 + (0.5)\cdot O_2 + O_3 + O_4 + (10)\cdot O_5$$
$$M_2 = O_1 + O_2 + O_3 + (-1)\cdot O_4 + (5)\cdot O_5$$
$$M_3 = O_1 + (0.5)\cdot O_2 + (6)\cdot O_3 + O_4 + (20)\cdot O_5$$
$$M_4 = O_1 + O_2 + (10)\cdot O_3 + (2)\cdot O_4 + (5)\cdot O_5$$
$$M_5 = O_1 + O_2 + O_3 + O_4 + O_5$$

R xusuredp lvý 1l

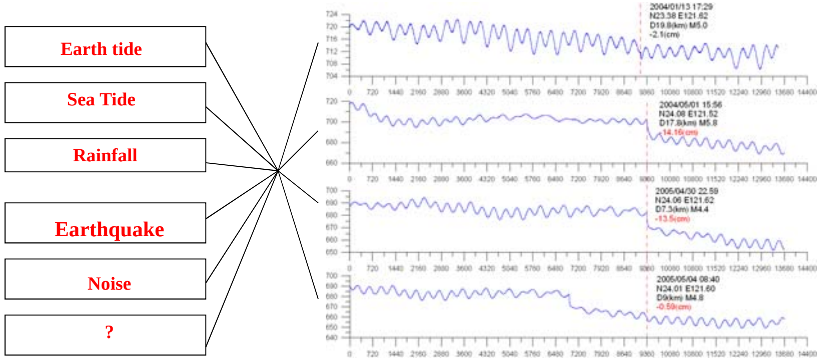

Generally, ICA requires that the number of sensors must be no less than the number of independent sources to ensure enough information for separation of all sources. However, this is usually not the case.

Wavelet methods

Decompose time series, $\boxed{X(t)}$, into local, time-dilated and time-translated wavelet components, ⌡ –complete (not necessarily orthogonal) basis

$$W(a,b) = \int \frac{1}{\sqrt{|a|}} \cdot f(t)\cdot \psi\left(\frac{t-b}{a}\right)dt$$

$$= \int_{-\infty}^{\infty} f(t)\cdot \psi^{*}_{a,b}(t)dt$$

$$\psi_{a,b}(t) = \frac{1}{\sqrt{|a|}} \cdot \psi\left(\frac{t-b}{a}\right)$$

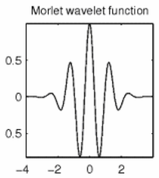

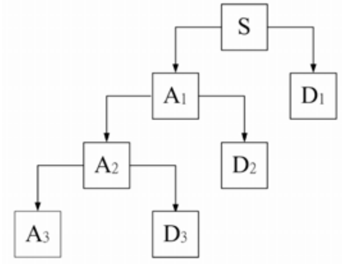

$S = A_1 + D_1$
$= A_2 + D_2 + D_1$
$= A_3 + D_3 + D_2 + D_1$

a is scaling function, control the **frequency domain**
b is translation function, control the **time domain**

Example of WICA application

x_1 is composed of four impulses, which is considered as feature to be isolated.

x_2 is a chirpy signal

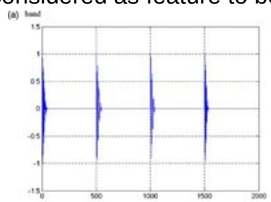

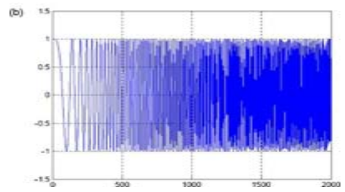

Waveform of the mixture of impulses and chirpy signals (mixed with 0.2:1).

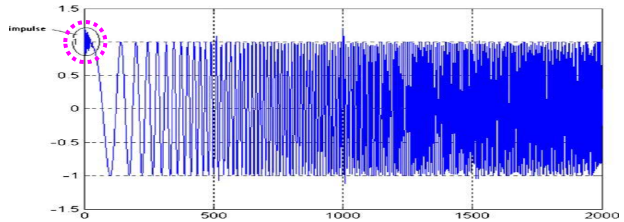

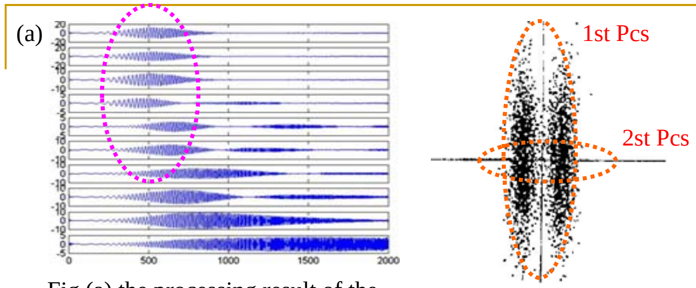

PCA Projection

Fig (a) the processing result of the wavelet decompositions by PCA

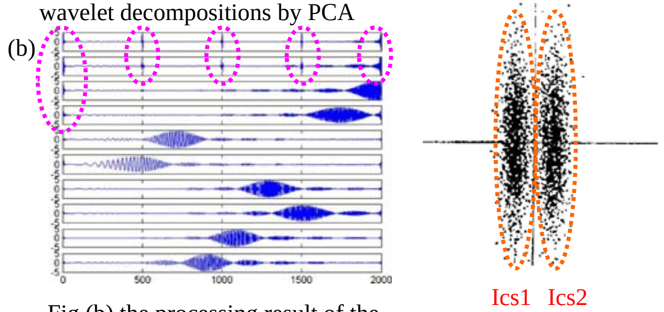

ICA Projection

Fig (b) the processing result of the wavelet decompositions by ICA

Case in Tono, Japan (King et al., 2000)

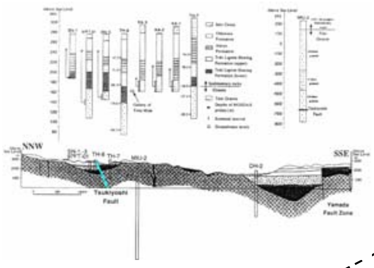

Original water levels

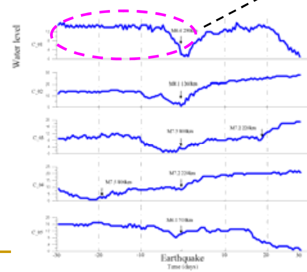

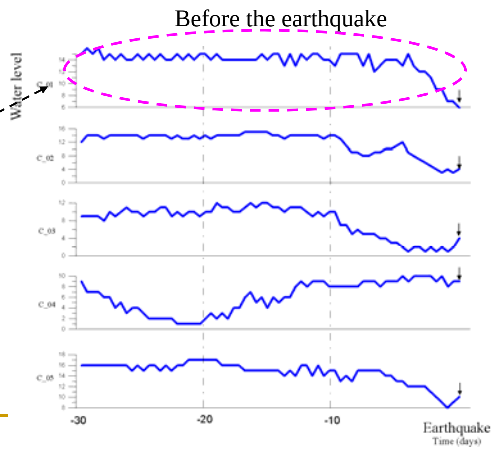

Case C_01~02 result of the WICA

C1

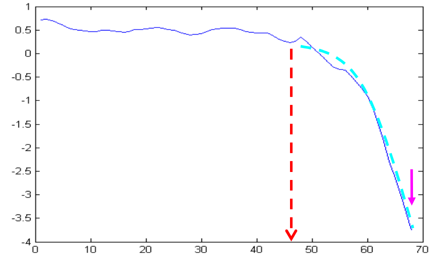

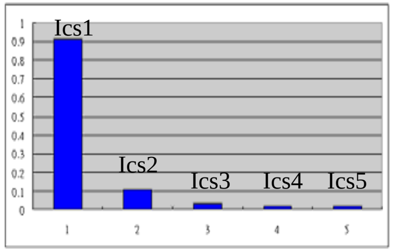

C2

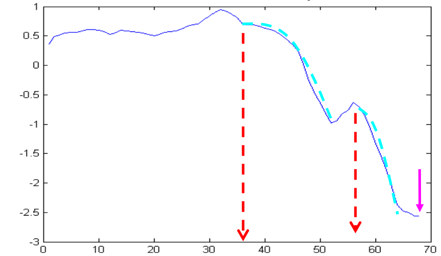

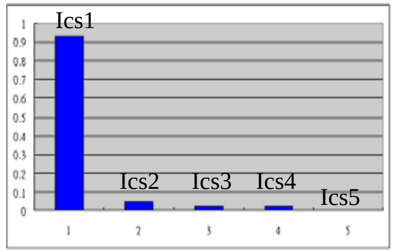

Earthquake time

Case C_03~04 result of the WICA

C3

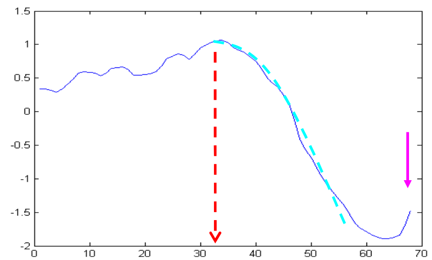

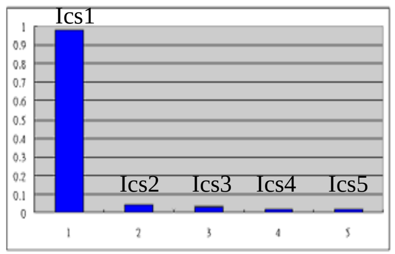

C4

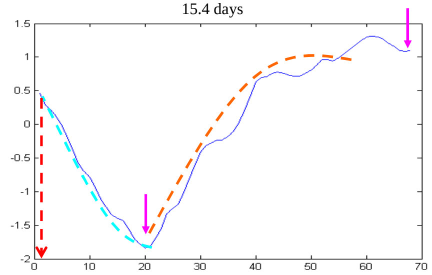

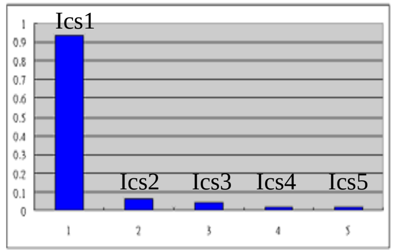

Earthquake time

Case C_05 result of the WICA

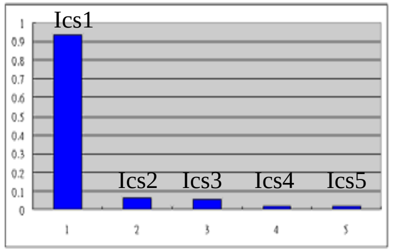

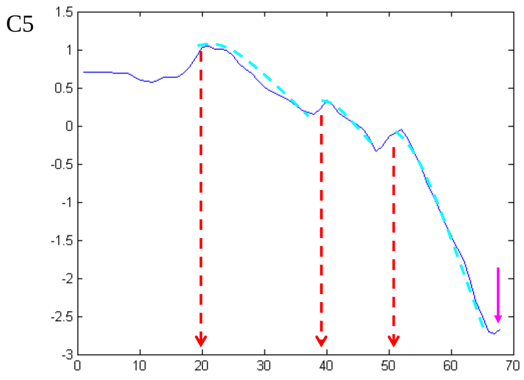

19.4 days 12.8 days 7.72 days

Earthquake time

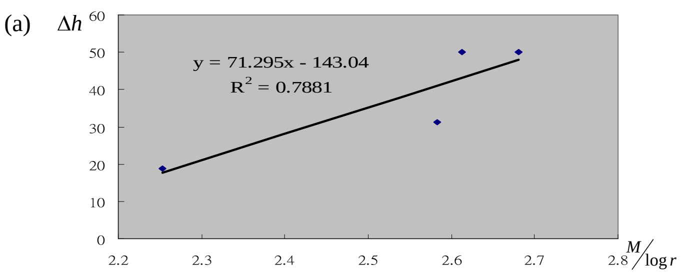

Fig (a) Result of WICA

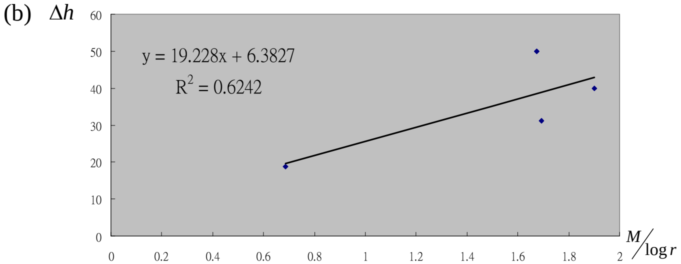

Fig (b) Result of original water levels

Δh is the difference of ten-day-before average water level and lowest water level

Conclusions

1. ICA has the capability to separate independent components sources from mixed signals.
2. The proposed WICA filter can extract the independent sources from one mixed signal.
3. The Tono case shows that the preseismic water level fluctuations have groundwater drop in 10~20 days before the earthquakes.
4. The regression relation of water level drop and earthquake parameters are improved by using WICA.

Evaluation of the effects of ground shaking and static volumetric strain change on earthquake-related groundwater level changes in Taiwan

Wen-Chi Lai[1、2], Kuo-Chin Hsu[2], Chjeng-Lun Shieh[1、3], Youe-Ping Lee [4],

Kuo-Chang Chung[4], Naoji Koizumi[5] and Norio Matsumoto[5]

1: Disaster Prevention Research Center, National Cheng-Kung University, Taiwan

2: Department of Resources Engineering, National Cheng-Kung University, Taiwan

3: Department of Hydraulic and Ocean Engineering, National Cheng Kung University, Taiwan

4: Water Resource Agency, Ministry of Economic Affair, Taiwan

5: Geological Survey of Japan, National Institute of Advanced Industrial Science and Technology

Abstract

During the period from 2001 to 2005, the Disaster Prevention Research Center of National Cheng-Kung University established a groundwater observation network composed of 16 wells mainly along active faults for research on earthquake-related groundwater changes. The 16 wells were mainly chosen from the 550 groundwater observation wells of Water Resources Agency (WRA), where WRA had been monitoring groundwater for managing groundwater resources. Groundwater level has been observed with a resolution of 0.2 mm at the wells. The depths of the screens range between 80 and 252 m. We analyzed groundwater level data at 6 of the 16 wells during the period from 2003 to 2006 and evaluated the ability for detecting earthquake-related groundwater level changes. At the 6 wells, strain sensitivities of the groundwater level range between 0.1 and 0.5 mm/10^{-9}. It means the 6 wells can detect the volumetric strain changes with the order of 10^{-9}. We also analyzed coseismic and/or postseismic groundwater level changes related to 17 earthquakes in and around Taiwan whose magnitudes are 6 or greater. The analysis showed that not the static coseismic volumetric strain changes but ground shaking is the main reason for the earthquake-related changes. It also showed that dynamic strain change might be important factor as well as the peak ground acceleration.

Tectono-Hydrology Research Group

Disaster Prevention Research Center,
National Cheng Kung University, Taiwan

AIST Geological Survey of Japan

Evaluation of the effects of ground shaking and static volumetric strain change on earthquake-related groundwater level changes in Taiwan

Wen-Chi Lai[1,2], Chjeng-Lun Shieh[1,3], Kuo-Chin Hsu[2], Norio Matsumoto [4], Naoji Koizumi [4]

1. Disaster Prevention Research Center, NCKU, Taiwan
2. Department of Resources Engineering, NCKU, Taiwan
3. Department of Hydraulic and Ocean Engineering, NCKU, Taiwan
4. Geological Survey of Japan, AIST, Japan

Observation wells

Well	Location		Depth (m)	Screened Depth (m)	Geology	Hydrological Conductivity (m/min)
	Lon.	Lat.				
TWN	121.782	24.746	130	112-124	Qs, Qm	2.22E-04
HUL	121.605	23.977	205	140-160	Qc	—
TLO	120.784	24.491	99	84-93	Qs	8.00E-04
DHR	120.561	23.688	258	222-252	Qg	4.15E-03
LUJ	120.342	23.227	228	204-222	Qs, Qm	2.67E-03
NBA	120.340	23.071	153	135-147	Qs, Qm	1.84E-03

* The monitoring well instrumented in the project
Qc: Quaternary conglomerate, Qg: Quaternary gravel, Qs: Quaternary sandstone, Qm: Quaternary shale and mudstone

I. Introduction

- Tectonic Setting of Taiwan.
- Highly Seismic hazard risk.
- Advantage of the research
  - High density monitoring network for water resources Groundwater Monitoring Networks of Taiwan
  - High density seismic monitoring network.
  - High seismic activity
- Good quality observation

→ ***Waiting for good news…***

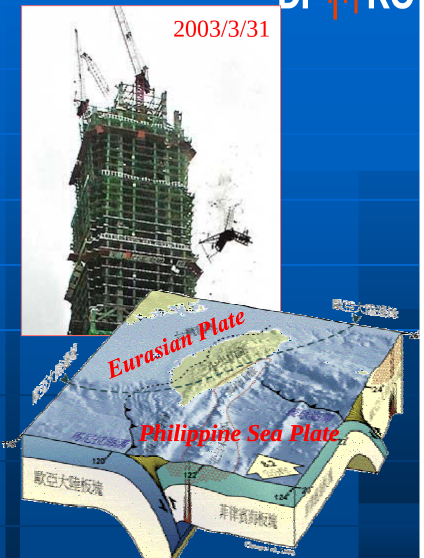

(Cheng et al.,2000)

Observation

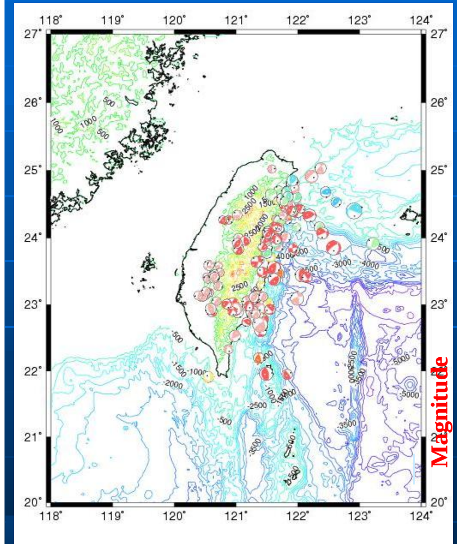

 CMT solution and distribution of events

Events of the earthquake M_L >3 in Taiwan 03'~06'

M_L	3~3.9	4~4.9	5~5.9	≧6.0
2003	118	181	43	2
2004	86	125	25	5
2005	277	140	24	3
2006	231	117	21	8

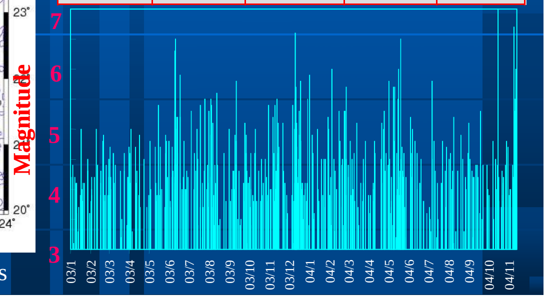

Observed coseismic events (03'~06')

DP RC

- Total 125 Observation, step changes (S) 26 events, oscillation (O) 76 events, O+S 23 events

Catalog	Events	HUL	TWN	LUJ	NAB	HRD	DHR	TLO	SIP
2003/4/3 Tainan, M=4.9	2			S	S				
2003/6/10 Taitung, M=6.5	4			S	O		O+S		O
2003/6/17 Taitung , M=5.9	2				O				O
2003/12/10 Taitung , M=6.6	7	O+S	O+S	S		S	O+S	O+S	O
2003/12/11 Taitung, M=5.7	1				S				
2003/12/18 Taitung, M=5.8	1	O							

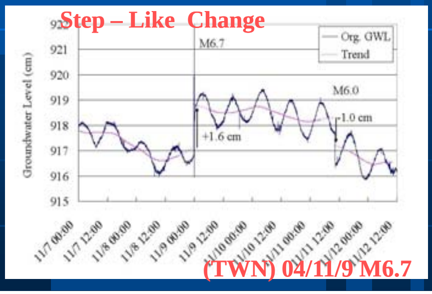

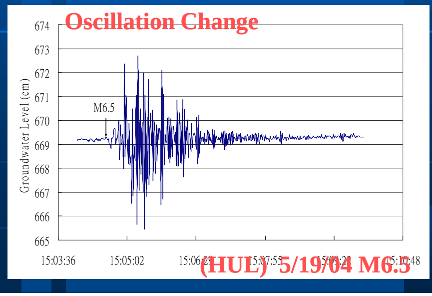

Estimation of the theoretical responses

DP RC

- Using Baytap-G Program to estimate the Tidal component of observed groundwater level
- Calculate the theoretic tidal potential from GOTIC II Program
- Derived the static strain volumetric sensitivity by

static volumetric strain sensitivity = (tidal responses ÷ tidal potential)

- Calculate the coseismic static volumetric strain using MICAP-G program.
- Derived the predicted amplitude estimated from tidal response by

Amp. Of Chg.= (calculated volumetric strain × strain sensitivity)

Decomposition and Extraction

DP RC

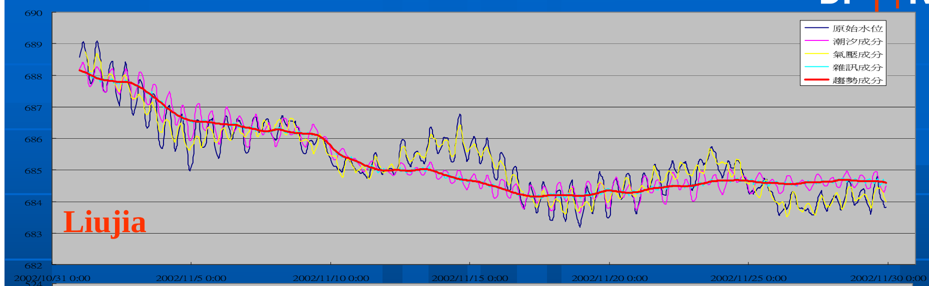

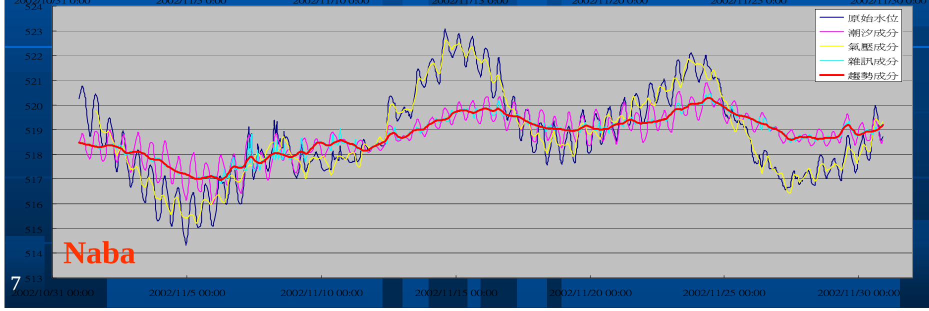

Verify of the Static Volumetric Strain Sensitivity

DP RC

Amplitude

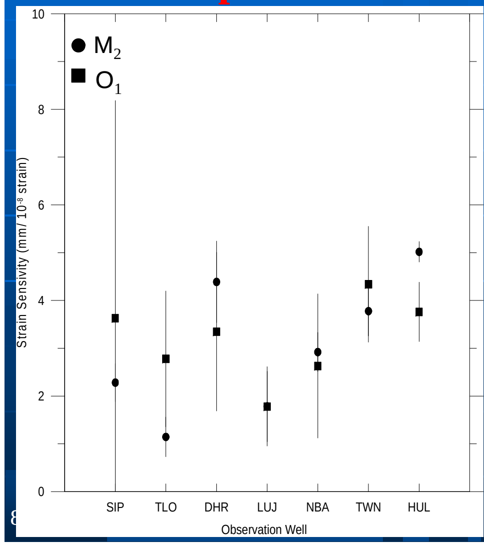

Phase Angle

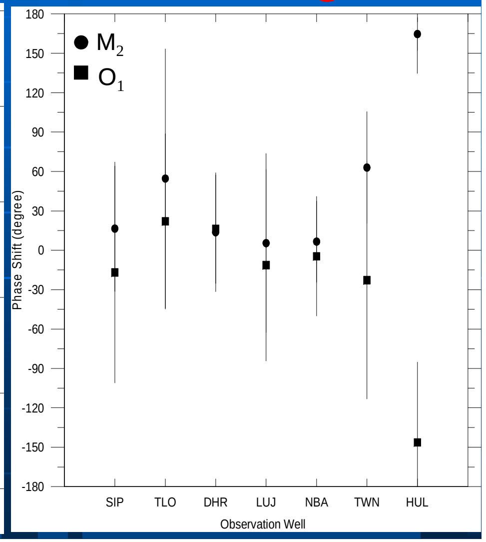

Static Volumetric Strain Sensitivity

	TLO	DHR	LUJ	NBA	TWN	HUL
	Amplitude (10^{-8}) [Phase Shift (degree)]					
Vol. strain by M_2 earth tide, t_e	1.35 [0]	1.37 [0]	1.38 [0]	1.38 [0]	1.35 [0]	1.37 [0]
Vol. strain by M_2 oceanic tidal loading, t_o	2.08 [-321]	0.18 [-276]	0.11 [-290]	0.11 [-301]	0.60 [-227]	6.10 [-184]
Vol. strain by earth + oceanic tide, $t_t = t_e + t_o$	3.25 [-336]	1.40 [-352]	1.42 [-356]	1.45 [-356]	1.04 [-335]	4.73 [-185]
M_2 amplitude(water level, t_w)	3.72±0.67 [-282±49]	6.17±0.60 [-339±23]	2.54±0.59 [-350±34]	4.24±0.29 [-349±15]	3.93±0.27 [-272±21]	23.77±0.50 [-21±6]
Strain sens. by **Water Level** M_2 tide, **Ws** = t_w/t_t (mm/10^{-8})	1.14	4.39	1.78	2.92	3.78	5.02

9

Static Volumetric Strain Sensitivity

	TLO	DHR	LUJ	NBA	TWN	HUL
	Amplitude (10^{-8}) [Phase Shift (degree)]					
Vol. strain by M_2 earth tide, t_e	1.35 [0]	1.37 [0]	1.38 [0]	1.38 [0]	1.35 [0]	1.37 [0]
Vol. strain by M_2 oceanic tidal loading, t_o	2.08 [-321]	0.18 [-276]	0.11 [-290]	0.11 [-301]	0.60 [-227]	6.10 [-184]
Vol. strain by earth + oceanic tide, $t_t = t_e + t_o$	3.25 [-336]	1.40 [-352]	1.42 [-356]	1.45 [-356]	1.04 [-335]	4.73 [-185]
M_2 amplitude(water level, t_w)	3.72±0.67 [-282±49]	6.17±0.60 [-339±23]	2.54±0.59 [-350±34]	4.24±0.29 [-349±15]	3.93±0.27 [-272±21]	23.77±0.50 [-21±6]
Strain sens. by **Water Level** M_2 tide, **Ws** = t_w/t_t (mm/10^{-8})	1.14	4.39	1.78	2.92	3.78	5.02
Strain sens. by **Coseismic Responses** (mm/10^{-8})	18.42	42.22	76.15	56.93	43.85	25.82

Comparison of the theoretic and observed responses

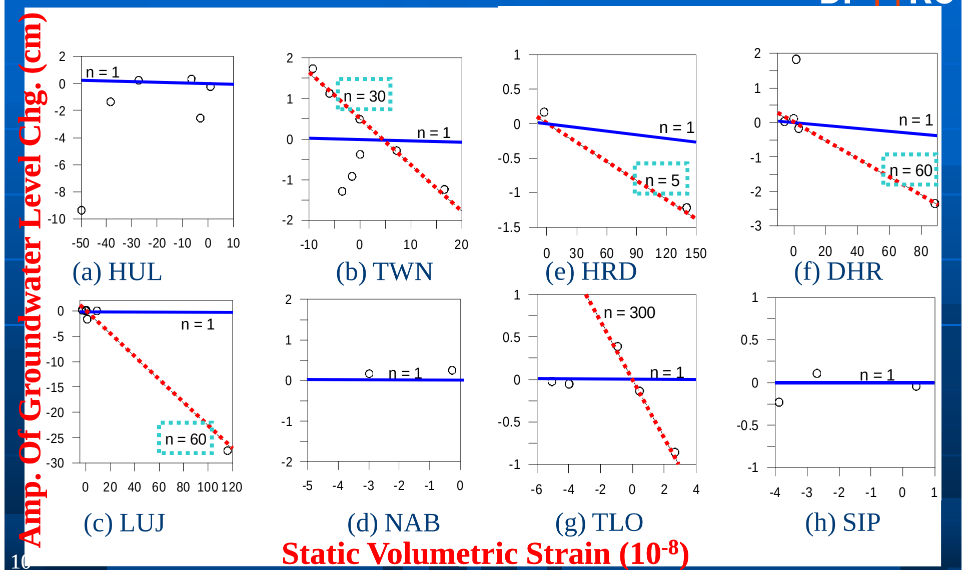

10

Problem statement

- Observed coseismic patterns can fit to strain model , but the amplitudes are amplify tens~hundreds times compare to the static strain sensitivity estimated from tidal response.
- Some wells seems always coseismic roses or coseismic lowering, them were not expected by the fault-dislocation volumetric strain .
- The mechanism of the coseismic groundwater level changes remains unknown.

12

Observed coseismic events (03'~06')

No.	Time	Lat.	Long.	Depth (km)	M_W
1	2003/6/10 8:40	23.50	121.70	27.59	**6.54**
2	2003/12/10 4:38	23.07	121.40	10	**6.6**
3	2004/2/4 3:24	23.38	122.15	4.07	**6.03**
4	2004/5/16 6:04	23.05	121.98	12.52	**6**
5	2004/5/19 7:04	22.71	121.37	8.68	**6.49**
6	2004/10/15 4:08	24.46	122.85	58.84	**7.03**
7	2004/11/8 15:54	23.79	122.76	10	**6.6**
8	2004/11/11 2:16	24.31	122.16	27.3	**6.04**
9	2005/9/6 9:16	23.96	122.28	16.8	**6.12**
10	2006/4/1 18:02	22.88	121.08	7.2	**6.35**
11	2006/4/16 6:40	22.86	121.3	17.9	**6.2**
12	2006/7/28 15:40	23.97	122.66	28	**6.06**
13	2006/8/28 1:11	24.8	123.07	135.3	**6.1**
14	2006/10/9 18:01	20.7	119.83	28	**6.1**
15	2006/10/9 19:08	20.77	119.93	8	**6.1**
16	2006/10/11 14:43	20.89	119.9	10	**6**
18	2006/12/26 20:34	21.95	120.39	47.03	**6.4**

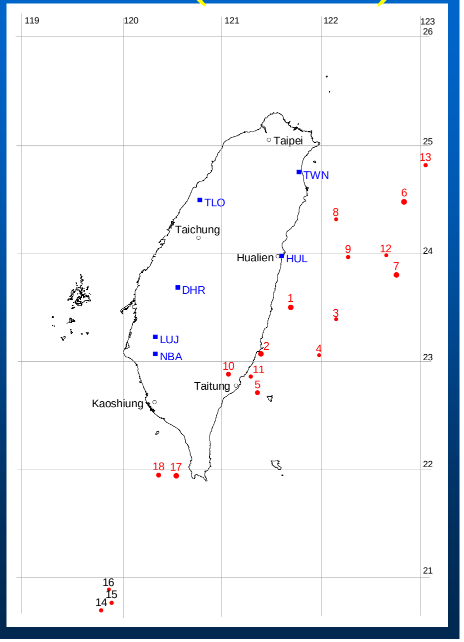

Observed coseismic events (03'~06')

No.	HUL					TWN					TLO				
	Gw_{obs}	Type	Vol. Strn.	GW_{exp}	PGA(gal)	Gw_{obs}	Type	Vol. Strn.	GW_{exp}	PGA(gal)	Gw_{obs}	Type	Vol. Strn.	GW_{exp}	PGA(gal)
1	-					-					-				
2	-13.47	O+S	-3.84E-09	7.65	29	11.24	O+S	-5.98E-10	1.58	6	-8.57	O+S	2.66E-10	-2.33	11
3	±2.36	O	9.28E-11	-0.18	29	4.92	O	-5.41E-12	0.01	6	±4.794	O	1.26E-11	-0.11	4
4	±3.60	O	2.54E-11	-0.05	13		N	-1.06E-11	0.03	8		N	1.92E-11	-0.17	3
5	3.20	S	-6.58E-10	1.31	13	-9.16	O+S	-1.51E-10	0.40	4	3.88	S	-9.30E-11	0.82	7
6	±0.04	O	-2.38E-09	4.75	53	-12.86	O+S	-3.47E-10	0.92	70	-0.23	O+S	-5.05E-10	4.43	23
7	2.39	S	2.27E-10	-0.45	14	15.92	O+S	-9.76E-10	2.58	38	±1.38	O	-2.04E-11	0.18	9
8	±2.21	O	-2.27E-10	0.45	9	-12.28	S	4.76E-10	-1.26	14		N	-7.04E-12	0.06	3
9	±16.03	O	2.09E-10	-0.42	18	-5.73	S	2.09E-10	-0.55	12		N	-6.67E-11	0.58	7
10	±11.88	O	-8.35E-10	1.66	5	-6.96	S	-1.46E-10	0.39	5		N	3.34E-10	-2.92	9
11	±18.57	O	-2.69E-10	0.54	11	-5.77	S+O	-5.09E-11	0.13	4		N	-3.88E-11	0.34	8
12		N	-5.05E-11	0.10	8	-19.56	S	1.72E-11	-0.05	31		N	-1.90E-11	0.17	3
13	±8.1	O	-1.64E-12	0.00	11		N	-6.71E-12	0.02	4		N	-2.14E-11	0.18	8
14		N	9.29E-12	-0.02	4		N	-2.68E-12	0.01	2		N	-3.19E-12	0.03	6
15		N	-1.30E-12	0.00	4		N	-1.15E-12	0.00	2		N	-4.11E-12	0.04	9
16		N	-9.94E-12	0.02	7		N	-5.06E-12	0.01	4		N	-5.21E-12	0.05	6
17	±15.76	O	-2.39E-09	4.76	15	-2.14	S	-9.60E-10	2.54	6		N	-5.61E-10	4.92	12
18	±5.3	O	-4.61E-10	0.92	18	-6.86	S	-3.13E-10	0.83	7		N	-2.84E-10	2.49	9

Observed coseismic events (03'~06')

No.	LUJ					NBA					DHR				
	Gw_{obs}	Type	Vol. Strn.	GW_{exp}	PGA(gal)	Gw_{obs}	Type	Vol. Strn.	GW_{exp}	PGA(gal)	Gw_{obs}	Type	Vol. Strn.	GW_{exp}	PGA(gal)
1	-16.70	S	1.13E-10	-0.64	31	±3.51	O	7.15E-11	-0.24	20	-1.69	O+S	3.09E-10	-0.70	28
2	-275.66	S	1.16E-08	-65.32	17		N	1.09E-08	-37.32	11	-23.51	O+S	7.91E-09	-18.02	27
3		N	1.77E-11	-0.10	3		N	1.52E-11	-0.05	8		N	-2.77E-15	0.00	2
4	0.93	S	3.16E-11	-0.18	4		N	2.51E-11	-0.09	6		N	-1.02E-14	0.00	2
5	-0.51	S	9.01E-10	-5.06	10		N	1.20E-09	-4.11	16	18.23	S	1.50E-10	-0.34	19
6		O	-4.01E-10	2.25	17		N	-3.71E-10	1.27	4	0.28	S	-1.50E-09	3.42	20
7	±1.20	O	2.23E-11	-0.13	5	±1.50	O	6.68E-11	-0.23	5		N	5.54E-10	-1.26	10
8	±2.40	O	-4.11E-11	0.02	6		N	3.77E-11	-0.13	6		N	-3.36E-11	0.08	5
9		N	6.11E-12	-0.03	5		N	1.08E-11	-0.04	4		N	-1.78E-11	0.04	5
10	7.76	S+O	4.19E-09	-23.54	18		N	2.63E-09	-9.00	10		N	3.20E-09	-7.28	5
11		N	4.71E-10	-2.65	3		N	5.91E-10	-2.02	6		N	7.79E-11	-0.18	7
12		N	-2.40E-12	0.01	3		N	-7.51E-13	0.00	2		N	-9.82E-12	0.02	5
13		N	5.54E-12	-0.03	2		N	5.56E-11	-0.20	5		N	-9.12E-12	0.02	4
14		N	4.38E-11	-0.25	6		N	5.04E-11	-0.17	7		N	2.12E-11	-0.05	4
15		N	-1.66E-11	0.09	3		N	-2.00E-11	0.07	5		N	-8.93E-12	0.02	2
16		N	-1.79E-11	0.10	2		N	-2.27E-11	0.08	4		N	-1.12E-11	0.03	2
17		N	8.25E-10	-4.64	45	-12.23	O+S	1.81E-09	-6.21	59	±27.13	O	-8.75E-10	1.99	38
18		N	4.55E-09	-25.56	37	-25.75	O+S	7.74E-09	-26.52	106	±15.29	O	4.33E-10	-0.99	58

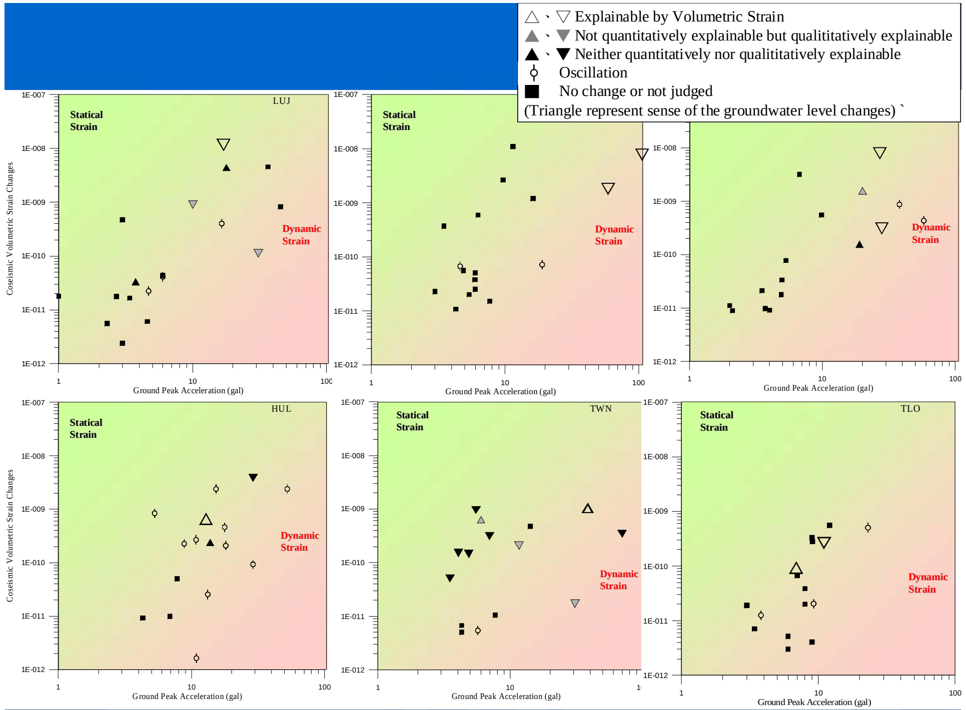

Mechanism of coseismic groundwater level changes

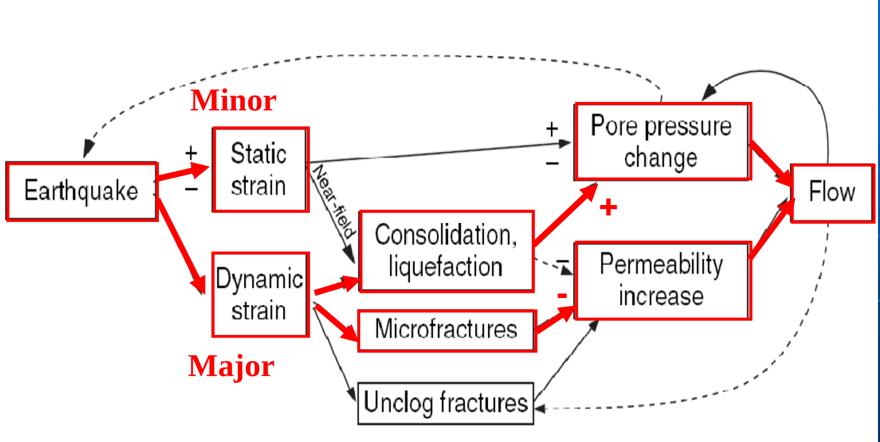

M. Manga and C.-Y. Wang (2007)

2008/5/12 Wenchuan, China Earthquake (M_L 8.0)

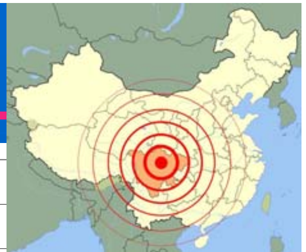

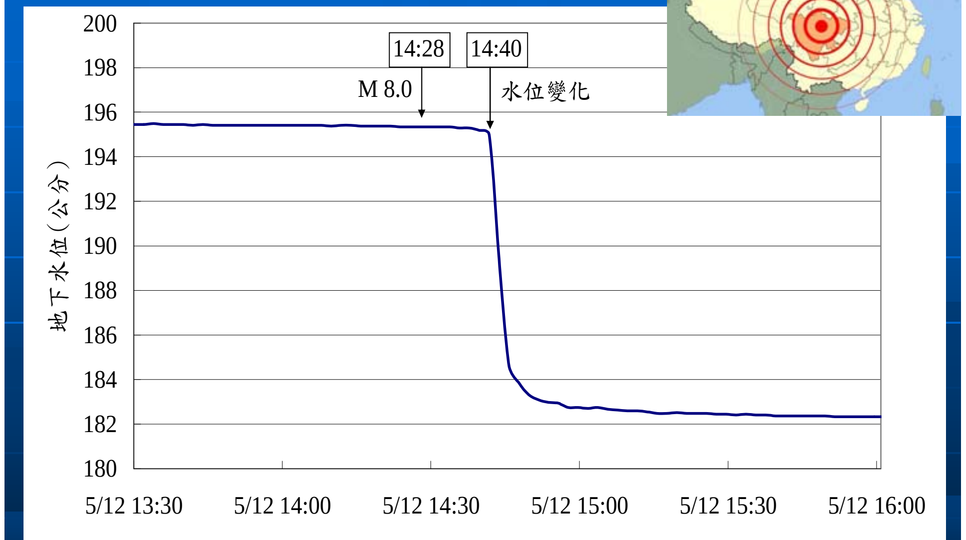

Conclusion

- The results show that the dynamic strains induced by ground shaking could be another possible factor for the coseismic groundwater level changes.
- It seems to appear especially in shallow aquifers with high hydraulic conductivity in lose-cemented and permeable sedimentary deposits.
- The similar effects can also be recognized in the coseismic groundwater level changes related to the 1999 Chi-Chi earthquake and 2004 Wenchuan earthquake .

DPRC
Disaster Prevention Research Center,
National Cheng Kung University, Taiwan

Tectono-Hydrology Research Group
AIST Geological Survey of Japan

Thank you !